INSTITUTO DE NEUROCIENCIAS

TESIS DOCTORAL

Desregulación transcripcional y desacetilación de lisinas en trastornos neurológicos: La enfermedad de Huntington y el síndrome de Rubinstein-Taybi.

Lysine deacetylation and transcriptional dysregulation in neurological disorders: Huntington's disease and the Rubinstein-Taybi syndrome

Deisy Mariela Guiretti

San Juan de Alicante, 2015

Director de Tesis: Dr. Ángel Barco Guerrero

Co-director de Tesis: Dr. Luis Miguel Valor Becerra

Consejo Superior de Investigaciones Científicas
Universidad Miguel Hernández
Instituto de Neurociencias

Dr. Ángel Barco
Científico Titular CSIC

Dr. Ángel Barco Guerrero, Investigador Científico de la Agencia Estatal Consejo Superior de Investigaciones Científicas- CSIC en el Instituto de Neurociencias de Alicante, centro mixto UMH-CSIC, y

Dr. Luis Miguel Valor Becerra, Investigador Ramón y Cajal de la Agencia Estatal Consejo Superior de Investigaciones Científicas- CSIC en el Instituto de Neurociencias de Alicante, centro mixto UMH-CSIC

CERTIFICAN,

Que D.ª **Deisy Mariela Guiretti,** ha realizado bajo su dirección el trabajo experimental que recoge su Tesis Doctoral titulado: **"**Lysine deacetylation and transcriptional dysregulation in neurological disorders: Huntington's disease and the Rubinstein-Taybi syndrome**"** y tras revisar los contenidos científicos y los aspectos formales del trabajo da su conformidad para su presentación y defensa públicas.

Para que así conste, y a los efectos oportunos, firman el presente Certificado en San Juan de Alicante, a 14 de Julio de 2015

Fdo. Ángel Barco Guerrero

Fdo. Luis Miguel Valor Becerra

abarco@umh.es
lmv@umh.es

www.ina.umh.es

Tel.: +34 965 919232
Tel.; + 34 965 919531

Av Ramón y Cajal s/n
Campus de San Juan
03550 SAN JUAN DE ALICANTE– ESPAÑA

INSTITUTO DE NEUROCIENCIAS

EXCELENCIA SEVERO OCHOA
Centro de Excelencia «Severo Ochoa» 2014-2018

Consejo Superior de Investigaciones Científicas
Universidad Miguel Hernández
Instituto de Neurociencias

Prof. Juan Lerma
Director

A QUIEN CORRESPONDA:

Prof. Juan Lerma Gómez, Director del Instituto de Neurociencias, centro mixto de la Universidad Miguel Hernández (UMH) y el Consejo Superior de Investigaciones Científicas,

CERTIFICA:

Que la Tesis Doctoral "Lysine deacetylation and transcriptional dysregulation in neurological disorders: Huntington's disease and the Rubinstein-Taybi syndrome" ha sido realizada por D.ª Deisy Mariela Guiretti (NIE Y0151110Z) bajo la dirección del Dr. Ángel Luis Barco Guerrero y co-dirección del Dr. Luis Miguel Valor Becerra y da su conformidad para que sea presentada a la Comisión de Doctorado de la Universidad Miguel Hernández.

Para que así conste a los efectos oportunos, firma el presente certificado en San Juan de Alicante a 15 de julio de 2015

INSTITUTO DE NEUROCIENCIAS
CSIC

Juan Lerma
Director

direccion.in@umhc.es
director.in@umh.es
www.ina.umh.es

Tel: +34 965-919221(d)
+34 965-919220 (s)
Fax: +34 965 919561

Av Ramón y Cajal s/n
Campus de San Juan
03550 SAN JUAN DE ALICANTE– ESPAÑA

Abstract

Sinopsis

Desregulación transcripcional y desacetilación de lisinas en trastornos neurológicos: La enfermedad de Huntington y el síndrome de Rubinstein-Taybi

Los déficits cognitivos y otros síntomas neurológicos asociados con el envejecimiento, las enfermedades neurodegenerativas, la enfermedad de Alzheimer, patologías PolyQ como la enfermedad de Huntington (EH), y ciertos trastornos congénitos que manifiestan discapacidad intelectual, tales como el síndrome de Rubinstein-Taybi (SRT), han sido relacionados con niveles alterados de acetilación de histonas neuronales. Sin embargo, la relación entre cambios transcripcionales y alteraciones epigenéticas en estas dolencias es aún poco claro. En este estudio examinamos la correlación a nivel genómico de los defectos de la acetilación de histonas y los cambios de expresión génica en un modelo de ratón de la EH (HD82Q). Nuestro análisis identificó cientos de loci que presentaron hypoacetilación para las marcas epigenéticas H3K9/14ac and H4K12ac en la cromatina de dichos ratones. Sólo unos pocos de estos genes presentaron niveles de transcripción significativamente alterados y *viceversa.* Sin embargo, dicho grupo de genes aparecen consistentemente afectados en diferentes áreas del cerebro y modelos de ratón, y en tejido de pacientes, lo cual sugiere un papel clave en la etiología de esta patología. De forma general, el rastreo genónico realizado en este estudio demuestra que la desregulación de la acetilación de histonas y la expresión génica se comportan como dos eventos tempranos pero independientes en la patología de la EH. En análisis posteriores, hemos extendido a otros modelos animales y celulares de la EH nuestra observación acerca del impacto limitado de la patología causada por polyQ en cambios globales en la acetilación de histonas. Como en el caso de los ratones HD82Q, encontramos que la desacetilación de histonas no es global sino que se localiza en el sitio de inicio de la transcripción de genes relevantes para el funcionamiento neuronal. Además pudimos detectar que estos cambios locales a veces coinciden con una reducción en la trimetilación de la histona 3 en K4 (H3K4me3), otra modificación epigenética relacionada con genes activos, lo que podría determinar una mayor susceptibilidad de estos loci a la desregulación transcripcional.

En la segunda parte de esta tesis se llevó a cabo la caracterización de la línea de ratón Nes-cre::CBP$^{f/f}$. En estos ratones, la función acetiltransferasa de histonas (KAT) de CBP es eliminada selectivamente de la línea neural. Por ello estos ratones resultan útiles para determinar el papel de CBP en el desarrollo del sistema nervioso y la etiología del SRT que está causado por mutaciones en el gen que codifica dicha proteína en humanos. La falta de CBP en la línea neural da lugar a muerte perinatal y a un defecto severo en el crecimiento de neuritas en cultivos primarios de embriones homocigotos. Ambos fenotipos están asociados a una desacetilación severa de histonas. Con el objetivo de revertir la hypoacetilación de histonas presente en SRT desarrollamos una herramienta genética que consiste en un lentivirus (LV) recombinante que sobre-expresa la actividad KAT de CBP específicamente en neuronas (KAT-LV). Observamos que la herramienta KAT-LV incrementó eficientemente la acetilación de histonas en los cultivos de embriones homocigotos y restableció parcialmente la integridad del árbol dendrítico. Dicha estrategia podría facilitar un nuevo abordaje terapéutico no sólo para el SRT, sino también en otras enfermedades neurológicas asociadas a la desacetilación patológica de histonas neuronales, como la EH.

Abstract

Lysine deacetylation and transcriptional dysregulation in neurological disorders: Huntington's disease and the Rubinstein-Taybi syndrome

Cognitive decline and other neurological symptoms associated with aging, neurodegenerative diseases such as Alzheimer's diseases or poliglutamines (polyQ) diseases (e.g. Huntington's disease (HD)) and congenital intellectual disability disorders (e.g., Rubinstein-Taybi syndrome (RSTS)) have been associated with reduced level of neuronal histone acetylation. Here we investigate the genome-wide correlation of histone acetylation and gene expression defects in a HD mouse model (HD82Q). Our analyses identified hundreds of loci that were hypoacetylated for H3K9/14 and H4K12 in the chromatin of HD82Q) mice. Surprisingly, few genes with altered transcript levels in mutant mice showed significant changes in these acetylation marks and *vice versa*. Genes in this group were consistently affected in different brain areas, mouse models and tissue from patients, which suggests a role in the etiology of this pathology. Overall, our histone acetylation and gene expression screens demonstrate that these phenomena are two early, largely independent, manifestations of polyQ disease. Subsequently, we extended the observation of the limited impact of polyQ pathology in global histone acetylation profiles to other animal and cellular HD models. In the absence of bulk chromatin changes, we documented histone deacetylation events at the transcription start sites (TSS) of relevant genes for neuronal functioning. These local deficits can be associated with an increased susceptibility for transcriptional dysregulation and defective trimethylation of histone H3 at lysine 4 (H3K4me3), another covalent modification of the histone tails related with active transcription that is also altered in HD. Overall, this study provides further insight into the nature and extent of epigenetic dysregulation in HD pathology.

In the second part of this thesis we addressed the role of the CREB-binding protein (CBP), a transcriptional co-activator which mutation is linked to the RSTS. To this end, we generated and characterized a Nes-cre::CBP$^{f/f}$ mouse line. These mice presents the ablation of CBP in neural-derived cells, hence, they are usefull to determine the role of CBP in the development of the nervous system and the etiology of the RSTS). The absence of CBP in neural-derived cells caused perinatal death and severe neuronal growth defects in primary hippocampal cultures. Both

phenotypes were associated with a severe histone hypoacetylation. In order to counteract the reduced histone acetylation observed in RSTS, we have designed and generated recombinant lentiviruses (LV) that overexpress the KAT activity of CBP specifically in neurons (KAT-LV). The KAT-LV vector efficiently reverted histone acetylation deficits and led to a partial recovery of the dendritic tree integrity in primary hippocampal cultures from homozygous embryos. This strategy may represent a novel therapeutic approach not only for RSTS but also for others neurological diseases associated with neuronal histone deacetylation like HD.

Front cover illustration: At the top, it is presented an image of a cultured hippocampal neuron infected with a lentivirus that expresses a mutant huntingtin protein (green) and transfected with DsRed for whole cell labeling (red).

Back cover illustration: A primary hippocampal culture from a control embryo of the Nes-cre::CBP$^{f/f}$ mouse line labeling with the neuronal marker MAP2 (red), the glial cell marker GFAP (green) and the DNA stain DAPI (blue).

A mi viejo, por enviarme, no sé desde donde, rayos de felicidad gigantes.

«Ahora sabemos que olvidar es tan importante como recordar, tal cual lo había anticipado el escritor J.J. Borges en su cuento *Funes el memorioso*, de 1942". Sin memoria o con memoria absoluta, tareas extremadamente simples se vuelven imposibles»

Rodrigo Quian Quiroga

«Eppur Si Muove»

Galileo Galilei

Agradecimientos

No creo tener muchos problemas de expresividad pero esto me cuesta más que la Intro. Aunque se escribe con mucha alegría, es el final. En estos laaargos años quiero agradecerles a muchas personas. Primero al Dr. Ángel Barco por haberme dado la oportunidad de trabajar en su grupo. Por despertar la curiosidad en temas que eran totalmente nuevos para mí. Cuando llegué me sentía como recién llegada de Krypton, ya después me fui afianzando, aunque tampoco terminé como Superman, pese a todo, aprendí mucho, gracias Ángel. En segundo lugar al Dr. Luis Miguel Valor por haberme guiado siempre, en las buenas y malas, ya nos lo hemos dicho todo, como bien dijiste "la confianza da asco". Millón de gracias. Tenés todo el potencial para ser un buen jefe.

También quiero agradecerle a todo mi grupo y primero a ellas: ¡Marilyn, por no decirme nunca que no! Lo valoro mucho, te ayudaré en tu "ristorante" *ad honorem*. A Anna por su sonrisa y optimismo, hemos llegado en el mismo estado al final "con los guantes puestos pero sentadas". A Eva y María, mis primeras amigas europeas, me llevo su amistad para siempre. A Satomi por sus risas locas y lágrimas (aunque más lágrimas que risas). A las más nuevas: Bea (la vasca) por la discusión diaria (muy importante y necesaria para mí) y a Romana por arribar con sus métodos de cultivo salvadores (podría haber sido antes, je!).

A ellos: a José, por intentar dar vuelta los resultados hasta sacar lo mejor de ellos, suerte en esta etapa "dorada". A Román por los innumerables genotipados y seguimos expandiéndonos…no me odies! A Michal por su perseverancia, juntos podemos contra CBP. ¡Hasta la victoria, siempre! A los últimos fichajes del *team*: Alejandro y a Jordi, por transmitir tanta motivación científica, suerte chicos. ¡Se lo merecen!

A los ex-miembros del grupo: al mefistófeles de Manu (por enseñarme un nuevo lenguaje☺), a Sven, a Pierrick (por defenderme de los fantasmas del animalario), J. Viosca, Alexandro, Matías y Gianmarco. Así como también a muchas personas del Instituto: A la Dra. Eloísa Herrera y todo su grupo, en especial a Vero, Santi, Rocío y Gerald por los momentos compartidos en el "rincón de los inmigrantes" (aunque luego fue "invadido por españoles"), y a Yaiza por tener esas "manos de cristal". Al Dr. Eduardo Puelles y Diego Echeverría por sus consejos y a

muchos talentosos postdocs del INA por las charlas enriquecedoras. A Cristina por “iluminarme” en la electroporación, a Giovanna por estar siempre disponible (y viva el café colombiano). A todo mi grupo del “master de excelencia” incluídas mis super-amigas: Isa, Vale y Mariajo.

Y fuera del INA, y de España, quiero agradecer a mis anteriores jefas y codirectoras que me mantuvieron activamente en ciencia: Dra. Rocío Hassan (por su inteligencia descomunal), Dra. Dorothy Crawford *(I'm a huge fan of your books),* Dra. Karen McAuley, Dra. Paola Chabay, Dra. M. Victoria Preciado. También al Dr. Gustavo Stefanoff (por su apoyo incondicional), al Dr. Claudio Bidau y a Flavia, Elina, Pachi, el enano y muchos más que me ayudaron en el camino.

A los grupos: ‘La familia alicantina’, ‘Las brujas’, ‘Y hoy donde tangueamos?’, ‘Chulitas’, ‘Los hermanos Viyegas’, ‘la Antito’, ‘Elda’, ‘Rosa’ y ‘Kakkmaddafakka’, (para algo sirven los grupos de wassap).

A mi familia, chica, pero de las buenas, gracias a vos Ma, Marianita y Marcos, por la energía inmensurable que transmiten. A sus asociados Luján y Pablo, y a sus asociaditos Joaquín, Juliana, Aramei y Jerónimo. A la chicha, por sus tangos vía skype. ¡Sos una grande abu!

A mi tierra y su gente in-cre-í-ble, ya me vuelvo, pongo todas mis fichas en lograr el experimento de hacer “ciencia tercermundista”.

A Nahuel, por todo. Se acabó esta tesis psicológica para los dos. Ahora solo cocinarás 4 días a la semana. ¡Gracias compañero! ¡Te quiero!

Ah, y también a Tim Hunt (por dimitir) y a Isaac B Hilton *et al.* (por mi soñado *paper* estos últimos años).

Index

GENERAL INDEX

Abbreviations and acronyms……..…1-3
INTRODUCTION…….....7-45
1.1 Transcriptional and epigenetic regulation of brain function……....7
1.1.1 Basic principles of transcriptional regulation……....7
1.1.2 Basic principles of epigenetic regulation…….....8
1.1.3 Lysine acetylation and the regulation of gene expression……....10
1.1.4 Relevance of transcriptional and epigenetic mechanisms in the adult brain.....13
1.1.5 Relevance of histone acetylation and transcriptional dysregulation in neurological disorders…….....17
1.2 Huntington's disease…….....19
1.2.1 Historical background…….....19
1.2.2 Huntington's disease pathoetiobiology…….....21
1.2.3 The molecular genetics of Huntington's disease……....23
1.2.4 Role of huntingtin in phisiology and pathobiology…….....24
1.2.5 Transcriptional dysregulation in Huntington's disease……..26
1.2.6 Epigenetic dysregulation in Huntington's disease……..29
1.2.7 Experimental models of Huntington's disease and relevant phenotypes.....32
1.2.8 Epigenetic and transcriptional dysregulation in others polyglutamine diseases.....34
1.3. Rubinstein-Taybi syndrome……....37
1.3.1 Molecular genetics of Rubinstein-Taybi syndrome ……...37
1.3.2 Impaired lysine acetylation and transcriptional dysregulation in Rubinstein-Taybi syndrome…….....37
1.3.3 Experimental models of Rubinstein-Taybi syndrome 39
1.3.4 Developmental and adult component of Rubinstein-Taybi syndrome…….....41
1.4. Epigenetic therapies in Huntington's disease and Rubinstein-Taybi syndrome..43
1.4.1 Pharmacological approaches…….....43
1.4.2 Genetic approaches ……...45

OBJECTIVES…….....49

MATERIALS AND METHODS……..53-71

3.1 Mouse models of neurological diseases…….....53
3.1.1 Mouse models of Huntington's disease…….53
3.1.2 Mouse models of RSTS.....54
3.2 Behavioral procedures.…….54
3.2.1 Morris water maze..……..54
3.2.2 Rotarod.……...55
3.2.3 Grip strength…….....55
3.2.4 Feet clasping……...55
3.3 DNA constructs.……..55
3.4 Cell lines and primary cultures……....60
3.4.1 Established cell lines cultures.....60
3.4.2 Primary dissociated hippocampal culture…….....60
3.4.3 Cell culture infection ……...61
3.4.4 Transient transfection.……...61
3.4.5 Cell death assays……...61
3.5 Lentiviral vectors……....61
3.5.1 Lentivirus production, titration and infection ……...61
3.5.2 Biosafety measures……....63
3.6 *In utero* electroporation protocol……....63
3.7 Immunodetection and Immunoblotting analysis……....63
3.7.1 Antibodies…….....63
3.7.2 Immunocytochemistry and Immunohistochemistry.……...65
3.7.3 Protein extraction and western blot…….....65
3.8 Microscopy and morphometric analysis……....66
3.9 MRI imaging…….....67
3.10 RNA extraction, purification, RT-PCR and qRT-PCR.……....68
3.11 Microarray analysis……....69
3.12 ChIP assays and ChIPseq analyses……....70
3.13 Functional genomics analyses……...70

RESULTS…….....75-116
4.1 Genomic landscape of transcriptional and epigenetic dysregulation in early onset polyglutamine disease.....75
4.1.1 Summary.....75

4.1.2 Reprint: The Journal of Neuroscience, June 19, 201333(25): 10471–10482 ...76
4.2 Deacetylation of histone H3 in Huntington's disease is locus-specific.....77
4.2.1 Bulk histone acetylation levels are preserved in several animal models of HD.....77
4.2.2 Bulk histone acetylation levels are also preserved in cellular models of HD.....82
4.2.3 Other epigenetic marks are unaffected at the bulk level in polyQ pathology....85
4.2.4 Histone H3 acetylation is perturbed at specific neuronal loci.....86
4.2.5 Deficits in acetylation and trimethylation of histone H3 concur at relevant neuronal loci……..88
4.2.6 Discussion: H3 deacetylation and demethylation in HD.....90
4.3 CBP deficiency and impaired lysine acetylation in neural-derived cells cause....93
perinatal death and severe neuronal growth defects in primary hippocampal cultures
4.3.1 Characterization of Nes-cre::CBPf/f mice……...93
4.3.2 Severe neuronal growth defects of primary cultures from Nes-cre::CBPf/f mice.....96
4.4 KAT-expressing viral vector as a potential therapeutic tool to reverse neurological deficits associated with impaired lysine acetylation.....100
4.4.1 Generation and characterization of a KAT-expressing viral vector.....100
4.4.2 KAT-overexpression causes an increase in the number of synaptic protrusions in hippocampal neurons.....111
4.4.3 The genetic reversal of lysine acetylation deficits ameliorates the neuronal growth defects ……113
4.4.4 Discussion: KAT-LV as a potential therapeutic tool in neuropathologies.....114

GENERAL DISCUSSION……119-121
5.1 The link between histone acetylation and transcription: an open debate.....119
5.2 Future perspectives…….....120

CONCLUSIONS……..125-126

BIBLIOGRAPHY……...129-143

ANNEX: Published review during the thesis period.....147

FIGURE INDEX

Figure 1. KAT and HDAC activities……11
Figure 2. Mechanisms that regulate activity-dependent transcription of Fos.....17
Figure 3. Original paper published as: "On Chorea," by George Huntington……..20
Figure 4. The cortico-striatal system.……22
Figure 5. Scheme of the human huntingtin protein ……26
Figure 6. Transcriptional dysregulation in Huntington's disease.....29
Figure 7. Summary of the disrupted epigenetic mechanisms in HD and the ameliorative strategies tested……..32
Figure 8. PolyQ disease affects chromatin modification and usage…….36
Figure 9. Structure of KAT3 proteins: CBP and p300 ……38
Figure 10. mHTT fusion protein cloning strategy ……...57
Figure 11. KAT domain cloning strategy.……..58
Figure 12. R6/1 mice show motor, cognitive and transcriptional deficits but preserved bulk histone acetylation levels. …….....78
Figure 13. YAC128 mice also show HD molecular and phenotypic traits but preserved bulk histone acetylation levels. …….....80
Figure 14. mHTT-electroprated mice show preserved bulk histone acetylation levels.....81
Figure 15. mHTT-infected neurons show preserved bulk histone acetylation levels.83
Figure 16. Stably HTT-expressing PC12 cells show preserved bulk histone acetylation levels. …….....84
Figure 17. Other bulk histone modifications are also preserved in HD hippocampus.....85
Figure 18. Histone H3 deacetylation is altered at specific neuronal loci.....87-88
Figure 19. Promoters with H3 deacetylation can be also demethylated at histone H3 lysine 4…….....89
Figure 20. General characterization of Nes-cre::CBP$^{f/f}$ mouse line……....93-94
Figure 21. MRI images from sagital head and coronal head…….94
Figure 22. Three-dimensional reconstruction of MR images.....……95-96
Figure 23. NeuN and GFAP staining in Nes-cre::CBP$^{f/f}$ ……..96-97
Figure 24. Nes-cre::CBP$^{f/f}$ mice show acetylation deficits in the four-nucleosome histones……...98
Figure 25. Nes-cre::CBP$^{f/f}$ mice show acetylation abnormal neuronal morphology...99

Figure 26. KAT-LV tool design……100
Figure 27. Selective infection of pSyn-NLS-KAT-GFP in neurons……101
Figure 28. Experimental design and timing for KAT-overexpression experiments..102
Figure 29. Representative images of hippocampal neurons under different conditions……..103
Figure 30. pSyn-NLS-KAT-GFP induce hyperacetylation selectively in neurons….....105-106
Figure 31. pSyn-NLS-KAT-GFP increase acetylation of the four-nucleosome histones…….107
Figure 32. pSyn-NLS-KAT-GFP increase the acetylation of NF-κB and p53 TFs….....108-109
Figure 33. pCAG-NLS-KAT-GFP increase histone acetylation in an *in vivo* system.....110
Figure 34. pSyn-NLS-KAT-GFP increase the number of filopodia like-spines.112-113
Figure 35. pSyn-NLS-KAT-GFP can restore hypoacetylation and the altered MAP2 expression pattern in Nes-cre::CBP$^{f/f}$ mice …….....114

TABLE INDEX

Table 1. Summary of known acetyltransferases and deacetylases enzymes and representative substrates.....12
Table 2. Summary of the cellular and animal HD models used in this work.……..33
Table 3. Neurological traits in mouse strains with deficient CBP activity.……....40
Table 4. Cloning primers…….....59
Table 5. Plasmids used in this work……...59
Table 6. Antibodies used in this study……..64
Table 7. RT-qPCR primers ……....68

Abbreviations

aa	amino acid
AD	Alzheimer disease
ADTF	Activity-dependent transcription factor
ALS	Amyotrophic lateral sclerosis
AR	Androgen receptor
BD	Bromodomain
BDNF	Brain-derived neurotrophic factor
CBP	CREB binding protein
Chip	Chromatin immunoprecipitation
Chip-seq	Chromatin immunoprecipitation sequencing
CoREST	REST corepressor 1
CRE	cAMP Response Element
CREB	cAMP response element binding protein
CRTC2	CREB-regulated transcription coactivator 2
CTF	Constitutive transcription factors
CH	Cysteine/histidine-rich regions
cyt-mHtt	Cytoplasmic mutant huntingtin
DAB	3,3'-Diaminobenzidine substrate
DAPI	4´,6-diamidino-2-phenylindole
DRPLA	Dentatorubral pallidoluysian atrophy
DG	Dentate gyrus
DINF	Days after infection
DIV	Days in vitro
DMEM	Dubelcco's modified eagle medium
DMSO	Dimethylsulfoxide
DNMT	DNA methyltransferase
EE	Environmental enrichment
eIF3k	elongation factor 3
EGR	Early growth response
FC	Fear conditioning
FOS	FBJ murine osteosarcoma viral oncogene homolog
GABA	γ-Aminobutyric acid
GFAP	Glial fibrillary acidic protein
GFP	Green fluorescent protein
GO	Gene ontology
GOF	Gain-of-function
GTF	General transcription factors
H	Histone
HAP1	Huntingtin-associated protein-1
HD	Huntington disease
HDAC	Histone deacetylases
HDACi	Histone deacethylases inhibitors
HIP1	Huntingtin-interacting protein 1
HP	Hidden platform
Htt	Huntingtin
IC	Immunocytochemistry
IDDs	Intellectual disability disorders
IEG	Immediate early genes
IHC	Immunohistochemistry
Inr	Initiator

IGF	Insulin-like growth factor
ITF	Inducible transcription factors
Jun	Jun proto-oncogene
K	Lysine
KAT	Histone acetyl transferases
kDa	Kilodalton
KO	Knock out
KREs	Krox response elements
LDH	Lactate dehydrogenase
L-LTP	Late LTP
LOF	Loss-of-function
LTD	Long-term depression
LTP	Long- term potentiation
LV	Lentiviruses
MAP2	Microtubule-associated protein 2
MAPK	Mitogen- activated protein kinases
me	Methylation
MeCP2	Methyl-CpG binding protein 2
MEFs	Mouse embryonic fibroblasts
MEF2	Myocyte enhancer factor 2
mHtt	mutant Huntingtin
miRNA	microRNA
mRNA	messenger RNA
MSK-1	Mitogen- and stress-activated protein kinase 1
MSN	Medium spiny neurons
NCoR	Nuclear corepressor
ncRNA	non-coding RNA
NGS	Next-generation sequencing
Nf-κB	Nuclear Factor kappa-light-chain enhancer of activated B cells
NLS	Nuclear localization signal
NMDA	N-methyl-D-aspartate
NMDAR	NMDA receptor
NRSE	Neuron restrictive silencing element
nuc-mHtt	nuclear mutant Huntingtin
O/N	Over night
P	Proline
PBS	Phosphate buffer saline
PcG	Polycomb-group complex
p53	Tumor suppressor protein
PFA	Paraformaldehyde
PP2A	PR65/A subunit of protein phosphatase 2A
polyQ	Polyglutamine
PSD95	Postsynaptic density 95
PTMs	Post-translational modifications
Q	Glutamine
RT-qPCR	quantitative reverse transcription polymerase chain reaction
R	Arginine
REST	Repressor element 1-silencing transcription factor
RNApolII	RNA polymerase II
RORα	Retinoid acid receptor-related orphan receptor alpha

RSTS	Rubinstein-Taybi syndrome
RT	Room temperature
SAHA	Suberoylanilide hydroxamic acid
SB	Sodium butyrate
SBMA	Spinal and bulbar muscular atrophy
SCA	Spino cerebellar ataxia
Ser	Serine
SP1	Specificity protein 1
SRE	Serum response element
SRF	Serum response factor
TBP	TATA-binding protein
TFs	Transcription factors
TFBS	Transcription factor binding site
Tip60	Tat-interactive protein 60 kDa
TOR	Target of rapamycin
TQ	Target quadrant
TSA	Trichostatin A
TSS	Transcription star site
Ub	Ubiquitylation
UPS	Ubiquitine proteasome system
VP	Visible platform
VSV-G	Vesicular stomatitis virus G
WB	Western blot
WPRE	Woodchuck hepatitis virus posttranscriptional regulatory element
YAC	Yeast artificial chromosome

Introduction

1. Transcriptional and epigenetic regulation of brain function

1.1.1 Basic principles of transcriptional regulation

Mechanisms of transcription and translation take the information encoded in the DNA to synthesize proteins via an RNA intermediate. Transcription is the first step in which a particular segment of DNA is copied into RNA by the enzymes RNA polymerases. In particular, RNA polymerase II (RNApol II) forms a protein complex for the expression of messenger RNA (mRNA) to copy coding genes and a majority of non-coding RNAs such as small nuclear RNAs, small nucleolar RNAs and miRNA (Porrua and Libri, 2015).

Transcription proceeds through multiple stages: preinitiation, initiation, elongation and termination. A key controlling point for transcription is the initiation, in which *trans*-acting proteins (the so-called transcription factor, TFs) bind to the *cis*-acting elements that are present in the DNA. The interaction with evolutionarily conserved proteins called general transcription factors (GTF) are required for RNApol II recruitment and activity (Goodrich and Tjian, 1994) at the core promoter. The core promoter, generally defined as the minimal stretch of DNA that is sufficient to direct the accurate initiation of transcription by RNApol II (Kadonaga, 2012), can include several DNA elements, such as the TATA box, recognized by the GTF TFIID (Lifton et al., 1978), the transcription start site (TSS, the location where transcription starts at the 5'-end of a gene sequence) (Orphanides and Reinberg, 2002), the Initiator (Zajac et al. 2010; Smale and Baltimore, 1989), the BRE motif (TFIIB recognition element) (Lagrange et al., 1998), among others, although no universal core promoter element exists. In addition to the core promoter, other *cis*-acting DNA sequences can also regulate RNApoll II transcription, such as the proximal promoter (the region immediately upstream (up to a few hundred base pairs) from the core promoter, which are bound by sequence-specific factors, enhancers, silencers, and boundary/insulator elements (Bondarenko et al., 2003, Kadonaga, 2004).

Overall, TFs can cooperate in activating or suppressing gene expression by interacting with *cis*-acting elements and GTF/RNA pol II, as a result of the cellular circumstances, general activity in the nucleus, spatial organization (Bergqvist and Rice, 2001), their affinity for the DNA binding sites, interaction/recruitment events, etc (Herdegen and Leah, 1998). TFs can also have a role in transcriptional elongation and termination in gene regulation. Therefore, these factors bind specific sites on the

DNA at both the promoter and distal positions (even 1 Mb away). In general terms, prior to binding, members of the same family recognize variations of specific sequences; for instance, the CREB family members bind to cAMP Response Element (CRE) (Mayr and Montminy, 2001), SRF to SRF Response Elements (SRE) (Norman et al., 1988), Zn-finger proteins to the highly GC-rich sequences of KREs ("Krox Response Elements" by EGR members), GC-boxes (by Sp members), etc (Poirier et al., 2007). In the case of distal positions, TFs interacts with enhancer regions that modify the promoter activity but are not effective alone. Thus, distant enhancer sites can be positioned by bending and distorting the DNA close to the basal machinery already located at the initiation site.

1.1.2 Basic principles of epigenetic regulation

In 1942, Conrad Waddington coined the term "epigenetic" to describe how the genetic information in a 'genotype' manifests itself as a set of characteristics, or 'phenotype' (Waddington, 2012) (reprinted). The concept continues evolving and *"epigenetics"* has become a common word in modern biology without a satisfactory consensual definition into the broader scientific society (Jablonka and Lamb, 2002). Currently, the term 'epigenetic regulation' refers to the presence of dynamic chemical markers in genes that do not involve a change in the DNA sequence (Rountree et al., 2001; Baylin, 2005; Feinberg et al., 2006) but contribute to define how genetic information is expressed. Thus, every cell in a human body containing exactly the same genetic material can behave in different ways. Another well-known example of epigenetic variety comes from monozygotic twin studies where the discordance rates for common diseases have revealed the existence of epigenetic differences that diverge as they become older, despite been considered genetically identical (Fraga et al., 2005).

Epigenetic mechanisms can be classified as follows:

- DNA covalent modification: e.g., methylation and hydroxymethylation of cytosines (Guibert and Weber, 2013).
- Post-translational modifications (PTM) of histone proteins: e.g., acetylation (Ac), methylation (me), phosphorylation (S), ubiquitylation (Ub), SUMOylation, ADP ribosylation (Kouzarides, 2007).
- Exchange of histone variants (e.g., H1; H3.3; H2A.Z, H2A.X; macroH2A) (Soria et al., 2012).

- Chromating remodeling and 3D organization.
- An additional layer of epigenetic regulation is certain non-coding RNA species (ncRNA), such as piwiRNAs, which play an important role organizing the chromatin architecture by recruiting the chromatin modifying machinery (Esteller, 2011, Gomes et al., 2013).

Epigenetic mechanisms are associated with compaction degree and stability of the chromatin and chromosomal functional partitioning. Chromatin is a densely packed nucleoprotein complex composed by DNA, proteins and RNA. The repeating core subunit of chromatin is the nucleosome (147 bp of DNA wrapped around the histone octamer complex (two dimers of each histone protein H2A, H2B, H3 and H4)) (Kornberg, 1977, McGhee and Felsenfeld, 1980). Therefore the nucleosome structure has an impact in transcription. In the case of histone PTMs, some of them are associated with transcriptional activation while others are associated with transcriptional repression. Specifically, active genes are marked by tri-methylation on lysine 4 of histone H3 (H3K4me3) (Heintzman et al., 2007) and the acetylation of histones is, in general, related with transcriptionally active genes. However, histone methylation (me) can serve as both an activator and repressor of transcription, depending on the residue being modified and the degree of modification (i.e. mono-, di(me2)-, or tri(me3)-methylation). The best studied repressive histone modifications are the methylation of lysines 9 and 27 of histone H3 (H3K9me2/3 and H3K27me3) (Choukrallah and Matthias, 2014). In contrast H3K4/36/79me is higher in the transcribed region than at the promoter, suggesting a link with transcription elongation stage (Gerber and Shilatifard, 2003). In general, acetylation of histones is related with transcriptionally active genes whereas DNA methylation establishes a silent chromatin state.

Epigenetic modifications are mediated both by general and tissue-specific cofactors with enzymatic activity (acetylases, deacetylases, kinases, phosphotases, methylases and demethylases), whose interaction with TFs contribute to determine the extent to which genes are expressed (Zaidi et al., 2005). As an example, we can mention the Polycomb-group complexes (PcG) that play essential roles in the epigenetic regulation of gene expression during development. One of these complexes is the PRC1, which includes the E3 ubiquitin ligase responsible for the monoubiquitylation of H2A at K119 and has been linked to the silencing of developmental genes. Albeit, another event is involved, the H3K27 trimethylation by

the PRC2 complex is a prerequisite for the chromatin association of PRC1. In contrast, the monoubiquitylation of H2B at K120 is associated with gene activation. One main function of monoubiquitylated H2B is the regulation of other histone modifications, that is, the modification of H3K4 and H3K79 by histone methyltransferases (Braun and Madhani, 2012, Cao and Yan, 2012). Another example is the SWI/SNF-family complexes, which are large chromatin-remodeling proteins that physically alter nucleosome positioning using energy generated by ATP hydrolysis, providing an appropriate nucleosome location and density at a large number of genes (Kasten et al., 2011).

A fundamental role for epigenetic mechanisms has been described during development and cellular differentiation, contributing to generate an environment that allows cell type-specific gene expression underlying cellular identity (Bonasio et al., 2010). Nonetheless epigenetic mechanisms in the control of both normal cellular processes and abnormal events in disease have gained a relevant attention over the past decade. Moreover, as we will see in the particular case of the nervous system, epigenetic can also play a relevant role in both physiological and pathological processes in adulthood.

1.1.3 Lysine acetylation and the regulation of gene expression

Among the multiple histone PTMs, the acetylation of lysines (K) at their N-terminus is the most studied in the context of cognition and neuropathology. Histone (or lysine) acetyltransferases (HAT/KAT) and histone deacetylases (HDAC) (Valor et al., 2013b) catalyze the acetylation and deacetylation of histone proteins at K residues, respectively (**Fig. 1**) (Valor et al., 2013b). The interplay between KATs and HDACs alters the net balance of histone acetylation levels, thereby promoting changes in the chromatin structure. In general, an increase in protein acetylation by the addition of an acetyl group to K residues located at the histone-tails neutralizes the basic charge of this residues and weaken the contact between histones and DNA, which causes the relaxation of the chromatin, thus facilitating or enabling the access of transcription factor to the gene promoter and allowing gene expression. HDACs often function as a component of transcriptional repressor complexes to silence gene expression and induce chromatin compaction through histone protein deacetylation. However, the proposed causal flow histone acetylation → chromatin relaxation → gene activation is not clear (Chuang et al., 2009). Correlation is not sufficient for the establishment of

causality (Lopez-Atalaya and Barco, 2014), genomic data indicates that the real situation *in vivo* is more complex than previously envisaged (see section 1.1.4 and 1.1.5) and active genes contain both KAT and HDAC activities at the same time (Wang et al., 2009b). This is especially relevant for poised genes (inactive but ready for transcription), as the balance between both enzymatic reactions determines future gene activation or inactivation. In addition, an important aspect to have into consideration is that KAT and HDAC enzymes also target non-histone substrates (Choudhary et al., 2009, Gaub et al., 2010) such as transcription and chromatin remodeling factors and regulatory subunits of the RNApol II complex (See **Table 1** for the description of the different KAT/HDACs enzymes and their targets) that can contribute to transcriptional processes (Fischle et al., 2002, Sterner et al., 2002, Lahm et al., 2007, Bedford and Brindle, 2012, Sun et al., 2013).

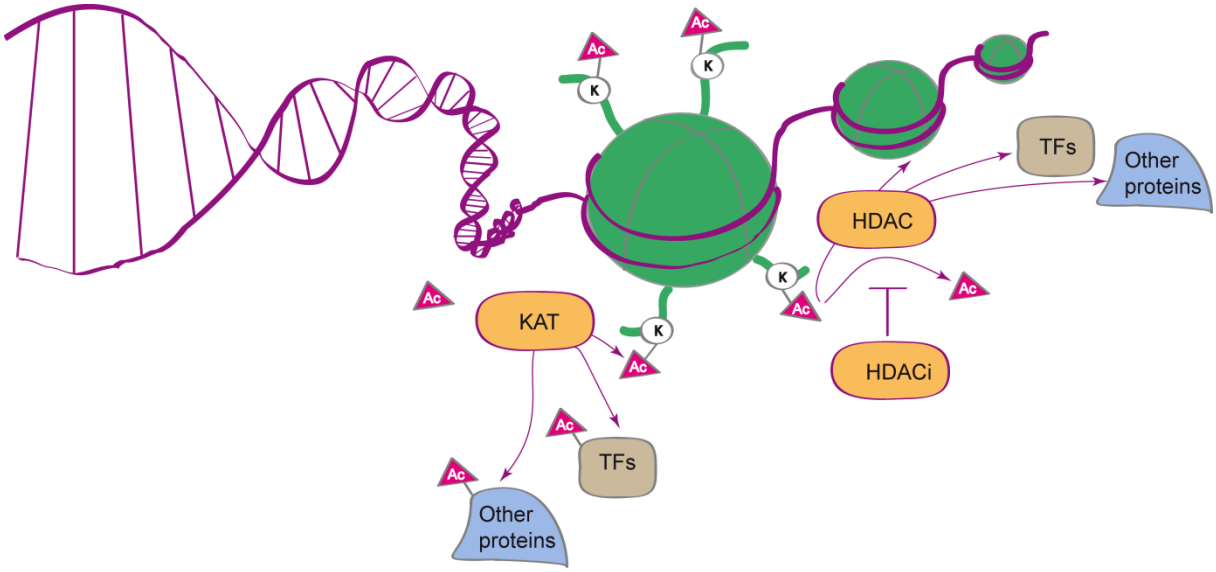

Figure 1. KAT and HDAC activities. The illustration shows the dynamic state of histone acetylation/deacetylation cycle regulated by KAT and HDAC activities. Transcription factors and others proteins also are substrates of KAT and HDAC enzymes. HDACi binds to HDAC and inhibits its function. KAT, histone acetyl transferase; HDAC, histone deacetylases; HDACi, histone deacethylases inhibitors; Ac, acetylation; TFs, transcription factors. Adapted from Lopez-Atalaya and Barco, 2014.

Table 1. Summary of known acetyltransferases and deacetylases enzymes and representative substrates

Name	*Enzyme*	*Substrates specificity*	*Reference*
KAT3 A/B	CBP/p300	H2AK5, H2B (K5, 12, 15, 20), H3 (K9, 14, 18, 27), H4 (K5,8)	Valor et al. Tie et al. Selvi et al.
		CREB	Lundblad et al.
		RNApol II complex (TFIIEbK52 and TFIIF)	Imhof et al.
		p53	Gu et al.
		Nf-κB	Romano et al.
		pRb	Chan et al.
		others TFs	Yeh et al. Boyes et al.
KAT2B	PCAF	H3K9/14	Love et al.
KAT5	Tip60	H4, H2A, H3	
KAT13B	ACTR	H3, H4	
Class I HDAC (Zn-dependent)	HDAC1	All core, p53	
	HDAC2		Turner et al.
	HDAC3	All core	
	HDAC8		
Class II HDAC (Zn-dependent)	HDAC4	MEF2A	Zhao et al.
	HDAC5	GCM1	Chang et al.
	HDAC6	H4K5,8	Marks et al.
		Tubulin	Hubert et al.
	HDAC7		
	HDAC9		
	HDAC10		
Class III HDAC (NAD+-dependent)	Sirt1	MEF2A	Zhao et al.
		FOXO proteins	Saunders et al.
		E2F1	Wang et al.
		p53	Saunders et al.
	Sirt2	p53	Langley et al.
		H3K9/14 and H4K16	Imai et al.
		H3K56	Xu et al.
		tubulin	Saunders et al.
	Sirt3		
	Sirt4		
	Sirt5		
	Sirt6		
	Sirt7		
Class IV HDAC (Zn-dependent)	HDAC11		Gao et al.

All core: histones H2A, H2B, H3 and H4.

1.1.4 Relevance of transcriptional and epigenetic mechanisms in the adult brain

A considerable amount of literature has vastly described the link between neurons and their response to external environment. One of the consequence of neuron-stimuli connection is the induction of the transcription of activity-responsive genes and the expression of synaptic effectors at the nuclear level (Loebrich and Nedivi, 2009).

The effects of sensory experience are manifested by the release of neurotransmitter at excitatory synapses. For instance, the primary neurotransmitter in vertebrates (glutamate) is released from the presynaptic terminal and binds to its receptors (NMDAR and AMPAR) on the postsynaptic neuron. As a result, the postsynaptic cell membrane depolarizes (as the Na^+ and K^+ ions enter the cell via AMPAR) leading to an activation of channels (NMDAR and VGCC) followed by a primary influx of calcium into the cytoplasm as a principal activator of a program of gene expression in the nucleus (Greenberg et al., 1986, Sheng and Greenberg, 1990, Zhang et al., 2007). Recently, a mechanism describing the functional connection between presynapse sites and neuronal gene expression has been also reported (Ivanova et al., 2015, Kravchick and Jordan, 2015).

Neuronal responses to stimuli can be classified as early and late responses at the level of transcription. The early response occurs rapidly after stimulation and lasts from milliseconds to minutes. This “first wave of gene expression” is represented by the so-called immediate early genes (IEG), which encode TFs, secreted and synaptic proteins, intracellular signaling molecules and enzymes (Herdegen and Leah, 1998, Loebrich and Nedivi, 2009). IEG definition refers to their rapid and transient induction, which occurs in the absence of *de novo* protein synthesis making possible to track neurons that have been recently activated. Greenberg and co-workers in 1985 were the first in demonstrate the importance of stimulus-dependent regulation of IEG transcription in neuronal cells. They observed that the nerve growth factor and epidermal growth factor (EGF) induced Fos transcription in the neuroendocrine cell line PC12 (Ghosh and Greenberg, 1995). These initial findings opened many subsequent studies that established activation of signaling pathways by second messengers, such as calcium, as a central mechanism for synaptic activity-regulated transcription in neurons (Ebert and Greenberg, 2013). Conversely, the late response lasts from hours to days. This “second wave of gene expression” is thought to be prominently controled by the TFs generated in the primary response. Overall, both

the first and second transcriptional responses provide effectors molecules implicated in functional or structural synaptic remodeling that may help in strengthen or weaken the synaptic connections (Kandel, 2001).

Depending on their basal expression level, two classes of TFs can be distinguished "constitutive" and "inducible" (i.e., CTF and ITF). CTFs are constitutively expressed but only become activated upon cellular stimulation. In neurons, CTFs include cyclic adenosine monophosphate (cAMP) Response Element Binding Protein (CREB) and members of the Activating Transcription Factor (ATF) family, as well as Serum Response Element (SRF), Myocyte Enhancer Factor 2 (MEF2), and Nuclear Factor kappa-light-chain enhancer of activated B cells (NF-κB). ITFs are not expressed under basal conditions and they are downstream of CTF. ITF, are represented by members of FOS (FBJ murine osteosarcoma viral oncogene homolog), JUN (proto-oncogene) and EGR (Early Growth Response) families. Both CTF and ITFs can be classified as "activity-dependent TFs" (ADTF), as their activation and/or expression are regulated by activity (Flavell and Greenberg, 2008).

In addition, the covalent modification of the chromatin can also be regulated by neuronal activity. Many of the enzymes responsible for PTMs of histones are modulated by upstream activity-dependent signaling cascade (**Fig. 2**) (Roh et al., 2005, West and Greenberg, 2011). As an illustrative example, the Mitogen- and Stress-activated protein Kinase 1 (MSK-1) (a nuclear protein kinase activated downstream of the MAPK/ERK signaling pathway) induce transient serine (Ser) 10 H3 phosphorylation which has been related to transcriptional activation of IEGs (Nowak and Corces, 2000) via the EGF-signaling pathway (Mahadevan et al. 1991), playing a key role in neuronal plasticity (Mahadevan et al., 1991, Crosio et al., 2003). Moreover, the phosphorylation of Ser10 in H3 is functionally linked to both the repression of methylation at K9 and the acetylation at K14 (Cheung et al., 2000; Fischle et al., 2005; Lo et al. 2000). MSK-1 also has a dual role in gene regulation given that it can phosphorylate the TF CREB at Ser133 (Deak et al., 1998).

Overall, transcriptional and epigenetic mechanisms may subserve modulation of different forms of plasticity like:

- Synaptic plasticity → the capacity of synapses to strengthen or weaken in response to activity. In particular, two forms of synaptic plasticity, namely Long-Term Potentiation (LTP) and Long-Term Depression (LTD) have been widely used as cellular "analogues of memory". Transcription is a hallmark for

long but not short-term synaptic plasticity. A reasonable number of cognitive-associated genes are epigenetically modified in response to experience, such as *Bdnf, Reln, Egr1, PP1, Arc* and *Caln* (Day and Sweatt, 2011). There are increasing evidence implicating both DNA methylation and histone PTMs that shape the epigenetic state of chromatin in the nervous system in response to induction of plasticity and formation of memory. Specifically, the co-occurrence of acetylation at H3K9/14, H4K5/8, and H4K12 after fear conditioning in young mice have been associated with hippocampal transcriptional changes in hundreds of genes (Peleg et al., 2010). In contrast, aged mice exposed to the fear conditioning show low acetylation levels at H4K12 and very modest changes in gene expression in concomitance with learning deficits. Like histone modifications, DNA methylation has been also implicated in learning and long term memory processes (Day and Sweatt, 2011). The first indications that DNA methylation may play a role in cognition came from Miller and Sweatt (2007) who showed that contextual fear conditioning caused the upregulation of different subtypes of DNA methyltransferase enzymes (DNMT) gene expression in the adult rat hippocampus. This upregulation was associated with rapid methylation and downregulation of the memory suppressor gene PP1 and demethylation and upregulation of the synaptic plasticity gene reelin, indicating that enzymatic activities, methyltransferase and demethylase, act during consolidation (Miller and Sweatt, 2007, Rudenko and Tsai, 2014). It is also important to indicate that the same epigenetic mark occuring at different genomic sites (TFs binding sites, TSS, etc) or in different context (cell type, brain structure, etc) migh cause different effects on gene transcription.

- Intrinsic plasticity → this particular form of plasticity can significantly affect the input-output relationship of neuronal networks (e.g., the modulation of voltage- and calcium-gated ion channels to regulate synaptic integration and action potential generation) (Sehgal et al., 2013). There is growing evidence from the pain and epilepsy fields demonstrating that epigenetic mechanisms underlie neuronal hyperexcitability in these disease states (Beck and Yaari, 2008). For example, the Repressor Element 1-Silencing Transcription factor (Carninci et al., 2006) has been involved in the control of fundamental transcription programs that drive circuit excitability, seizures and epilepsy. REST enables

many histone modifications on its Neuron Restrictive Silencing Element (NRSE)-containing target genes by recruiting lysine-modifying enzymes via multiple corepressors such as the histone deacetylase complex subunit (Sin3a), the transcriptional repressor Methyl-CpG binding Protein 2 (MeCP2) and the REST corepressor 1 (CoREST). It has been shown in animal models of neuropathic pain, the downregulation of genes encoding for sodium channel and potassium channel. These decreased transcript levels were associated with enhanced binding of REST and hypoacetylation of histone H3 and H4 at NRSEs in the promoter regions of these genes (Uchida et al., 2010).

- Synaptic scaling → this is a cell-autonomous form of homeostatic plasticity to compensate excessive excitation or inhibition of neuronal activity, both from membrane-to-synapse and from synapse-to-membrane. The most commonly studied form of homeostatic plasticity is mediated by AMPA (α-Amino-3-hydroxy-5-methyl-4-isoxazolepropionic acid) receptors, which consists on a cell-wide multiplicative increase in the quantal amplitudes of spontaneous AMPAergic currents after chronic reductions in AMPAergic transmission (Fong et al., 2015).

For additional information see the review (Guzman-Karlsson et al., 2014).

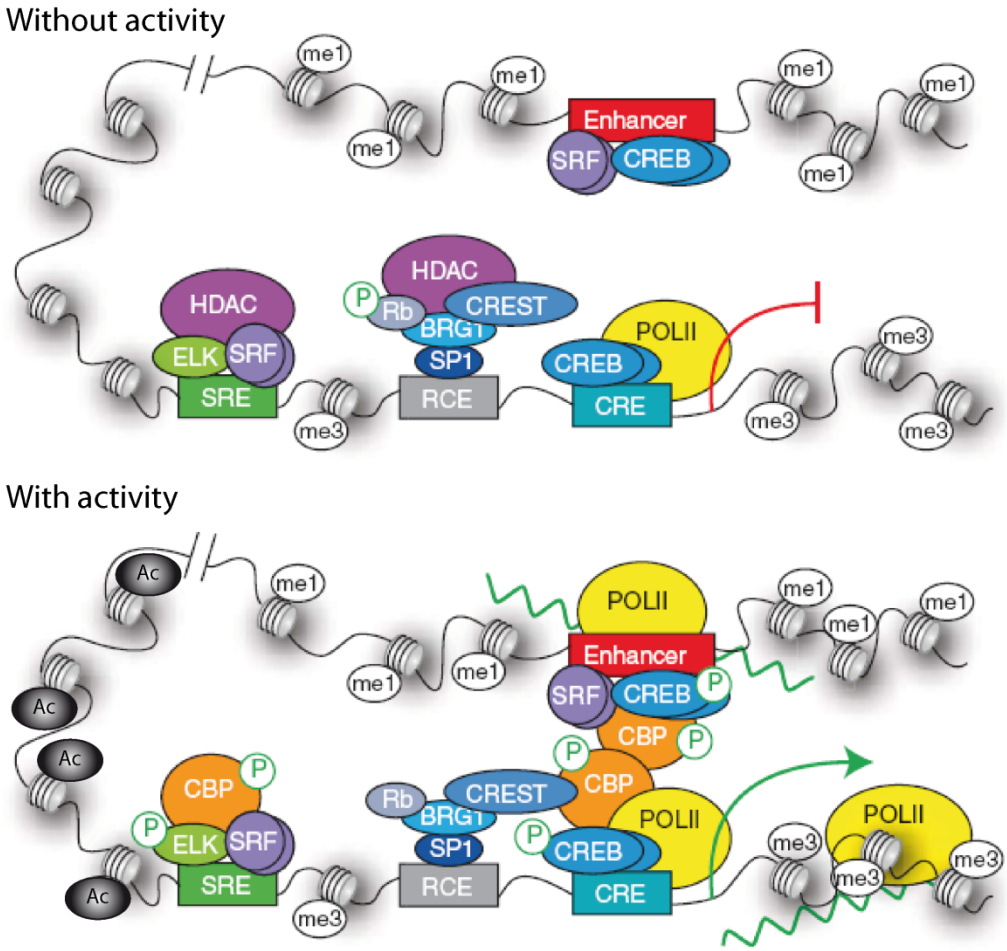

Figure 2. Mechanisms that regulate activity-dependent transcription of Fos. The top panel shows a repressed state of Fos in absence of activity. Without activity, HDAC is recruited by Elk-1 and the Retinoblastoma (Rb)-BRG1-CREST complex. RNA polymerase II (POLII) is also located at the promoter, which has the presence of H3K4me3 at promoter histones. The bottom panel shows Fos transcription after activation of calcium-dependent signaling pathways. CBP is recruited to phosphorylated CREB, inducing local histone acetylation whereas Rb is desphosporilated and releases the HDAC. POLII and CBP are also recruited to H3K4m1 enhancer regions that are prebound by SRF and CREB. The enhancer and the Fos promoter interact through long distance looping inducing transcription of Fos mRNA and of eRNAs (green lines). Ac, acetylation; me1, monomethylation; me3, trimethylation; P, phosphorylation. Adapted from West and Greenberg, 2011.

1.1.5 Relevance of histones acetylation and transcriptional dysregulation in neurological disorders

The complexity in the functioning of the nervous system relies on multiple cellular and molecular processes that are intimately connected. As commented in the section 1.1.4, epigenetic modifications are critical for basic cellular processes such as synaptic plasticity, and for complex cognitive behaviors such as learning and memory. It has been proposed that alteration in the level of neuronal lysine acetylation in the brain may underlie cognitive decline and other neurological

symptoms associated with aging, neurodegenerative diseases, etc (i.e, Huntington's and Alzheimer's diseases (AD).

In general, we can observe three different lines of evidence (Lopez-Atalaya and Barco, 2014) that support a role for aberrant lysine acetylation in pathological conditions in the brain:

(i) Genetic evidence, in which mutations in histone- modifying enzymes, including activities that regulate the acetylation of histone tails, are found in patients with cognitive impairment. An example of this scenario is the mutations in epigenetic genes linked to intellectual disability disorders (IDDs) i.e.: Rubinstein-Taybi syndrome (RSTS) (Padfield et al., 1968; Petrij et al., 1995; Graff and Tsai, 2013), see section 1.3 for more detail.

(ii) Pharmacological evidence, which emanate from the beneficial effect of inhibitors of histone deacethylase (HDACi) and small KAT activator molecules in multiples models of cognitive disorders. These compounds also improve memory in wild type animals (Fischer et al., 2010).

(iii) Correlative evidence, in which different conditions like aging, Huntington's or AD exhibit neuronal histone hypoacetylation associated with gene expression defects. However, the consequential or causal relationship between transcriptional and acetylation alterations remain under discussion (Govindarajan et al., 2011; Peixoto and Abel, 2013; Valor et al., 2013a).

In spite of histone hypoacetylation being the most frequently observed change in neurological diseases others PTMs also have a relevant impact in neurological disorders. For example, histone phosphorylation alterations are typical in AD and epilepsy, and H3K9 hypertrimethylation has been described in both HD (Urdinguio et al., 2009) and Friedreich's ataxia (Al-Mahdawi et al., 2008). Moreover, the IDDs caused by mutations in genes that encode proteins involved in epigenetics regulation of gene expression form a long list (Kleefstra et al., 2014). To cite some examples, the Kleefstra syndrome is caused by the loss of EHMT1, a gene that encodes for euchromatic histone methyltransferase and catalyzes mono- and dimethylation of histone H3K9, leading to derepression of non-neuronal genes in adult neurons and resulting in defects in learning, motivation, and environmental adaptation (Schaefer

et al. 2009; Parkel et al., 2013). Also, the histone demethylase PHF8 has been involved in X-linked mental retardation (Kleine-Kohlbrecher et al., 2010).

Epigenetic and transcriptional dysregulation can be early manifestations of particular psychiatric or neurodegenerative diseases, which may provide a powerful means for pharmacological treatments. For example, a study conducted in HD blood samples identified a panel subset of up-regulated mRNAs that was able to discriminate controls, presymptomatic individuals carrying the HD mutation, and symptomatic HD patients. In addition, these transcripts were also alered in postmortem HD caudate, indicating that these mRNAs could be good candidates as biomarkers, useful in monitoring the progression of HD in blood (Borovecki et al., 2005). Another example for potential use in early diagnosis comes from gene expression profile in fibroblasts from different individuals of three familial AD. In this case, the mutation carriers share a common gene expression profile significantly different from that of their wildtype siblings. The results indicate that the disease process starts several decades before the onset of cognitive decline, suggesting that presymptomatic diagnosis of AD and other progressive cognitive disorders may be quite worthy (Nagasaka et al., 2005).

In the next section, I will introduce in greater detail two disorders, Huntington's disease, as an example of neurodegenerative disease, and RSTS, as an example of intellectual disability disorders, that have provided relevant clues for understanding the interplay between transcriptional dsyregulation and histone deacetylation in neuropathology.

1.2 Huntington´s Disease

1.2.1 Historical background

The first description of HD was provided in 1872 by George Huntington (1850-1916) shortly after being graduated from the medical school at Columbia's University. His paper entitled 'On Chorea', in the Medical and Surgical Reporter of Philadelphia (Huntington G: On chorea. Med Surg Rep 1872; 26:317–321), has become a classical in neurological disease descriptions. Since its publication the illness bore his eponym "Huntington's chorea". The disease was also called "Vitus Dance" in the late Middle Ages, due to its resemblance of a dancing festivity after the name of a

local Christian Patron Saint in the region of Prague and Bohemia, a name that was also assigned to different movement disorders (Bates et al., 2002). The name "Huntington's chorea" was later discarded as some patients do not present the chorea symptom (Heathfield, 1973; Lanska, 2000, 2010) (**Fig. 3**) and at the same time it does not show the real complexity of the disease (see next section).

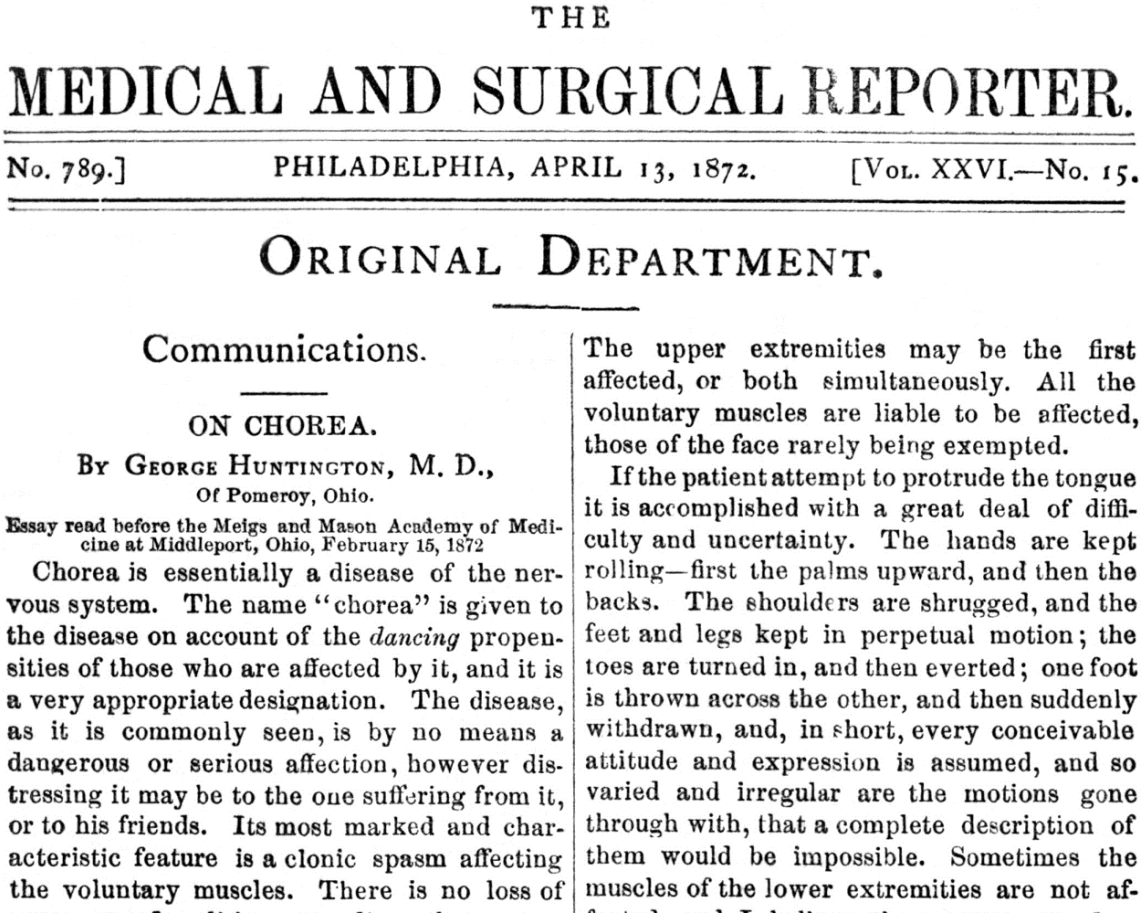

THE

MEDICAL AND SURGICAL REPORTER.

No. 789.] PHILADELPHIA, APRIL 13, 1872. [Vol. XXVI.—No. 15.

ORIGINAL DEPARTMENT.

Communications.

ON CHOREA.

By George Huntington, M. D.,

Of Pomeroy, Ohio.

Essay read before the Meigs and Mason Academy of Medicine at Middleport, Ohio, February 15, 1872

Chorea is essentially a disease of the nervous system. The name "chorea" is given to the disease on account of the *dancing* propensities of those who are affected by it, and it is a very appropriate designation. The disease, as it is commonly seen, is by no means a dangerous or serious affection, however distressing it may be to the one suffering from it, or to his friends. Its most marked and characteristic feature is a clonic spasm affecting the voluntary muscles. There is no loss of

The upper extremities may be the first affected, or both simultaneously. All the voluntary muscles are liable to be affected, those of the face rarely being exempted.

If the patient attempt to protrude the tongue it is accomplished with a great deal of difficulty and uncertainty. The hands are kept rolling—first the palms upward, and then the backs. The shoulders are shrugged, and the feet and legs kept in perpetual motion; the toes are turned in, and then everted; one foot is thrown across the other, and then suddenly withdrawn, and, in short, every conceivable attitude and expression is assumed, and so varied and irregular are the motions gone through with, that a complete description of them would be impossible. Sometimes the muscles of the lower extremities are not af-

Figure 3. Original paper published as: "On Chorea," by George Huntington, M.D. The Medical and Surgical Reporter: A Weekly Journal, (Philadelphia: S.W. Butler), vol. 26, no. 15 (April 13, 1872), pp. 317-321.

Given that the disease struck members of the same family, it hereditary nature was clear from the beginning. In consequence, researchers attempted to track back its geographical origin with the naïve hope of finding the first patient. In 1932, Percy R. Vessie, utilized witchcraft record accusations as an indicator of the disease and traced almost 1000 cases spanning twelve generations in 300 years, to three individuals (Vessie, 1932). He suggested that the disorder might have originated in the village of Bures in Suffolk, England. Unfortunately his work led to the prejudicial

view that those with HD were connected with witchcraft practices, stigmatized as criminals, alcoholics and insane people.

As history shown, the cure for the "Vitus dance" in the middle ages included the flames due to the beliefs that the genetically-afflicted were possessed by the devil and that their involuntary movements were a mere parody of Christ upon the Cross. It was not until 1968 when the psychoanalyst Milton Wexler, for personal reasons, created the Hereditary Disease Foundation (HDF) in Los Angeles when this condition started to be studied extensively (Wexler, 2012). The foundation was involved in the recruitment of over 100 scientists to finally constitute the Huntington's disease Collaborative Research Project. Over a 10-year period this consortium worked to identify the gene causative of HD. Finally, this goal was achieved thanks to the analysis of a highly endogamic population in Lake Maracaibo, Venezuela, which permits the study of a relatively rare allele. Successfully, in 1993 they reported the identification of the gene causative of HD (Huntington's Disease Collaborative Research Group, 1993).

1.2.2 Huntington's disease pathoetiology

HD is a fatal neurological disorder that is inherited in an autosomal dominant manner. The disease affects both sexes with the same frequency and the total prevalence is of 5–10 cases per 100,000 individuals worldwide (Landles and Bates, 2004). Death occurs with an average of 15 years after onset, which commonly is in the 30s and 40s influenced by several factors, such as sex and age of the transmitting parent (Cattaneo et al., 2001). However, a 10% of all HD cases are represented by the HD juvenile form, including the so-called Westphal variant, characterized by a predominance of paternal inheritance and onset before the age of 21 (Myers, 2004).
The classical HD variant is characterized by:

(i) personality changes: such as affective disorders, suicide tendency, mania, apathy that can worsen over time, schizophrenia-like symptoms, etc;
(ii) motor abnormalities: including the hallmark feature of chorea (involuntary jerky movements of the face and limbs), gait abnormalities, and in later stage of the disease, bradykinesia and rigidity;
(iii) cognitive deficits: poor planning and judgment, attention problems, and motor skill learning deficits;
(iv) others: sleep disturbance and weight loss (Walling et al., 1998).

The juvenile HD form typically manifests as dystonia, bradikinesia and rigidity (rather than chorea) that gradually becomes generalized, and parkinsonism, which may be the dominant feature in young patients (Quarrell et al., 2012).

A prominent neuropathologic feature of HD is a marked degeneration in medium spiny GABAergic neurons (MSN) of the caudate (**Fig. 4**) (McGeer and McGeer, 1976; Vonsattel et al., 1985), although several neuronal types become more and more affected during the progression of the disease (Bates et al., 2004). In consequence, the medial paraventricular region and tail of the caudate, along with the dorsal putamen, are the first brain regions to show significant atrophy (Vonsattel et al., 1985). The functional consequences of this malfunction are depicted in **Fig. 4**. Neuronal death spreads later to the cortex (mainly in the sensorimotor areas), white matter and thalamus (Sax et al., 1983; de la Monte et al., 1988) with abundant evidence for hippocampal dysfunction accumulating in recent years (Ransome et al., 2012; Ransome and Hannan, 2013). In juvenile patients the same areas are affected but in a more severe and widespread way with the inclusion of cerebellum (Seneca et al., 2004; Paradiso et al., 2008).

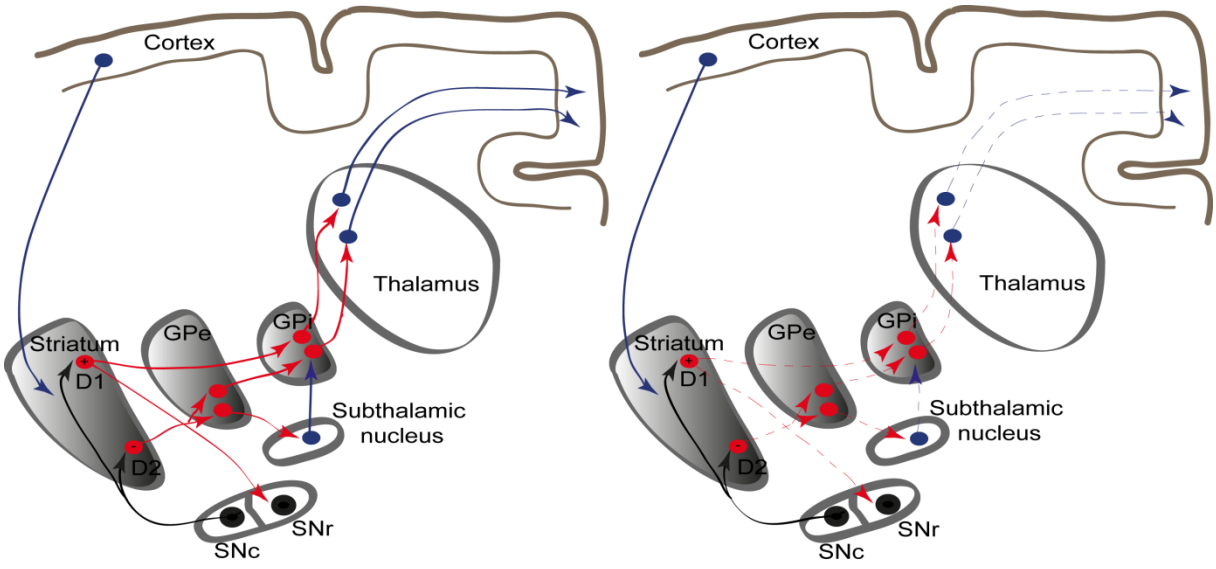

Figure 4. The cortico-striatal system. The striatum receive excitatory glutamatergic input from the cortex (blue) and dopaminergic innervation from substantia nigra pars compacta (black). These two types of afferent projections shape the activity of MSNs. The striatal GABAergic projection neurons provide an inhibitory control of globus pallidus and pars reticulata of the substantia nigra (red). In HD the malfunction of MSNs results in disinhibition of pallidal outflow (right) inducing severe impairments in both motor and cognitive functions. Substantia nigra pars compacta (SNc); Substantia nigra pars reticulata (SNr); Globus pallidus externo (GPe) and interno (GPi). Dopamine activates D1 and inhibits D2 receptors. Adapted from Bjorklund and Lindvall, 2000.

The precise relationship between topological alterations in brain structures and clinical symptoms of HD remains to be elucidated (Pillai et al., 2012). Attempts to ascribe the symptoms of HD to striatal degeneration or to dysfunction of cortico-striatal circuitry have been unsatisfying. For example, there is no good correlation between striatal atrophy and motor symptoms (Aylward et al., 1997; Aylward et al., 2000). However, it has been reported that pathophysiological effects of HD may precede the development of overt clinical symptoms and detectable cerebral atrophy (Novak et al., 2012). In addition, a growing body of evidence suggests that the natural history of gradually progressive motor and cognitive dysfunction in HD, which may begin years prior to a clinical diagnosis (Huntington Study Group. Mov Disord Group, 1996), is related to regionally specific changes affecting diverse brain regions (Kipps et al., 2005, Rosas et al., 2005).

1.2.3 The molecular genetics of Huntington's disease

HD is one of the most common forms of monogenic neurodegenerative diseases. The disease is caused by a trinucleotide sequence CAG expansion encoding a polyQ in the N-terminus of the protein huntingtin (HTT), which is codified near the telomere of chromosome 4. Disease occurs when the repeat expands to an abnormal length of consecutive glutamines, suggesting a pathogenic threshold in the length of the polyQ. Therefore, the CAG/polyQ expansion in HD patients is in the range of 37–121 repeats at the N-terminus end of the protein while normal individual has between 6 to 35 units (Huntington's Disease Collaborative Research Group, 1993). Repeat length between 27 and 35 CAGs is often described as the 'gray area' attributed to intermediate alleles that may explain the phenomenon of anticipation that worsen the symptomatology in the descendants (**Fig. 5**) or reduced penetrance, although still uncertain, for carriers of these alleles. CAG expansion is inversely correlated with age of disease onset that accounts for 44 to 73% of the observed variance (Harper and Jones, 2002a, 2002b; Langbehn et al., 2004). The clearest example with large CAG lengths/early onset is the juvenile HD type with more than 60 CAG repeats (Nance and Myers, 2001). The remaining variance not accounted for by CAG repeat length is attributable to other genetic factors (i.e.: inheritance of others deleterious modifying genes not associated with the *HTT* gene) or environmental modifiers factors (i.e.: socioeconomic strata, diet, effluvia exposition ambient) (Trembath et al., 2010; Shang et al., 2012; Burgunder, 2014). This type of mutation can be also found

in other genes and constitutes the main feature of the family of polyglutamine (polyQ) diseases within the more ample trinucleotide repeats disorders: spinal and bulbar muscular atrophy (SBMA), dentatorubral pallidoluysian atrophy (DRPLA), and spinocerebellar ataxia (SCA) types 1, 2, 3, 6, 7 and 17 (Li and Li, 2004; Orr and Zoghbi, 2007) (see section 1.2.8). Due to its prevalence in the human population, HD is the most common polyQ disorder.

1.2.4 Role of huntingtin in physiology and pathobiology

The 67 exons of the *HTT* gene encodes for a large protein of 348 kDa (Landles and Bates, 2004) with several domains. As already mentioned, located at the N-terminal part of the protein there is the polyQ domain, immediately followed by two proline-rich domains (poly-P) (composed by 11 and 10 prolines), three main groups of HEATs repeats (Andrade and Bork, 1995) named for: **HTT**, elongation factor 3 (**e**IF3k), the PR65/A subunit of protein phosphatase 2A (PP2**A**) and the lipid kinase **T**OR (target of rapamycin), which are involved in intracellular transport and chromosomal segregation (Harjes and Wanker, 2003), and NES and NLS nuclear export and nuclear localization signals respectively (**Fig. 5**).

The protein has no homology with other proteins and is expressed ubiquitously in humans and rodents, with the highest levels in CNS neurons and testes (Trottier et al., 1995; Ferrante et al., 1997; Fusco et al., 1999). However, both in peripheral organ tissues and the brain, huntingtin appeared to be localized in the cytoplasm. Also, in neurons, the protein appears to be partly associated in part with the membranes of vesicles (DiFiglia et al., 1995; Velier et al., 1998; Hilditch-Maguire et al., 2000; Hoffner et al., 2002; Kegel et al., 2002; Li et al., 2003). This widespread localization complicates the definition of a clear function of the protein. It has been described that HTT likely plays a variety of roles, such as endocytosis and vesicular transport (Metzler et al., 2001; Qin et al., 2004; Smith et al., 2009b; Pardo et al., 2010), trafficking of growth factor complexes (del Toro et al., 2006; Liot et al., 2013) and cell adhesion (Lo Sardo et al., 2012). HTT also has a pro-survival function against apoptotic stress (Reiner et al., 1988; White et al., 1997; Rigamonti et al., 2000; Reiner et al., 2003), and it is required for normal embryonic development and neurogenesis (Nasir et al., 1995; Zeitlin et al., 1995; White et al., 1997; Seong et al., 2010). Other roles of HTT in transcriptional regulation in adulthood will be discussed in the next section.

The polyQ mutation has two different consequences (Zuccato et al., 2010): (i) a loss-of-function (Tallaksen-Greene et al., 2005) effect because one allele is not available for the physiological roles of normal HTT, and (ii) a gain-of-function (GOF) effect, characterized by the presence of a misfolded mutant Htt (mHTT) that interferes with multiple intracellular activities through aberrant interactions and accumulation into insoluble aggregates.

mHTT conversely to wild type HTT, is located mainly in cell nuclei and to a lesser extent in the cytoplasm, neurites and terminals (Sapp et al., 1997). Proteolytic cleavage of N-terminus mHTT protein is thought to lead to the generation of mHTT fragments and to increase aggregation in the nucleus and cytoplasm (Martindale, et al., 1998) while inhibition of cleavage with specific protease inhibitors reduces the frequency of aggregate formation (Gafni and Ellerby, 2002; Gafni, et al., 2004; Lunkes, et al., 2002; Wellington, et al., 2000). mHTT aggregates constitutes a hallmark of HD and are present in brains of human patients and several HD models, but it is still controversial whether mHTT inclusions are pathogenic (Davies et al., 1997), benign biomarkers (Kim et al., 1999), or neuroprotective (Arrasate et al., 2004). Some studies did not show correlation between the formation of nuclear inclusions and the degree of apoptotic cell death (Saudou et al., 1998) and it has been suggested that the principal toxic species might be an early intermediate of inclusion bodies or a form of diffuse intracellular mHTT (Arrasate et al., 2004; Graham et al., 2006; Miller et al., 2010; Arrasate and Finkbeiner, 2012). In any case, abnormal interaction of mHTT with other proteins has been identified, including transcription factors (see next section), vesicular structures and microtubule components such as the huntingtin-associated protein-1 (HAP1) (a protein that is transported in axons and associates with a dynactin subunit (essential in the dynein/dynactin microtubule-based motor complex). mHTT binds also to huntingtin-interacting protein 1 (HIP1), which binds to α-adaptin and clathrin, and is implicated in cytoskeleton assembly and in endocytosis. In addition, it has been reported that mHtt can affect the regulation of synaptic plasticity since it can interact with the postsynaptic density 95 (PSD-95) among others (Harjes and Wanker, 2003).

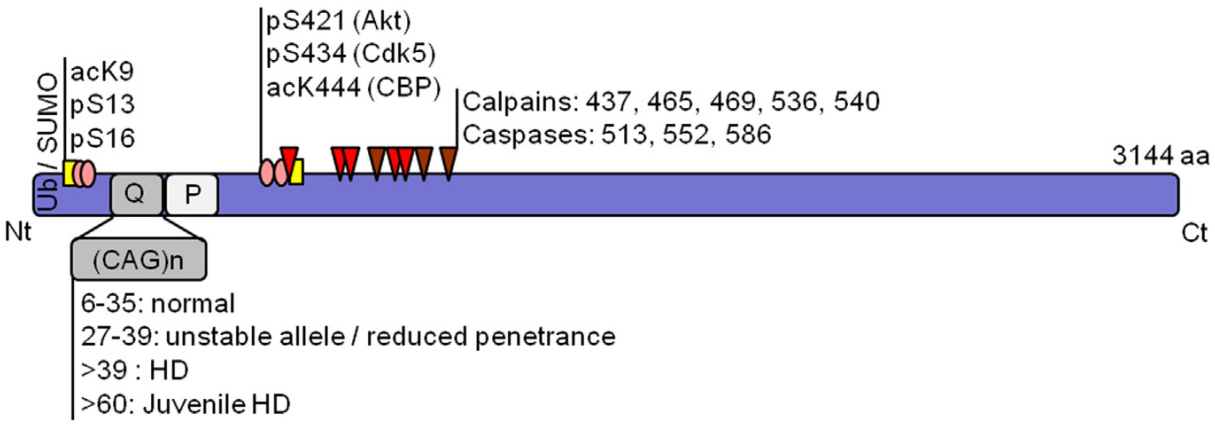

Figure 5. Scheme of the human huntingtin protein. Poly-Q (glutamine) and poly-P (proline) tracts are indicated, in addition to the polymorphic range of CAG repeats found in human population. Cleavage sites and post-translational modifications are also shown, together with the residue number: Ub/SUMO, ubiquitylation/SUMOylation; yellow square, acetylation; pink oval, phosphorylation; red and brown triangles, calpain and caspase cleavage sites, respectively. aa: amino acid, Nt and Ct, amino- and carboxy-termini, respectively.

1.2.5 Transcriptional dysregulation in Huntington's disease

Accumulating evidence from the last two decades indicates that transcriptional dysregulation is a central and early pathogenic mechanism in HD. The activity of transcriptional regulators can be affected in several ways, with a bias towards inhibition of positive regulators and desinhibition of negative regulators, including transcription factors, chromatin-remodeling proteins, and non-coding RNAs. Different groups have been identified an altered expression in a number of genes, such as neurotransmitter receptors and neuropeptides, first in patients´s brains and later in animals models (Emson et al., 1980; Young et al., 1988; Augood et al., 1997; Cha et al., 1998). The importance of transcriptional dysregulation in HD pathology emerges from studies that analyze separately the impact of nuclear and cytoplasmic mHTT on the initiation and evolution of the symptoms. Thus nuclear mHTT was able to induce cytoplasmic neurodegeneration (in the form of degenerate organelles and dystrophic neurites) and transcriptional dysregulation in parallel to reproducing part of the HD symptomatology (Schilling et al., 2004; Benn et al., 2005; Hodges et al., 2008; Moumne et al., 2013).

Further demonstrations of the presymptomatic transcriptional alterations has been provided from both animal and cellular HD models, in which gene expression changes occur before the onset of mHTT aggregation, cell death and mitochondrial abnormalities (Valor, 2014). Importantly, changes between mouse models and early-grade patient brains show an important overlap (Moumne et al., 2013) pinpointing to

the suitability of animal models to study the transcriptional dysregulation associated to this pathology.

In LOF normal Htt experiments, Zuccato and colleagues in 2003 demonstrated the interaction between wildtype HTT and REST in the cytoplasm. REST associates with NRSE to affect the nuclear transcription of neuronal genes, including that of brain-derived neurotrophic factor (*Bdnf*). The interaction of HTT with REST/NRSE in the cytoplasm is able to avoid REST/NRSE translocation to the nucleus leading to normal expression of its target genes. mHTT, however, interacts weakly with or fails to bind REST/NRSE, resulting in an accumulation of REST/NRSE in the nucleus which alters the expression of neuronal genes (Zuccato et al., 2003).

In GOF mHTT experiements, aberrant interaction and/or apparent sequestration of essential proteins into mHTT aggregates has traditionally been proposed in the literature as one of the modes by which mHTT can alter the activity of transcriptional regulators. Diverse nuclear proteins, such as CBP, Sin3a, p53, the transcription elongation regulator 1 (Tcerg1/CA150), the specificity protein 1 (SP1), the nuclear corepressor (NCoR) and TATA-binding protein (TBP), among others (Huang et al., 1998; Boutell et al., 1999; Kazantsev et al., 1999; Steffan et al., 2000; Holbert et al., 2001; Nucifora et al., 2001; Yamanaka et al., 2008) were found within the mHTT aggregates, suggesting a depletion in their activity (**Fig. 6**), although other studies have claimed that this is not the case. For example, a number of studies have proved that transcription factors and cofactors are not apparently affected by polyQ aggregates (Steffan et al., 2001; Yu et al., 2002; Obrietan and Hoyt, 2004; Tallaksen-Greene et al., 2005). Moreover, soluble mHTT versions showed better interactions with the aforementioned proteins than aggregative versions (Choi et al., 2012) or even preceded the formation of visible inclusions (Cong et al., 2005). mHTT can also disrupt the binding activities of many transcription factors by acting directly over the DNA (Cui et al., 2006; Benn et al., 2008) or by affecting the process of protein degradation. In this last case, mHtt can promote the removal of regulators such as the cofactor CBP (Nucifora et al., 2001) or prevent the degradation of other proteins like the Wnt-dependent transcriptional coactivator β-catenin (Godin et al., 2010). As a consequence of these alterations, transcription can be affected (Valor, 2014).

There is increasing evidence showing that neuronal dysfunction largely precedes the appearance of neuronal death, which permits investigate transcriptional alterations without the confounding factor of changes in the cellular composition of

the tissue due to neuronal death (Leegwater-Kim and Cha, 2004). Importantly, alterations of gene expression correlate with the progression of the HD phenotype, as confirmed by concurrent changes in behavior and the expression of related genes (Hodges et al., 2008). More precisely, downregulation of many genes in HD is associated with neuronal signaling processes such as neurotransmitters, neurotrophin receptors, neuropeptides, synaptic transmission, calcium signalling and homeostatic genes, as well as factors related to transcription and chromatin remodelling. On the other side, genes related with RNA metabolism, protein folding, and stress markers are generally associated with an upregulated gene expression profile.

A substantial number of HD models are nowadays available to investigate the progression of the disease. In fact, different HD animal models had revealed a high degree of concordance when gene expression profile analysis has been carried out in their respective brain tissue samples (Kuhn et al., 2007). Furthermore, gene expression studies have been performed in human samples validating important transcriptional features of animal models (Cha, 2007). Important factors need to be considered in this type of analysis because they can generate model-specific changes. For instance, the intrinsic properties of the tissues, such as sensitivity to degeneration and tissular-specific transcription, even different cell types within the same structure. This can be clearly seen in the striatum, where GABAergic projections are more susceptible to damage in HD than cholinergic interneurons (Calabresi et al., 2000; Van Raamsdonk et al., 2007). Another important factor that could add variability to the analysis is the intrinsic properties of the models including features like the transgene employed in the model (e.g. ubiquitous *versus* neuronal-restricted), the length of the mHTT (full-length *versus* N-terminal truncated protein) (Jeong et al., 2009; Lee et al., 2013a) as well as the number of CAG repeats, since important transcriptional changes has been associated with higher CAG size (Jacobsen et al., 2011; Lee et al., 2013b; Galkina et al., 2014). This complexity is accompanied by the presence of multiple gene expression regulators that are altered in HD.

In summary, the study of transcriptional dysregulation in HD can open new avenues to better comprehend the chain of events underlying the manifestation and progression of the disease.

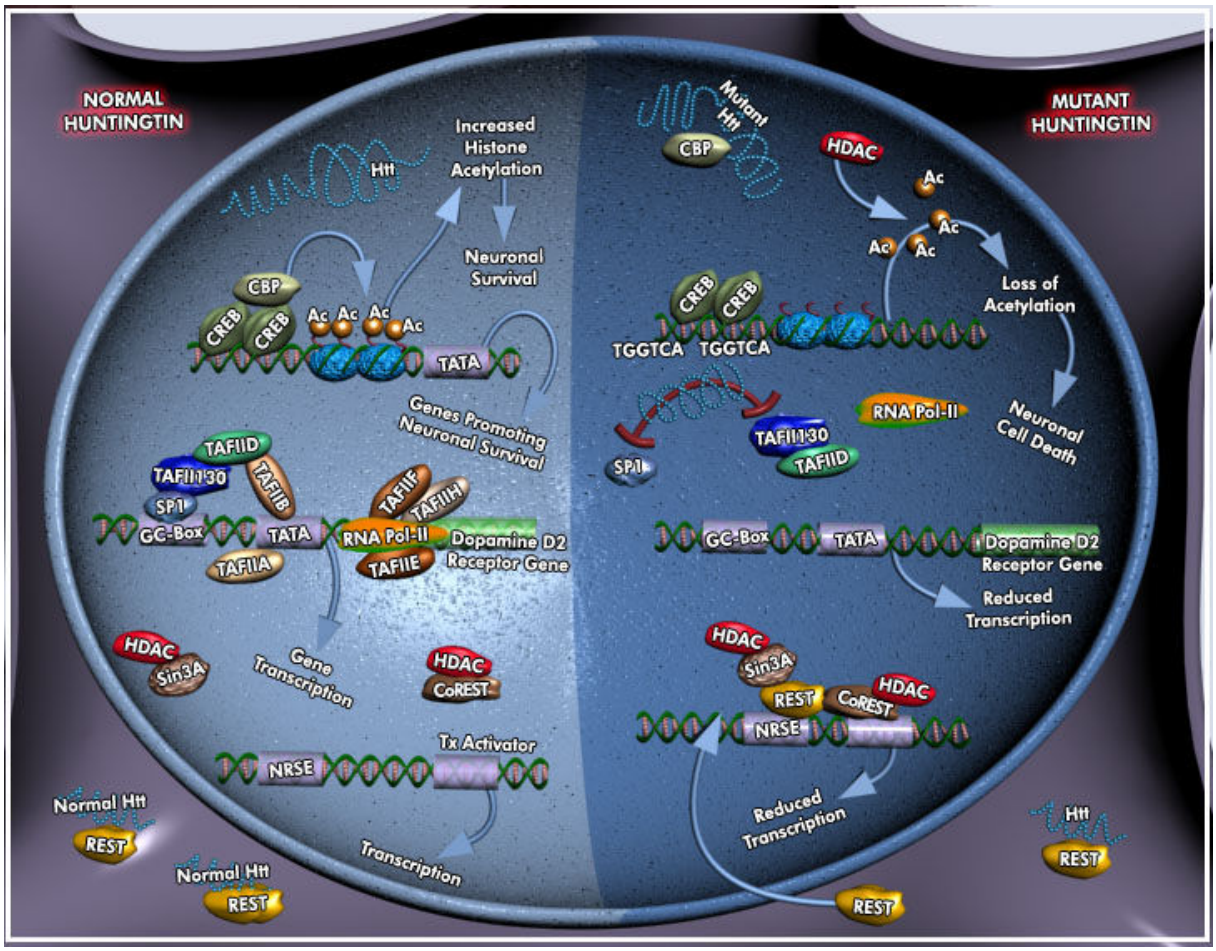

Figure 6. Transcriptional dysregulation in Huntington's disease. Normal huntingtin can associate with dozens of signal transduction proteins, including transcription factors complexes (like basal transcription factors: SP1, TAFII130; transcriptional co-repressors and co-activators: CBP, NCOR1, Sin3A, CTBP, REST. Mutant huntingtin alters protein conformation, resulting in aberrant protein interactions. Taken from www.qiagen.com

1.2.6 Epigenetic dysregulation in Huntington's disease

Several histones PTMs and DNA methylation (**Fig. 7**) have been described to be affected in HD (Valor and Guiretti, 2014). In fact, HD has emerged as an exemplary paradigm of epigenetic dysregulation in a neurodegenerative condition due to the pioneering work suggesting a relevant role of epigenetics in neuronal malfunction and cell loss (Bates et al., 2004). As other neuropathologies, including AD, also show epigenetic dysregulation, the hypothesis of an epigenetic imbalance as a key aspect of neurodegeneration has been pushed forward during the last years.

More precisely, the relevance of altered KAT activity in HD pathogenesis is highlighted by a number of studies showing that HDACi ameliorate neurodegeneration in Drosophila and mouse models of HD (McCampbell et al., 2001; Steffan et al., 2001). It has been proposed that imbalances between the activities of

KATs and HDACs could lead to disease states (Saha and Pahan, 2006). Several studies have revealed the co-localization between CBP (which has KAT activity) and mHTT in a number of HD models suggesting the possibility that histone acetylation levels can be altered in HD (Kazantsev et al., 1999; Steffan et al., 2000; Nucifora et al., 2001; Jiang et al., 2006). In consequence, diminished CBP activity can alter the expression of cell survival genes. In harmony with this view, Ferrante and colleagues demonstrated decreased acetylation of histone H4 in immunoblots and Stack and collaborators revealed, in mouse models (both N171-82Q and R6/2 strains), a significant chromatin modification that led to histone hypoacetylation with concomitant hypermethylation (Ferrante et al., 2003; Stack et al., 2007). Hence alteration in bulk histone acetylation have been addressed in an ample variety of HD models (Ferrante et al., 2003; Igarashi et al., 2003; Gardian et al., 2005; Jiang et al., 2006; Stack et al., 2007; Chiu et al., 2011; Lim et al., 2011; Giralt et al., 2012) including, recently, samples from patients (Yeh et al., 2013), while others did not find such profound molecular changes, even using the same murine models. For example, Klevytska et al. have demonstrated that the levels of acetylated histone H4 were marginally lower in the brains of N171-82Q and HD/CBP$^{+/-}$ mice (double mutants harboring a disrupted CBP gene and expressing mHTT) compared with non-transgenic mice (Klevytska et al., 2010). Sadri-Vakili et al. found no evidence for a diminution of the level of acetylated histone H3 in the brains of symptomatic R6/2 mice, albeit, they detected reductions in the levels of acetylated histone H3 restricted to promoter sequences of genes known to be downregulated in these mice (Sadri-Vakili et al., 2007). Others studies have observed histone acetylation deficits at the specific loci level rather than having global effects (Thomas et al., 2008; McFarland et al., 2012).

Different proteins and mechanisms can contribute to acetylation deficits in HD that are not necessarily mutually exclusive: in the case of CBP, this protein can be (i) sequestrated into mHTT aggregates (e.g., by the interaction between polyQ fragments of mHTT and the C-terminus of CBP) (Kazantsev et al., 1999; Nucifora et al., 2001); (ii) inhibited by soluble mHTT (e.g., by the binding of soluble mHTT form to acetyltransferase domains of CBP) (Steffan et al., 2001; Cong et al., 2005; Choi et al., 2012) and/or (iii) degradated (e.g., by the ubiquitine proteasome system (UPS) (Jiang et al., 2003; Giampa et al., 2009; Giralt et al., 2012). Thus, both mHTT versions, aggregate or soluble, might interact with chromatin-remodeling proteins to

mediate pathological changes. Nevertheless, the precise role of CBP in HD is not clear since depletion of this protein have shown a reduction in bulk histone acetylation and unaffected cell viability (Chen et al., 2010; Valor et al., 2011) implying that other factors are responsible for neuronal degeneration.

HDACs have been widely study in HD. The knockdown of single HDACs (namely HDAC3, 6, 7 and Sirt2) in R6/2 strain is not sufficient to ameliorate physiological or behavioral phenotypes and did not restore dysregulated transcripts (Benn et al., 2009; Bobrowska et al., 2011; Bobrowska et al., 2012; Moumne et al., 2012). On the other hand, in cell lines challenged with cytotoxic insults, the overexpression of HDAC7 resulted in neuroprotection acting by a mechanism that is independent of its deacetylase activity (Ma and D'Mello, 2011). Similarly the overexpression of wild-type HTT, interacts physically with HDAC3 to damper its activity (a protein known to promote neuronal death) (Bardai et al., 2013). Although mHTT neurotoxicity is greatly reduced in the absence of HDAC3 in R6/2 mice. In summary, these results add more complexity for understanding the precise roles of HDACs in HD.

Another important epigenetic mark is histone methylation, also involved in cognition and linked to intellectual disabilities, especially in the case of histone H3 (Parkel et al., 2013). The repressive marks H3K9m2/m3 are elevated in brain tissues of R6/2 and N171-82Q mice and in HD patients (Ferrante et al., 2004; Gardian et al., 2005; Ryu et al., 2006; Stack et al., 2007). In contrast, the methylation mark associated with active genes, H3K4me3 (Parkel et al., 2013), exhibited reduced binding at the promoters of representative downregulated genes in cortical and striatal areas of R6/2mice and patients (Vashishtha et al., 2013). A summary of the disrupted epigenetic mechanisms in HD is depicted in **Fig. 7**.

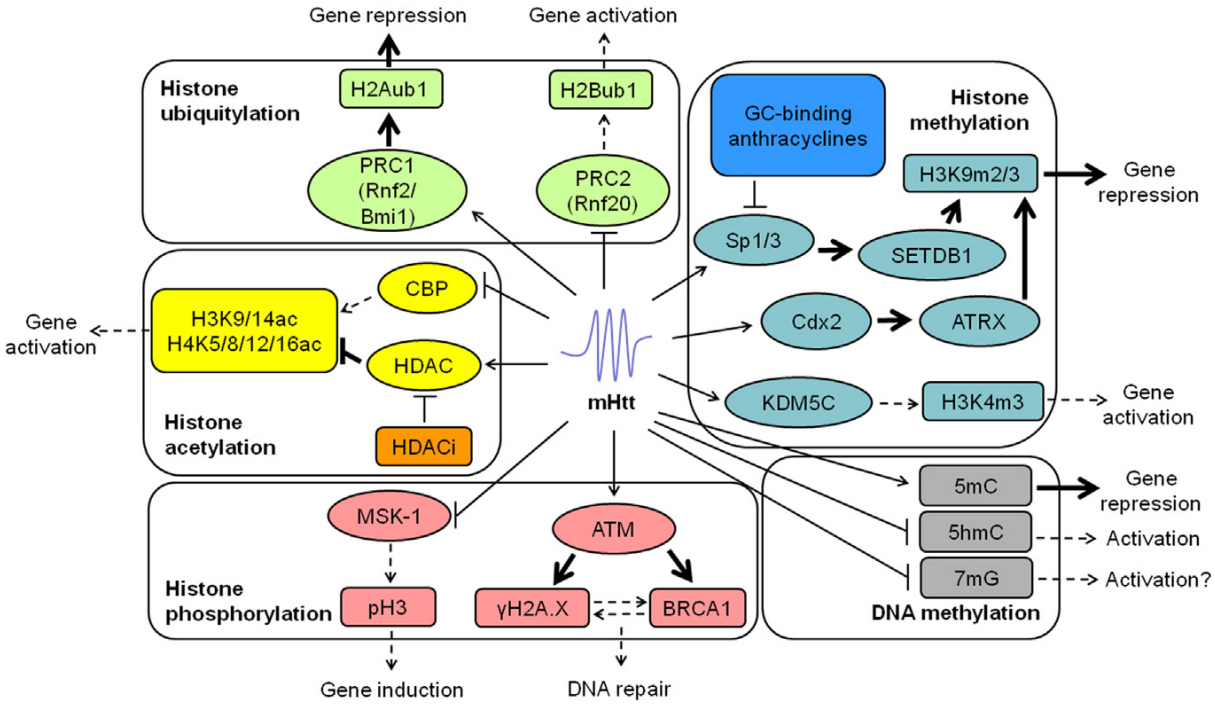

Figure 7. Summary of the disrupted epigenetic mechanisms in HD and the ameliorative strategies tested. A gain-of-function effect is inferred because most of the HD models are based on transgenic or exogenous mHTT expression. Nonetheless, altered interactions between wt-HTT and chromatin-remodeling proteins are possible in HD (e.g., HTT-HDAC3). Actions by mHTT: regular arrow, activation; blunt end, inhibition. Resulting effects in the relationship between transcription factors and chromatin-remodeling proteins and their downstream targets and related processes are represented by dashed (reduced activity/effect) and thick arrows (enhanced activity/effect). No intermediate enzyme has been examined in altered DNA methylation. Ameliorative pharmacological compounds are also depicted.

1.2.7 Experimental models of Huntington's disease and relevant phenotypes

HD models can be divided in two types: chemical and genetic. Chemical models were developed before the identification of the disease gene in 1993 where HD animal models were produced by injecting neurotoxins into the striatum. These models mimic the regional selectivity of HD neuropathology but are unable to reproduce the pathophysiological mechanisms induced by the *HTT* gene. Nonetheless, they may be still useful to study neuroprotection and neurorestorative therapies in HD. In contrast, there is a wide range of models available to the HD community, including a variety of species like *Caenorhabditis elegans* and *Drosophila melanogaster* (invertebrate models), non-mammalian species as zebrafish and mammals, such as mouse and rat. In addition, a transgenic non-human primate has been described (Yang et al., 2008). **Table 2** lists the animal and cellular models of HD investigated in this thesis.

Table 2. Summary of the cellular and animal HD models used in this work

HD model	*Construct*	*Promoter*	*CAG repeat size*	*Symptoms*
N171-82Q Transgenic mouse	First 171 aa of human HTT randomly inserted into mouse genome (Schilling et al. 1999)	Prion	82	11 wk: Rotarod deficits, clasping behavior, weight loss (McBride et al. 2006). 14 wk: Deficits on radial arm water maze text of reference and working memory (Ramaswamy et al. 2004).
R6/1 Transgenic mouse	First 90 aa of human HTT randomly inserted into mouse genome (Mangiarini et al. 1996)	Human huntingtin	116	22 wk: Body weights plateau after which they begin to decline. Gait abnormalities as measured by footprint analysis and hindlimb clasping behavior (Naver et al. 2003). 23-24 wk: Decreased anxiety on open-field test (Naver et al. 2003).
YAC128 Transgenic mouse	Yeast artificial chromosome expressing entire human HTT protein (Slow et al., 2003)	Human huntingtin	128	3 months: Hyperkinesia on an open-field test. 12 months: hypokinesia on open-field test (Slow et al., 2003). 2 months: Deficits on T-maze 4 months: Progressive decline on the rotarod test. (Van Raamsdonk et al. 2007)
mHTT-electroprated mice	In utero electroporation of wt and mHtt version in the striatum.	CAG promoter	15, 128	16-19wk: Presence of feet clasping in mice electroporated with mHTT version (unpublished results)
mHTT-infected neurons	Infection of wt and mHTT version in primary hippocampal culture	Synapsin promoter	15, 128	
Stably HTT-expressing PC12	PC12 cell line that express exon 1 *HTT* with varying CAG repeat lengths under doxycycline control	pTRE-Tight plasmid	23, 72	Aggregate formation, caspase-dependent cell death and decreased neurite outgrowth (Wyttenbach et al. 2001)

aa: aminoacids; HTT: huntingtin; wt, wildtype; mHTT: mutant huntingtin; wk: weeks; CAG: cytomegalovirus early enhancer/β-actin promoter.

1.2.8 Epigenetic and transcriptional dysregulation in others polyglutamine diseases

As previously indicated HD is part of a group of related neurological diseases known as polyQ disorders. The deregulation of gene expression seems to be a common pathogenetic mechanism in these disorders (Paulson and Fischbeck, 1996; Cha, 2000). The pathologic consequences of polyQ expansion include progressive spinal, cerebellar, and neural degeneration. Increasing evidence suggests that polyQ proteins in their native form regulate gene expression and indeed, as many of the nine CAG-expanded genes are transcription factors, transcriptional coactivators, and regulators of RNA stability (**Fig. 8**). Thus, analysis of gene expression profiles indicates that a large number of genes are deregulated in mouse models of polyQ disease (Luthi-Carter et al., 2002). Thus, polyglutamines might have a role either in protein–DNA interactions or in the protein–protein interactions that occur when transcription factors form transcriptionally active complexes reviewed in Mohan et al., 2014. As examples:

- Spinal and bulbar muscular atrophy (SBMA) is caused by the polyQ expansion in the transactivation domain of the androgen receptor (AR) (La Spada et al., 1991). AR, normally functions as a nuclear TF that binds to androgen response elements in target genes while polyQ expansion of its glutamine-rich transactivation domain interferes with AR binding to coactivators and components of the basal transcription apparatus (Chamberlain et al., 1994; Nakajima et al., 1996). In addition, it has been shown that transcriptional activation by AR is accompanied by a cascade of distinct covalent histone modifications, including methylation in the arginine 17 (R17) of H3 (H3R17me), H3S10 phosphorylation and H3K4me. However, it remains to be determined if these PTMs are impacted by its polyQ expansion (Kang et al., 2004).
- Dentatorubral pallidoluysian atrophy (DRPLA) is caused by polyglutamine expansion of the gene encoding the atrophin-1 protein, which triggers degeneration both in the brain and spinal cord (Yazawa et al., 1995). Atrophin-1 can repress transcription in reporter gene assays and sequesters transcriptional regulators into nuclear inclusions like Sin3A, HDACs and ETO/MTG8 corepressor complex subunit (Wood et al., 2000). Furthermore, analysis of gene expression profiles indicates that a large number of genes

are deregulated in a mouse model for this pathology (Luthi-Carter et al., 2002).

- Spinocerebellar ataxia (SCA) type 1 (SCA1) is caused by polyglutamine expansion of the Ataxin-1 (ATXN1), a disease characterized by dominantly inherited cerebellar degeneration and early transcriptional derangements that occurs before behavioral features (Lin et al., 2000; Serra et al., 2004). Normal ATXN1 interacts with a variety of TFs. Several nuclear proteins that interact with ATXN1 have been identified as possible mediators of SCA1 pathogenesis (Okazawa et al., 2002; Tsai et al., 2004; Tsuda et al., 2005). Yet, even with these advances, the molecular mechanism by which a mutant ATXN1-induced alteration in gene expression results in the degeneration of only certain neurons, such as cerebellar Purkinje cells, remains unclear. A likely mechanism mediating SCA1 pathogenesis is the ability of mutant ATXN1 to induce the loss of *ROR-α* (a transcription factor critical for cerebellar development) from Purkinje cell nuclei. This leads to a reduced expression of *RORα*-mediated genes that are critical for Purkinje cell functioning. In addition, ATXN1 interacts with RORα and the Tat-interactive protein 60 kDa (Tip60), a histone acetyltransferase and a nuclear receptor coactivator (Brady et al., 1999). Tip60 mediates the interaction between ATXN1 and *ROR-α* (Gold et al., 2003) and it directly interacts with ATXN1 (Serra et al., 2006). It has been shown that under partial loss of Tip60, *RORα* expression is increased in SCA1 transgenic mice (Gehrking et al., 2011) http://www.ncbi.nlm.nih.gov/pmc/articles/PMC3655547/ - R100 and these mice show delayed disease progression; indicating Tip60 interaction with the mutant SCA1 accelerates pathogenesis, likely through epigenetic modifications at Tip60 targeted genes (Gold et al., 2003; He et al., 2011).
- SCA type 3 (SCA3) (also known as Machado–Joseph disease) is caused by the mutation in the ataxin-3 gene. Its protein binds chromatin directly and can be found in gene promoters. It can activate and repress transactivation. It is a deubiquitinase and this activity is indespensible for transactivation function. Interacts with FOXO-4, TAFII130, CBP, NCoR, HDACs, RAD23. PolyQ expansion reduces Ataxin-3 transcrional repression function reviewed in Mohan et al., 2014.

- SCA type 7 (SCA7) is caused by mutations in the gene ataxin-7, which encodes a component component of the KAT GCN5-containing coactivator complexes (McCampbell et al., 2000). In vitro experiments indicate that although mutant ataxin-7 does not disrupt such complexes, it interferes with their KAT activity (McMahon et al., 2005; Palhan et al., 2005). The scenario in vivo is more complex because KAT activity is apparently not affected in mouse models of the disease, but these mice exhibit a general chromatin de-condensation and aberrant histone acetylation in transcriptionally altered genes (Blennow et al., 2006).

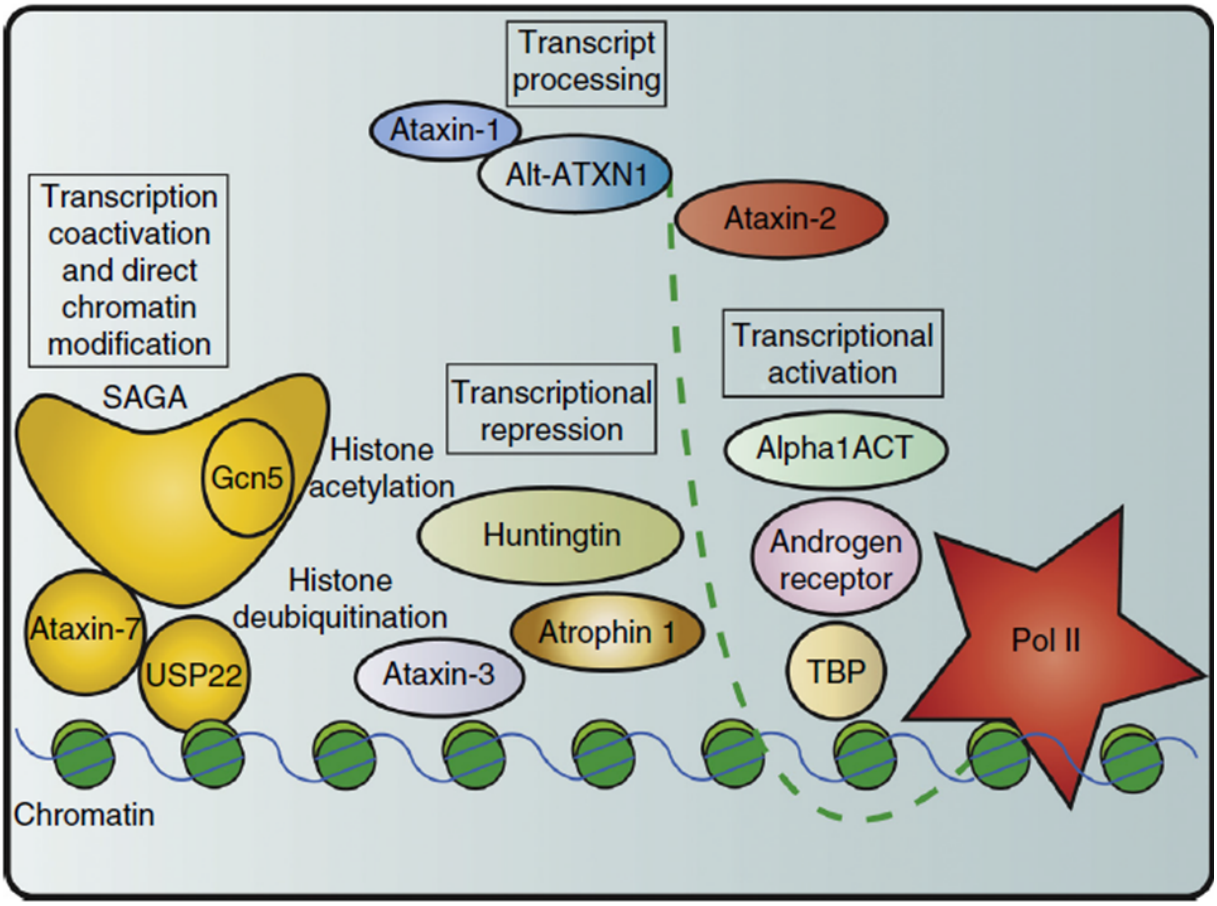

Figure 8. PolyQ disease affects chromatin modification and usage. The polyglutamine expanded proteins huntingtin, Androgen receptor (SBMA), Atrophin 1 and Alt-ATXN1 (Alt-ATXN1 (alternative Ataxin-1) (DRPLA), Ataxin-1 (SCA1), Ataxin-2 (SCA2), Ataxin-3 (SCA3), alpha-1A voltage-dependent calcium channel subunit and alpha1ACT transcription factor (SCA6), Ataxin-7 (SCA7), and TBP, TATA box binding protein (SCA17) are all important regulators of gene expression and chromatin modification. The causative disease is written between brackets: HD, Huntington disease; SBMA, spinal and bulbar muscular atrophy; DRPLA, dentatorubral pallidoluysian atrophy; SCA, spinocerebellar ataxia; Pol II, RNA polymerase II; SAGA, chromatin modifying Spt-Ada-Gcn5-Acetyltransferase complex; Gcn5, histone acetyltransferase, USP22, histone deubiquitinase. Taken from Mohan et al., 2014.

1.3 Rubinstein-Taybi syndrome

1.3.1 Molecular genetics of Rubinstein-Taybi syndrome

Rubinstein-Taybi syndrome (RSTS) is a rare and complex autosomal dominant disease with an incidence of 1:100 000–125 000 at birth (Hennekam, 2006). This disorder was first described by Michail *et al*. in 1957 (Michail et al., 1957) and later was precisely defined as a syndrome in 1963 by Rubinstein and Taybi (Rubinstein and Taybi, 1963). In general, RSTS occurs as the result of a *de novo* mutation. People suffering RSTS present craniofacial abnormalities, mental retardation, growth deficiency and physical features including broad thumbs and toes that are used in diagnosis. An important number of patients also show other neurological symptoms such as seizures (28%) and abnormal electroencephalograms (60%) (Schorry et al., 2008). In addition, approximately a third of RSTS patients has heart malformations and may present abnormalities in other tissues, such as the kidney and skin. In fact, complications from congenital heart disease and infections of the respiratory tract have been reported as the primary causes of morbidity and mortality in RSTS (Lopez-Atalaya et al., 2014). Behavioral studies have shown that RSTS patients have low levels of intelligence, short attention spans and poor motor coordination (Wiley et al., 2003) as well as a high risk of developing lymphoma (Mullighan et al., 2011; Pasqualucci et al., 2011; Lopez-Atalaya et al., 2012).

Most cases (60%) are associated with mutations in one allele of the gene encoding CBP (*CREBBP*) (Petrij et al., 1995) and a small percentage (3% of cases) are caused by mutations in the gene encoding p300 (*EP300*), which is highly homologous to CBP (> 70 % homology) (Roelfsema et al., 2005). CBP and p300 constitutes their own family of transcriptional co-activators with intrinsic KAT activity, the KAT3A family, and have recently being renamed as KAT3A and KAT3B, respectively.

1.3.2 Pathoetiology of Rubinstein-Taybi syndrome

The proteins affected in RSTS, CBP and p300, have diverse functions related to transcription activation and regulation. CBP/p300 are nuclear and ubiquitously expressed proteins of ~250 kDa approximately, that interact physically or functionally with over 400 different proteins including multiples TFs (Kasper et al., 2006; Bedford et al., 2010). They are normally described as molecular scaffolds proteins between

DNA-binding TFs and the RNApol II complex. Together with their capability of acetylation of histones and TFs, CBP/p300 are proposed to play a key role role in transcriptional initiation (Imhof et al., 1997). Thus, both proteins also display widespread occupancy of transcriptional regulatory regions including many putative enhancers (Heintzman et al., 2009; Wang et al., 2009b).

The multiple actions of CBP and p300 can be explained by the high number of domains including (i) three cysteine/histidine-rich regions (CH1 to CH3) involved in protein-protein interaction (ii) the KAT domain in the center of the protein; (iii) the bromodomain (Abdolmaleky et al., 2005) that binds acetylated lysines in histones and specific transcription factors (Polesskaya and Harel-Bellan, 2001); (iv) two transactivation domains located at either end of the protein; and (v) the KIX domain that mediates interaction with phosphorylated CREB and other TFs (**Fig. 9**) (Parker et al., 1996).

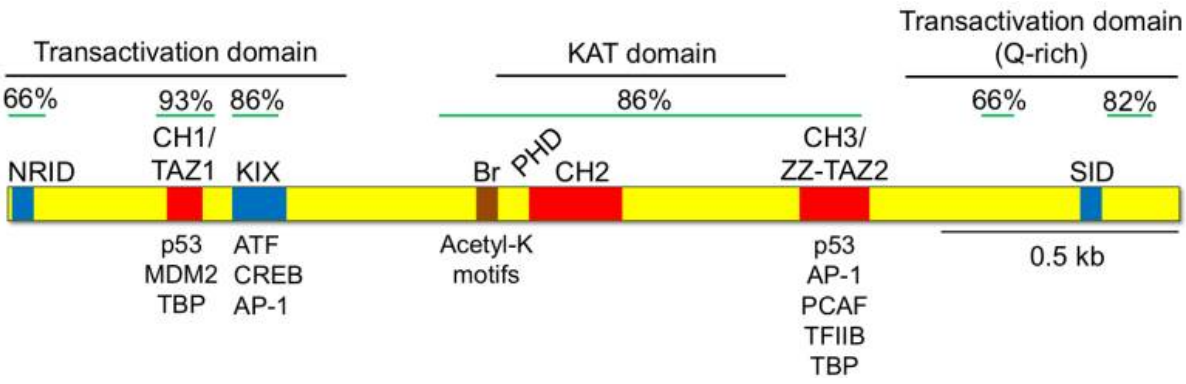

Figure 9. Structure of KAT3 proteins. CBP and p300 share a number of structural domains including three cysteine/histidine rich regions (CH1-CH3) for protein-protein interaction, the KIX domain that mediates the interaction with CREB and other transcription factors, and the KAT domain. Regions of high homology between the human CBP and p300 proteins expressed as % identity. NRID, nuclear hormone receptor interacting domain; CH1-3, cysteine/histidine-rich regions 1-3; TAZ1-2, transcripcional adaptor Zn-finger domain 1-2; KIX, kinase inducible domain; Br, bromodomain; PHD, plant homeodomain; ZZ, ZZ-type Zn-finger domain; SID, SRC-1 interacting domain; MDM2, p53 E3-ubiquitin protein ligase homolog; ATF, activation transcription factors; TBP, TATA-binding protein. Taken from Valor et al., 2013.

However, several studies have demonstrated by gene profiling analysis that the loss of CBP and p300 proteins only caused a reduced number of transcriptional changes, which were in some cases very modest in magnitude (Chen et al., 2010; Viosca et al., 2010; Lopez-Atalaya et al., 2011; Valor et al., 2011). Furthermore, transcriptional events related to plasticity, such as activity-driven gene expression in KAT3-deficient mice, seem largely spared (Alarcon et al., 2004; Valor et al., 2011)

although in long-term synaptic rearrangements CBP is required for environmental enrichment-induced neurogenesis and cognitive enhancement (Lopez-Atalaya et al., 2011). In addition, experiments in mouse embryonic fibroblasts (MEFs) derived from the KIX knock-in mice revealed a significant impact in only a small subset of CREB-targets genes (Xu et al., 2007). The key features that determine the extent to which an endogenous CREB target gene requires CBP/p300 are not completely clear. It is possible that the number of CREB binding sites may be one limiting factor (Kasper et al., 2010). Similar evidences were observed from the study of hypoxia-responsive gene expression in MEFs deficient for both CBP/p300 CH1 domain function (Kasper and Brindle, 2006). These findings suggest that there are others coactivator mechanisms independent that can provide compensatory coactivation functions in certain target genes (Xu et al., 2007). Regarding the KAT activity, the loss of CBP in forebrain neurons of adult mice also indicates the limited impact over transcription of dramatic reduction of histone acetylation (Valor et al., 2011). Indeed, experiments in MEFs from double knockout mice for CBP and p300 showed almost complete loss of histone H3K18 and H3K27 acetylation but limited transcriptional effects (Jin et al., 2011). Interestingly, some of these transcriptional deficits were rescued by overexpressing the CREB-regulated transcription coactivator 2 (CRTC2), a protein without KAT activity (Bedford and Brindle, 2012). As H3K27ac is an active transcription mark that can be used to discriminate active from inactive or poised genes (Creyghton et al., 2010), this data raise the question regarding which is the particular stage or conditions for these epigenetic marks to act as stimulators of transcription.

1.3.3 Experimental models of Rubinstein-Taybi syndrome

A wide number of CBP- and p300-deficient mouse strains have been developed making possible the modeling of specific endophenotypes of RSTS in the mouse. **Table 3** briefly summarizes different mouse models currently available for investigating RSTS.

Table 3. Neurological traits in mouse strains with deficient CBP activity

RSTS model	*Mutation*	*Pattern of expression of the mutation*	*Phenotypic features*
$CBP^{+/-}$	Null allele heterozygous: 50% reduction of CBP level	Ubiquitous	Skeletal abnormalities, growth retardation, genetic background effect on viability (Alarcon et al. 2004, Levine et al. 2005, Tanaka et al. 1997,2000).
$CBP^{+/\Delta}$	Truncated allele heterozygous: expression of dominant-negative truncated protein	Ubiquitous	Skeletal abnormalities, growth retardation, reduced viability (Oike et al. 1999a, Bourtchouladze et al 2003, Oike et al. 1999b, Yamauchi et al 2002).
$CBP^{+/-}$	Monoallelic inactivation of the CBP gene: deletion of the CH1 domain (aa 340–443) and replaced by a neomycin resistance cassette	Ubiquitous	Abnormal skeletal patterning, defects in hematopoietic differentiation, growth retardation and craniofacial abnormalities (Kung et al. 2000).
$p300^{+/-}$	Truncation of the protein after CH1 by removing the aa 302–509	Ubiquitous	Defects in neurulation, cell proliferation, and heart development (Yao et al. 1998).
CBP/$p300^{+/-}$	Inactivating point mutations in the KAT domain of either CBP (residues W1503 and Y1504) or p300 (W1466 and 1467)	Ubiquitous	Delayed terminal differentiation and a reduced muscle mass in $p300^{+/-}$ (Roth et al. 2003).
$cbp^{KIX/KIX}$	Triple point mutation in the KIX domain in homozygosis	Ubiquitous	Smaller body size and reduced thymus volumen (Wood et al. 2006, Kasper et al. 2002)
CBP/$p300^{CH1/+}$	Deletions the CH1 domain of CBP (aa 342–393) and p300 (aa 329–379)	Ubiquitous	Lung defects in $CBP^{CH1/+}$ (Kasper et al. 2005).
Cre;$CBP^{flox/flox}$	Introduction of loxP sites flanking exon	Disruption of CBP in	Phenotype comparable to the two previously

	7 of CBP	principal forebrain neurons	established mutant *CBP* alleles: $CBP^{+/-}$ and $CBP^{+/\Delta}$ (Tanaka *et al.*, 1997, 2000; Oike *et al.*, 1999; Zhang et al. 2004).
Cre;$CBP^{flox/flox}$/ Cre;$p300^{flox/flox}$	Introduction of loxP sites flanking exon 9 of CBP Introduction of loxP sites flanking exon 9 of p300	Disruption in mammary gland, salivary gland, skin, and hematopoietic cells in bone marrow, thymus, and spleen.	T-cell lymphomagenesis (Kang-Decker et al. 2004). Increased number of $CD8^+$ single+ thymocytes in *CBP* mutants (not observed in *p300* mutants). T cells completely lacking both CBP and p300 did not develop normally and are rare in the periphery (Kasper et al. 2006).
CBP(HAT-)	Tetracycline-inducible transgene encoding a CBP protein lacking HAT activity	CA1, dentate gyrus, caudate putamen and neocortex	Impaired NOR (24h) and MWM performance (Korzus et al. 2004).
CBPΔ1	Transgenic overexpression of dominant negative truncated protein	Hippocampus, amygdala, striatum and cortex	Impaired FC-Cx (24h) and MWM performance (Wood et al. 2005)
p300Δ1	Truncated p300 (aa 1–1031) lacking the KAT domain and the C-terminal half of the protein		Impaired long-term recognition memory and contextual fear memory (Oliveira et al. 2013)

aa: amino acids, NOR: novel object recognition, MWM: Morris water maze, FC-Cx: contextual fear conditioning; null mutants (gray), knock-in mutants (pink), conditional knock out mutants (violet), transgenic mutants (green).

1.3.4 Developmental and adult component of Rubinstein-Taybi syndrome

Developmental programs are critically affected by changes in epigenetic mechanisms (Gifford et al., 2013; Xie et al., 2013; Zhu et al., 2013). In particular, the relevance of epigenetic mechanisms in the maintenance and regulation of cell fate decisions have been clearly demonstrated in reprogramming experiments in which adult cells are forced to go backwards in development to generate induced pluripotent stem cells followed by re-differentiation toward different cell types. The residual epigenetic signature characteristic of the original somatic cell (epigenetic memory) not only favors the subsequent differentiation to lineages related to the tissue of origin but also restrict the differentiation toward alternative cell fates (Kim et al., 2010). Hence,

not surprisingly, the mutation of genes encoding epigenetic factors can severely alter developmental processes. However, epigenetic mechanisms also can contribute to control specific differentiation programs in adult somatic cells (Berdasco and Esteller, 2013).

CBP and p300 knockout suffer early embryonic lethality, which complicate the investigation of the role of CBP and p300 in adult cell lineages (Kasper et al., 2010). Fortunately, this problem can be circunvent by the creation of conditional knockout (Novak et al., 2012) strains using the Cre/LoxP system, i.e., mice bearing cbp^{flox} and $p300^{flox}$ alleles. The investigation of these cKO mice has indicated that both proteins have distinct roles in defined cell lineages and that the loss of both genes extremely severely affects cell proliferation (Kasper et al., 2006; Xu et al., 2006).

In mammals, both CBP and p300 proteins are first required for neural tube closure at the three-layer embryonic stage and later their expression decay (Partanen et al., 1999; Bhattacherjee et al., 2009). But still, these two proteins are also involved in the differentiation of neurons and glial cells from cortical precursors at later stages (Wang et al., 2010; Tsui et al., 2014). During development, early lethality has been detected. In homozygous mice bearing cbp- or p300-null alleles (Yao et al., 1998; Oike et al., 1999; Tanaka et al., 2000) it has been observed that death may occur by exencephaly (Yao et al., 1998; Kung et al., 2000; Tanaka et al., 2000), abnormal blood vessel formation (Oike et al., 1999, Tanaka et al., 2000) and heart development defects (Yao et al., 1998) whereas heterozygous mice ($cbp^{+/-}$ and $p300^{+/-}$) are viable and fertile but exhibit craniofacial dysmorphia (prominent forehead, blunt nose, and large anterior fontanel) and other RSTS-associated skeletal abnormalities (Tanaka et al., 1997; Oike et al., 1999; Viosca et al., 2010).

In adulthood, animal models indicate that the lack of proteins with KAT activity, like CBP or p300 in the brain, also contributes to the cognitive impairment in RSTS (Alarcon et al., 2004; Korzus et al., 2004; Viosca et al., 2010; Lopez-Atalaya et al., 2011) revealed for instance by defect in environment-induced neurogenesis as well as impaired EE-mediated enhancement of spatial memory and pattern separation ability. In addition, these changes were accompanied with an attenuation of the transcriptional programme induced in response to EE and with deficits in histone acetylation at the promoters of EE-regulated and genes related with neurogenesis (Lopez-Atalaya et al., 2011). These phenotypes seem relatively modest when compared with the dramatic consequences of KAT ablation during development. This

observation is in concordance with the idea that epigenetic marks are more critical during cell differentiation and lineage specification than the maintenance of transcription programs in differentiated cells (Lopez-Atalaya et al., 2014). In the context of IDDs a challenging point would be to distinguish the role of altered epigenetic mechanism in both developmental and adult stages.

1.4 Epigenetic therapies in Huntington's disease and Rubinstein-Taybi syndrome

Currently, HD and RSTS have no effective therapy. In spite of extensive research, treatment options for patients continue limited, and generally, only provide modest symptomatic relief. The approaches as potential treatments for these diseases can be divided in pharmacological and genetic treatments.

1.4.1 Pharmacological approaches

The development of HDACi has allowed the pharmacological manipulation of histone acetylation levels to attempt the treatment of multiples neurological disorders as well as cancer (Kazantsev and Thompson, 2008). The use of these compounds lead to an accumulation of acetylated targets including histone and non-histone substrates both in nucleus and cytoplasm (Chueh et al., 2014). Administration of HDACi (see **Fig. 7**) has consistently showed therapeutic potential in models of HD, aimed at restoring histone acetylation deficits caused by diminishion of KAT activity (section 1.2.6). Therefore the final target of the pharmacological approach is restorement of the transcriptional dysregulation for relevant genes involved in neuronal functioning and survival. In fact, some studies demonstrate phenotypical amelioration with transcriptional rescue of specific genes (Steffan et al., 2001; Ferrante et al., 2003; Gardian et al., 2005; Sadri-Vakili et al., 2007; Kazantsev and Thompson, 2008; Thomas et al., 2008) although genome-wide studies revealed that in most of the cases the impact over transcription of this type of approach is complex. Unfortunately, the benefits of pharmaceuticals therapies still are quite limited. On top of this, an important caveat is that overdose may have deleterious effects (Valor et al., 2013).

HDACi generally exert a broad action on HDACs (excluding HDAC class III), although HDACi 4b and related compounds may have more specificity against HDAC1 and 3 (Jia et al., 2012). Regardless of a specific HDAC suppression in transformed cells sensitive to HDACi-induced cell death in HD (Dokmanovic et al., 2007), the beneficial effect of HDACi seems to be not predominantly mediated through the inhibition of a particular HDAC (Benn et al., 2009; Bobrowska et al., 2011; Moumne et al., 2012). The situation is more complex when considering that HDACs have many protein substrates, in addition to histones, involved in the regulation of gene expression, cell proliferation and cell death (Kazantsev and Thompson, 2008). This is well exemplified by Dompierre et al., 2007. Consequently, they can produce pleiotropic effects. Also, the chronic treatment with these compounds might involve significant side effects due to the indiscriminate promotion of high levels of acetylation. The molecular mechanisms by which HDACi exerts its beneficial and toxic effects are currently not clear, nor whether these opposite effects can be dissociated.

In the case of epigenetic therapy for RSTS, a crucial experiment came from the Kandel´s lab. This group showed that the HDACi SAHA restored the deficits in hippocampal L-LTP and long-term fear memory observed in the null allele mouse model for RSTS (Alarcon et al., 2004). Similarly, Korzus and colleagues demonstrated that memory deficits in mice lacking CBP KAT activity were rescued by TSA (Korzus et al., 2004). Additionally, other studies in homozygous $CBP^{KIX/KIX}$ showed impairment in object recognition (Wood et al., 2006) that were reverted by HDACi (Stefanko et al., 2009). Importantly, acetylation levels were normal in those mutants. Furthermore, $CBP^{KIX/KIX}$ mutant mice have shown that TSA-treatment increases the expression of specific genes during memory consolidation and synaptic plasticity (Vecsey et al., 2007; Haettig et al., 2011). However, the situation is different in mice showing complete loss of CBP function in forebrain. In this case HDACi was not efficient rescuing short- or long-term memory alterations (Chen et al., 2010). In agreement with this, memory deficits generated by ablation of CBP in CA1 hippocampal area were not rescued when treated with the HDACi sodium butyrate (SB) (Barrett et al., 2011).

Other chromatin remodeling approaches are the anthracyclines antibiotics such as mithramycin and chromomycin. The anti-tumor properties are ascribed to their inhibitory effects on replication and the transcription process. These compounds

directly bind via the minor groove to DNA sequences with guanosine-cytosine (GC) specificity and may interfere with binding of transcription factors to DNA. It is possible to manipulate histone methylation indirectly, by using GC-binding anthracyclines (Chakrabarti et al., 2000; Piekarski and Jelinska, 2013). It has been demonstrated that interaction of mithramycin with the minor groove of DNA can inhibit transcription factors of the Sp family, suppressing the expression of the methyltransferase SETDB1/ESET expression and reducing hypermethylation of histone H3K9 in HD animal models (Ryu et al., 2006). Anthracycline compounds have also been demonstrated to interact directly with core histone proteins H3 and H4 (Rabbani et al., 2004), as they can also reverse the hypoacetylation of histones H3 and H4 (Stack et al., 2007). In any case, amelioration has been achieved in the tested animal models (Ferrante et al., 2004; Ryu et al., 2006; Stack et al., 2007), in the latter case concomitant to a partial reversal of the HD transcriptional dysregulation.

1.4.2 Genetic approaches

Genetic approaches are based on the addition of a corrected copy of a defective gene or the inactivation of a mutated gene that is operating improperly. Although such approaches currently have very limited usability in humans, their use in animal models is essential to clarify the etiology of specific symptoms. HD is caused by a single mutation at a defined locus, thereby this disease is potentially amenable to gene therapy (Zhang and Friedlander, 2011). On the other hand, there are therapies that target a specific gene mutation by RNA interference (RNAi) avoiding the translation of a key mRNA. Most gene therapy studies employ viral vectors to express a gene of interest in host cells (McBride and Kordower, 2002; Gasmi et al., 2007; Ramaswamy et al., 2007). This approach has allowed the over-expression of CBP in mouse models mimicking AD with promising results (Liu et al., 2012), in Drosophila model of polyQ disease (Taylor et al., 2003) as weel as models of amyotrophic lateral sclerosis (ALS) (Rouaux et al., 2003).

Objectives

1. To characterize the progression of neuropathology in HD82Q mice, a mouse model of early-onset polyQ disease, with special emphasis on the onset of transcriptional dysregulation.

2. To perform the first genomic profiles for histone deacetylation in an animal model of polyQ disease using state-of-the-art ChIPseq methodology.

3. To investigate both locally and genome-wide the correlation between altered levels of histone acetylation and transcriptional dysregulation in neurons in the brain of HD82Q mice.

4. To identify genes in which transcriptional and epigenetic dysregulation concur to define a disease signature conserved across different experimental models of the disease.

5. To investigate the existence of changes in bulk histone acetylation levels for the four-nucleosome histone in different experimental models of HD.

6. To explore the co-ocurrence of histone acetylation changes with other epigenetic alterations at pathology's relevant dysregulated genes.

7. To characterize the developmental consequences of CBP ablation and lysine hypoacetylation in the nervous system.

8. To develop a genetic tool for increasing lysine acetylation levels in neurons and validate its therapeutic potential in an experimental model of RSTS.

Materials and Methods

3.1 Mouse models of neurological diseases

All animals were bred and maintained in our SPF facilities. Experimental protocols were consistent with European regulations and approved by the Institutional Animal Care and Use Committee.

3.1.1 Mouse models of Huntington's disease

- *N171-82Q mouse strain:* The transgenic strain PrP-htt-N171-82Q mice express a transgene of 171 amino acid mHTT protein with 82 polyQ residues under the control of prion promoter (restricted to neurons in the CNS) (Schilling et al., 1999). In our study these mice were acquired from Jackson Laboratories (stock No. 003627) and maintained in a DBA and C57BL/6J mixed background (50:50) because the viability of the strain is compromised in a pure C57BL/6J background.

Sodium butyrate (SB) (1.2 mg/kg in PBS) was administered by intraperitoneal injection in N171-82Q mice. Vehicle-treated mice received an injection of PBS. Sampling was performed 30 min later, before the decay of the transient increase of acetylation (Valor et al., 2011).

- *R6/1 mouse strain:* These mice were acquired from Jackson laboratorIes (stock number 006471) and maintained in a pure C57BL/6J background. R6/1 strain shows like the N171-82Q an early onset and rapid progression of the disease (Mangiarini et al., 1996). R6/1 mice express *exon* 1 of the human *HTT* gene with 115 CAG repeats. The transgene expression is driven by the human *HTT* promoter, which permits the ubiquitous expression throughout the mouse brain.

- *YAC128 mouse line:* These mice were acquired from Jackson laboratories (stock number 004938) and maintained in a pure C57BL/6J background. YAC128 line expresses multiple copies of full-length human HTT with 128 glutamine repeats on a yeast artificial chromosome (Slow et al., 2003). The advantage of full-length transgenic models is that includes all the local conserved regions of *mHTT* human gene, which are highly conserved across species allowing a better reproduction of the HD symptoms (Kent et al., 2002). Thus, it would be expected that is regulated in the mouse as it is in humans, defined by its native promoter and internal regulatory elements. One characteristic of this reproducibility is that YAC128 mice line presents a slow progression of the disease as is observed in HD patients. However, YAC128

mice presents relatively robust motor dysfunction (i.e. rotarod deficits), psychiatric-related behaviors and cognitive deficits, and selective atrophy in the striatum and cortex that later extent to the cerebellum (Hodgson et al., 1999; Van Raamsdonk et al., 2005; Gray et al., 2008).

3.1.2 Mouse model of RSTS

- *Nes-cre::CBP$^{f/f}$ mouse strain:* In our group, we have generated mice lacking CBP in the neural line through the crossing of CBP floxed mice (CBP$^{f/f}$) with transgenic mice that express the cre recombinase under the control of the nestin promoter (Stock number 003771, The Jackson Laboratory) and the CBP floxed allele (Nestin-cre $^{+/-}$ / CBP$^{f/-}$ mice). We will refer to this line as Nes-cre::CBP$^{f/f}$.

3.2 Behavioral procedures

For all behavioral tasks, transgenic mice were analyzed with wild-type (wt) littermates of the indicated age, and procedures were conducted during the light phase of the light cycle. Experimenters were blind to genotypes. The result of the PCR-based genotyping was provided as a factor for statistical analysis of the behavioral data after task analysis. If not indicated, a Student's t-test was used for statistical analysis in all the behavioral experiments.

3.2.1 Morris water maze

Experiments were carried out in a 170-cm pool using SMART software (S.L. Panlab). The basic water maze experiment was divided in two phases:

1) In the visible platform (VP) task, the animal was forced to swim in a pool filled with opaque water and learnt to associate escape from the pool with finding a platform submerged 1 cm under the water. The platform location changed every trial and was cued with a black bar (Viosca et al., 2009). Mice received four trials of 120 sec maximum, separated by a 60–120 min intertrial interval every day.

2) In the hidden platform task, the basic procedures were the same as in the visible platform task, but the submerged platform was not cued and its position did not change during the task. Therefore, the animal is forced to remember the position of the hidden escape platform using distal surrounding cues. Probe trials of 60 sec, in which the platform was removed, were performed on specific days (8 and 12) during

the HP procedure to assess memory formation. After 60 sec, mice were gently guided to the original platform location and allowed to remain in this position for 15 sec to avoid extinction. For the analysis of probe trials, a series of parameters were calculated: quadrant occupancy (percent of time) including target (platform) quadrant (TQ), number of crossings in an annulus (the double area surrounding the platform), thigmotaxis (tendency to follow the wall around the outer perimeter of the tank), speed, path length, etc.

3.2.2 Rotarod

To assess motor coordination and balance, mice were trained to maintain on a rotating rod at fixed or accelerating speeds. Mice were first habituated to the RotaRod (Panlab S.L, Barcelona) at a constant speed (4 rpm) until they were able to stay on the rod for 5 min in both genotypes. On testing day, the Rotarod was set to accelerate from 4 to 40 rpm over 5 minutes. The latency to fall (first slippery) was measured.

3.2.3 Grip strength

Grip strength has been developed to measure muscle strength in rodent forelimbs as an indicator of neuromuscular function. Each mouse was held gently by the base of its tail over the top of the grid so that only its front paws were able to grip the trapeze-like horizontal bar of the grip strength meter (Ugo Basile, etc). With its torso in a horizontal position the mouse was pulled back steadily until the grip was released down the complete length of the grid/bar and the maximum force applied as the peak tension (in grams) is measured. Grip strength values were the average of six measures.

3.2.4 Feet clasping

In a 5-min tail suspension, feet clasping was classified in mild and severe according to the number and duration of the hind-paw clasping (threshold: 1-2 times of <3 s each).

3.3 DNA constructs

All cloning primers used for cloning can be found in **Table 4**. Plasmids and sources

thereof used in this study can be found in **Table 5**.

- *pSyn-wtHTT-GFP and pSyn-mutHTT-GFP*: Shorter Htt fragments of the pCI-neo1955-15Q and pCI-neo1955-128Q plasmids were obtained by conventional PCR using the Pfu DNA polymerase (Fermentas, ThermoFisher) following *suppliers' instructions.* Primers end contained sites for XhoI and BamHI to permit an open reading frame cloning into the vector with GFP. Next, the wtHTT-GFP and mHTT-GFP fragments were digested with BglII and NotI and subcloned into the lentiviral vector (Gascon et al., 2008) (where the second synapsin promoter has been removed (pSyn-WPRE)) at the BamHI and NotI cloning site to get different versions of plamids: pSyn-cyt wtHTT-GFP, pSyn-nuc wtHTT-GFP, pSyn-cyt mHTT-GFP and pSyn-nuc mHTT-GFP. Next, the production of lentiviral pseudovirions (LV) was carried out as described in (Gascon et al., 2008) with minor modifications (Benito et al., 2011). Both wild-type fragments were undistinguishable in the culture preparations, and therefore only the longest version (cyt) is shown and referred to as pSyn-wtHTT-GFP.

- *pCAG-GFP-wtHTT and pCAG-GFP-mutHTT:* The pCI-neo1955-15Q and pCI-neo1955-128Q plasmid, were digested with XhoI restriction enzyme and subcloned into the pEGFP-C3 vector in order to fusion the EGFP protein with the protein of interest. The entire fragment was obtained after digestion with NheI and KpnI restriction enzimes and cloned into the NheI/KpnI site of pCAGGS/ES vector (kindly provided by Eloisa Herrera´s lab) (**Fig. 10**). Expression of the fluorescent protein was under the control of the CAG promoter, a modified chicken-actin promoter with a cytomegalovirus immediate (CMV) early enhancer (Garcia-Frigola et al., 2007).

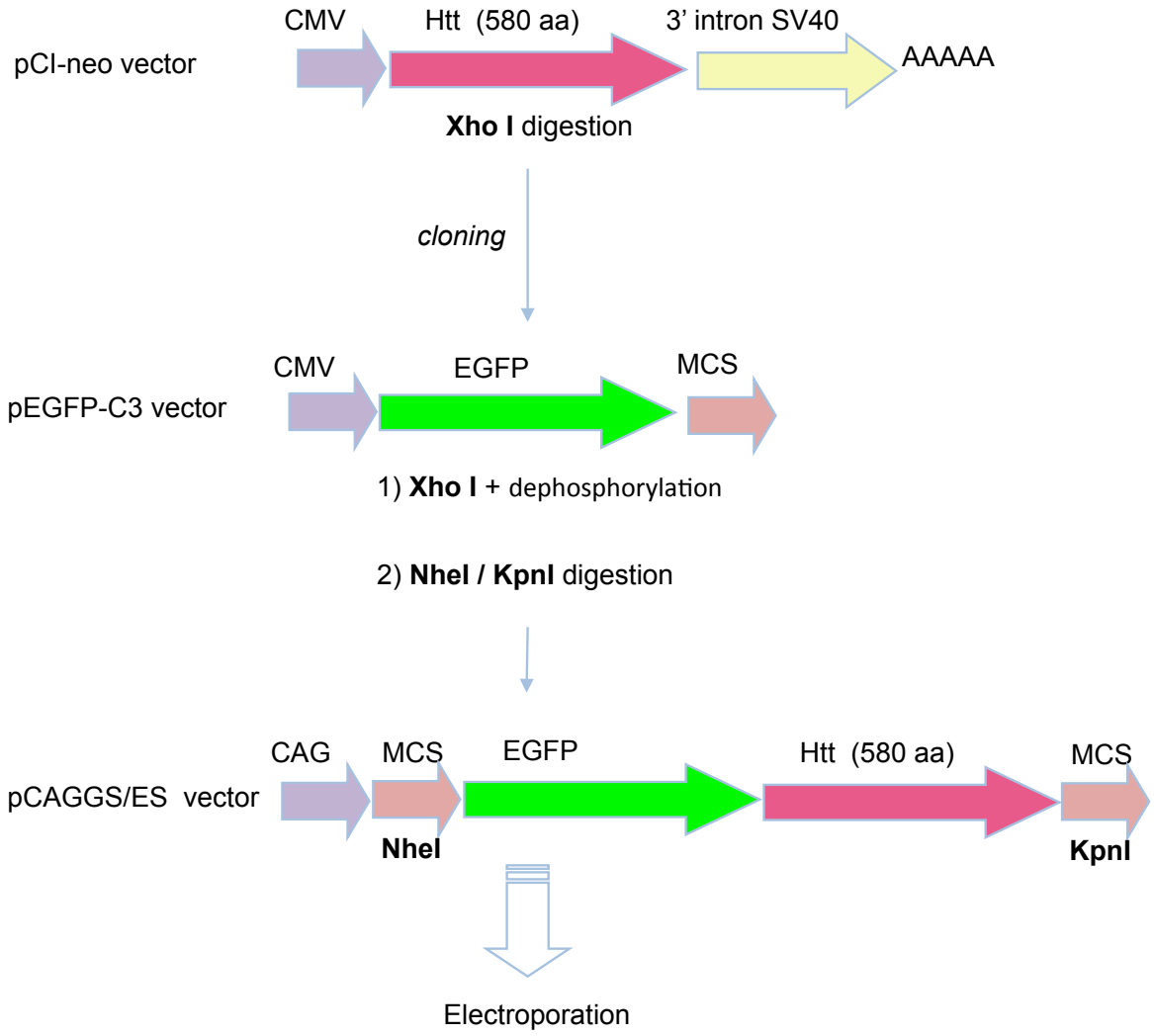

Figure 10. mHTT fusion protein cloning strategy. CMV: cytomegalovirus promoter; CAG: promoter (chicken β-actin promoter with CMV enhancer), restriction enzymes are depicted in bold type.

- *pSyn-NLS-GFP and pSyn-NLS-KAT-GFP:* The lentiviral plasmid in primary cultures infection of the fusion protein NLS-KAT-GFP in neurons was generated by fusioning the KAT domain of CBP with a nuclear localization signal (NLS) into the pEGFP-N3 vector (Clontech). First, NLS fragment headed by a Kozaq signal was obtained by hybridizing two pairs of primers (**Fig. 11**) with cohesive ends to permit cloning at BglII and HindIII sites of the pEGFP-N3 vector. Second, the KAT domain (from 1099 to 1758 aa) as defined by Bannister and Kouzarides (Bannister and Kouzarides, 1996), 1996 was obtained by PCR using the primers KAT-forward and KAT-reverse (see

Table 4) containing the sites for HindIII and BamHI at their 5' end to permit an oriented cloning into the vector with the NLS. Third, The NLS-KAT-GFP fragment was digested with BglII and NotI and subcloned into the lentiviral vector (pSyn-WPRE) at the BamHI and NotI cloning site. A negative control plasmid was similarly obtained but without the KAT domain insertion.

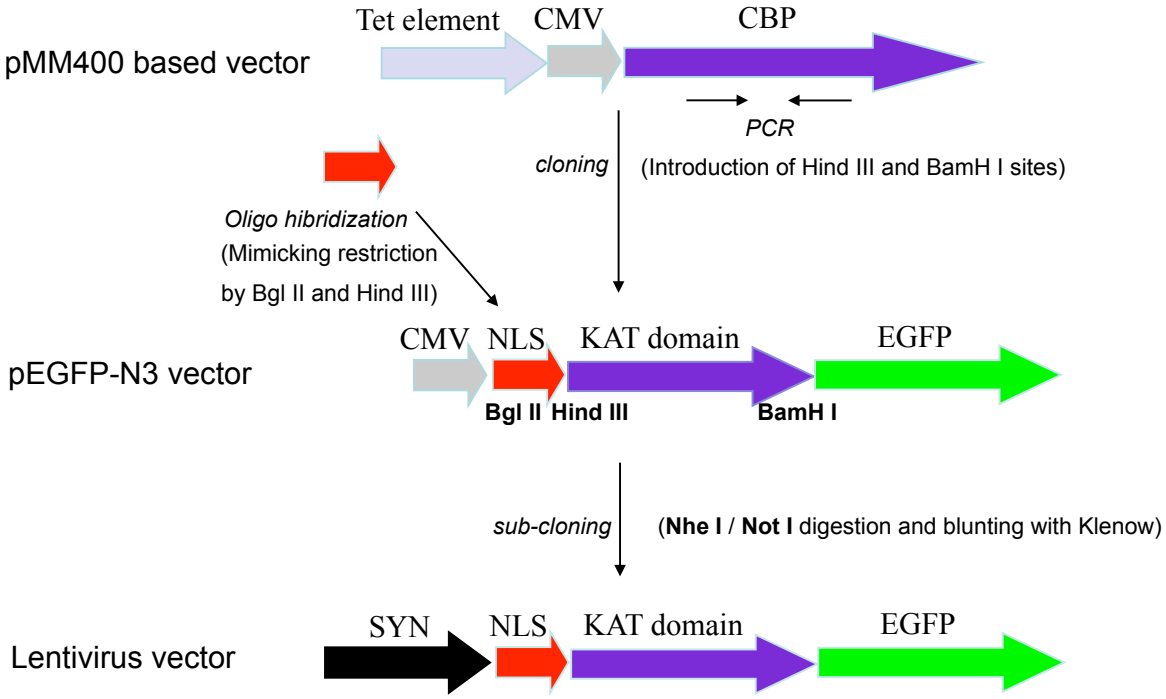

Figure 11. KAT domain cloning strategy. CMV: cytomegalovirus promoter; CBP: CREB binding protein, NLS: nuclear localization signal, Syn: synapsin promoter, restriction enzymes are depicted in bold type.

- *pCAG-NLS-KAT-GFP:* The entire fragment NLS-KAT-GFP was obtained after digestion with NheI and NotI restriction enzymes and cloned into the XbaI/NotI site of pCAGGS/SE vector. A negative control plasmid was similarly obtained but without the KAT domain insertion.

Table 4. Cloning primers

Primer name	*Sequence (5' -> 3')*
5' CBP KAT F	CGAGCTCAAGCTTCTAGAAGCACTCTATCGACAG
3' CBP KAT R	GGTGGCGATGGATCCACCCTGACTGCTGCCCTC
5' Htt F	AGATCTCTCGAGATGGCGACCCTGGAAAAGC
3' Htt R	AAGCTTGGATCCCTGA GGAAGCTGAGGAGG

Table 5. Plasmids used in this work

Plasmid name	*Source*
pCI-neo1955-15Q	Dr. Hayden, British Columbia University
pCI-neo1955-128Q	Dr. Hayden, British Columbia University
pSyn-WPRE-Syn-WPRE	Dr. Francisco Gomez Scholl, University of Sevilla
pSyn-WPRE	De novo cloning
pSyn-cyt wtHTT-GFP	De novo cloning
pSyn-cyt mHTT-GFP	De novo cloning
pSyn-nuc mHTT-GFP	De novo cloning
pCAG-GFP-wtHTT	De novo cloning
pCAG-GFP-mHTT	De novo cloning
pSyn-NLS-GFP	De novo cloning
pSyn-NLS-KAT-GFP	De novo cloning
pCAG-NLS-KAT-GFP	De novo cloning
pCAG-NLS-GFP	De novo cloning

3.4 Cell lines and primary cultures

3.4.1 Established cell lines cultures

HEK293 and HEK293T (bearing the large T antigen from SV40) cells were grown in a monolayer under optimum growth conditions (37°C, 5% CO_2) in DMEM (21969 and 11960 Gibco®, respectively) supplemented with 10% fetal bovine serum (FBS, Gibco®), 2 mM glutamine (Gibco®), 10,000 U/ml of penicillin and 10,000 µg/ml of streptomycin (Gibco®). All cell lines were maintained in 10 cm diameter plates and split every 3-4 days when they were 70-80 % confluence.

PC12-TetOn-HD23/72Q cells (kindly provided by Dr. Rubinsztein, Cambridge Institute of Medical Research (Wyttenbach et al., 2001)) were maintained in DMEM (Gibco, 11960 and 21969 respectively) supplemented with 10% horse serum (Gibco), 5% Tet System fetal bovine serum (FBS, Clontech), 1% penicillin-streptomycin (Gibco), 200 µg/ml G418 (Invitrogen) and 100 µg/ml of hygromycin B (Clontech). For the induction of the transgene, doxycycline (1 µg/µl) was applied to the medium at the indicated times. Doxycycline and G418/hygromycin B were replaced every 2 and 3-4 days, respectively.

3.4.2 Primary dissociated hippocampal cultures

The procedure was based in (Benito et al., 2011). Briefly, the day before culture, 24-well plates (BD Falcon™) containing coverslips were treated with Poly-D-Lysine (0.5 mg/ml, Sigma-Aldrich) at room temperature O/N. The next day, a pregnant mouse was sacrificed by cervical dislocation. Experimental animals were Swiss Albino wild-type mouse embryos at E17.5. Embryos heads were separated and the brains were pulled out from the skull and transferred into a Petri dish with pre-cooled HBBS (Gibco®). Then the brains were cut along midline and the hippocampi region was extracted. Subsequently the tissue was digested with 0.25% trypsin, 0.1 mg/ml of DNase I (Invitrogen) and incubated in a water bath at 37°C for 15 min. The tissue was washed three times with fresh plating medium (PM) (DMEM 11960 Gibco® supplemented with 10% FBS, 0.45% glucose, 2mM glutamine and penicillin/streptomycin 100U/ml-100 µg/ml) to inactivate the trypsin. After dissociation of the tissue the cell density were determined by measuring the cell number in a Neubauer chamber (Marienfeld) and seeded at a density of ~130.000 cells per well. The cells were incubated at 37ºC and 5% CO_2 during 2-3 h and the PM was replaced

for maintenance medium (MM) (Neurobasal Gibco®, supplemented with B27, 2 mM glutamine and penicillin/streptomycin 100U/ml-100 µg/ml). During the experiment the cells were maintained in MM. The day of plating is considered "Day *in vitro*" 0 (DIV0).

3.4.3 Cell culture infection

The day of virical introduction is considered "Day of infection" 1 (1DINF). Primary hippocampal neurons were infected at 1DINF by adding the necessary volume of the concentrated viral preparation to achieve a theoretical MOI (Multiplicity Of Infection) of 1000 (Benito et al., 2011). Due to the tittering procedure employed (see item 5.1), we estimated that the effective MOI was 1-10. In all cases, percentage of infection was visually estimated to be close to 80% for the neurons.

3.4.4 Transient transfection

Neuronal transfection for morphometric assays were performed with Lipofectamine™ 2000 (Invitrogen) according to the manufacturer's instructions. Briefly, the medium was replaced with prewarmed culture medium devoid of Neurobasal and cells were returned to the incubator for recovery. 0.8 µg of DNA was used per well of a 24-well plate. DNA and lipofectamine (2 µl per well of a 24-well plate) were independently mixed with DMEM/Neurobasal and incubated for 5 min at RT. Later, they were mixed and incubated for 20 min at RT and added dropwise to the cell culture. The transfection medium was replaced with fresh culture medium after 1-2 h.

3.4.5 Cell death assays

Cell death estimation was based on lactate dehydrogenase (LDH) activity, which was was measured with kit "Cytotoxicity Detection kit PLUS" (Poirier et al.). Briefly, 50 µl Reaction mix were added to each well and the plate was incubated at RT for 20-30 min. Finally, 25 µl Stop buffer was added to each well and absorbance was measured at 490 nm in a Benchmark microplate reader (BioRad). LDH activity was expressed as mean fold activity vs. untreated control. Manufacturer's instructions were followed.

3.5 Lentiviral vectors

3.5.1 Lentivirus production, titration and infection

The production of lentiviral pseudovirions (LV) was carried out as described in

(Gascon S. et al. 2008). Briefly, HEK293T cells were plated in 15 cm plates (Starsted) at a density of 10 x 10^6 cells per plate and left to recover overnight (o/n). 24 h later, when cells were 70-80% confluent approximately, the co-transfection was performed by the Calcium Phosphate ($CaPO_4$) Method. The following plasmids were mixed: 20 µg of transgene-bearing plasmid, 15 µg of pCMV-*∂*8.9 which contains the *gag* and *pol* viral genes (that encodes for the viral capsid proteins and the reverse transcriptase respectively) and 10 µg of pCAG-VSVg plasmid encoding the VSV-G protein from the vesicular stomatitis virus (VSV) for pseudotyping and achieving pleiotropic infection. For each transfection 1.8 ml of H_2O, 2 ml of phosphate buffer (2X HBS: 50 mM HEPES and 1.5 mM Na_2HPO_4, 280 mM NaCl) and 0.2 ml of 2.5M $CaCl_2$ was added dropwise to the abovementioned suspension to induce precipitation of calcium phosphate particles bearing the three plasmids required for viral production. This mixture was added dropwise to the cells and media was replaced 4-6 h after transfection to prevent cell toxicity. 48-60 h post-transfection, the cell supernatant was collected, centrifuged at low speed (5min at 2000 rpm) and filtered (0.45 µm filters, Nalgene) to eliminate cellular debris in suspension. The filtered medium was transferred to a conical ultracentrifuge tube (Beckman 358654), which was sealed to avoid biological spills. The viruses were concentrated by ultracentrifugation at 25000 rpm in Optima L-100XP (Beckman) for 90 min to pellet viral particles. Then the supernatant was eliminated and the viral pellet was resuspended in 1% PBS volume 3 orders of magnitude smaller than the initial volume of cell supernatant. The viral suspension was stored at 4ºC O/N to facilitate manual resuspension and aliquoted for long-term storage at -80ºC.

Titration of the LV vector particles was performed by qRT-PCR. First of all, viral RNA was extracted with QIAamp Viral RNA Mini kit (QIAGEN). Next, the retrotranscription was performed using the procedures described section 3.12. A standard curve of known concentration of lentiviral plasmid copies was amplified in parallel in order to estimate the number of viral genomes in the original unconcentrated preparation. Unconcentrated viral preparations regularly fell in the order of 10^8–10^9 particles/ml. The effective titter is estimated at the range as the correction of 1000-fold concentration factor is the same as the overestimation of the titter due to contaminating genomic DNA and/or defective viral particles in the original preparation (Sastry et al., 2002). PyroTaq EvaGreen qPCR Mix Plus (Trembath et al., 2010) (Cultek) were used to quantitatively amplify the cDNA copies of the viral

genomes (see section 3.10).

3.5.2 Biosafety measures

All procedures were revised and approved by the in-house biosafety committee, and carried out in a designated area according to P-2 risk level.

3.6 In utero electroporation protocol

Pregnant females were deeply anesthetized with 5% isofluorane and placed under binocular microscope. Anesthesia during surgery with 1.5% isofluorane was administered through a facemask. An electrode puller was used to prepare fine-tipped micropipettes: borosilicate glass capillaries with 1.2 mm/0.68mm outer /inner diameter (1B120F-4; WPI, Saratosa, FL, USA), with a tip 8mm long and 40–50 µm of outer diameter, approximately. Capillaries loaded with DNA solution (1 µg/µl) was introduced into the embryo brain with 0.03% fast green in PBS (Sigma-Aldrich), and approximately 1 µl of DNA was pressure-injected into the cortico-striatal area. Next, a pin-and-paddle tweezers-type electrode (CUY650 P5; NEPA Gene, Chiba, Japan) was used to electroporate the DNA into the striatum. Square electric pulses (50 ms) were passed using an electroporator (CUY21EDIT; NEPA Gene). Electric pulses were set at constant voltage of 45V for E14 embryos. Under these conditions, amperage readings were 75 ± 3mA (mean ± S.E.M.) for E14 embryos (Garcia-Frigola et al., 2007). The dam skin was suture-closed, and the animal was allowed to recover from the anesthesia. The electroporated animals were processed at different adult states after behavioral experiments and histological analysis.

3.7 Immunodetection and Immunoblotting analysis

3.7.1 Antibodies

Secondary biotinylated antibodies, streptavidin peroxidase conjugated and 3,3'-Diaminobenzidine (DAB) substrate were obtained from Sigma-Aldrich (**Table 6**).

Table 6. Antibodies used in this study

Antibody	*Host*	*Usual dilution*	*Source*
α-AcH2A (K5, 9, 13,15)	Rabbit	1:500	Millipore
α-AcH2B (K5, 12, 15, 20)	Rabbit	1:1000	Barco's lab (Sanchis-Segura et al., 2009)
α-AcH3 (K9, 14)	Rabbit	1:3000	Barco's lab (Sanchis-Segura et al., 2009)
α-AcH4 (K5, 8, 12, 16)	Rabbit	1:500	Barco's lab (Sanchis-Segura et al., 2009)
α-H3 K4me3	Rabbit	1:300	Millipore
α-H3 K9me2/3	Mouse	1:1000	Abcam
α-H3 K27me3	Mouse	1:500	Abcam
α-H2Aub	Mouse	1:100	Millipore
α-Huntingtin clone mEM48	Mouse	1:200	Chemicon
α-H2B (07-371)	Rabbit	1:5000	Millipore
α-H3 (05-499)	Rabbit	1:5000	Abcam
α-MAP2 (clone HM-2)	Mouse	1:800	Sigma-Aldrich
α-ß actin (clone AC-15)	Mouse	1:10000	Sigma-Aldrich
α-tubulin acetylated	Mouse	1:10000	Sigma-Aldrich
α-GFP	Chicken	1:1000	Ave Labs
α-GFAP	Rabbit	1:1000	Sigma-Aldrich
α-NeuN	Mouse	1:3000	Millipore
α-NF-κB p65 (acetyl K310)	Rabbit	1:1000	Abcam
α-NF-κB p65	Rabbit	1:1000	Abcam
α-Acetyl p53	Mouse	1:1000	Abcam
α-Acetyl Lys	Rabbit	1:1000	Millipore
α-CBP (C-1)	Mouse	1:200	Santa Cruz
α-DARPP32	Rabbit	1:400	Abcam
α-DsRed	Rabbit	1:1000	Clontech
α-Rabbit-HRP	Goat	1:7500	Cell Signaling
α-Mouse-HRP	Goat	1:10000	Cell Signaling
α-Calbindin-D-28K	Rabbit	1:1000	Sigma-Aldrich

α-chiken-Alexa-488	Goat	1:500	Invitrogen
α-mouse-Alexa-594	Goat	1:500	Invitrogen
α-mouse-Alexa-555	Goat	1:500	Invitrogen
α-rabbit-Alexa-633	Goat	1:500	Invitrogen

3.7.2 Immunocytochemistry and Immunohistochemistry

After transfection or LV infection the cells were fixed with 4% paraformaldehyde (PFA) (Sigma-Aldrich) for 12 minutes. The cells were next rinsed 3 times with PBS (10 min each) and permeabilized for 10 min with PBS-T (PBS with 0.2% Triton-X100). Following permeabilization, they were incubated for 20 min in blocking buffer composed of 1.5% Newborn Calf Serum (NCS, GIBCO) in PBS. Cells were then incubated with a suitable primary antibody diluted in PBS-T + 1% NCS at 4ºC followed by washes with PBS and PBS-T and further incubation with secondary antibody for 1.5 h at room temperature. After additional washes, the cells were stained with 4'-6-diamidino-2-phenylindole (DAPI) 1 μM for 2 min. Subsequently, the coverslips were mounted with *SlowFade*® Antifade Reagent. The same procedure was applied with slides brain sections. Regarding DAB, to quench endogenous peroxidase (HRP) activity, the slides sections were incubated with peroxidase blocking reagent (3% H_2O_2) for 15 minutes. The subsequent steps were as mentioned above. Following, the samples were incubated with the biotinylated secondary antibody. For the detection, samples were incubated with Streptavidin-HRP conjugate (HSS-HRP) for 1 h at room temperature (RT) (due to the large enzyme to antibody ratio there is a degree of signal amplification which provides high sensitivity). Lastly, tissue sections were rinsed with peroxidase substrate solution (DAB Chromage/Substrate solution) carefully monitoring the intensity of the tissue Colored precipitate localized to the sites of antigen expression as the chromogenic substrate was converted by HRP enzyme into insoluble end product and mounting with an organic Mounting media.

3.7.3 Protein extraction and western blot

Cells were placed on ice and the culture supernatant was removed. 100 μl of Protein Extraction Buffer (PEB: 50 mM Tris-HCL, 150 mM NaCl, 1 mM EDTA, 1% NP-40) containing Protein Inhibitor Mix (PIM, Roche) was added to each well and cells were

scraped from the glass coverslips. The protein extract was transferred to fresh tubes and SDS was added to a final concentration of 2% v/v. Samples were centrifugated at 13.000 rpm at 4ºC for 5 min and finally, loading buffer and 10% β-mercaptoethanol (Sigma-Aldrich M7154) were added from concentrated solutions to a final concentration of 1X. Prior to loading, samples were heated at 95ºC for 5 min to denaturalize the proteins.

For tissues samples, mice cortical, striatal, hippocampal and cerebellar samples were rapidly dissected using a chilled acrylic mouse brain slicer matrix (Zivic Instruments), frozen in dry ice and stored at -80ºC until further protein extraction (see the procedure above). Sample protein concentration was determined and equal amounts of protein were loaded in each lane.

Proteins extracts were separated by SDS-PAGE in gels containing 12-15% polyacrylamide/bisacrylamide and they were transferred to a nitrocellulose membrane (Pall Life Sciences) for immunodetection. The Ponceau solution (Sigma-Aldrich) was used to check the transfer. Blocking and primary antibody incubation was performed in PBS-T + 5% BSA. The secondary antibody was diluted in PBS-T + 1% BSA. Membranes were revealed with chemioluminiscence with the kit “Western Lighting Plus-ELC” (PerkinElmer) and image acquisition was done in an Intelligent Dark BpxII apparatus (FUJIFILM LAS-100 equipment (Fuji photo Film Co.)) and quantified using Quantity One 4.6 software (Bio-Rad, Inc.).

3.8 Microscopy and morphometric analysis

Immunostaining was examined by using Leica DM2500 fluorescence microscope. Images were recorded with a Leica DFC300 FX digital color camera and processed with Leica Application Suite (LAS) V3.8.0 imaging software. For Multi-Area Time-Lapse that enables multiple measurement points in glass slides, Confocal Laser Scanning Microscope Olympus FV1200 implemented with Olympus FV-ASW software was used. The IHC staining was performed as described above. Cell counting and signal intensities quantification was performed using ImageJ64 software. Morphological analysis was performed 24 h post-transfection after staining with the appropriate antibodies (see **Table 6**). Confocal images were acquired with a 1024 x 1024 resolution and the pixel intensity within the dynamic range of the detector. For spine density analysis, the 60X objective was used and approximately

6-10 sequential planes in Z were acquired with a step size of 0.5 µm. Spines count were manually performed in random order with the software ImageJ and are expressed as the normalized fold change in spine density (number of spines/10 µm length of dendrite).

3.9 MRI Imaging

Experiments were carried out in a horizontal 7T scanner with a 30 cm diameter bore (Biospec 70/30v, Bruker Medical, Ettlingen, Germany). The system had a 675 mT/m actively shielded gradient coil (Bruker, BGA 12-S) of 11.4 cm inner diameter. A ^{1}H rat brain receive-only phase array coil with integrated combiner and preamplifier, no tune/no match, in combination with the actively detuned transmit-only resonator (Bruker BioSpin MRI GmbH, Germany) was employed. Phantoms containing a mouse head in agarose were placed in a custom-made holder and positioned fixed in the magnet isocenter. T_2 weighted anatomical images were collected using a rapid acquisition relaxation enhanced sequence (RARE), applying the following parameters: field of view (FOV) 30x30mm, 15 slices, slice thickness 1mm, matrix 256 x 256, effective echo time (TE_{eff}) 56ms, repetition time (TR) 2s and a RARE factor of 8.The B0 field distribution in a large voxel (40x40x40 mm^3) containing the volume to be imaged was acquired (FieldMap). Samples were localized with a T_2weighted RARE sequence, and first- and second-order shims adjusted with MAPSHIM application in a sufficiently large voxel containing the brain. 3D data were acquired using a RARE 3D sequence with TR 1500 ms, TE_{eff} 46.8 ms, RARE factor 16 and 16 averages in a total acquisition time of 13.6 h. The matrix size was 300x200x170 using a FOV of 30x20x17 mm^3, which yielded an isotropic resolution of 100 µm. Data were acquired and processed with Paravision5.1 software (Bruker Medical GmbH, Ettlingen, Germany). After 3D data acquisition, new orthogonal planes were generated using Jive 7.9.0 application running under Paravision 5.1 software. Briefly, after rotating the image to obtain the desired orientations, new 2D images were created. Image resolution was digitally increased by linear interpolation rendering a final isotropic resolution of 30 µm.

3.10 RNA extraction, purification, RT-PCR and qRT-PCR

Total RNA from whole hippocampus, cortex, striatum, cerebellum and neuron cell culture were purified using TRI reagent (Sigma-Aldrich) according to the manufacturer´s instructions. For microarray experiments, RNA from 3 to 4 mice of the same age, sex, and genotype were pooled and further cleaned up using the RNeasy Mini Kit (Qiagen) according to manufacturer's recommendations. RNA concentration and purity was measured with a Nanodrop and the same amount of sample was retrotranscribed with the kit RevertAid (Fermentas) using hexamer random primer. Quantitative RT-PCRs (RT-qPCR) were performed in an Applied Biosystems 7300 real-time PCR unit using PyroTaq EvaGreen qPCR Mix Plus (Trembath et al.) (Cultek). Primers used are in the listed in **Table 7**. All primers pairs were tested for efficiency. Each independent sample was assayed in duplicate and normalized using glyceraldehyde 3-phosphate dehydrogenase (GAPDH) levels. Relative quantifications were performed with the ΔΔCT method with GAPDH as a normalizer.

Table 7. RT-qPCR primers

Gene	*Primer*	*Sequence (5´-> 3´)*
GFP	Forward	GGGCACAAGCTGGAGTACAACT
	Reverse	ATGTTGTGGCGGATCTTGAAGT
Nfya	Forward	ACAAGGGACGGTCACTGTGAC
	Reverse	TTTGGATAGCAGGCACAGAGC
Nfyb	Forward	GACAGCTACGTGGAGCCTCTG
	Reverse	AGTCCATCTGTGGCGGAGAC
Igfbp-5	Forward	AACACTGCCCACCCCAGAG
	Reverse	TTGAACTCCTGGAGGGAAGCT
Bdnf CS	Forward	GAAGGTTCGGCCCAACGA
	Reverse	CCAGCAGAAAGAGTAGAGGAGGC
Bdnf Prom. I	Forward	AAGTCACACCAAGTGGTGGGC
	Reverse	GGATGGTCATCACTCTTCTCACCT
Bdnf Prom. IV	Forward	GTAAGAGTCTAGAACCTTGGGGACC
	Reverse	GGATGGTCATCACTCTTCTCACCT

Arc	Forward	AAGACTGATATTGCTGAGCCTCAA
	Reverse	GCAGGAGAACTGCCTGAACAG
Penk	Forward	TCCCAGATTTTGAAAGAAGGCA
	Reverse	GACCATGTGATCGCGCTTCTCGTT
Nr4a1	Forward	GGCCTAGCACTGCCAAATTG
	Reverse	GCAGCACCAGTTCCTGGAAC
Npas4	Forward	CTGGCCCAAGCTTCTTCTCA
	Reverse	TCCATGCTTGGCTTGAAGTCT
cFos	Forward	GCTTCCCAGAGGAGATGTCTGT
	Reverse	GCAGACCTCCAGTCAAATCCA
Hpca	Forward	CTACATCAGCCGGGAGGAGAT
	Reverse	ATCTTGTAAATGGCCTGCACAA
Gapdh	Forward	CATGGACTGTGGTCATGAGCC
	Reverse	CTTCACCACCATGGAGAAGGC
Rin1	Forward	GCGGCTGCCAGAAGCTAGT
	Reverse	CCTGGAACATGAGCTCTGAGC
Iptka	Forward	TACACTCGGCTTTCGCATTG
	Reverse	CAAAGACACGGGTCACTTGCT

3.11 Microarray analysis

Total RNA (3-5 ug) for microarray analysis was sent to an external service (Servicio de Análisis Multigénico, Unidad Central de Investigación de Medicina (UCIM), Universidad de Valencia) for assessing RNA quality by Bioanalyzer. Subsequent labeling, hybridization into Affymetrix arrays, image scanning and retrieval of CEL files were performed following Affymetrix recommendations. Microarray data were background corrected, normalized, summarized, and statistically analyzed using R and Bioconductor (Gentleman et al., 2004). Both Affymetrix Mouse Gene 1.0 and 2.0 ST arrays were read using *oligo* package, using RMA algorithm as normalization method. The *limma* package (Smyth, 2005) was used for extracting statistically

significant changes between genotypes (moderated *t* tests) after removal of control transcript cluster IDs. Specifically, Mouse Gene 1.0 ST arrays allow the identification of the majority of protein-coding transcripts (total RefSeq transcripts covered: 26,166). A newest platform, Mouse Gene 2.0 ST Array, increases the number of long non-coding transcripts and microRNA precursors for differential expression analysis (total RefSeq transcripts covered: 35,240). For more detail see the section 4.1.2 (Reprint: The Journal of Neuroscience, June 19, 201333(25): 10471–10482).

3.12 ChIP assays and ChIP-seq analyses

Mouse were sacrificed by decapitation and the brain of interest (whole hippocampus, cerebellum or striatum with associated cortical tissue) were dissected to proceed with the ChIP-qPCR assay as previously described (Lopez-Atalaya et al., 2011), qPCR on immunoprecipitated DNA was performed as described in the previous section using specific primers close to the TSS.

ChIP-seq was performed as described previously (Lopez-Atalaya et al., 2013). For the ChIPseq-based screen, we generated four deeply sequenced libraries after IP of hippocampal chromatin (pooled crude chromatin extracts from the hippocampi of 16 10-week-old male mice) using antibodies against AcH3K9/14 (06-599 from Millipore) and AcH4K12 (ab46983 from Abcam). Libraries were prepared using indexed adapters following standard Illumina library preparation kits and protocols (for further detail see section 4.1.2 Reprint: The Journal of Neuroscience, June 19, 201333(25): 10471–10482).

3.13 Functional genomics analyses

For Gene Ontology (GO) terms enrichment, we used the functional annotation tools implemented in DAVID (Huang da et al., 2009) using the whole mouse genome as background list. Only enrichments with a *P*-value < 0.05 were considered. Significant GO terms retrieved from different gene expression datasets were compared using Venny software (Oliveros, 2007); redundant (highly related but nonexactly matched) terms were not considered in the analysis. The resulting GO terms were manually collapsed. To predict enrichment of transcription factor binding sites (TFBS), Pscan software was used to scan motifs from the Jaspar database in promoter regions (-950/ + 50; (Zambelli et al., 2009). As datasets we used the lists of differentially expressed and differentially acetylated genes at their TSS. For Spearman correlation,

all the Jaspar motifs (130) were ranked according to their Z-score, independently of their significance, for each dataset. Only enrichments with $P < 0.05$ were considered significant.

Results

4.1 Genomic landscape of transcriptional and epigenetic dysregulation in early onset polyglutamine disease

4.1.1 Summary

Transcriptional dysregulation is an important early feature of polyglutamine diseases. One of its proposed causes is defective neuronal histone acetylation, but important aspects of this hypothesis, such as the precise genomic topography of acetylation deficits and the relationship between transcriptional and acetylation alterations at the whole-genome level, remain unknown. The new techniques for the mapping of histone post-translational modifications at genomic scale enable such global analyses and are challenging some assumptions about the role of specific histone modifications in gene expression. We examined here the genome-wide correlation of histone acetylation and gene expression defects in a mouse model of early onset Huntington's disease. Our analyses identified hundreds of loci that were hypoacetylated at lysines 9 and 14 of histone H3 (H3K9/14ac) and lysine 12 of histone H4 (H4K12ac) the chromatin of these mice. Surprisingly, few genes with altered transcript levels in mutant mice showed significant change in these acetylation marks and vice versa. Our screen, however, identified a subset of genes in which H3K9/14 deacetylation and transcriptional dysregulation concur. Genes in this group were consistently affected in different brain areas, mouse models, and tissue from patients, which suggests a role in the etiology of this pathology. Overall, the combination of histone acetylation and gene expression screenings demonstrates that histone deacetylation and transcriptional dysregulation are two early, largely independent, manifestations of polyglutamine disease and suggests that additional epigenetic marks or mechanisms are required for explaining the full range of transcriptional alterations associated with this disorder.

My specific experimental contribution to this article was:

- full behavioral characterization of the HD82Q mouse line, which included a large battery of behavioral experiments,
- anatomical and histological analyses,
- MRI images analysis,
- quantification of bulk acetylation levels of the four nucleosome-histones by IC

- qPCR validation of transcriptional deficits and ChIP-qPCR validation of altered histone acetylation profiles.

4.1.2 Reprint: The Journal of Neuroscience, June 19, 201333(25): 10471–10482.

Neurobiology of Disease

Genomic Landscape of Transcriptional and Epigenetic Dysregulation in Early Onset Polyglutamine Disease

Luis M. Valor,* Deisy Guiretti,* Jose P. Lopez-Atalaya,* and Angel Barco

Instituto de Neurociencias de Alicante (Universidad Miguel Hernández-Consejo Superior de Investigaciones Científicas), Sant Joan d'Alacant, 03550, Alicante, Spain

Transcriptional dysregulation is an important early feature of polyglutamine diseases. One of its proposed causes is defective neuronal histone acetylation, but important aspects of this hypothesis, such as the precise genomic topography of acetylation deficits and the relationship between transcriptional and acetylation alterations at the whole-genome level, remain unknown. The new techniques for the mapping of histone post-translational modifications at genomic scale enable such global analyses and are challenging some assumptions about the role of specific histone modifications in gene expression. We examined here the genome-wide correlation of histone acetylation and gene expression defects in a mouse model of early onset Huntington's disease. Our analyses identified hundreds of loci that were hypoacetylated for H3K9,14 and H4K12 in the chromatin of these mice. Surprisingly, few genes with altered transcript levels in mutant mice showed significant changes in these acetylation marks and vice versa. Our screen, however, identified a subset of genes in which H3K9,14 deacetylation and transcriptional dysregulation concur. Genes in this group were consistently affected in different brain areas, mouse models, and tissue from patients, which suggests a role in the etiology of this pathology. Overall, the combination of histone acetylation and gene expression screenings demonstrates that histone deacetylation and transcriptional dysregulation are two early, largely independent, manifestations of polyglutamine disease and suggests that additional epigenetic marks or mechanisms are required for explaining the full range of transcriptional alterations associated with this disorder.

Introduction

Polyglutamine (polyQ) diseases are autosomal dominant neurodegenerative disorders caused by an aberrant expansion of CAG triplet-repeats in neuronal genes (Orr and Zoghbi, 2007). In the case of Huntington's disease (HD), this expansion takes place in the huntingtin (*HTT*) gene (MacDonald et al., 1993). HD is usually diagnosed in adulthood on the basis of characteristic symptoms, such as involuntary movement, changes in character, and cognitive deficits (Zuccato et al., 2010). Previous studies have indicated that transcriptional dysregulation is an important early feature of HD and other polyQ diseases (Cha, 2000; Bowles et al., 2012; Seredenina and Luthi-Carter, 2012). One of the proposed causes of this dysregulation is defective neuronal histone acetylation (Saha and Pahan, 2006; Stack et al., 2007; Valor et al., 2013) but different aspects of this hypothesis remain controversial and require further investigation. Thus, not all studies on HD animal models have confirmed the deacetylation of histones in bulk chromatin assays (Hockly et al., 2002; Sadri-Vakili et al., 2007; Klevytska et al., 2010; McFarland et al., 2012) and the genomic topography of the possible acetylation deficits remains unknown. To address these questions, we chose the transgenic mouse strain N171-HD82Q (subsequently referred as HD82Q), which expresses a truncated version of mutant Htt (mHtt) bearing an 82-residue long polyQ tract and reproduces many features of HD, including progressive weight loss and tremors, motor impairment, cognitive deficits, and premature death (Schilling et al., 1999).

We present here the first parallel genome-wide analysis of transcriptional and histone acetylation deficits in a polyQ disease model. The combination of ChIPseq and microarray technologies supported the hypothesis that transcriptional and epigenetic dysregulation, particularly aberrant acetylation of neuronal chromatin, are important early features of HD, and identified the sites of epigenetic and transcriptional dysregulation with nucleosome resolution. The comparison of these two differential screens demonstrated that most local histone acetylation deficits were not associated with transcriptional dysregulation except for a subset of genes that showed both reduced transcript levels and deficits in H3K9,14 acetylation at the transcription start site (TSS). Genes in this group were consistently altered in different brain areas, mouse models, and in transcriptomic data derived from human patients, and therefore, represent suitable candidates as progression biomarkers or therapeutic targets for this devastating disease.

Received Feb. 13, 2013; revised May 8, 2013; accepted May 20, 2013.

Author contributions: L.M.V. and A.B. designed research; L.M.V., D.G., and J.P.L.-A. performed research; L.M.V., D.G., J.P.L.-A., and A.B. analyzed data; L.M.V. and A.B. wrote the paper.

This work was supported by the Spanish Ministry of Science and Innovation (Grants SAF2008-03194-E (part of the coordinated ERA-Net NEURON project Epitherapy) and SAF2011-22855 to A.B., SAF2011-22506 to L.M.V., and CSD2007-00023) and grants from the Generalitat Valenciana (Prometeo/2012/005), Fundació La Marató de TV3 (063510) and Fundació Gent per Gent. We thank the support of Asociación Valenciana de Enfermedad de Huntington (AVAEH). L.M.V.'s research is supported by a Ramón y Cajal contract from the Spanish Ministry of Economy and Competiveness. D.G. and J.P.L.-A. hold, respectively, a predoctoral fellowship (JAE-pre) and a postdoctoral contract (JAE-doc) from the Program "Junta para la Ampliación de Estudios" cofunded by the Fondo Social Europeo (FSE). We thank Santiago Canals and Jesús Pacheco for their help in the acquisition and analysis of MRI data, Román Olivares for excellent technical assistance in the maintenance of the mouse colony, and Eva Benito for the help with initial bioinformatics analyses.

The authors declare no competing financial interests.

*L.M.V., D.G., and J.P.L.-A contributed equally to this work.

Correspondence should be addressed to either Angel Barco or Luis M. Valor, Instituto de Neurociencias de Alicante, Campus de San Juan, Apartado 18, Sant Joan d'Alacant 03550, Alicante, Spain. E-mail: abarco@umh.es or lmv@umh.es.

DOI:10.1523/JNEUROSCI.0670-13.2013

 0270-6474/13/3310471-12$15.00/0

Materials and Methods

Animals. The transgenic strain *PrP-htt-N171-82Q* (Schilling et al., 1999) was acquired from Jackson Laboratories (stock No. 003627) and maintained in a DBA and C57BL/6J mixed background (50:50) because the viability of the strain is compromised in a pure C57BL/6J background. In both the microarray-based and ChIPseq-based differential screenings, tissue from several animals was pooled together to minimize the potential genetic variability that could result from this mixed background. Sodium butyrate was administered as previously described (Valor et al., 2011); mice were intraperitoneally injected with vehicle (PBS) or sodium butyrate (1.2 mg/Kg) and killed 30 min later. Experimental protocols were consistent with European regulations and approved by the Institutional Animal Care and Use Committee.

Behavioral testing. For all behavioral tasks, we compared HD82Q animals and wild-type littermates of the indicated age. RotaRod and Morris water maze tasks were performed as described previously (Valor et al., 2011). Grip strength values are the average of six measures in the Grip Strength Meter (Ugo Basile).

MRI analysis. For magnetic resonance imaging (MRI), mice were anesthetized, perfused with 4% paraformaldehyde, and decapitated. The whole head was postfixed overnight and included in agarose before data acquisition as reported (Lopez-Atalaya et al., 2011). Length and volume measurements were performed using ImageJ software.

Histological and Western-blot analyses. Nissl staining, immunohistochemistry, and Western-blot analyses were performed as previously described (Lopez de Armentia et al., 2007; Sanchis-Segura et al., 2009). Cell counting and signal intensities quantification were performed using ImageJ software. The following antibodies were used: acetyl-histone antibodies specific for the panacetylated forms of H2A (K5, K9), H2B (K5, K12, K15, K20), H3 (K9, K14), and H4 (K5, K8, K12, K16) produced in our laboratory (Sanchis-Segura et al., 2009); α-Huntingtin, clone mEM48 (MAB5374), α-AcH3K9,14 (06-599), α-H2B (07-371), α-H3 (05-499), α-NeuN (MAB377) from Millipore; α-AcH4K12 (ab46983) from Abcam; α-GFAP (G9269), α-MAP2 (M4403), α-β-actin (F5441), and biotinylated and HRP-conjugated secondary antibodies from Sigma-Aldrich Química S.A., and Alexa Fluor 594 secondary antibody (A-21209) from Invitrogen.

RNA extraction, RT-qPCR, and microarray analyses. Quantitative RT-PCR (RT-qPCR) assays were performed as previously described (Valor et al., 2011). Each independent sample was assayed in duplicate and normalized using glyceraldehyde 3-phosphate dehydrogenase (GAPDH) levels. All primer sequences are available upon request. For microarray experiments, RNA from 3 to 4 mice of the same age, sex, and genotype were pooled and cleaned up using the RNeasy Mini Kit (Qiagen). Three independent pooled samples per genotype and brain area were hybridized to Mouse Gene 1.0 ST expression arrays (Affymetrix). All the mice (mutant and controls) used in the 10-week analysis were males, whereas all the mice used in the 20-week analysis were females. We did not observe apparent sex differences in histopathology, premature death, and gene-specific RT-qPCR assays. Microarray data were background corrected, normalized, summarized, and statistically analyzed using R and Bioconductor (Gentleman et al., 2004). Mouse Gene 1.0 ST arrays were read using *oligo* package, using RMA algorithm as normalization method. The *limma* package (Smyth, 2005) was used for extracting statistically significant changes between HD82Q and control samples (moderated *t* tests). Fold-change >1.25 and adjusted $P < 0.05$ were used as filters. These files can be downloaded from the Gene Expression Omnibus (GEO) database using the accession number GSE44855. Striatal profiles were obtained from the datasets GSE9803 and GSE9804 corresponding to 12-week-old R6/2 mice (Kuhn et al., 2007) and processed in a similar manner than HD82Q arrays except for the use of the *affy* package to read the CEL files. Gene expression changes in caudate nucleus of postmortem brain from HD patients were obtained from Hodges et al. (2006). The same reported *P* value threshold was used ($p < 0.001$) but additionally we applied a fold-change (FC) filter (>1.25) to minimize the impact of very weak changes in our subsequent analyses.

ChIP assays and ChIPseq analysis. Chromatin immunoprecipitation (ChIP) was performed as described previously (Lopez-Atalaya et al., 2011). ChIP-qPCR validation of candidate genes and ChIPseq experiments were performed in independent cohorts of animals. For conventional ChIP assays, we used dissected tissue from two mice for the hippocampal samples and from a single animal for the cerebellar samples. qPCR on IP chromatin was performed as described for RT-qPCR using specific primers close to the TSS. All primer sequences are available upon request. Because initial two-way ANOVA analyses did not reveal significant age effects or age-genotype interaction, we pooled the data corresponding to 10- and 20-week-old animals. For the ChIPseq-based screen, we generated four deeply sequenced libraries after IP of hippocampal chromatin (pooled crude chromatin extracts from the hippocampi of 16 10-week-old male mice) using antibodies against AcH3K9,14 (06-599 from Millipore) and AcH4K12 (ab46983 from Abcam). Libraries were prepared using indexed adapters following standard Illumina library preparation kits and protocols. High-throughput sequencing was performed using a HiSeq-2000 apparatus (Illumina) with 50 TruSeq SBS v3 sequencing kit following the manufacturer's instructions. Indexed reads were demultiplexed into individual samples, filtered for low-quality reads and adaptor sequences. Fifty base-pair long single-read datasets were obtained for AcH3K9,14 (wt and HD82Q mice), AcH4K12 (wt and HD82Q mice), input (wt mice), and preimmune serum (wt mice and HD82Q mice). To achieve sufficient genome depth coverage to identify post-translational chromatin modifications, the depth of the sequencing run was between 8.4 and 14.5×10^6 reads per sample ($AcH3K9,14_{WT}$: 13,867,710; $AcH4K12_{WT}$: 14,187,515; $AcH3K9,14_{HD82Q}$: 9,053,780; $AcH4K12_{HD82Q}$: 9,935,242; input sample: 7,904,594; IgG condition: 9,220,090). A saturation analysis indicated that the depth of sequencing was sufficient for reliable detection of histone acetylation peaks in our samples (data not shown). Reads were aligned to the NCBI-M37/mm9 reference genome using BWA (Li and Durbin, 2010), and BAM files were parsed using the SAMTOOLS (Li et al., 2009) to extract uniquely mapped reads ($AcH3K9,14_{WT}$: 88%; $AcH4K12_{WT}$: 86%; $AcH3K9,14_{HD82Q}$: 89%; $AcH4K12_{HD82Q}$: 85%; input sample: 80%; IgG condition: 80%). SICER algorithm (Zang et al., 2009) was used to extract acetylation-enriched chromatin regions. To further increase the depth of coverage and to exclude false positive enriched-regions due to eventual local deficits of coverage in the control dataset, acetylation-enriched regions were identified using pooled input and IgG libraries as control library. SICER parameters for island identification were as follows: redundancy threshold = 100, window size = 200, gap size = 2 (AcH3K9,K14) (3 for AcH4K12), fragment size = 150, effective genome fraction = 0.77, FDR (enriched islands) = 10^{-8}. For the differential screen, we set a threshold of FDR adjusted $p < 10^{-3}$ to identify the most reliably changed histone acetylation islands. The large islands at the *Prnp* promoter corresponding to the detection of the transgene were not considered in subsequent analyses. Overlap and annotation of significantly enriched islands was done with ChipPeakAnno (Zhu et al., 2010). RefSeq gene annotations were obtained from the University of California at Santa Cruz (UCSC) Genome Bioinformatics website. Seqmonk and Integrative Genomics Viewer (IGV; Robinson et al., 2011) were used for data visualization and coverage snapshots at discrete loci. Wig files containing the coverage data (normalized read density per million bp; RPM) across the enriched regions for the two acetylated histones were obtained using IGV Tools. Read length was extended 200 bp. The files were then normalized to the size of the dataset using Wigreader. The high-throughput sequencing data generated in this study has been deposited at NCBI's GEO and can be consulted through the accession number GSE44855.

Meta-analysis of microarray and ChIPseq data. Log_2 fold-change values from hippocampal microarray and ChIPseq data were directly correlated. We also performed a Pearson correlation analysis using *P* values that did not reveal any significant association. In those cases in which more than one island were associated with the same gene, fold-changes were averaged with the assumption that all the islands similarly contribute to gene expression. As an alternative to average, the nearest island to the gene was tested without further improvement in the correlation coefficients. In the χ^2-square tests the expression data corresponding to the whole array was first ranked according to the *P* values of TC IDs (MG 1.0 ST) or probesets (MG 430, HU133A, and B). The rank of the TC IDs/probesets corresponding to Exp-AcH3 genes was determined and χ^2

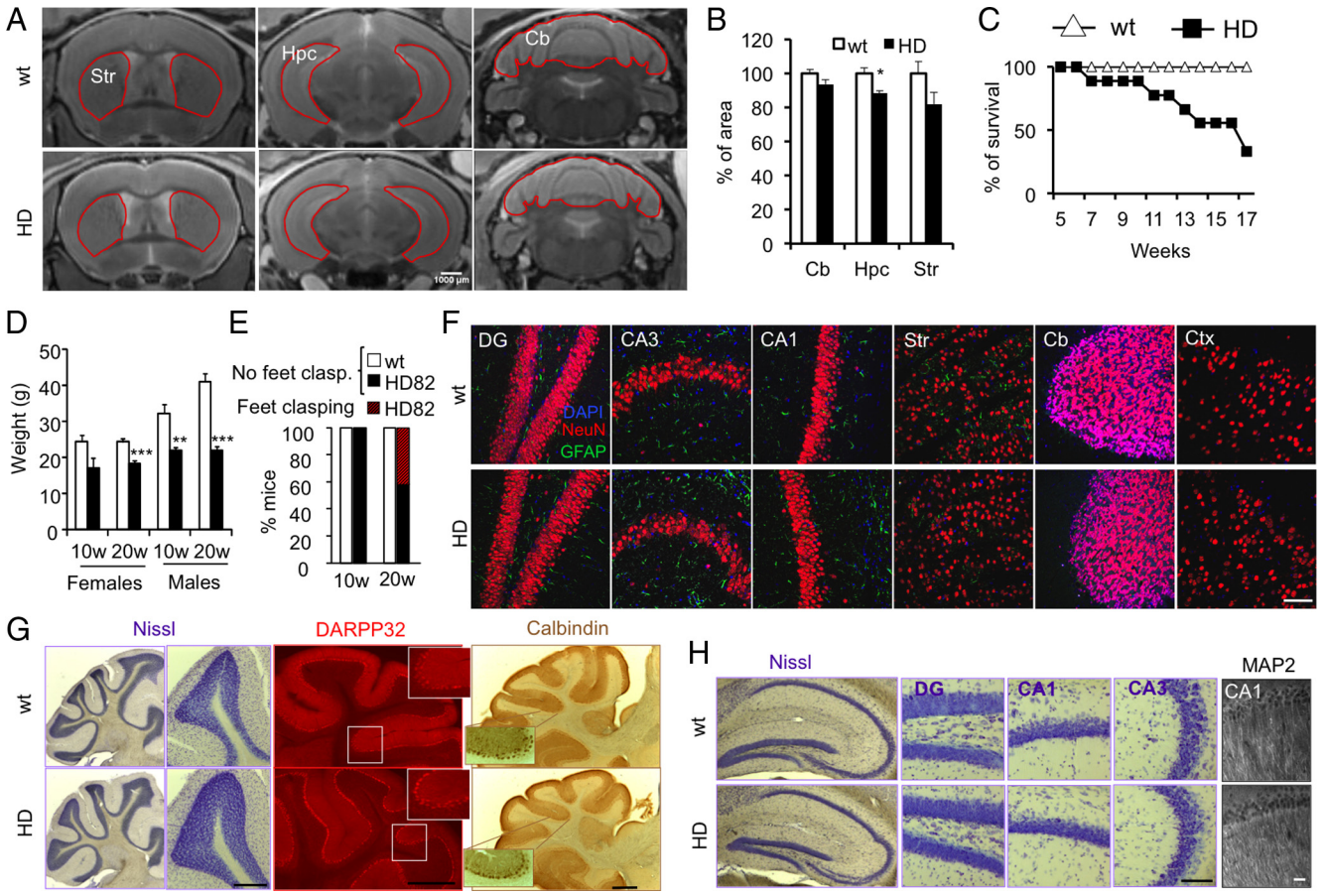

Figure 1. HD82Q mice show neuropathological traits in the absence of neurodegeneration. ***A***, Representative MRI images showing the striatum (Str), hippocampus (Hpc), and cerebellum (Cb) of a 20-week-old HD82Q mouse and a control littermate. Red line denotes the area considered for quantification. ***B***, Volume quantification of these brain areas (three animals per genotype). Mutant mice had smaller brains. However, morphometric ratios were maintained between different brain regions and there was no apparent enlargement of lateral ventricles. Data are represented as mean ± SEM $*p < 0.05$, Student's *t* test HD versus wt. ***C***, HD82Q (HD) mice had a short life span. Premature death was occasionally observed at early symptomatic stages ($n = 9$ for each genotype). ***D***, HD82Q mice did not gain weight in the same progression that control littermates. This phenotype was especially severe in males. ***E***, Percentage of 10- and 20-week-old mice showing feet clasping during 1 min tail suspension test. ***F***, Double immunostaining of brain sections of 12-week-old HD82Q mice and control littermates with a marker for neurons (NeuN) and glial cells (GFAP) showed no significant difference in the number of either cell type, indicating that there is neither neuronal cell loss nor gliosis. Scale bar, 10 μm. ***G***, Cerebellar morphology in 12-week-old HD82Q mice and control littermates were undistinguishable; the quantification of layers thickness did not reveal any significant change (data not shown). Left, Nissl staining. Right, Immunostaining of cerebellar sections with the cerebellar markers DARPP32 and calbindin. Scale bars: Nissl, 200 μm; DARPP2 and calbindin, 500 μm. ***H***, Hippocampal morphology in 12-week-old HD82Q mice and control littermates were undistinguishable; the quantification of layers thickness did not reveal any significant change (data not shown). Left, Nissl staining. Right, Immunostaining with the neuronal marker MAP2. Scale bars: Nissl, 100 μm; DARPP2 and MAP2, 25 μm.

values were calculated related to a random distribution. For Gene Ontology (GO) terms enrichment, we used the functional annotation tools implemented in DAVID (Huang et al., 2009) using the whole mouse genome as background list. Only enrichments with a *P*-value <0.05 were considered. Significant GO terms retrieved from different gene expression datasets were compared using Venny software (Oliveros, 2007); redundant (highly related but nonexactly matched) terms were not considered in the analysis. The resulting GO terms were manually collapsed. To predict enrichment of transcription factor binding sites (TFBS), Pscan software was used to scan motifs from the Jaspar database in promoter regions (−950/+50; Zambelli et al., 2009). As datasets we used the lists of differentially expressed and differentially acetylated genes at their TSS. For Spearman correlation, all the Jaspar motifs (130) were ranked according to their Z-score, independently of their significance, for each dataset. Only enrichments with $P < 0.05$ were considered significant.

Results

HD82Q mice show neuropathological traits in the absence of neurodegeneration

HD82Q mice exhibit slight brain atrophy but grossly normal anatomy (Fig. 1*A*,*B*). Despite their premature death (Fig. 1*C*), severe weight loss (Fig. 1*D*), and motor dysfunction (Fig. 1*E*), no apparent neurodegeneration or active gliosis were observed even in the late stages of the disease (Fig. 1*F*–*H*; Schilling et al., 1999; Klevytska et al., 2010). We reasoned that the dissociation between neuronal malfunction and death could allow us to investigate transcriptional and epigenetic dysregulation without the confounding factor of changes in the cellular composition of the tissue. Detailed histological analysis of mHtt aggregates identified the cerebellum and the hippocampus as the two main brain areas of transgene expression (Fig. 2*A*,*B*). In agreement with this observation, processes that depend on proper functioning of these regions, such as motor performance in the rotarod task (Fig. 2*C*), grip control (Fig. 2*D*), and spatial learning in the water maze (Fig. 2*E*–*G*), were severely affected in HD82Q mice (Fig. 2, see legend for additional detail). Importantly, cerebellar and hippocampal functions are also altered in HD patients (Snowden et al., 2002; Seneca et al., 2004). We focused our subsequent analyses on these two tissues.

Severe transcriptional dysregulation in mHtt-expressing tissues

To investigate genome-wide transcriptional dysregulation in HD82Q mice, we performed microarray analysis on hippocam-

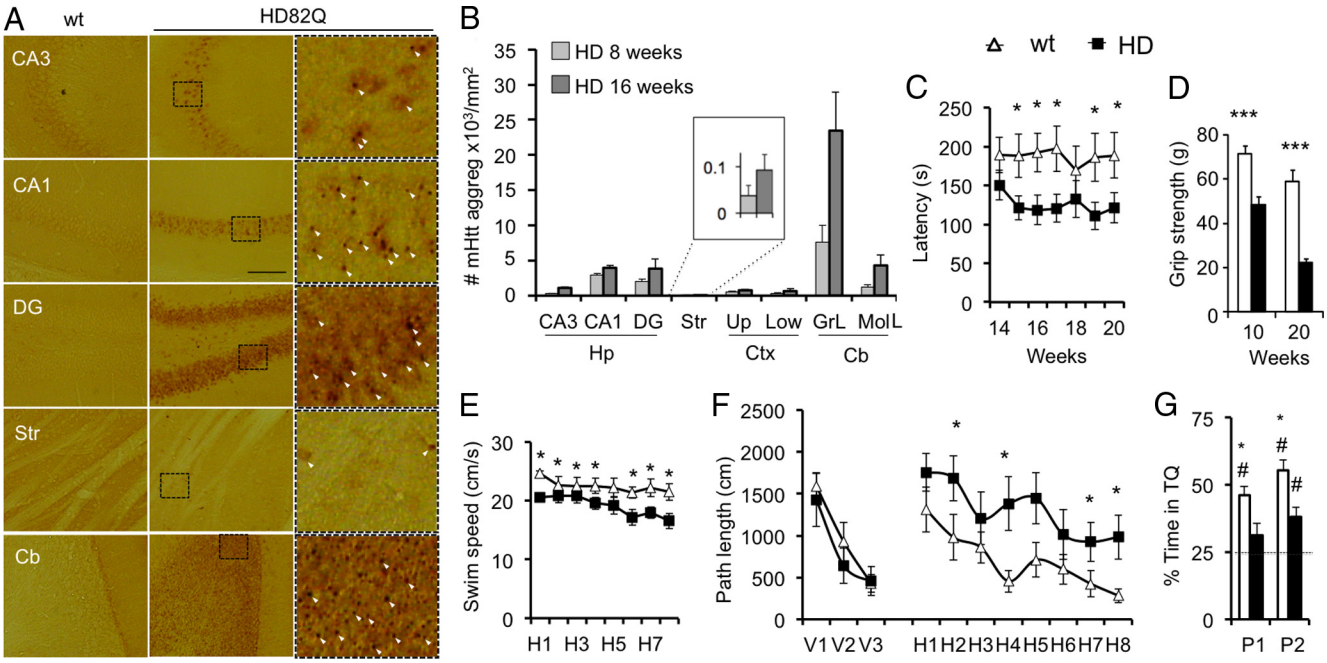

Figure 2. Impaired cerebellar and hippocampal function in HD82Q mice. ***A***, Transgene expression in HD82Q mice. Strong mHtt immunoreactivity was detected in hippocampus and cerebellum of HD82Q mice. Aggregates were also detected in lower amount in the cortex and striatum of HD82Q mice, but were absent in sections from wt littermates. Representative images corresponding to the CA1, CA3, and dentate gyrus (DG) subfields in the hippocampus, striatum (Str), and cerebellum (Cb) of 16-week-old HD82Q mice are shown. Insets in HD82Q show higher-magnification images of mHtt aggregates labeled with white arrowheads. Scale bar, 100 μm. ***B***, Quantification of mHtt immunoreactivity in brain sections of 8- and 16-week-old HD82Q mice. The strongest expressions were detected in the hippocampus and cerebellum, followed by the cortex and striatum ($n = 3$ per genotype). Hp, Hippocampus; Cb, cerebellum; Str, striatum; Up, cortical upper layers; Low, cortical lower layers; GrL, granular layer; MoL, molecular layer. Note that the presence of mHtt aggregates in the cerebellum was 100-fold higher than that in the striatum or cortex. This result is in agreement with images presented in the original publication describing this strain (Schilling et al., 1999). ***C***, Mutant mice slipped from the rod earlier than control littermates in an accelerated speed rotarod task ($n = 10$ for wt, $n = 11$ for HD82Q). The weak mHtt staining observed in striatal tissue suggests that the motor deficits in HD82Q mice may be largely cerebellum-dependent. ***D***, 10- and 20-week-old HD82Q mice showed a significant reduction of grip strength. ***E–G***, 3-month-old HD82Q mice were severely impaired in the Morris water maze task ($n = 11$ for wt, $n = 8$ for HD82Q). Mutant mice showed reduced swimming speed (***E***) and longer path lengths to reach the platform in the hidden version of the task (F: H1–H8), but normal learning in the visible platform task (F: V1–V3). Mutant mice also performed worse than wild-type littermates in the probe trials in day 5 (G: P1) and 9 (G: P2). These results suggest the existence of spatial learning defects in addition to the motor impairment, although these two defects are difficult to dissociate. Data are presented as mean ± SEM *$p < 0.05$; **$p < 0.01$; ***$p < 0.001$ (Student's t test) for differences between genotypes. #, $p < 0.05$ (Student's t test) for comparison with random performance.

pal RNA using Affymetrix Mouse Gene 1.0 ST arrays at two different stages of disease: early symptomatic (10 weeks old) and terminal (20 weeks old; Fig. 3*A*). Differential gene profiling analysis identified 436 transcript cluster IDs (TC IDs), corresponding to 405 annotated genes, that showed a significant genotype effect (FC > 1.25, adjusted $p < 0.05$). The profiles of transcriptional dysregulation in HD82Q mice were very similar at the two investigated time points, as shown both in the hierarchical clustering (Fig. 3*B*) and correlation plot (Fig. 3*C*) analyses. Pairwise contrast tests retrieved the lists of TC IDs significantly altered at specific time points and confirmed the early onset of most transcriptional deficits and their moderate progression with age (Fig. 3*C*,*D*). No TC IDs showed a significant interaction between genotype and age. The progression of the pathology in terms of gene profiling was reflected in a modest increase in the severity of the changes ($FC_{Down\ TCIDs}$: 0.71 ± 0.01 in 10-week-old mice vs 0.67 ± 0.01 in 20-week-old mice, $p = 0.005$; $FC_{Up\ TCIDs}$: 1.27 ± 0.02 vs 1.52 ± 0.02, $p = 6.5 \times 10^{-13}$) and a larger number of affected TC IDs (two- and eightfold increase for down- and upregulations, respectively). These results indicate that mHtt expression is initially strongly associated with impaired gene expression (up/down ratio = 0.09) and later leads to numerous gene upregulations (up/down ratio = 0.43), which might reflect the emergence of a homeostatic or defense response to polyQ pathology.

To extend our transcriptomic analysis to a different tissue, we also performed microarray analysis with RNA from cerebellar tissue of the same 10-week-old animals. As shown in Figure 2*B*, this tissue presented the highest density of mHtt aggregates in the brain of HD82Q mice. The comparison between control and HD82Q samples detected 1624 TC IDs corresponding to 1413 annotated genes (FC > 1.25, adjusted $p < 0.05$). These results indicate that the extension of transcriptional dysregulation correlates with the abundance of mHtt aggregates and suggest that the cerebellum may be more sensitive to polyQ pathology than the hippocampus (Fig. 3*E*). Only 111 genes were consistently affected in both tissues, indicating that a majority of mHtt transcriptional targets are tissue specific. Among the affected transcripts in both tissues, we found relevant genes known to be altered in HD (Seredenina and Luthi-Carter, 2012) like the ones encoding the neuropeptide enkephalin (*Penk*), subunits of glutamate (*Grm2*) and GABA receptors (*Gabrd*), and the GTP-binding protein Rasd2 (also known as Rhes). Among the upregulated transcripts we found Nfya, which encodes for a subunit of the transcription factor NF-Y that is sequestered in mHtt aggregates (Yamanaka et al., 2008). As a positive control for our screen, the analysis of individual probesets confirmed the overexpression of *Htt* exon 1, which is part of the transgene construct, in all HD82Q samples (Fig. 3*F*).

We next examined the expression of a number of candidate genes, both common and region-specific, at different stages of the pathology, from presymptomatic to terminal mice through RT-qPCR assays using independent samples (Fig. 3*G*). Our assays

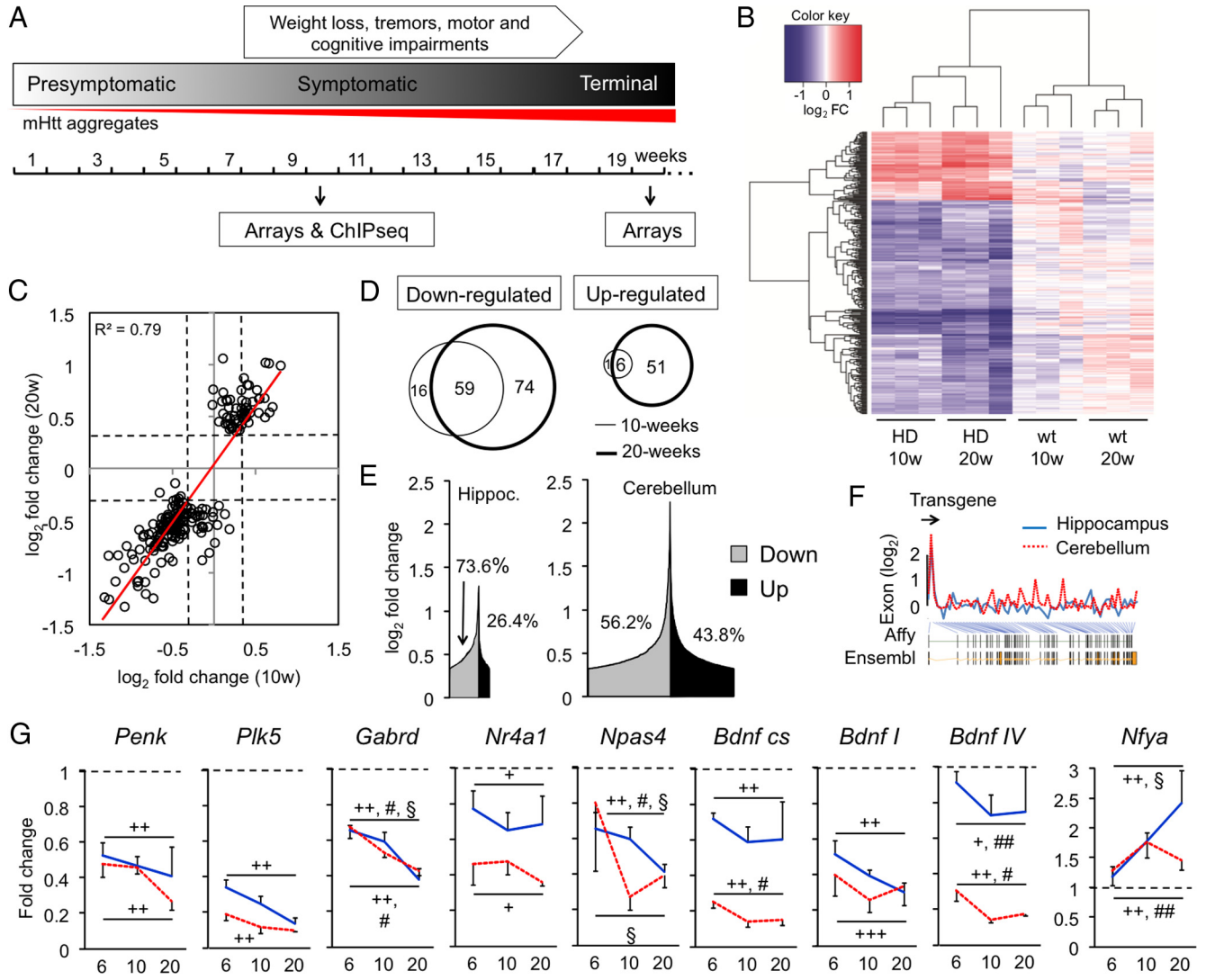

Figure 3. Transcriptional dysregulation in the hippocampus and cerebellum of HD82Q mice. ***A***, The time points for RNA and chromatin samples collection are indicated along with a schematic representation of the progression of neuropathological traits and presence of mHtt aggregates. ***B***, Heatmap showing the 436 TC IDs showing a significant genotype effect. ***C***, Scatter plot showing the FC (log2) of differentially expressed transcripts in the hippocampus of 10- and 20-week-old HD82Q mice. Note the deviation from the diagonal indicating that the progression of the pathology was associated with a slight worsening of the transcriptional deficits. This deviation was more prominent among upregulated TC IDs. ***D***, Venn diagram showing the number of significant TC IDs retrieved in the contrast tests for 10- and 20-week-old mice (six arrays each). ***E***, Distribution of differentially expressed genes in hippocampus and cerebellum. The areas are proportional to the number of genes affected in each tissue and the percentage values correspond to the areas under the curve. ***F***, The analysis of individual probesets confirmed the overexpression of *Htt* exon 1 in HD82Q samples. ***G***, Validation and early onset of transcriptional deficits in hippocampus and cerebellum. RT-qPCR analysis of the temporal course of transcriptional dysregulation of selected genes retrieved in our differential screen. We confirmed the transcript level changes in both hippocampus (blue) and cerebellum (red) of HD82Q mice. The discontinous line at Fold change 1 indicates the expression in wild-type littermates. In all panels, RNA samples were collected from 6-, 10-, and 20-week-old mice. Data are represented as the mean ± SEM. Student's *t* test ($p < 0.05$; $p < 0.005$): *, ** for pairwise comparisons. Two-way ANOVA ($p < 0.05$; $p < 0.005$): +, ++ for genotype effect; #, ## for age effect; § for genotype *x* age interaction.

included activity-induced transcription factors (*Nr4a1*, *Npas4*) and BDNF isoforms. Our assays confirmed the downregulation of plasticity-related immediate early genes (IEG) in HD82Q mice and revealed that the two main activity-regulated promoters of *Bdnf*, P-I, and P-IV, were both affected by HD pathology. In agreement with array data, the transcriptional deficits were, in general, more severe in cerebellar tissue. Overall, these experiments validated the microarray screen, confirmed the modest progression of transcriptional defects (only *Gabrd*, *Npas4*, and *Nfya* showed a significant progression with age), and demonstrated that transcriptional deficits in HD82Q mice precede the onset of chorea and weight loss, which suggests a possible role for these alterations in the etiology of these symptoms.

Hundreds of genomic loci are deacetylated in hippocampal chromatin of HD82Q mice

To examine the relationship between transcriptional and epigenetic dysregulation associated with mHtt expression, we first assessed the level of acetylation of the four nucleosome histones by Western blotting and immunohistochemistry. In agreement with previous studies (Hockly et al., 2002; Sadri-Vakili et al., 2007; Klevytska et al., 2010; McFarland et al., 2012), but in contrast to others (Gardian et al., 2005; Stack et al., 2007; Giralt et al., 2012), neither one of these techniques revealed significant deficits in bulk chromatin of mHtt expressing tissues (Fig. 4).

We next used ChIPseq technology to tackle the identification of histone acetylation deficits with a resolution and genomic coverage

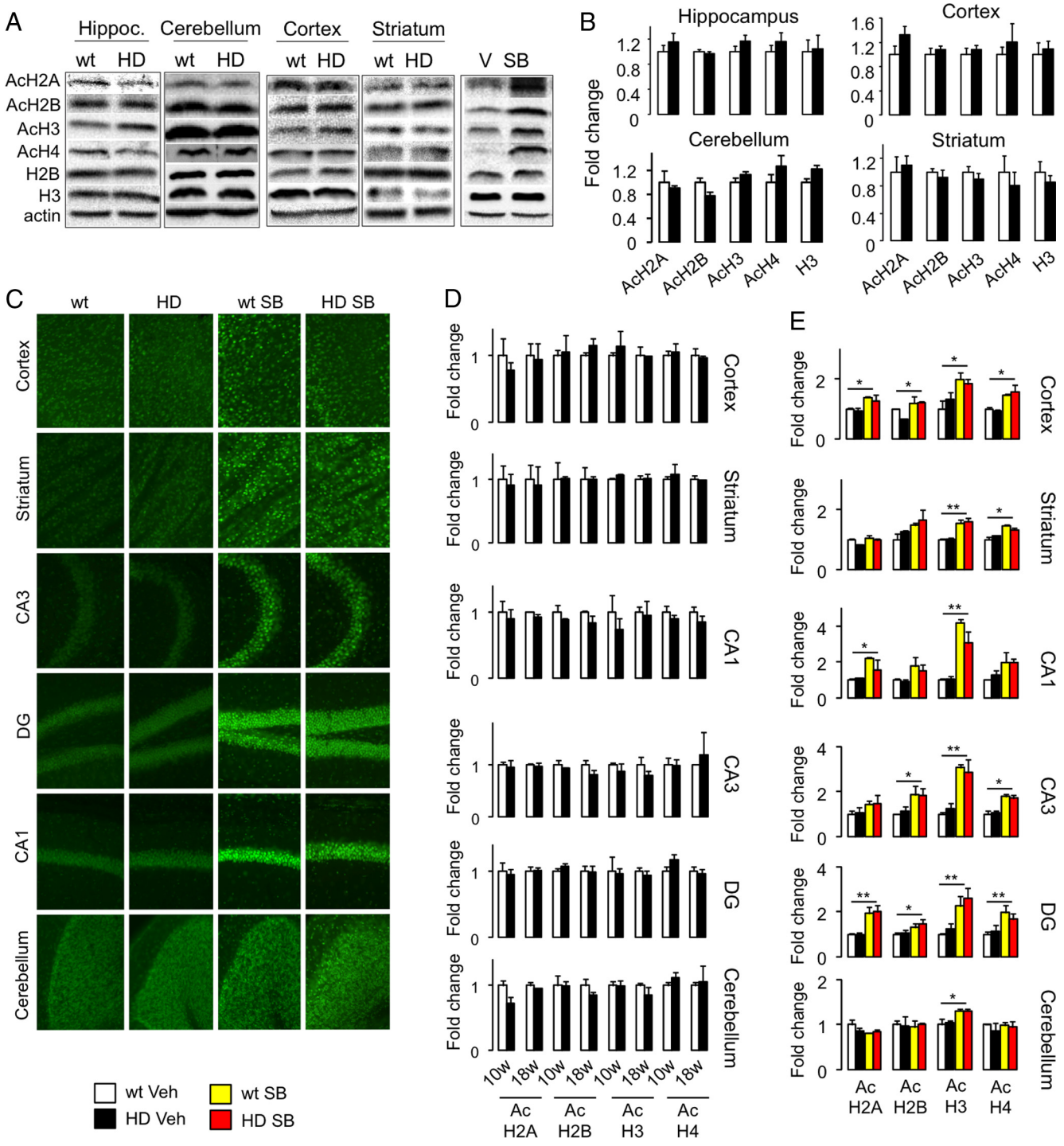

Figure 4. Bulk chromatin acetylation is not reduced in the brain of HD82Q mice. ***A***, Representative Western blots analysis of hippocampal extracts from terminal HD82Q (HD, 20-week-old) and wt littermate mice against different pan-acetylated histones. As a positive control, we also show histone acetylation levels in murine cortex after treatment with vehicle (V, PBS) or sodium butyrate (SB). ***B***, Quantification of the Western blots. Hippocampus, striatum and cortex: $n = 6$ (wt), $n = 8$ (HD); cerebellum: $n = 7$ (wt), $n = 6$ (HD). ***C***, Representative immunohistochemistry images of different brain areas from 18-week-old HD82Q (HD) and wt mice using an antibody against AcH3K9,14. Mice treated with SB were used as a positive control for the detection of significant changes in histone acetylation. This HDACi caused similar hyperacetylation of histones in HD82Q and wild-type littermates. Similar results were obtained for acetylated forms of the four nucleosome histones. Scale bar, 100 μm. ***D***, Quantification of immunohistochemistry assays in 10- (10w) and 18-week-old (18w) mice; $n = 4$ for both genotypes and times. ***E***, Quantification of immunohistochemistry assays in an independent set of HD82Q and wt littermate mice treated with vehicle or SB; $n = 2$ per group; two-way ANOVA analysis did not reveal any genotype effect or genotype *x* treatment interaction, but a significant HDACi treatment effect for different histones and brain areas. Data are represented as mean ± SEM $^{*}p < 0.05$; $^{**}p < 0.005$ (two-way ANOVA, treatment effect).

that is unattainable through Western blot, locus-specific ChIP assays and ChIP-on-chip techniques. Given the relevance of the hippocampus in cognitive processes affected by HD, we performed the ChIPseq screen in hippocampal chromatin of early symptomatic mice so that we could explore the predictive value of early deacetylation in late transcriptional dysregulation. We focused on two relevant histone acetylation marks associated with active transcription: AcH3K9,14, which is regulated during memory processes (Levenson et al., 2004) and has been found reduced in some models of HD (Stack et al., 2007); and AcH4K12, which has been linked to age-

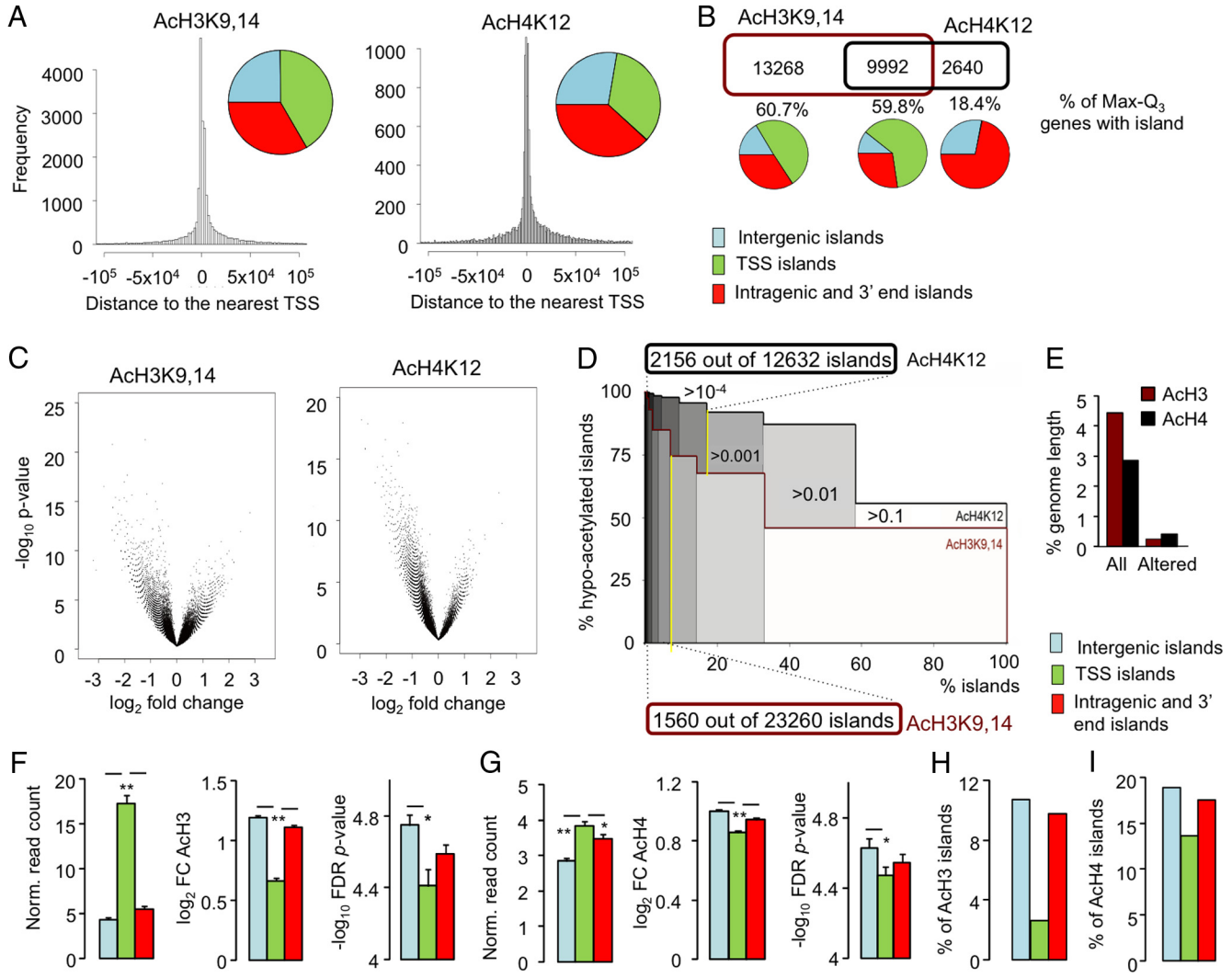

Figure 5. Genomic topography of histone acetylation deficits in HD82Q mice. ***A***, Genomic distribution of AcH3K9,14 and AcH4K12 represented as frequencies of reads referred to the nearest TSS (frequency graphs) and percentages of islands located in different gene features (sector graphs): green, overlapping with TSS (including islands comprising the whole gene); red intragenic islands (inside exons or introns) and islands overlapping with the 3′-end; blue, intergenic islands (upstream and downstream of genes). ***B***, Venn diagram showing the physical overlap between AcH3K9,14 and AcH4K12 islands. The percentages indicate the proportion of genes associated with these islands that were highly expressed in the hippocampus (top 25%, between the maximum and Q_3 values). The sector graphs show the distribution of these islands according to gene feature. The coloring is the same as in ***A***. ***C***, Volcano plots demonstrate the hypoacetylation of many enrichment islands in HD82Q samples for both marks. Note the asymmetric distribution of dots toward the left half of the graphs, which corresponds to negative $\log_2$ fold-change values. The outlier dots corresponding to the promoter region of *Prnp* (which is present in high copy number as part of the transgene) fall beyond the scale of the plot. ***D***, Percentage of hypoacetylated islands according to their associated FDR *p* value in the genotype comparison. Yellow lines label the significance threshold (FDR $p < 10^{-3}$) used in all subsequent analyses. ***E***, Percentage of effective genome size (i.e., excluding centromeric regions) occupied by the indicated acetylation marks. ***F***, ***G***, Normalized read count in control animals (left), magnitude (fold-change in absolute $\log_2$ value) and significance ($-\log_{10}$ FDR *P* value) of differentially acetylated H3K9,14 (***F***) and H4K12 (***G***) islands in HD82Q chromatin distributed according to their location referred to the nearest gene. Note that one island may fall in more than one category. ***H***, ***I***, Only a small percentage of genes showed significant changes at the TSS for the AcH3K9,14 (***H***) and AcH4K12 (***I***) marks according to our filtering criteria.

related memory impairment (Peleg et al., 2010). The SICER algorithm, which is particularly suitable for identifying local enrichments for histone post-translational modifications (Zang et al., 2009), was used to identify acetylation-enriched chromatin regions. We found that both acetylation marks tended to accumulate in the proximity of the TSS (Fig. 5*A*) defining thousands of enrichment islands, most of which were located at promoters and intragenic sequences. The physical overlap between the two labels was high and revealed their convergence at active loci (Fig. 5*B*). Notably, there was a dramatic reduction in the number of islands detected in HD82Q chromatin compared with control samples (criterion FDR $p < 10^{-8}$; 27.7% reduction for AcH3K9,14 and 71.7% reduction for AcH4K12).

SICER also allows the direct comparison of acetylation profiles between genotypes. The comparison revealed a general reduction of hippocampal chromatin acetylation in HD82Q mice that was especially severe for the AcH4K12 mark (Fig. 5*C*). To retrieve the most prominent changes, we set an arbitrary threshold (FDR $p < 10^{-3}$) that identified 1560 AcH3K9,14 islands and 2156 AcH4K12 islands altered by mHtt expression (Fig. 5*D*). Notably, the top ranked islands for both histone marks mapped onto the promoter of the prion protein gene (result not shown). Because this sequence is part of the HD82Q transgene and thereby it is in high copy number in the chromatin of mutant mice, their prominent position in the lists of differential islands represented a first validation of our differential screen. The great majority of the acetylation changes that passed our filtering criteria corresponded to hypoacetylation in HD82Q chromatin (87.7 and 96.9% of the islands for AcH3K9,14 and AcH4K12, respectively). As a whole, these differentially acetylated islands accounted for a small proportion (<0.5%) of the murine genome

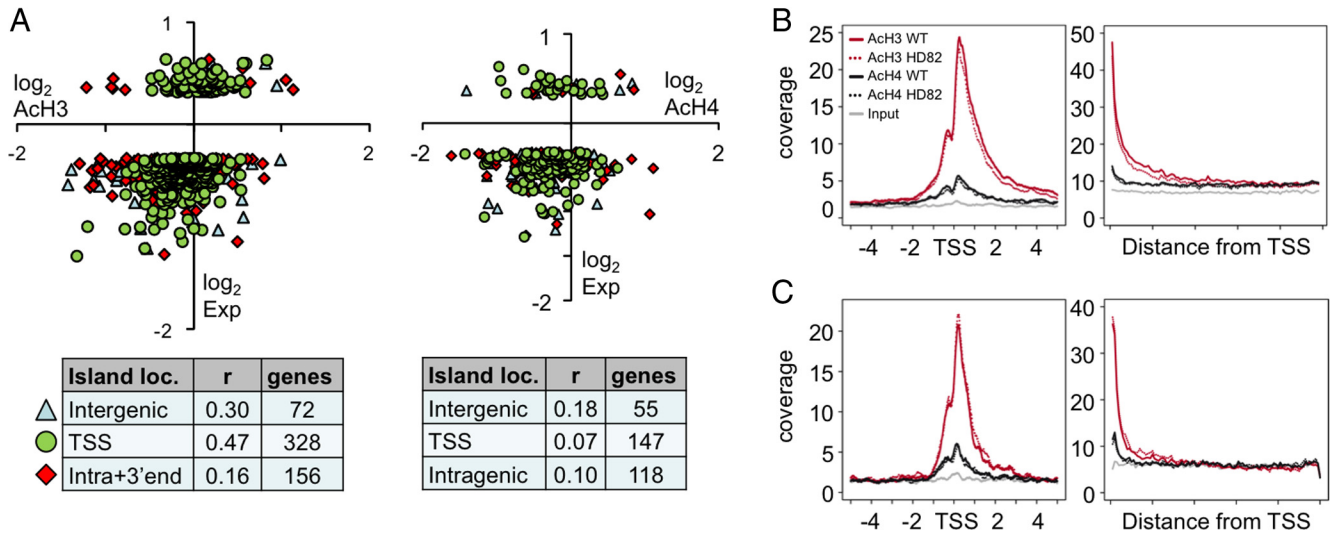

Island loc.	r	genes
Intergenic	0.30	72
TSS	0.47	328
Intra+3'end	0.16	156

Island loc.	r	genes
Intergenic	0.18	55
TSS	0.07	147
Intragenic	0.10	118

Figure 6. Correlation between gene expression and histone acetylation deficits. ***A***, Correlation between fold changes in gene expression and histone acetylation profiles among differentially expressed genes (*r*, Pearson coefficient). The correlation for the AcH3 mark (left) was better considering those genes with TSS islands (green circles) compared with those located on intragenic (red diamonds) or intergenic (blue triangles) regions. No correlation was observed for the AcH4K12 mark in any subgroup of genes (right). ***B***, ***C***, Mean enrichment profiles presenting the genomic distribution of reads for AcH3K9,14 and AcH4K12 across the TSSs (left) and gene length (right) for genes down- (***B***) or upregulated (***C***) in HD82Q mice according to our array screen.

(Fig. 5*E*), which is consistent with the absence of significant changes in the acetylation of bulk chromatin reported above.

Most of these differentially acetylated islands mapped onto inter- and intragenic regions. Moreover, although the islands that overlapped with a TSS were in general larger than those located in inter- and intragenic regions, mHtt-induced deacetylation at TSSs was less prominent and had lower statistical significance, particularly in the case of AcH3K9,14 (Fig. 5*F*,*G*). Overall, the changes at the TSS affected 2.6% of AcH3K9,14 islands (Fig. 5*H*) and 13.6% of AcH4K12 islands (Fig. 5*I*).

Transcriptional and histone acetylation defects show low global correlation

To investigate the correlation between ChIPseq and microarrays data, we discriminated between islands located in the TSS or in intra- and intergenic regions because we reasoned that islands at these different locations could distinctly contribute to transcription. The most prominent H3K9,14 and H4K12 acetylation changes detected in our ChIPseq screen showed no correlation with expression changes of the nearest gene (Pearson correlation indexes: $r_{TSS} = 0.17$; $r_{Intragenic} = 0.03$; $r_{Intergenic} = 0.04$). In contrast, when we compared the genes significantly altered at the transcript level (genotype main effect, adjusted $p < 0.05$) with nonfiltered fold-change values for the nearest H3K9,14 and H4K12 acetylation islands, a moderate correlation was observed in the case of AcH3K9,14 islands located at the TSS ($r = 0.47$; Fig. 6*A*). Consistently with these results, we observed a slight reduction or increase of acetylation levels at the TSS in HD82Q samples, respectively for down- or upregulated genes (Fig. 6*B*,*C*).

Genes showing both transcriptional and deacetylation defects are part of a consistent HD gene signature

Only 42 genes exhibited both a significantly reduction of transcript levels and H3K9,14 deacetylation at the TSS according to our filtering criteria (Fig. 7*A*). This gene set, thereafter referred as Exp-AcH3, showed a good correlation between the changes in gene expression and acetylation (Fig. 7*B*; $r = 0.69$). Independent RT-qPCR and ChIP-qPCR assays confirmed this association. In particular, we examined the loci encoding enkephalin, the modulator of Ras signaling Rin1 and the regulator of dendritic growth Itpka (Fig. 7*C*). Additional ChIP-qPCR assays were performed at the TSS region of two candidate genes, the regulator of neuritic growth *Plk5* (de Cárcer et al., 2011) and the epilepsy-related gene *Gabrd* (Dibbens et al., 2004), that were affected in both cerebellum and hippocampus (Fig. 7*D*). The assays demonstrated that the deacetylation of H3K9,14 detected in our ChIPseq experiment in the hippocampus also occurs in cerebellar chromatin. However, as reported above, the changes in gene expression and promoter acetylation did not always run in parallel. Thus, the promoter region of the gene encoding the activity-regulated cytoskeleton-associated (Arc) protein, which is downregulated in HD82Q samples, did not show any apparent change at the acetylation level (Fig. 7*E*).

We also investigated whether the genes exhibiting altered transcript levels specifically in the cerebellum were associated with H3K9,14 deacetylation of the promoter. We assessed the promoters of the cerebellar ataxia-associated gene *Igfbp5* (Gatchel et al., 2008), the transcription factor *Eomes* (also known as *Tbr2*), the IEG *Fos*, and the substrate of protein kinase C *Marcks* (Fig. 7*F*). Like in the hippocampus, these gene specific assays confirmed the association of histone deacetylation events at TSS with relevant transcriptional deficits in HD tissue, but also indicated that additional epigenetic marks or mechanisms are required for explaining the full range of transcriptional alterations in polyQ disease as exemplified by *Marcks*.

To further investigate the relevance of the group of genes that exhibited concurrent changes in histone acetylation and gene expression in the hippocampus, we performed a GO enrichment analysis for this gene set and found a significant enrichment for ion binding proteins, particularly Ca^{2+}-binding proteins, and components of the synapse (Fig. 7*G*), which is consistent with the important synaptic dysfunction reported for these mice (Li et al., 2003). We also asked whether the same genes were altered in other tissues and HD models. To address this question, we examined the datasets corresponding to cerebellar gene expression in HD82Q mice, to striatal gene expression in R6/2 mice (a mouse model of early onset HD that exhibits striatal degeneration; Kuhn et al., 2007) and to postmortem caudate nucleus from HD patients (Hodges et al., 2006). GO and

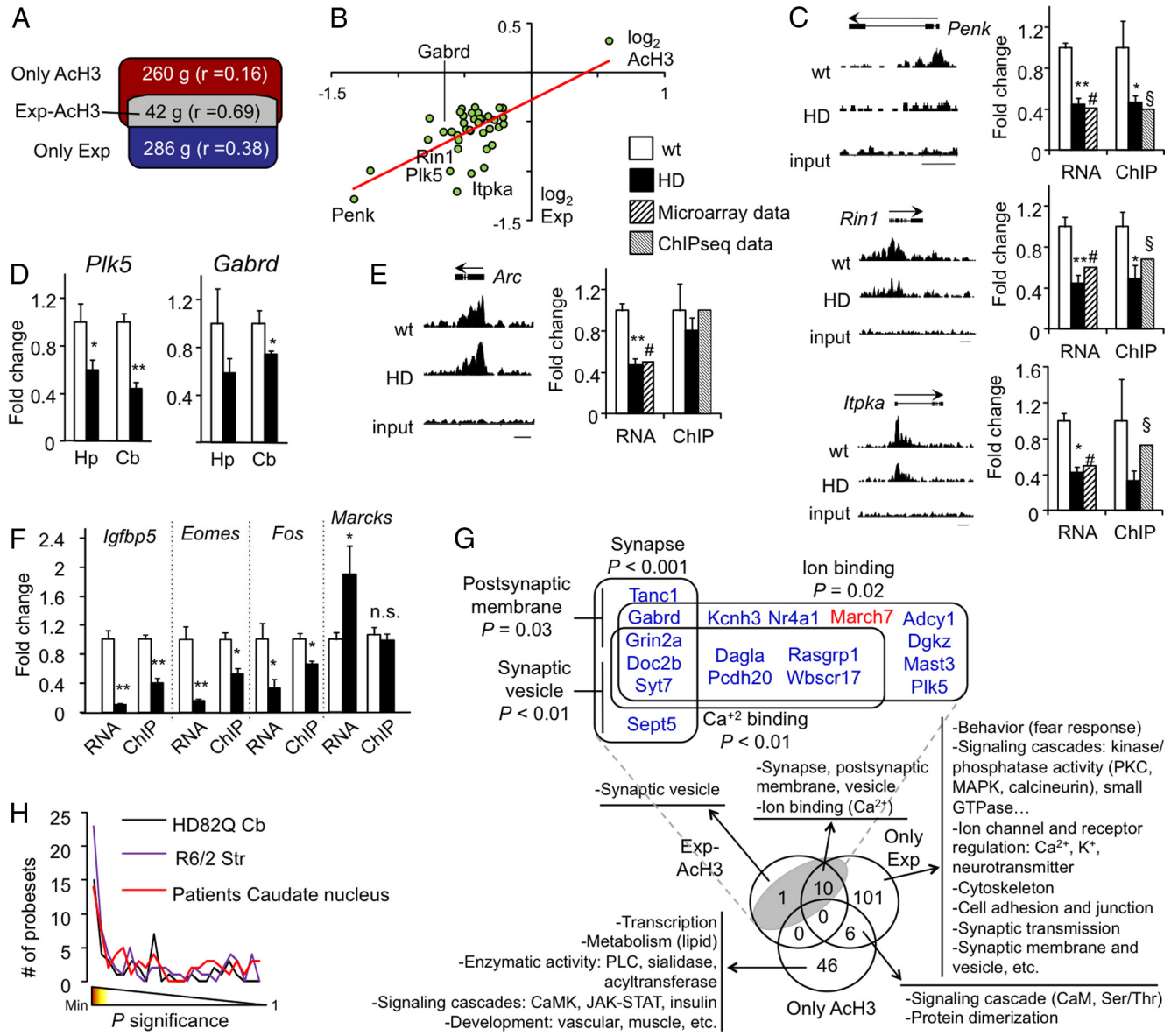

Figure 7. Genes showing both transcriptional and deacetylation defects are part of a consistent HD gene signature. ***A***, Venn diagram shows the overlapping between the genes differentially expressed and the genes differentially acetylated at the TSS. ***B***, Correlation graph for the Exp-AcH3 subset. ***C***, Bar graphs: ChIP-qPCR at the TSS of the genes *Penk*, *Rin1*, and *Itpka* and parallel RT-qPCR assays for the corresponding transcripts validated ChIPseq and microarray experiments ($n = 5$ for wt and $n = 6$ for HD82Q; results from 10- and 20-week-old mice were pooled). ChIPseq profiles are presented at the left of the bar graph for the same gene. Each region is depicted by the accumulation of reads around the 5′-end of the gene. Scale bar, 2 kb. Data are presented as the mean ± SEM. Comparisons refer to wt control: $*p < 0.05$ and $**p < 0.005$ (Student's *t* test); #, $p < 0.05$ (adjusted *p* value in LIMMA analysis); §, $p < 10^{-3}$ (FDR *p* value in SICER analysis). ***D***, ChIP-qPCR assays using AcH3K9,14 antibody were performed with cerebellar (Cb, $n = 3$ for both genotypes) and hippocampal (Hp, $n = 5$ for wt and $n = 6$ for HD82Q) chromatin on the promoter of genes that were differently expressed in both brain areas. Comparisons refer to wt control: $*p < 0.05$; $**p < 0.005$ (Student's *t* test). ***E***, Dissociation of transcript downregulation and promoter deacetylation for the gene *Arc*. Samples and legends are the same than for ***C***. ***F***, ChIP-qPCR assays using AcH3K9,14 antibody were performed with cerebellar (Cb, $n = 3$ for both genotypes) chromatin on the promoter of genes showing cerebellum-specific transcript changes. Data are represented as the mean ± SEM $*p < 0.05$ and $**p < 0.005$ (Student's *t* test). ***G***, Venn diagram shows the number and overlap of significantly enriched GO terms (in the categories of "Biological process", "Molecular function", and "Cellular component") in the subsets of genes retrieved in ***A***: genes that only exhibit changes in expression (Only Exp), only changes in H3K9,14 acetylation at the TSS (Only AcH3) or significant changes in both expression and TSS acetylation (Exp-AcH3, gray). A more detailed summary of the GO terms for the Exp-AcH3 subset is also depicted; blue, downregulated; red, upregulated. ***H***, Distribution of the TC IDs/probesets corresponding to Exp-AcH3 genes in the differential expression profiles obtained in the cerebellum of HD82Q mice ($\chi^2 = 124$, df = 22, $p < 10^{-5}$), the striatum of R6/2 mice ($\chi^2 = 176$, df = 23, $p < 10^{-5}$), and the caudate nucleus of HD patients ($\chi^2 = 67$, df = 22, $p < 10^{-5}$). χ^2 values are referred to a random distribution.

KEGG pathways enrichment analyses also revealed a large overlap between these the four datasets. More than 50% of the biological processes affected in the hippocampus were also enriched in the other datasets, including terms related to behavior (learning, memory, fear response), synaptic transmission, signaling pathways (phosphorylation, cAMP, small GTPase), and ion transport (mainly K^+). The KEGG pathways calcium signaling, gap junction, MAPK signaling, and neuroactive ligand-receptor interaction were affected in all the examined datasets. In the three cases, we observed a highly significant enrichment for Exp-AcH3 probesets among the top ranked changes (Fig. 7*H*).

Interestingly, we also observed a good correlation between the enrichment for TFBS in the promoter of deacetylated genes and that in downregulated genes for the different HD models (Fig. 8*A*). Furthermore, downregulated genes showed high correlation indexes between all the gene profiles whereas upregulated genes were poorly

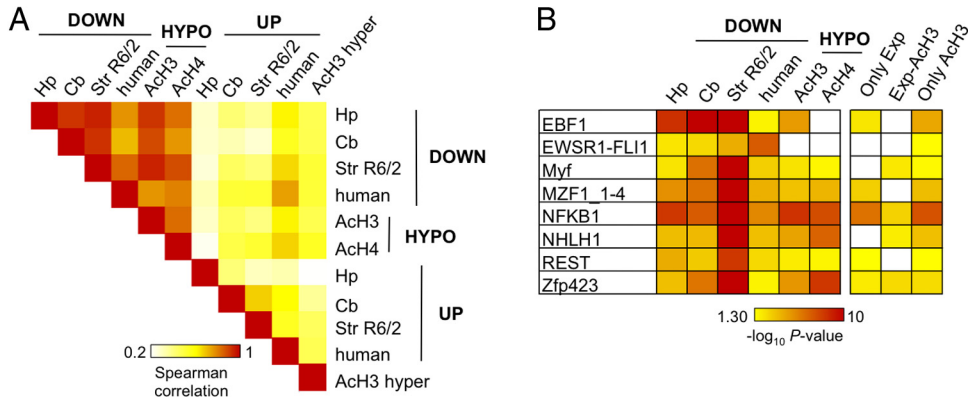

Figure 8. Functional genomics identifies transcriptional activities affected by mHtt. ***A***, Spearman correlation coefficients for TFBS enrichment in each dataset pair are presented as a heatmap. We compared the gene lists corresponding to significantly altered transcripts in HD82Q hippocampus (Hp) and cerebellum (Cb), R6/2 striatum (Str R6/2), caudate nucleus of HD patients (human) and hypo- and hyperacetylated TSS retrieved in our ChIPseq screen in HD82Q hippocampus. A good correlation was observed between the enrichment for TFBSs in the promoter of deacetylated genes (HYPO) and that in downregulated genes (DOWN) for the different HD models. In contrast, the enrichment in hyperacetylated genes (HYPER, only shown for AcH3K9,14 given the rarity of H4K12 hyperacetylation events) did not correlate with that in upregulated genes (UP). ***B***, Heatmap presenting the significance of TFBS enrichment for motifs that were consistently retrieved in the analysis of downregulated genes in the different expression profiles described above. The significance of the enrichment for the same TFBSs in the three gene sets defined in Figure 7*A* is also shown. The color palette indicates the *P* value range; white: nonsignificant ($P > 0.05$).

correlated. Together, these results suggest that common transcriptional mechanisms might be involved in the aberrant gene downregulation and deacetylation, whereas homeostatic responses (which are likely to contribute more prominently to gene upregulations) might depend on tissue-specific mechanisms. Among the most significant and consistent motifs detected in this meta-analysis were the binding sites of NRSF/REST and NF-κB that have both been previously involved in HD (Buckley et al., 2010; Marcora and Kennedy, 2010; Ravache et al., 2010; Datta and Bhattacharyya, 2011) (Fig. 8*B*). This analysis (limited to the motifs represented in the Jaspar database) did not identify DNA motifs unique to the Exp-AcH3 subset and that could thereby establish a specific link histone acetylation and gene expression deficits.

Discussion

Genomic landscape of transcriptional and epigenetic dysregulation in polyQ disease

Distinctive clinical features and brain imaging studies suggest that hippocampal and cerebellar malfunction may be especially relevant in early onset HD, an aggressive form of the disease associated with very long CAG repeats (Rodda, 1981; Rosas et al., 2003; Seneca et al., 2004; Paradiso et al., 2008; Ruocco et al., 2008). Moreover, other polyQ pathologies, such as different types of spinocerebellar ataxias, have the cerebellum as the main target (Orr and Zoghbi, 2007; Seidel et al., 2012). The regional pattern of transgene expression and the severity and fast progression of neuropathological traits in HD82Q mice made this strain especially suitable for investigating early onset polyQ pathology in these structures.

Our experiments demonstrate that the acetylation deficits observed in HD82Q mice are not global but are restricted to specific loci and associated with specific TFBS and genomic features. Although the two acetylation marks explored here have been linked to active loci, their profiles revealed remarkable differences. The enrichment profile of AcH3K9,14 showed sharp peaks that overlapped with the TSS, whereas AcH4K12 enrichment was characterized by wider and blunter islands that frequently occupied intra- and intergenic regions. The impact of HD pathology on the two profiles was also different. Although deacetylation of AcH4K12 islands in HD82Q chromatin was more severe than that of AcH3K9,14 islands, these changes were not associated with significant transcriptional deficits. As a result, we observed a much better correlation between reduced transcript levels and deacetylation at the TSS for AcH3K9,14 than for AcH4K12. Importantly, deregulated H4K12 acetylation has been also observed in the aging mouse hippocampus and linked to age-related memory impairment (Peleg et al., 2010). Our data therefore support the notion that neuronal H4K12 deacetylation may represent a biomarker for epigenetic dysregulation associated with hippocampal malfunction or degeneration, although the specific role of this mark in gene expression remains unknown.

Are histone acetylation and transcriptional dysregulation two independent manifestations of polyQ pathology?

Our appreciation of the complexity of epigenetic regulation of gene expression has dramatically increased with the development of new genomic techniques based on next generation sequencing (Dawson and Kouzarides, 2012). The novel insight that emerged from these studies has challenged many assumptions regarding the role of histone modifications in gene expression (Strahl and Allis, 2000; Schübeler et al., 2004; Wang et al., 2008) and basic questions, such as whether the transcriptional rate of a locus is determined by its histone acetylation level or vice versa, are now under debate (Henikoff and Shilatifard, 2011; Bedford and Brindle, 2012). One of the most striking conclusions of our comprehensive analysis is that histone deacetylation and transcriptional defects were, in general, not linked. This result is in good agreement with studies in yeast, flies, and mouse fibroblasts showing that the post-translational modification of histones may not be as essential for gene expression as anticipated. Thus, whole-genome analyses of gene expression changes in histone mutants have typically revealed modest phenotypes and relatively little phenotypic complexity resulting from the combination of histone mutations (Lenstra et al., 2011; Rando, 2012).

In agreement with a recent report based on a chip-on-chip screen (McFarland et al., 2012), our correlative analyses demonstrated an important mismatch between gene dysregulation and histone deacetylation in polyQ disorders, which indicates that the relationship between these two phenomena is more complex than anticipated (Saha and Pahan, 2006; Stack et al., 2007). With the exception of some H3K9,14 acetylation deficits located at TSS of genes that were part of a consistent signature found in different HD datasets, most of the differences in histone acetylation de-

tected in our differential screen mapped onto inter- and intragenic regions. Moreover, deacetylation events in inter- and intragenic regions were in average more prominent than those in TSSs. These acetylation defects did not have an apparent direct impact on the expression of the nearest gene. However, we still do not know the meaning of deacetylation events outside of the well studied protein-coding regions (Bernstein et al., 2012). For instance, a correlation between histone deacetylation at intergenic regions and noncoding RNA transcription (which are underrepresented in current microarrays) might still exist. These defects could also have trans and long-distance effects in other loci (Sanyal et al., 2012) or interfere with the transcriptional response of the cell to future challenges or insults. In fact, genes that are activated in response to stimuli, such as *Bdnf* (isoforms I and IV), the IEGs *Arc*, *Nr4a1*, and *Npas4* and others activity-regulated genes, were especially affected at the transcriptional level.

On the other hand, although we may have underestimated the number of genes that show a positive correlation between histone deacetylation and transcript downregulation due to the stringent filters used in our screen, the majority of the genes with reduced transcript levels in HD82Q samples did not exhibit significant changes in the two investigated acetylation marks. Therefore, other mechanisms, such as other post-translational modifications of histone (Kim et al., 2008), aberrant DNA methylation (Ng et al., 2013), and altered TF activities (Yamanaka et al., 2008; Buckley et al., 2010; Marcora and Kennedy, 2010; Ravache et al., 2010; Datta and Bhattacharyya, 2011), should also contribute to transcriptional dysregulation in HD. Because the compromised lysine acetyltransferase activity observed in the brain of HD82Q mice may also affect nonhistone substrates (Dompierre et al., 2007), including TFs like NF-κB whose activity is regulated by acetylation (Zhang et al., 2010), the histone deacetylation-independent transcriptional dysregulation may still be deacetylation-dependent. Consistently with this view, NF-κB binding sites were enriched in the promoters of both downregulated and deacetylated genes.

In conclusion, the combination of ChIPseq and microarray technologies supported the hypothesis that transcriptional and epigenetic dysregulation, particularly aberrant acetylation of neuronal chromatin, are early features of polyQ pathology. However, our results suggest that these are two largely independent manifestations of the pathology. Our screen also identified a relatively small subset of candidate genes that show potential as progression biomarkers or therapeutic targets for this fatal neurodegenerative disease. These results lead to new questions, such as how the expression of mHtt drives deacetylation to specific genomic regions and what causes the transcriptional deficits that were not associated with histone deacetylation. Regardless of the answers to those important questions, high-resolution description of the genomic topography of epigenetic and transcriptional alterations appears to be an essential requirement for a better understanding of the etiology of polyQ diseases and for the development of effective therapies aimed at correcting the deficits.

Notes

Supplemental material for this article is available at http://in.umh.es/IP/Barco-lab-DataSets.html. Access to: Tables that present the results of microarrays and ChIPseq differential screenings. This material has not been peer reviewed.

References

Bedford DC, Brindle PK (2012) Is histone acetylation the most important physiological function for CBP and p300? Aging 4:247–255. Medline

Bernstein BE, et al. (2012) An integrated encyclopedia of DNA elements in the human genome. Nature 489:57–74. CrossRef Medline

Bowles KR, Brooks SP, Dunnett SB, Jones L (2012) Gene expression and behaviour in mouse models of HD. Brain Res Bull 88:276–284. CrossRef Medline

Buckley NJ, Johnson R, Zuccato C, Bithell A, Cattaneo E (2010) The role of REST in transcriptional and epigenetic dysregulation in Huntington's disease. Neurobiol Dis 39:28–39. CrossRef Medline

Cha JH (2000) Transcriptional dysregulation in Huntington's disease. Trends Neurosci 23:387–392. CrossRef Medline

Datta M, Bhattacharyya NP (2011) Regulation of RE1 protein silencing transcription factor (REST) expression by HIP1 protein interactor (HIPPI). J Biol Chem 286:33759–33769. CrossRef Medline

Dawson MA, Kouzarides T (2012) Cancer epigenetics: from mechanism to therapy. Cell 150:12–27. CrossRef Medline

de Cárcer G, Escobar B, Higuero AM, García L, Ansón A, Pérez G, Mollejo M, Manning G, Meléndez B, Abad-Rodríguez J, Malumbres M (2011) Plk5, a polo box domain-only protein with specific roles in neuron differentiation and glioblastoma suppression. Mol Cell Biol 31:1225–1239. CrossRef Medline

Dibbens LM, Feng HJ, Richards MC, Harkin LA, Hodgson BL, Scott D, Jenkins M, Petrou S, Sutherland GR, Scheffer IE, Berkovic SF, Macdonald RL, Mulley JC (2004) GABRD encoding a protein for extra- or perisynaptic GABAA receptors is a susceptibility locus for generalized epilepsies. Hum Mol Genet 13:1315–1319. CrossRef Medline

Dompierre JP, Godin JD, Charrin BC, Cordelières FP, King SJ, Humbert S, Saudou F (2007) Histone deacetylase 6 inhibition compensates for the transport deficit in Huntington's disease by increasing tubulin acetylation. J Neurosci 27:3571–3583. CrossRef Medline

Gardian G, Browne SE, Choi DK, Klivenyi P, Gregorio J, Kubilus JK, Ryu H, Langley B, Ratan RR, Ferrante RJ, Beal MF (2005) Neuroprotective effects of phenylbutyrate in the N171–82Q transgenic mouse model of Huntington's disease. J Biol Chem 280:556–563. CrossRef Medline

Gatchel JR, Watase K, Thaller C, Carson JP, Jafar-Nejad P, Shaw C, Zu T, Orr HT, Zoghbi HY (2008) The insulin-like growth factor pathway is altered in spinocerebellar ataxia type 1 and type 7. Proc Natl Acad Sci U S A 105:1291–1296. CrossRef Medline

Gentleman RC, Carey VJ, Bates DM, Bolstad B, Dettling M, Dudoit S, Ellis B, Gautier L, Ge Y, Gentry J, Hornik K, Hothorn T, Huber W, Iacus S, Irizarry R, Leisch F, Li C, Maechler M, Rossini AJ, Sawitzki G, Smith C, et al. (2004) Bioconductor: open software development for computational biology and bioinformatics. Genome Biol 5:R80. CrossRef Medline

Giralt A, Puigdellívol M, Carretón O, Paoletti P, Valero J, Parra-Damas A, Saura CA, Alberch J, Ginés S (2012) Long-term memory deficits in Huntington's disease are associated with reduced CBP histone acetylase activity. Hum Mol Genet 21:1203–1216. CrossRef Medline

Henikoff S, Shilatifard A (2011) Histone modification: cause or cog? Trends Genet 27:389–396. CrossRef Medline

Hockly E, Cordery PM, Woodman B, Mahal A, van Dellen A, Blakemore C, Lewis CM, Hannan AJ, Bates GP (2002) Environmental enrichment slows disease progression in R6/2 Huntington's disease mice. Ann Neurol 51:235–242. CrossRef Medline

Hodges A, Strand AD, Aragaki AK, Kuhn A, Sengstag T, Hughes G, Elliston LA, Hartog C, Goldstein DR, Thu D, Hollingsworth ZR, Collin F, Synek B, Holmans PA, Young AB, Wexler NS, Delorenzi M, Kooperberg C, Augood SJ, Faull RL, et al. (2006) Regional and cellular gene expression changes in human Huntington's disease brain. Hum Mol Genet 15:965–977. CrossRef Medline

Huang da W, Sherman BT, Lempicki RA (2009) Systematic and integrative analysis of large gene lists using DAVID bioinformatics resources. Nat Protoc 4:44–57. CrossRef Medline

Kim MO, Chawla P, Overland RP, Xia E, Sadri-Vakili G, Cha JH (2008) Altered histone monoubiquitylation mediated by mutant huntingtin induces transcriptional dysregulation. J Neurosci 28:3947–3957. CrossRef Medline

Klevytska AM, Tebbenkamp AT, Savonenko AV, Borchelt DR (2010) Partial depletion of CREB-binding protein reduces life expectancy in a mouse model of Huntington disease. J Neuropathol Exp Neurol 69:396–404. CrossRef Medline

Kuhn A, Goldstein DR, Hodges A, Strand AD, Sengstag T, Kooperberg C, Becanovic K, Pouladi MA, Sathasivam K, Cha JH, Hannan AJ, Hayden MR, Leavitt BR, Dunnett SB, Ferrante RJ, Albin R, Shelbourne P, Delorenzi M, Augood SJ, Faull RL, Olson JM, et al. (2007) Mutant huntingtin's effects on striatal gene expression in mice recapitulate changes observed in human

Huntington's disease brain and do not differ with mutant huntingtin length or wild-type huntingtin dosage. Hum Mol Genet 16:1845–1861. CrossRef Medline

Lenstra TL, Benschop JJ, Kim T, Schulze JM, Brabers NA, Margaritis T, van de Pasch LA, van Heesch SA, Brok MO, Groot Koerkamp MJ, Ko CW, van Leenen D, Sameith K, van Hooff SR, Lijnzaad P, Kemmeren P, Hentrich T, Kobor MS, Buratowski S, Holstege FC (2011) The specificity and topology of chromatin interaction pathways in yeast. Mol Cell 42:536–549. CrossRef Medline

Levenson JM, O'Riordan KJ, Brown KD, Trinh MA, Molfese DL, Sweatt JD (2004) Regulation of histone acetylation during memory formation in the hippocampus. J Biol Chem 279:40545–40559. CrossRef Medline

Li H, Durbin R (2010) Fast and accurate long-read alignment with Burrows-Wheeler transform. Bioinformatics 26:589–595. CrossRef Medline

Li H, Wyman T, Yu ZX, Li SH, Li XJ (2003) Abnormal association of mutant huntingtin with synaptic vesicles inhibits glutamate release. Hum Mol Genet 12:2021–2030. CrossRef Medline

Li H, Handsaker B, Wysoker A, Fennell T, Ruan J, Homer N, Marth G, Abecasis G, Durbin R (2009) The sequence alignment/map format and SAMtools. Bioinformatics 25:2078–2079. CrossRef Medline

Lopez de Armentia M, Jancic D, Olivares R, Alarcon JM, Kandel ER, Barco A (2007) cAMP response element-binding protein-mediated gene expression increases the intrinsic excitability of CA1 pyramidal neurons. J Neurosci 27:13909–13918. CrossRef Medline

Lopez-Atalaya JP, Ciccarelli A, Viosca J, Valor LM, Jimenez-Minchan M, Canals S, Giustetto M, Barco A (2011) CBP is required for environmental enrichment-induced neurogenesis and cognitive enhancement. EMBO J 30:4287–4298. CrossRef Medline

MacDonald ME, Ambrose CM, Duyao MP, Myers RH, Lin C, Srinidhi L, Barnes G, Taylor SA, James M, Groot N, MacFarlane H, Jenkins B, Anderson MA, Wexler NS, Gusella JF, Bates GP, Baxendale S, Hummerich H, Kirby S, North M, et al. (1993) A novel gene containing a trinucleotide repeat that is expanded and unstable on Huntington's disease chromosomes. The Huntington's Disease Collaborative Research Group. Cell 72:971–983. CrossRef Medline

Marcora E, Kennedy MB (2010) The Huntington's disease mutation impairs Huntington's role in the transport of NF-kappaB from the synapse to the nucleus. Hum Mol Genet 19:4373–4384. CrossRef Medline

McFarland KN, Das S, Sun TT, Leyfer D, Xia E, Sangrey GR, Kuhn A, Luthi-Carter R, Clark TW, Sadri-Vakili G, Cha JH (2012) Genome-wide histone acetylation is altered in a transgenic mouse model of Huntington's disease. PLoS ONE 7:e41423. CrossRef Medline

Ng CW, Yildirim F, Yap YS, Dalin S, Matthews BJ, Velez PJ, Labadorf A, Housman DE, Fraenkel E (2013) Extensive changes in DNA methylation are associated with expression of mutant huntingtin. Proc Natl Acad Sci U S A 110:2354–2359. CrossRef Medline

Oliveros J (2007) Venny: an interactive tool for comparing lists with Venn diagrams. http://bioinfogp.cnb.csic.es/tools/venny/index.html.

Orr HT, Zoghbi HY (2007) Trinucleotide repeat disorders. Annu Rev Neurosci 30:575–621. CrossRef Medline

Paradiso S, Turner BM, Paulsen JS, Jorge R, Ponto LL, Robinson RG (2008) Neural bases of dysphoria in early Huntington's disease. Psychiatry Res 162:73–87. CrossRef Medline

Peleg S, Sananbenesi F, Zovoilis A, Burkhardt S, Bahari-Javan S, Agis-Balboa RC, Cota P, Wittnam JL, Gogol-Doering A, Opitz L, Salinas-Riester G, Dettenhofer M, Kang H, Farinelli L, Chen W, Fischer A (2010) Altered histone acetylation is associated with age-dependent memory impairment in mice. Science 328:753–756. CrossRef Medline

Rando OJ (2012) Combinatorial complexity in chromatin structure and function: revisiting the histone code. Curr Opin Genet Dev 22:148–155. CrossRef Medline

Ravache M, Weber C, Mérienne K, Trottier Y (2010) Transcriptional activation of REST by Sp1 in Huntington's disease models. PLoS ONE 5:e14311. CrossRef Medline

Robinson JT, Thorvaldsdóttir H, Winckler W, Guttman M, Lander ES, Getz G, Mesirov JP (2011) Integrative genomics viewer. Nat Biotechnol 29:24–26. CrossRef Medline

Rodda RA (1981) Cerebellar atrophy in Huntington's disease. J Neurol Sci 50:147–157. CrossRef Medline

Rosas HD, Koroshetz WJ, Chen YI, Skeuse C, Vangel M, Cudkowicz ME, Caplan K, Marek K, Seidman LJ, Makris N, Jenkins BG, Goldstein JM (2003) Evidence for more widespread cerebral pathology in early HD: an MRI-based morphometric analysis. Neurology 60:1615–1620. CrossRef Medline

Ruocco HH, Bonilha L, Li LM, Lopes-Cendes I, Cendes F (2008) Longitudinal analysis of regional grey matter loss in Huntington disease: effects of the length of the expanded CAG repeat. J Neurol Neurosurg Psychiatry 79:130–135. CrossRef Medline

Sadri-Vakili G, Bouzou B, Benn CL, Kim MO, Chawla P, Overland RP, Glajch KE, Xia E, Qiu Z, Hersch SM, Clark TW, Yohrling GJ, Cha JH (2007) Histones associated with downregulated genes are hypo-acetylated in Huntington's disease models. Hum Mol Genet 16:1293–1306. CrossRef Medline

Saha RN, Pahan K (2006) HATs and HDACs in neurodegeneration: a tale of disconcerted acetylation homeostasis. Cell Death Differ 13:539–550. CrossRef Medline

Sanchis-Segura C, Lopez-Atalaya JP, Barco A (2009) Selective boosting of transcriptional and behavioral responses to drugs of abuse by histone deacetylase inhibition. Neuropsychopharmacology 34:2642–2654. CrossRef Medline

Sanyal A, Lajoie BR, Jain G, Dekker J (2012) The long-range interaction landscape of gene promoters. Nature 489:109–113. CrossRef Medline

Schilling G, Becher MW, Sharp AH, Jinnah HA, Duan K, Kotzuk JA, Slunt HH, Ratovitski T, Cooper JK, Jenkins NA, Copeland NG, Price DL, Ross CA, Borchelt DR (1999) Intranuclear inclusions and neuritic aggregates in transgenic mice expressing a mutant N-terminal fragment of huntingtin. Hum Mol Genet 8:397–407. CrossRef Medline

Schübeler D, MacAlpine DM, Scalzo D, Wirbelauer C, Kooperberg C, van Leeuwen F, Gottschling DE, O'Neill LP, Turner BM, Delrow J, Bell SP, Groudine M (2004) The histone modification pattern of active genes revealed through genome-wide chromatin analysis of a higher eukaryote. Genes Dev 18:1263–1271. CrossRef Medline

Seidel K, Siswanto S, Brunt ER, den Dunnen W, Korf HW, Rüb U (2012) Brain pathology of spinocerebellar ataxias. Acta Neuropathologica 124:1–21. CrossRef Medline

Seneca S, Fagnart D, Keymolen K, Lissens W, Hasaerts D, Debulpaep S, Desprechins B, Liebaers I, De Meirleir L (2004) Early onset Huntington disease: a neuronal degeneration syndrome. Eur J Pediatr 163:717–721. CrossRef Medline

Seredenina T, Luthi-Carter R (2012) What have we learned from gene expression profiles in Huntington's disease? Neurobiol Dis 45:83–98. CrossRef Medline

Smyth G (2005) Limma: linear models for microarray data. New York: Springer.

Snowden JS, Craufurd D, Thompson J, Neary D (2002) Psychomotor, executive, and memory function in preclinical Huntington's disease. J Clin Exp Neuropsychol 24:133–145. CrossRef Medline

Stack EC, Del Signore SJ, Luthi-Carter R, Soh BY, Goldstein DR, Matson S, Goodrich S, Markey AL, Cormier K, Hagerty SW, Smith K, Ryu H, Ferrante RJ (2007) Modulation of nucleosome dynamics in Huntington's disease. Hum Mol Genet 16:1164–1175. CrossRef Medline

Strahl BD, Allis CD (2000) The language of covalent histone modifications. Nature 403:41–45. CrossRef Medline

Valor LM, Pulopulos MM, Jimenez-Minchan M, Olivares R, Lutz B, Barco A (2011) Ablation of CBP in forebrain principal neurons causes modest memory and transcriptional defects and a dramatic reduction of histone acetylation, but does not affect cell viability. J Neurosci 31:1652–1663. CrossRef Medline

Valor LM, Viosca J, Lopez-Atalaya JP, Barco A (2013) Lysine acetyltransferases CBP and p300 as therapeutic targets in cognitive and neurodegenerative disorders. Curr Pharm Des. Advance online publication. Retrieved Feb. 19, 2013. doi:10.2174/13816128113199990382. CrossRef Medline

Wang Z, Zang C, Rosenfeld JA, Schones DE, Barski A, Cuddapah S, Cui K, Roh TY, Peng W, Zhang MQ, Zhao K (2008) Combinatorial patterns of histone acetylations and methylations in the human genome. Nat Genet 40:897–903. CrossRef Medline

Yamanaka T, Miyazaki H, Oyama F, Kurosawa M, Washizu C, Doi H, Nukina N (2008) Mutant huntingtin reduces HSP70 expression through the sequestration of NF-Y transcription factor. EMBO J 27:827–839. CrossRef Medline

Zambelli F, Pesole G, Pavesi G (2009) Pscan: finding over-represented transcription factor binding site motifs in sequences from co-regulated or coexpressed genes. Nucleic Acids Res 37:W247–252. CrossRef Medline

Zang C, Schones DE, Zeng C, Cui K, Zhao K, Peng W (2009) A clustering

approach for identification of enriched domains from histone modification ChIP-seq data. Bioinformatics 25:1952–1958. CrossRef Medline

Zhang LX, Zhao Y, Cheng G, Guo TL, Chin YE, Liu PY, Zhao TC (2010) Targeted deletion of NF-kappaB p50 diminishes the cardioprotection of histone deacetylase inhibition. Am J Physiol Heart Circ Physiol 298: H2154–2163. CrossRef Medline

Zhu LJ, Gazin C, Lawson ND, Pagès H, Lin SM, Lapointe DS, Green MR (2010) ChIPpeakAnno: a bioconductor package to annotate ChIP-seq and ChIP-chip data. BMC Bioinformatics 11:237. CrossRef Medline

Zuccato C, Valenza M, Cattaneo E (2010) Molecular mechanisms and potential therapeutical targets in Huntington's disease. Physiological reviews 90:905–981. CrossRef Medline

4.2 Deacetylation of histone H3 in Huntington's disease is locus-specific

In this chapter of Results, we extend our research on histone deacetylation in the mouse model of poly-Q disease known as N171-82Q (*aka* HD82Q) (section 4.1) to other common models of HD. We also extend the analysis of altered histone PTMs to other epigenetic marks, primarily the trimethylation of histone H3 at K4.

4.2.1 Bulk histone acetylation levels are preserved in different animal models of HD

We have recently reported that the HD82Q strain does not show, even in advanced stages of the pathology, a net reduction of the global levels of histone acetylation in different brain areas, including those that show stronger mHtt expression, the hippocampus and the cerebellum (Valor et al., 2013a). To test whether this observation can be extended to other animal models or if it is, by contrast, a particular feature of the HD82Q strain, bulk histone acetylation levels were examined in other HD models that have different pattern of expression of mHtt and length of CAG repeats and that differ in the onset and progression rate of the pathology.

As in the case of HD82Q, the well-characterized HD murine model R6/1 shows early onset and rapid progression of the disease. Due to the use of the human HTT promoter (**Fig. 12A**), the transgene was ubiquitously expressed throughout the mouse brain, including the striatum, cortex, hippocampus and cerebellum (**Fig. 12B**). Mutant mice showed early motor and cognitive deficits (**Fig. 12C-G**). Consistent with these behavioral deficits, RT-qPCR assays revealed deregulation of several important neuronal genes identified in our previous study in HD82Q mice as part of the gene signature associated with polyQ disease (Valor et al., 2013a) (**Fig. 12H**). However, immunohistochemistry analyses revealed no apparent histone deacetylation in the brain of R6/1 mice (**Fig. 12I-J**), a finding that was further confirmed by Western blotting assays (not shown).

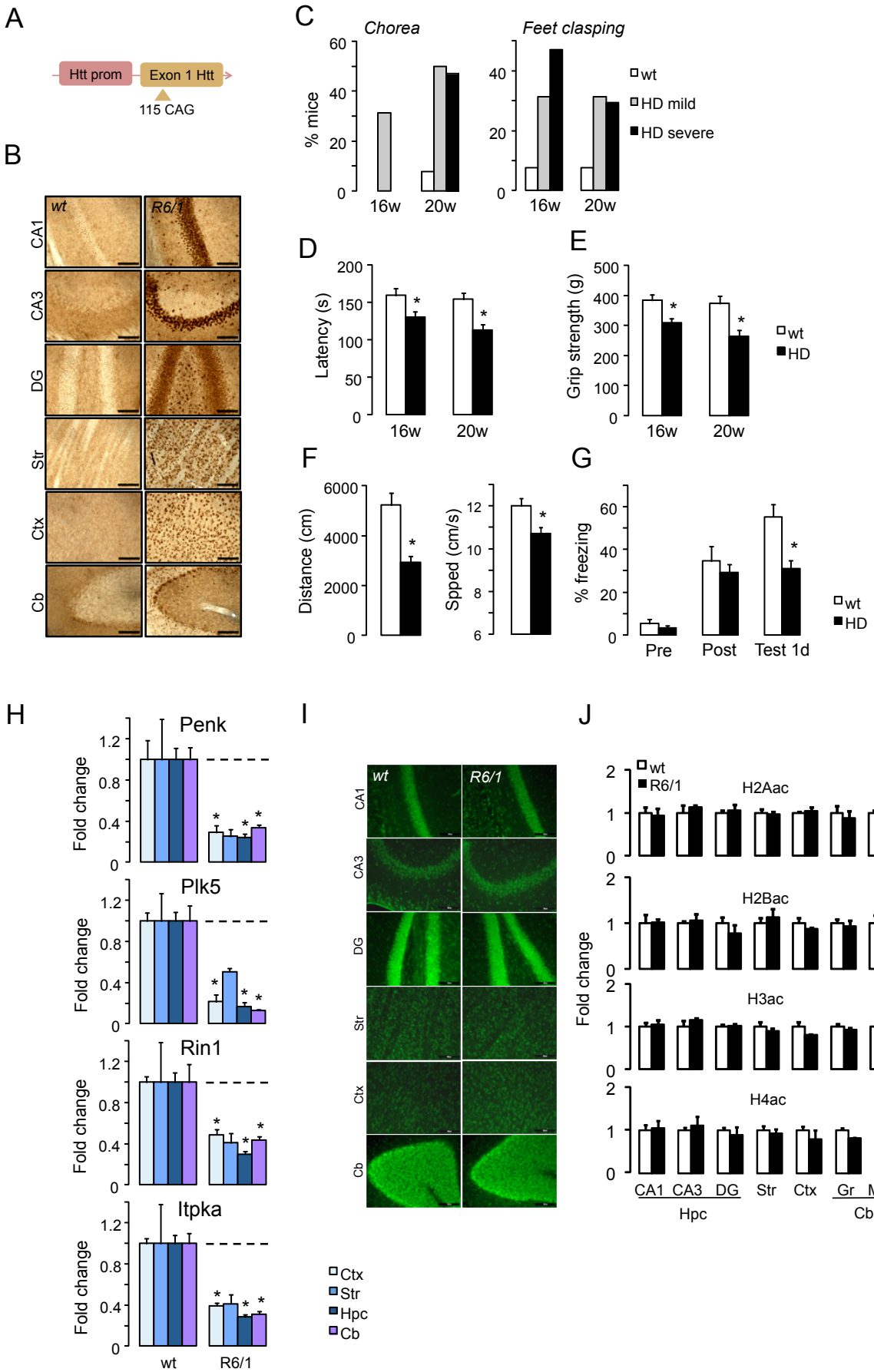
A
Htt prom
Exon 1 Htt
115 CAG
B
wt
R6/1
CA1
CA3
DG
Str
Ctx
Cb
C
Chorea
Feet clasping
% mice
wt
HD mild
HD severe
16w
20w
D
Latency (s)
E
Grip strength (g)
wt
HD
F
Distance (cm)
Spped (cm/s)
G
% freezing
Pre
Post
Test 1d
H
Penk
Plk5
Rin1
Itpka
Fold change
wt
R6/1
I
Ctx
Str
Hpc
Cb
J
H2Aac
H2Bac
H3ac
H4ac
CA1 CA3 DG Str Ctx Gr Mol
Hpc
Cb

Figure 12. R6/1 mice show motor, cognitive and transcriptional deficits but preserved bulk histone acetylation levels. A. Scheme of the HD transgene expressed in R6/1 strain. Mutant mice express exon 1 of the human *Htt* gene with 115 CAG repeats under the control of the human *HTT* promoter. **B.** mHTT expression in the R6/1 brain. A strong immunoreactivity was detected in all the brain areas tested in transgenic mice but absent in the wild-type littermates. Scale bar, 100 µm. **C-G.** Motor and spontaneous activity analysis of R6/1 mice and wild-type littermates: 16- and 20-weeks-old mutant animals exhibited chorea and feet clasping (**C**), and showed reduced latency in an accelerated speed rotarod task (**D**) and reduced the grip strength (**E**). In addition, 20-weeks-old R6/1 mice traveled less distance and moved slower than control littermate mice in an open field (**F**). *n* = 13 (wt), *n* = 16 (R6/1). **G.** Cognitive impairment in 12-weeks-old R6/1 mice prior to an overt motor phenotype, as revealed in the contextual fear conditioning paradigm as a deficit to remember the association between the chamber and the shock. Pre, pre-shock; post, post-shock. *n* = 6 (wt), *n* = 9 (R6/1). **H.** RT-qPCR assays in 20-weeks-old samples of selected transcripts, based in published data (Valor et al., 2013a): proenkephalin (Penk), polo-like kinase 5 (Plk5), Ras and Rab interactor 1 (Rin1), and inositol trisphosphate 3-kinase A (Iptka). *n* = 7 (wt), *n* = 5 (R6/1). **I.** Representative immunohistochemistry images of different brain areas from 25-week-old R6/1 and wild-type littermate mice using an antibody against H3K9/14ac. Scale bar, 100 µm. **J.** Quantification of immunohistochemistry assays of the four-nucleosome histones: acetylated lysines 5 and 9 of histone H2A (H2Aac), acetylated lysines 5, 12, 15 and 20 of histone H2B (H2Bac), acetylated lysines 9 and 14 of histone H3 (H3ac) and acetylated lysines 5, 8, 12 and 16 of histone H4 (H4ac). *n* = 5 (wt), *n* = 3 (R6/1). DG, dentate gyrus; Hpc, hippocampus; striatum, Str; Ctx, cortex; Gr, granular layer; Mol, molecular layer; Cb, cerebellum. Data are presented as mean ± s.e.m. *, $p < 0.05$ (Student's t-test); +, $p < 0.05$ (genotype effect, 2-way ANOVA).

We next investigated YAC128 mice, in which a mutant version of full length HTT is encoded in a yeast artificial chromosome (YAC) (**Fig. 13A**). In these animals, polyQ pathology is less aggressive (Slow et al., 2003) and shows a slower progression compared to HD82Q and R6/1 models. Both behavioral (**Fig. 13B-C**) and transcriptional (**Fig. 13D**) deficits were less prominent in YAC128 mice. However, like for the other two models, the brain of YAC128 mice did not exhibit sign of bulk histone hypoacetylation at time points in which transcriptional dysregulation and pathological behavior had become significant (**Fig. 13E-F**).

To gain more precision in our analyses of the impact of mHTT expression in neuronal histone acetylation levels, we used in utero electroporation technique. This approach allows the examination of global histone acetylation levels in a cell-by-cell analysis by quantifying acetylation in GFP positive (mHTT-expressing) cells in a non-expressing tissue background. For this purpose, the striata of wild-type embryos were monolaterally electroporated with constructs that express trackable transgenes encoding the N-terminus of the human HTT fused to EGFP and bearing either 128 (*mHTT*) or 15 CAG repeats (control) (**Fig. 14A**). Mice overexpressing the pathological version in the striatum (**Fig. 14B**) showed increased feet clasping behavior (**Fig. 14C**). Again, we found that the acetylation levels for the four core

histones remained unaltered in cells expressing the aberrantly expanded polyQ fragment (**Fig. 14D-E**).

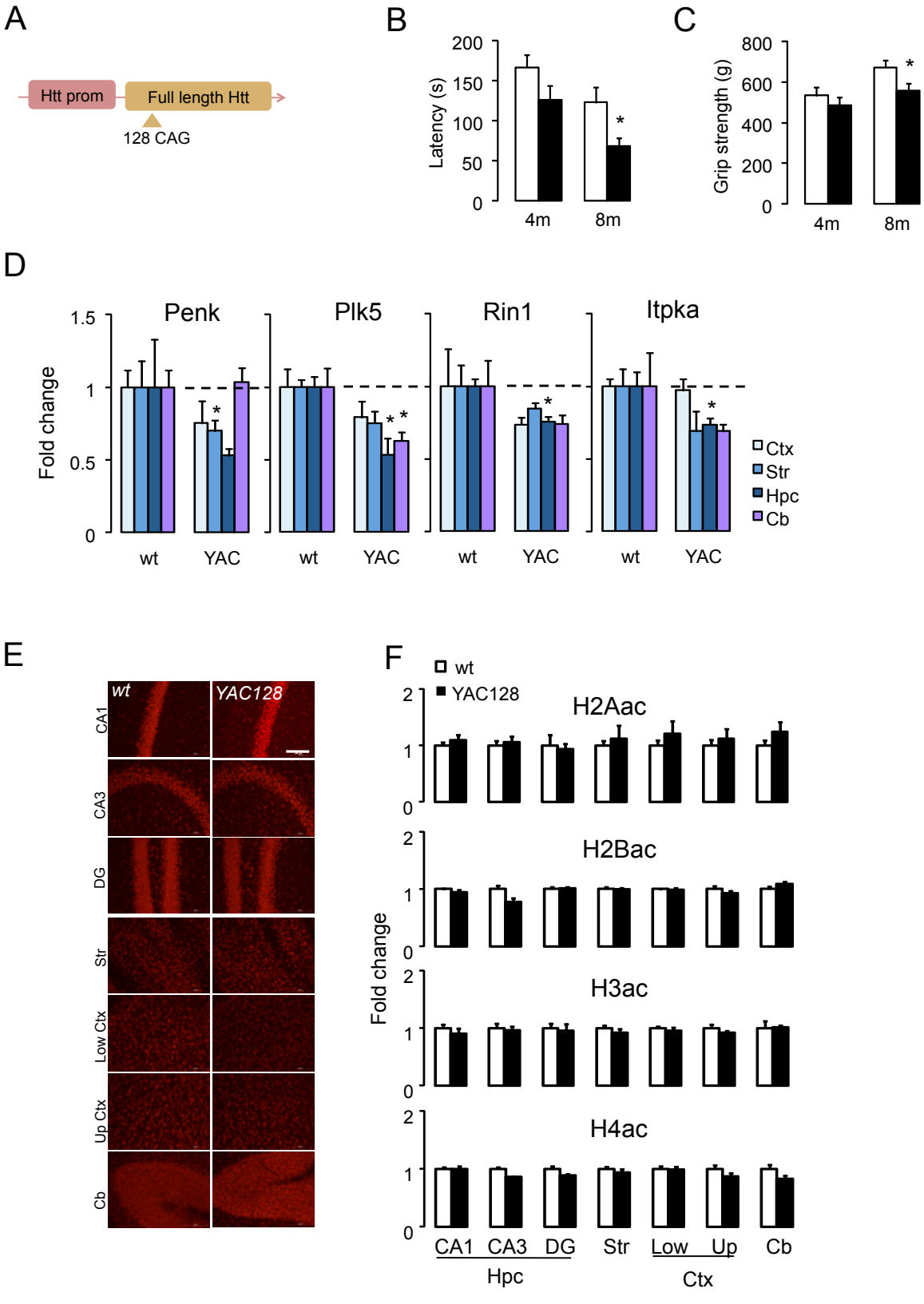

Figure 13. YAC128 mice also show HD molecular and phenotypic traits but preserved bulk histone acetylation levels. A. Squeme of the transgene expressed in YAC128 strain. Mutant mice express a full-length human *HTT* gene with 128 CAG repeats under the control of the human *HTT* promoter. **B-C.** Eight-months-old transgenic animals showed reduced latency in an accelerated speed rotarod task (**B**) and reduced grip strength (**C**). *n* = 11 (wt), *n* = 12 (YAC128). **D.** RT-qPCR assays of the same selected transcripts in Fig. 1. *n* = 4 (wt), *n* = 5 (YAC128). **E.** Representative immunohistochemistry images of different brain areas from early symptomatic (8-months-old) YAC128 and wild-type littermate mice using an antibody against H3K9/14ac. Scale bar, 100 µm. **F.** Quantification of immunohistochemistry assays of the four-nucleosome histones: H2Aac, H2Bac, H3ac and H4ac. *n* = 4 for each genotype. DG, dentate gyrus; Hpc, hippocampus; Str, striatum; Str; Low, lower cortical layers; Up, upper cortical layers; Ctx, cortex; Cb, cerebellum. Data are presented as mean ± s.e.m. *, $p < 0.05$ (Student's t-test); +, $p < 0.05$ (genotype effect, 2-way ANOVA).

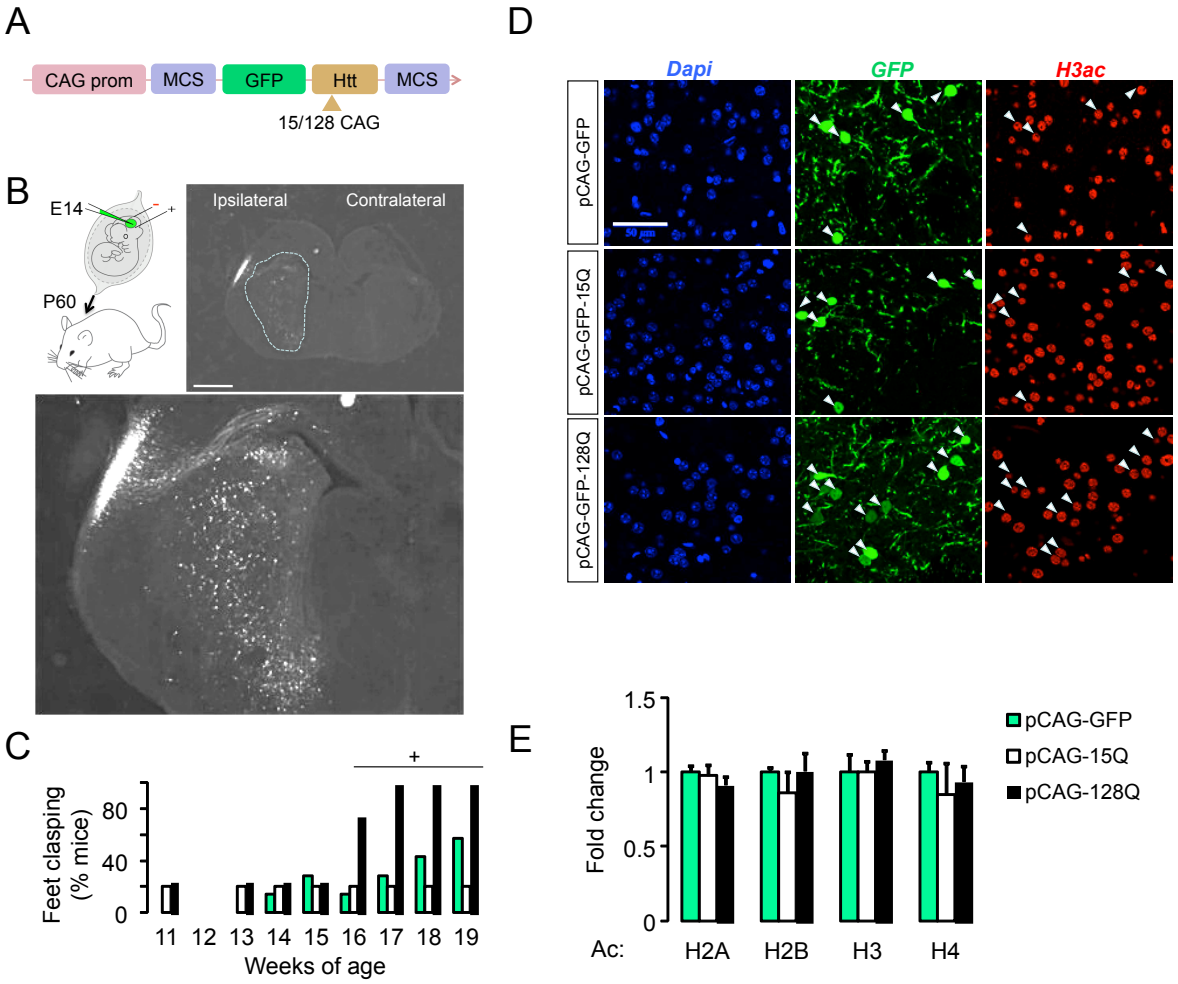

Figure 14. mHTT-electroprated mice show preserved bulk histone acetylation levels. A. Squeme of the constructs used in the *in utero* electroporation, containing two different expansions of the CAG stretch: 15 and 128 repeats. The expression of mHTT is under the control of the cytomegalovirus early enhancer/β-actin (CAG) promoter. The pCAG-GFP did not contain the HTT fragment. **B.** Coronal section from mHTT-electroporated striatum of an adult mouse. Scale bar, 500 µm. **C.** Percentage of 20-week-old mice showing feet clasping during 1 min tail suspension test. *n* = 7 (pCAG-GFP), *n* = 5 (pCAG-15Q), *n* = 4 (pCAG-128Q). **D.** Representative immunohistochemistry images of electroporated striatum with the GFP-HTT and GFP-alone constructs in 16-week-old mice using an antibody against H3K9/14ac. Note that fusion of the GFP upstream to the *HTT* sequence did not result in the formation of aggregates in the polyQ-expanded version, as already described (Choi et al., 2012). Scale bar, 500 µm. **E.** Quantification of the four-nucleosome acetylated histones in the cells expressing either mHTT

(pCAG-GFP-128Q), control HTT (pCAG-GFP-15Q) and GFP-alone (pCAG-GFP). *n* = 7 (pCAG-GFP), *n* = 5 (pCAG-15Q), *n* = 4 (pCAG-128Q). Data are presented as mean ± s.e.m.

4.2.2 Bulk histone acetylation levels are also preserved in cellular models of HD

The first studies showing a global reduction of histone acetylation were conducted in cellular preparations (Steffan et al., 2001; Igarashi et al., 2003). Due to the homogeneity and relative simplicity of *in vitro* models, we thought that changes in the levels of histone acetylation might be more easily observable in cellular models. To test this idea, primary neuronal cultures were infected with lentiviruses expressing different variants of N-terminal HTT fragments, bearing 15 CAG repeats (*wtHTT*) or 128 repeats (*mHTT*), and differing in the length of the 3'-end of the *HTT* sequence (**Fig. 15A**). The longest mHTT fragment produced perinuclear aggregates ("cytoplasmic" or cyt) whereas the shortest version was able to enter into the nucleus and form intranuclear aggregates ("nuclear" or nuc) (**Fig. 15B**). This result suggests that the differential segment between both constructs may contain a nuclear exclusion signal that is present in the longest mHtt version. Independently on the subcellular compartmentalization of soluble and aggregative-prone mHTT, the expression of neither variant had an overall impact on histone acetylation levels, indicating that accumulation of mHtt into the nucleus is not sufficient to produce a global alteration in histone acetylation (**Fig. 15C-D**). There results were also validated in Western blots (not shown).

The same biochemical analysis was extended to a well-established cellular model of HD: stably transfected PC12 cell lines that express in an inducible manner either a control (PC12-TetOn-HD23Q) or mutant (PC12-TetOn-HD72Q) N-terminus of the human HTT fused to GFP (**Fig. 16A**) (Wyttenbach et al., 2001). In these cells, treatment with doxycycline rapidly induced transgene expression (**Fig. 16B**). Whereas the fluorescent signal remained stable in the control cells, a decay of the signal was observed in the HD72Q cell line, probably due to toxicity-induced cell loss: cell counting after 7DIV revealed a reduction of 7.9 ± 1.6% and 23.5 ± 4.9% in HD23Q and HD72Q cell lines, respectively. This cell loss was more evident thereafter (**Fig. 16B** 14d images). Despite these changes, no net difference in bulk histone acetylation levels was observed between the two cell lines (**Fig. 16C-D**). Of note, both cell lines exhibited fluctuant levels of acetylated and total histones in cultured cells over time (**Fig. 16C-D**), This observation highlights the importance of

normalization procedures to properly estimate the net fraction of acetylated histones and illustrates how histone dynamics can act as a confounding factor in quantifications.

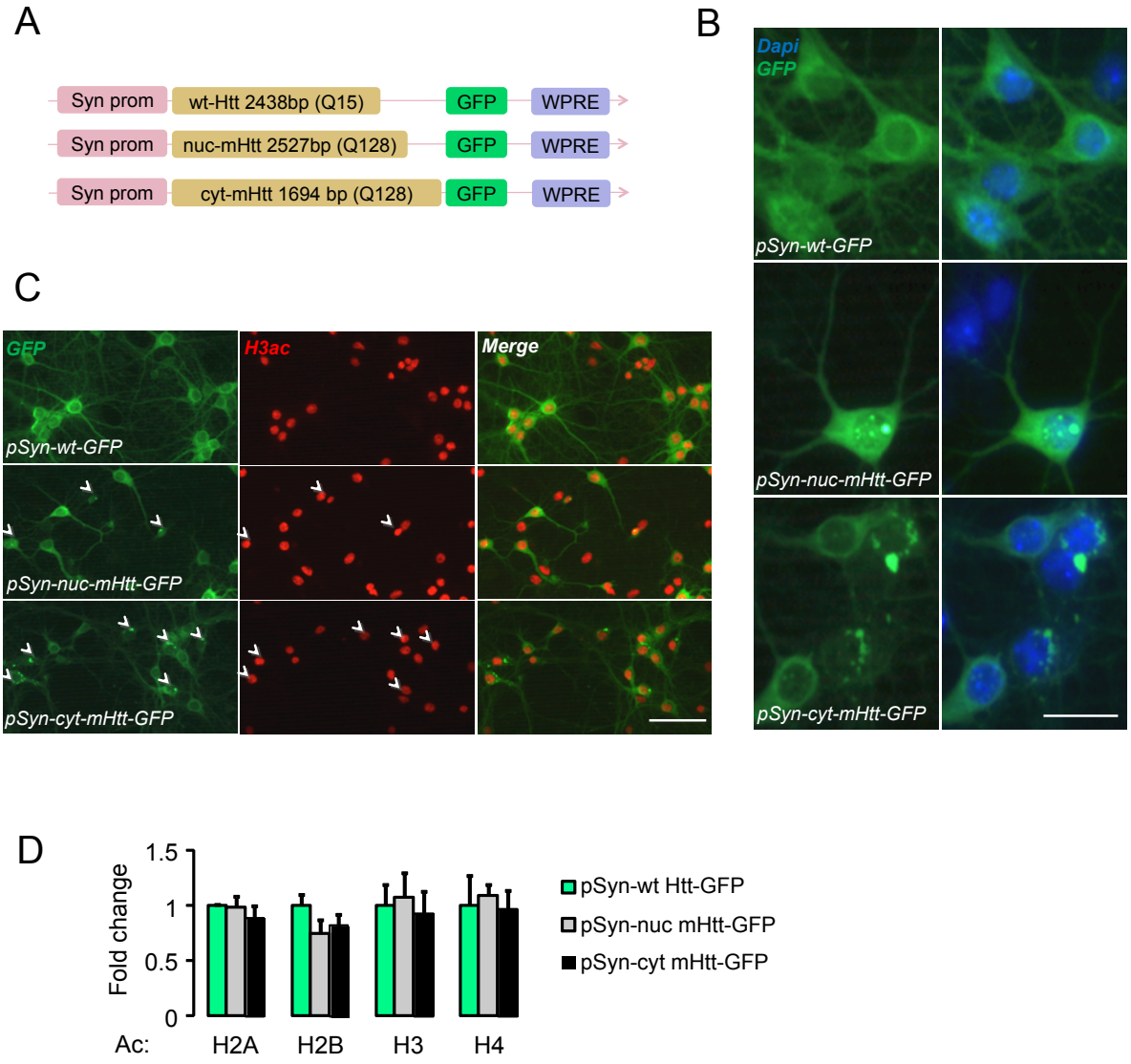

Figure 15. mHTT-infected neurons show preserved bulk histone acetylation levels. A. Schematic summary of the lentiviral vectors used to express variants of N-terminal fragments of the human HTT, with different number of repeats (15 for pSyn-wt HTT-GFP or 128 for pSyn-mHTT-GFP) and different length of the HTT sequence, denoted as Nuclear (nuc) or Cytoplasmic (cyt), depending on the predominant subcellular location of the mHTT aggregates. In the three constructs, HTT protein is fused upstream to GFP under the synapsin promoter. **B.** Representative image of cultured hippocampal neurons infected with the different viruses. Meanwhile pSyn-nuc mHTT-GFP can enter into the nucleus and form intranuclear aggregates, pSyn-cyt mHtt-GFP is retained in the cytoplasm and constitutes perinuclear aggregates. Blue, DAPI staining. Scale bar, 30 µm. **C.** Quantification of the four-nucleosome acetylated histones analyzed by immunocytochemistry (*n* = 6 wells for each condition). **D.** Representative immunocytochemistry of lentiviral-infected neurons (10DIV/6DINF) using anti-GFP and H3K9/14ac antibodies. White arrows indicate the insoluble aggregates. Scale bar, 100 µm.

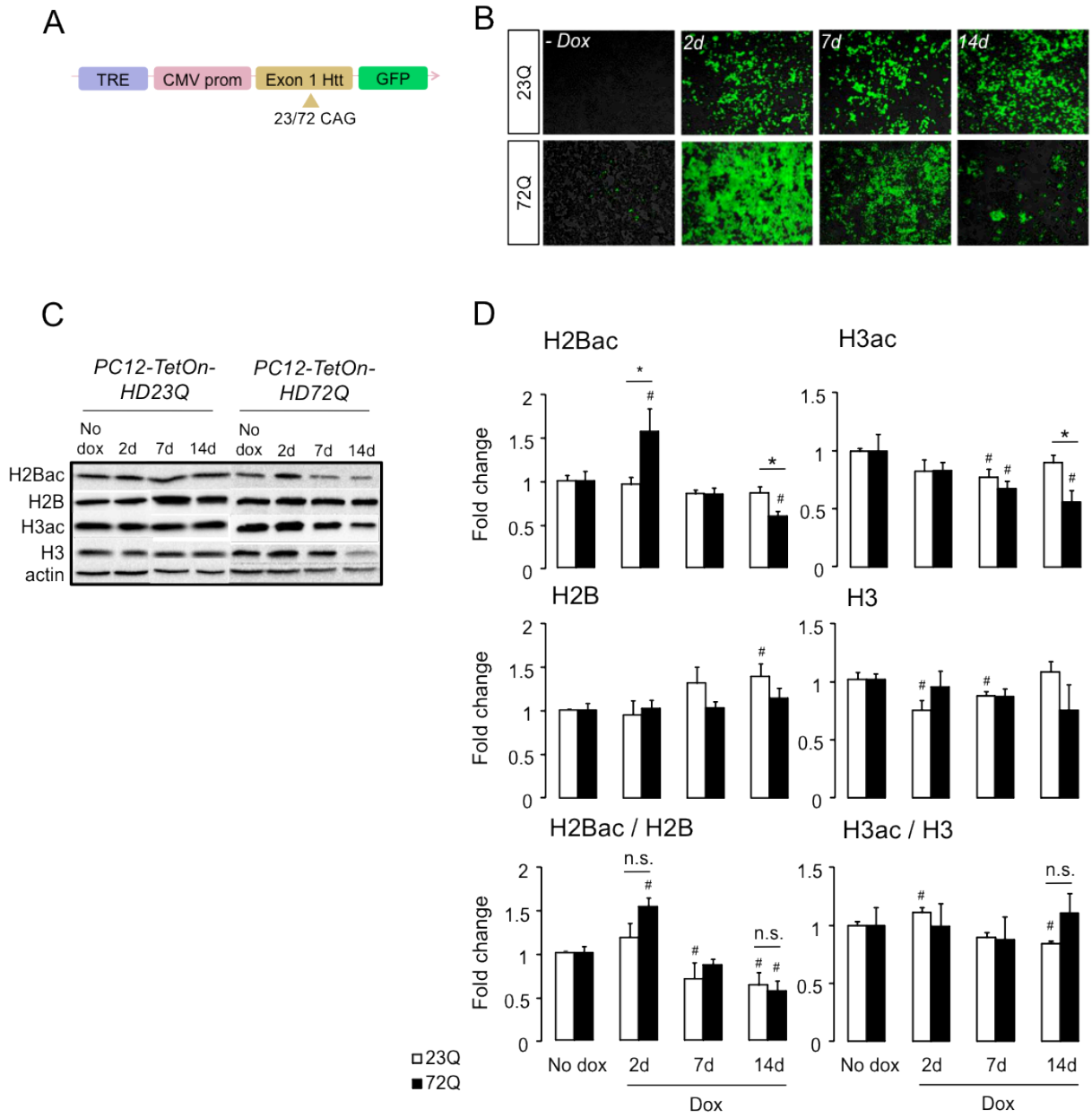

Figure 16. Stably HTT-expressing PC12 cells show preserved bulk histone acetylation levels. A. Squeme of the constructs that are integrated in rat phaeochromocytoma (PC12) cells to express GFP-tagged exon 1 of the Htt gene with either 23 or 72 CAG repeats (PC12-TetOn-HD23Q and HD72Q, respectively) in an inducible manner thanks to a doxycycline (dox)-dependent TetO operator and the minimal CMV promoter. **B.** Immunofluorescence superimposed to contrast phase of PC12 cells stably transfected with either HD23Q or HD74Q constructs. Cells were first grown in the absence of dox (No dox) and then 1 μg/μl of the compound was added to the medium for 2, 7, 17 days (Dox). **C.** Western blot of total cell extracts obtained from HD23Q and HD72Q transfected PC12 cell lines against the pan-acetylated histones H2B and H3 and their corresponding total histones. **D.** Quantification of the Western blots, expressed as fold change: acetylated histone fraction (upper), total histone (middle) and normalized acetylated fraction / total histone (lower). *n* = 4 for each condition. Data are presented as mean ± s.e.m. *, $p < 0.05$ (Student's t-test) between 23Q and 72Q; #, $p < 0.05$ (Student's t-test) related to "No dox" condition. n.s., not significant.

4.2.3 Other epigenetic marks are unaffected at the bulk level in polyQ pathology

Seeking other epigenetic marks that could show a better correlation with the transcriptional deficits associated with HD, we investigated the following histone PTMs: i) individual acetylable residues in histone H2B (K5, K12, K15 and K20) to explore the possibility that deficits on specific lysines could be masked by non-altered residues in the analysis of the pan-acetylated form of the histone, and ii) modifications of the histone tails defined as repressive marks: H3K9me2/3, H3K27me3 and the ubiquitylated histone H2A (H2Aub). To accelerate this screen, a series of Western blotting assays were conducted in our best characterized model of polyQ pathology, the hippocampus of late symptomatic HD82Q mice (Valor et al., 2013a). As shown in **Fig. 17**, all the explored marks were unaffected by mHTT expression.

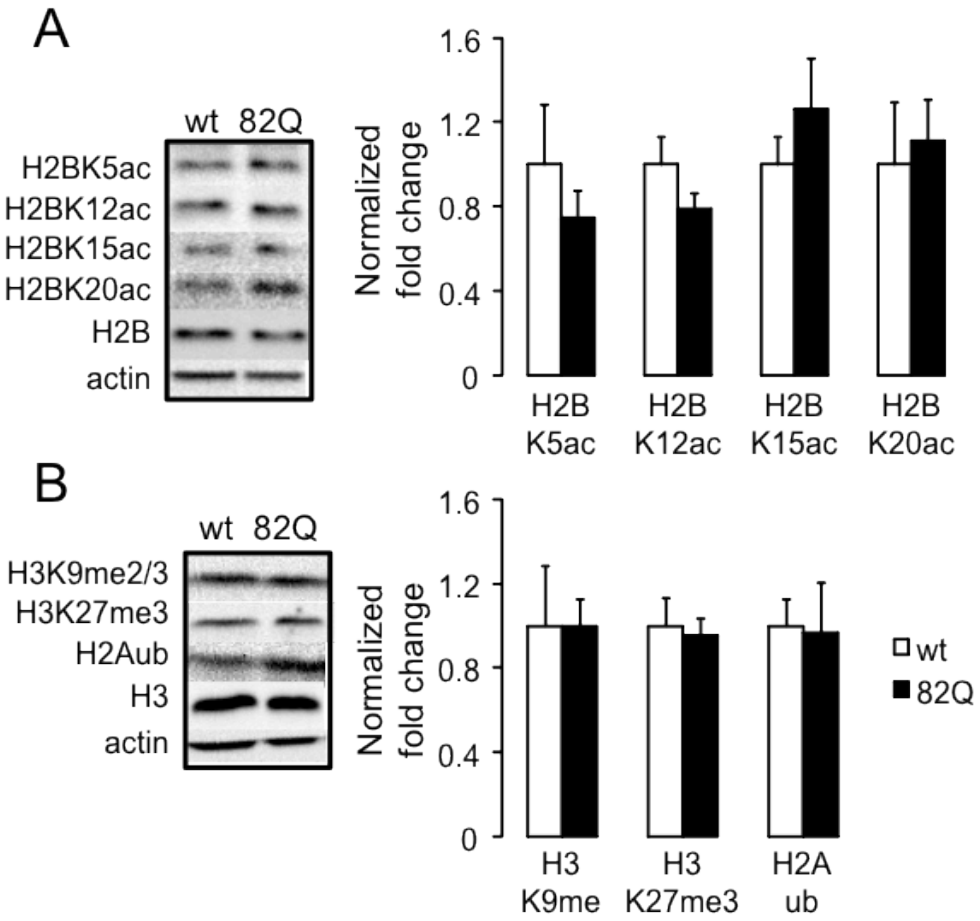

Figure 17. Other bulk histone modifications are also preserved in HD hippocampus. Screening of histone post-translational modifications in Western blot analysis of hippocampal extracts from 20-weeks-old HD82Q and wild-type littermates: specific acetylation of lysines 5, 12, 15 and 20 of histone H2B (H2BK5ac, H2BK12ac, H2BK15ac, H2BK20ac), methylation of lysines 9 and 27 of histone H3 (H3K9m2/3, H3K27m3) and ubiquitylation of histone H2A (H2Aub). **A.** Representative blots. **B.** Quantification of the blots as normalized fold change (acetylated histone fraction / total histone). *n* = 4 for wt, *n* = 7 for HD82Q.

4.2.4 Histone H3 acetylation is perturbed at specific neuronal loci

The exhaustive study of several animal and cell models confirmed the early conclusion that mHtt expression does not affect histone acetylation changes in bulk chromatin (Valor et al., 2013a). However, the genomic screen conducted in HD82Q mice revealed a significant, although moderate, correlation between H3 deacetylation in the TSS region and transcriptional dysregulation (Valor et al., 2013a). This correlation was more prominent in a relatively small subset of genes with a potential relevant role in this pathology, as they are prone to be altered in caudate nuclei from patients (Valor et al., 2013a). To determine whether these local changes were also found in another HD model, we performed a series of chromatin immunoprecitation (ChIP) assays in the promoter of the transcriptionally deregulated genes: *Penk*, *Plk5*, *Rin1*, *Itpka*, *Igfbp5*, *Eomes* and *Fos* (**Fig. 18A-B** and (Valor et al., 2013a)). In corticostriatal and cerebellar samples of R6/1 mice, these assays confirmed the occurrence of histone deacetylation events at specific regions in late symptomatic mice **(Fig. 18C-D**), thus extending our former observations of local perturbations at discrete loci to a different mouse HD model. In contrast, and supporting the specificity of the reported deficits, the housekeeping gene *Gapdh*, which had the same expression level than in controls, was unaffected.

Intriguingly, the immediate early gene *Fos* displayed a transcript change that was specific for the HD model: whereas in HD82Q it was downregulated (Valor et al., 2013), no significant alteration was detected in the R6/1 cerebellum (**Fig. 18B**). In any case, histone H3 deacetylation occurred at the promoter level in both models (Valor et al., 2013; **Fig. 18D**). Another example was found in the case of *Igfbp5*, a gene which expression is consistently affected in different brain areas (cortex, striatum and cerebellum in **Fig. 18A-B**) but not in the HD82Q hippocampus (**Fig. 18E** and (Valor et al., 2013a)). This observation led us to examined the subset of genes with differential H3K9/14ac occupancy at their TSSs in the hippocampus of early symptomatic HD82Q mice, as defined in our previous work (Valor et al., 2013a), for

transcript changes in other HD gene expression profiles. Pair-wise comparisons with gene expression datasets from different brain areas and HD models revealed statistically significant overlaps ($P < 0.05$, Fisher's exact test) with the hippocampal genes containing acetylation deficits, not only with HD82Q hippocampus but also for HD82Q cerebellum (Valor et al., 2013a), and both cortex and striatum of R6/2 mice (Vashishtha et al., 2013). Expectedly, most of these overlapping genes were also differentially expressed in the HD82Q hippocampus, confirming our previous definition of HD signature (Valor et al., 2013a). However, other genes that were not transcriptionally dysregulated in this tissue, but altered elsewhere, displayed altered hippocampal histone acetylation (at least 49 genes, **Fig. 18F**), suggesting that additional factors may converge to produce a final outcome of altered transcription. In fact, *Camk1g* and *Rasl11b* were eventually downregulated in the hippocampus in later stages of the pathology (**Fig. 18G**), indicating that they were susceptible to be altered at the gene expression level. However, disease progression was not sufficient for all the genes, as exemplified by *Igfbp5* (**Fig. 18E**), *Pde2a* and *Neu2* (not shown), and tissular and/or model-specific factors may account for effective transcriptional dysregulation.

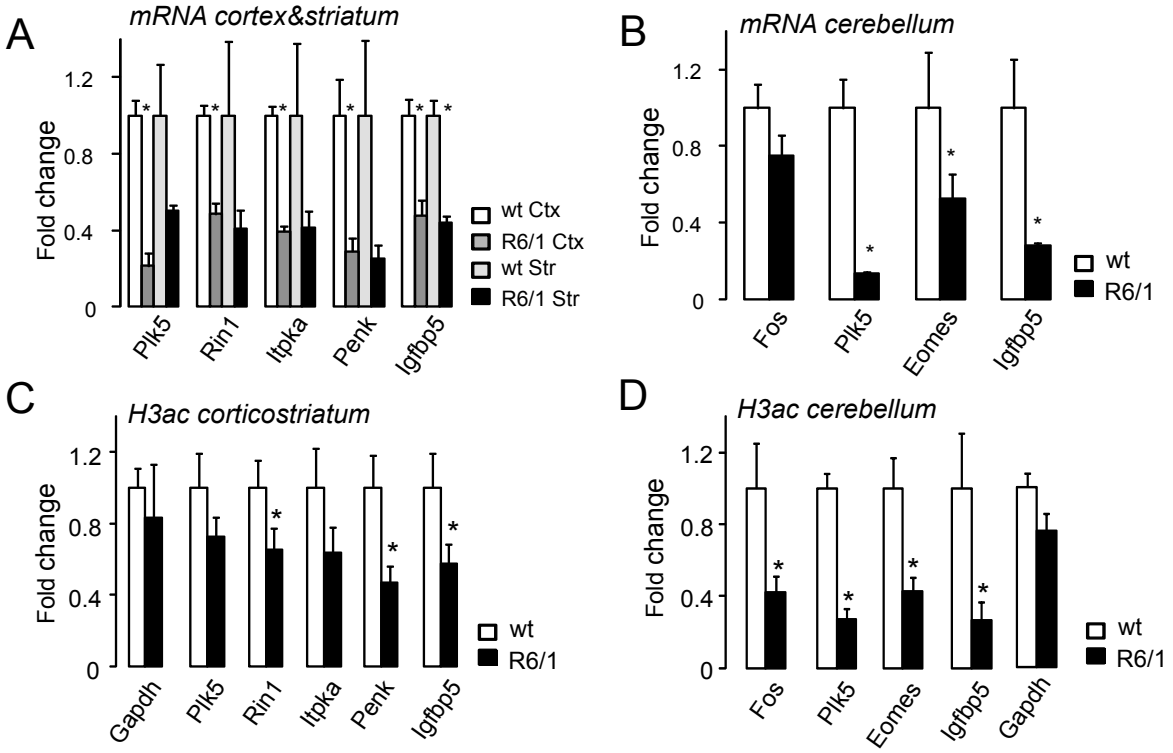

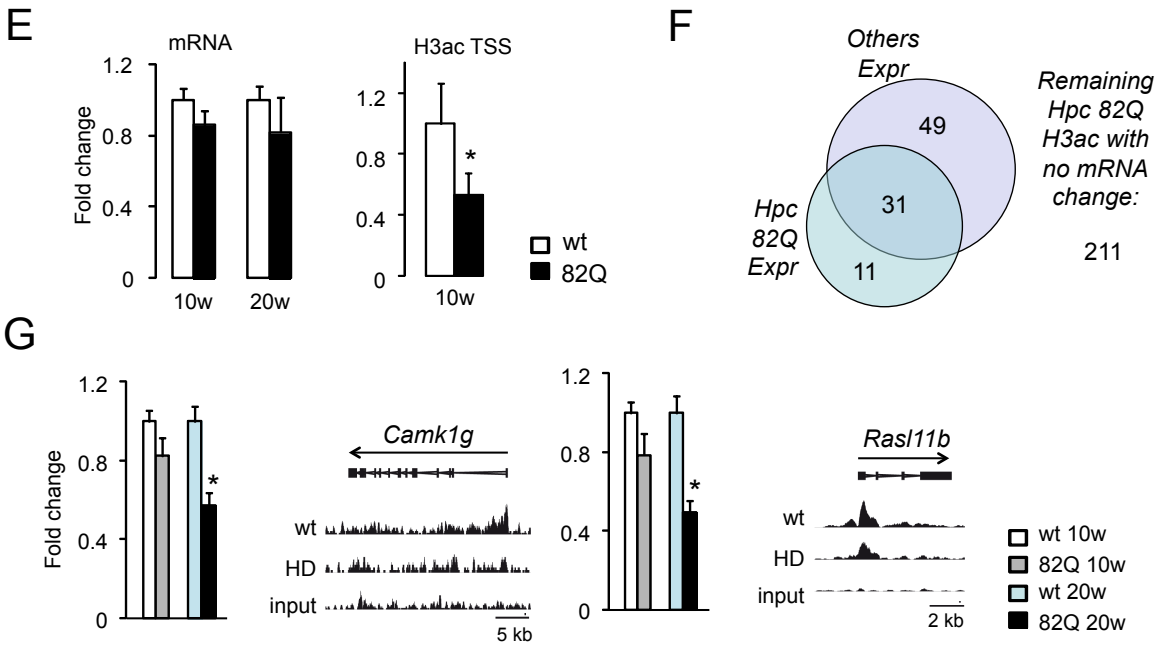

Figure 18. Histone H3 deacetylation is altered at specific neuronal loci. ChIP assays using an antibody against H3K9/14ac followed by qPCR of TSS of transcriptionally deregulated genes in HD in either corticostriatal (**A**, **C**) and cerebellar (**B**, **D**) samples of R6/1 mice, togethter with gliceraldehyde 3-phospahte dehydrogenase (*Gapdh*) as a control (**C**, **D**). *n* = 5 in corticostriatum and *n* = 3 in cerebellum for each genotype. **E.** qPCR assays of transcript (mRNA) and TSS-associated H3ac (H3ac TSS) of the insulin-like growth factor binding protein 5 (*Igfbp5*). **F.** Venn diagram of differentially acetylated H3ac in HD82Q hippocampus, including those that were also transcriptionally dysregulated in the same tissue and model, and in any of the following gene expression datasets: 10-week-old HD82Q cerebellum, 12-week-old R6/1 cortex and 12-week-old R6/1 striatum. Differentially changing genes were those according to the original publications (Valor et al., 2013a, Vashishtha et al., 2013). **G.** RT-PCR assays in early (10 weeks old) and late (20 weeks old) symptomatic hippocampal HD82Q for calcium/calmodulin-dependent protein kinase IG (*Camk1g*) and Ras-like family 11 member B (*Rasl11b*), accompanied by their associated genomic H3 acetylation profiles. *n* = 5 for each genotype (10 weeks old), *n* = 6 for wt and *n* = 8 for HD82Q (20 weeks old). Data are presented as mean ± s.e.m. *, $p < 0.05$ (Student's t-test).

4.2.5 Deficits in acetylation and trimethylation of histone H3 concur at relevant neuronal loci

Finally, we examined the pattern of H4K4me3 occupancy, another mark associated with H3ac (Lopez-Atalaya et al., 2013), to explore the putative concurrence of deficits for several epigenetic marks in HD. ChIP-qPCR assays were performed in the HD82Q cerebellum, a brain area showing high expression of mHtt in these transgenic mice and with a prominent role in juvenile manifestations of HD (Seneca et al., 2004; Nicolas et al., 2011) and other polyQ disorders (Orr and Zoghbi, 2007). In addition, the high amount of cerebellar chromatin allowed parallel IPs for multiple histone PTMs in the same samples. Thus, downregulated genes such as *Fos*, *Plk5*, *Eomes* and *Igfbp5* were concomitantly hypoacetylated and hypomethylated at their proximal promoter in cerebellar chromatin (**Fig. 19**), whereas the gene encoding the

GABA receptor subunit *Gabrd* only showed acetylation deficits. Overall, these results extend the previous finding of local perturbations of histone H3 acetylation in polyQ pathology (Valor et al., 2013a) to trimethylation of histone H3K4.

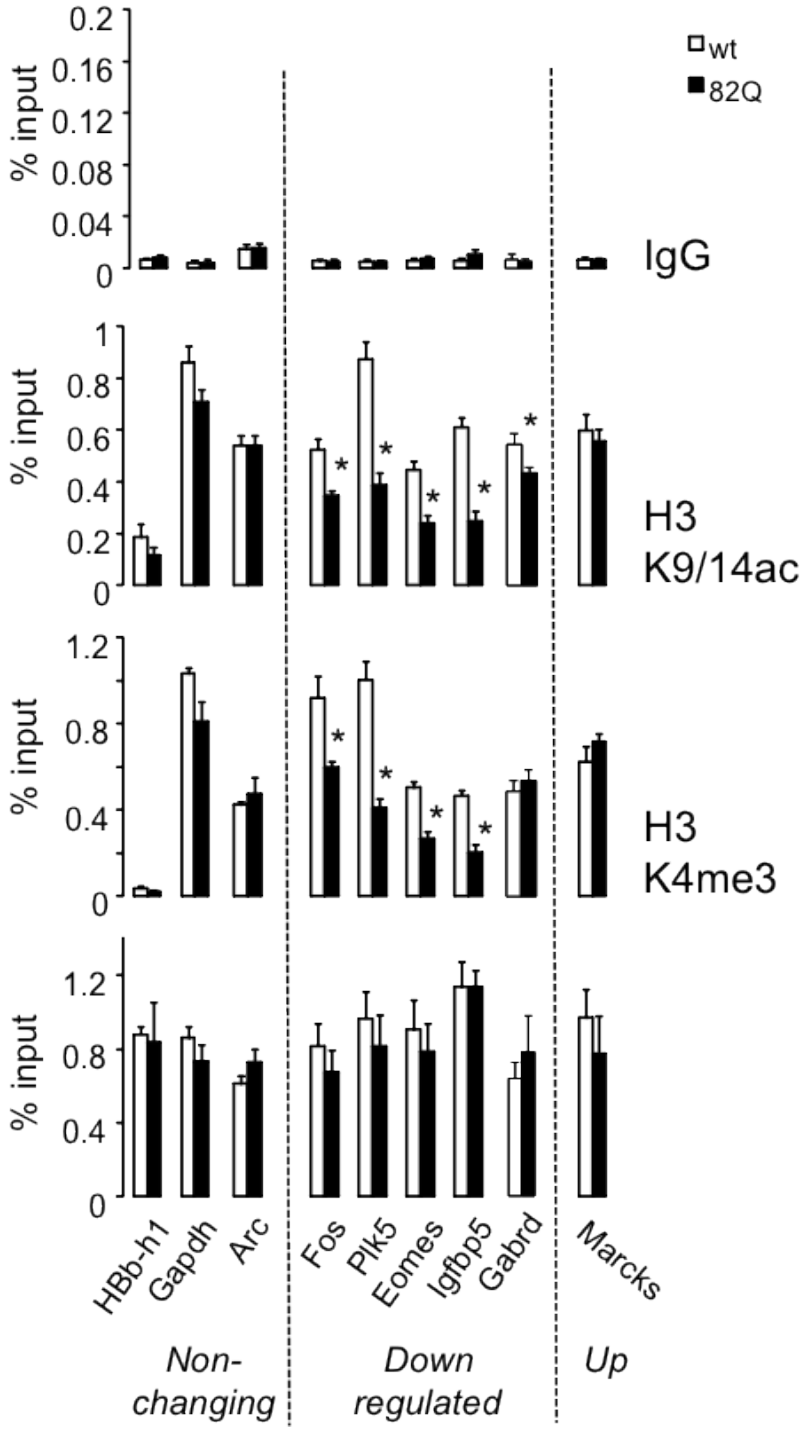

Figure 19. Promoters with H3 deacetylation can be also demethylated at histone H3 lysine 4. ChIP assays followed by qPCR of selected TSS in the cerebellum of HD82Q for *Plk5*, *Igfbp5*, FBJ murine osteosarcoma viral oncogene homolog (*Fos*), eomesodermin (*Eomes*), gamma-aminobutyric acid A receptor delta (*Gabrd*), and myristoylated alanine-rich protein kinase C substrate (*Marcks*).

Promoter regions of *Gapdh* and hemoglobin Z, beta-like embryonic chain (*HBb-h1*) were used as controls. Classification of non-changing, downregulated and upregulated genes in expression is made according to our published results (Valor et al., 2013a). n = 3 (ChIP) for each condition. Data are presented as mean ± s.e.m. *, $p < 0.05$ (Student's t-test).

4.2.6 Discussion: H3 deacetylation and demethylation in HD

In this work we present a comprehensive analysis of bulk histone acetylation in several experimental models of HD. Western blot, immunohistochemistry and immunocytochemistry experiments in diverse animal (N171-82Q, R6/1, YAC128 and striatal-electroporated mice) and cellular (primary neuronal cultures and stably transfected PC12 cells) models of HD demonstrate that the expression of mutant Htt variants is not sufficient to produce a global effect in the acetylation of lysines at the histone H3 and H4 tails, even in the presence of transcriptional dysregulation and overt manifestations of a pathological phenotype. Our results are in conflict with some previous experiment reporting bulk changes (Steffan et al., 2001; Ferrante et al., 2003; Igarashi et al., 2003; Gardian et al., 2005; Stack et al., 2007; Chiu et al., 2011; Lim et al., 2011; Giralt et al., 2012). Of note, few of those studies examined the levels of total histone levels and instead used cytosolic proteins such as tubulin or actin as the reference protein for normalization. In others, no quantification was performed. Our experiment in mHTT-expressing PC12 cells exemplifies how histone dynamics can produce misleading conclusions regarding acetylated histones levels. Although this phenomenon has been observed as part of the culture progression, such dynamics can be also a pathological consequence, as suggested by the increase of histone levels in post-mortem brains from AD patients (Narayan et al., 2015). Additional factors related with intrinsic properties of the HD models (e.g., interaction with genetic background, culturing conditions, overt degeneration) could also explain the divergence between our results and other previous studies.

In any case, the simple examination of bulk histone PTMs changes does not provide information about the impact of these epigenetic alterations in transcription. The use of next-generation sequencing techniques has greatly expanded the resolution of studies exploring the involvement of epigenetic alterations in pathological gene expression. As recently reviewed by the authors (Valor and Guiretti, 2014, Valor, 2015) there is still no conclusive evidence demonstrating a general correlation between epigenetic and transcriptional dysregulation in HD. Histone H3 deacetylation has been observed in specific genes that encode for

proteins of particular relevance in neuronal functioning, and therefore may have a significant contribution to the pathology. For example, Rin1 is a Ras effector protein that positively regulates ephrin-related endocytosis (Deininger et al., 2008) and negatively regulates conditioned fear memories (Dhaka et al., 2003; Bliss et al., 2010); Plk5 is highly expressed in the brain and modulates the neurite outgrowth in response to neurotrophic factors (de Carcer et al., 2011); Eomes (also known as Tbr2) is a transcription factor that regulates morphogenesis and neurogenesis in the developing central nervous system but whose role in adult brain remains obscure (Fink et al., 2006; Mione et al., 2008; Kahoud et al., 2014); Igfbp5 is a component of the insulin-like growth factor (IGF) pathway that antagonizes the action of IGF-1 in the bidirectional regulation of apoptosis (Zhong et al., 2005; Gatchel et al., 2008; Qiao et al., 2014); and *Fos* is an inducible transcription factor extensively used as a marker for neuronal activation. In conclusion, local alteration affecting histone PTMs may still have a profound impact in HD.

Much progress is still needed to understand the interplay between transcriptional and epigenetic alterations in neurons both under physiological conditions (Lopez-Atalaya and Barco, 2014) and in the context of polyQ diseases. In the absence of general rules, we propose here three alternative, although not necessarily exclusive, views: (i) Histone deacetylation and other forms of epigenetic dysregulation are a consequence of the transcriptional deficits and it can be more considered as a "passenger" event that does not contribute to the manifestation or progression of the pathology. (ii) Transcriptional dysregulation is a consequence of convergent epigenetic alterations (Valor, 2015). Thus, alteration of a single histone PTM cannot by itself explain the altered gene expression patterns. In this regard, we found that specific loci exhibited not only histone H3 hypoacetylation but also H3 demethylation at lysine 4. Regular altered genes in HD, such as *Igfbp5*, *Plk5* and *Rin1*, were not only hypomethylated in our experiments but also in the striatum and cortex of the R6/2 mice (Vashishtha et al., 2013) and the hippocampus of HD82Q mice (not shown). (iii) Epigenetic dysregulation might correlate better with susceptibility to transcriptional dysregulation than with effective change. According to this view, histone deacetylation in HD may act as a priming event that marks genes prone to change under appropriate conditions. Such conditions may be intrinsic to the affected brain area, animal model, or phase in disease progression, as demonstrated by our studies in the hippocampus of HD82Q mice. However, in the absence of a precise

characterization of these factors it is difficult to ascribe a predictive value for these epigenetic alterations.

Future studies investigating the profiles for other epigenetic marks and for transcription factor occupancy may distinguish between these possibilities and unveil stronger correlations and provide additional cues about the elusive relationship between epigenetic and transcriptional dysregulation in HD.

4.3 CBP deficiency and impaired lysine acetylation in neural-derived cells cause perinatal death and severe neuronal growth defects in primary hippocampal cultures

As indicated in the Introduction, a number of studies have demonstrated that neuropathology is often associated with reduced levels of histone acetylation in neurons. This is especially true in the case of RSTS, which is caused by mutations in KAT encoding genes in more than 65% of the patients (Valor et al., 2013b).

4.3.1 Characterization of Nes-cre::CBP$^{f/f}$ mice

We generated mice lacking CBP in neural-derived cells through the crossing of CBP floxed mice (CBP$^{f/f}$) with transgenic mice that express the cre recombinase under the control of the nestin promoter and the CBP floxed allele in heterozygosity (Nestin-cre::CBP$^{f/-}$ mice). In this line the nestin promoter drives cre-mediated recombination in the neural linaje. The characterization of these mice can importantly improve our understanding of the role of CBP during prenatal development period in the nervous system (Lopez-Atalaya et al., 2014) (**Fig. 20A)**.

Firstly, we characterized the genotypic distribution of the progeny and, as expected, the mouse line followed a Mendelian distribution. The expected ratio in the nestin conditional KO Nes-cre::CBP$^{f/f}$ line was approximately 25:25:25:25 nestin-cre::CBP$^{f/f}$, nestin-cre::CBP$^{+/f}$, no cre::CBP$^{f/f}$ and no cre::CBP$^{-/f}$ (the last two genotypes correspond to control conditions) (**Fig. 20B**), indicating that CBP ablation was not lethal during development. However, the newborn homozygotes became cyanotic and died minutes after birth (**Fig 20C**), probably due to respiration failure (under investigation).

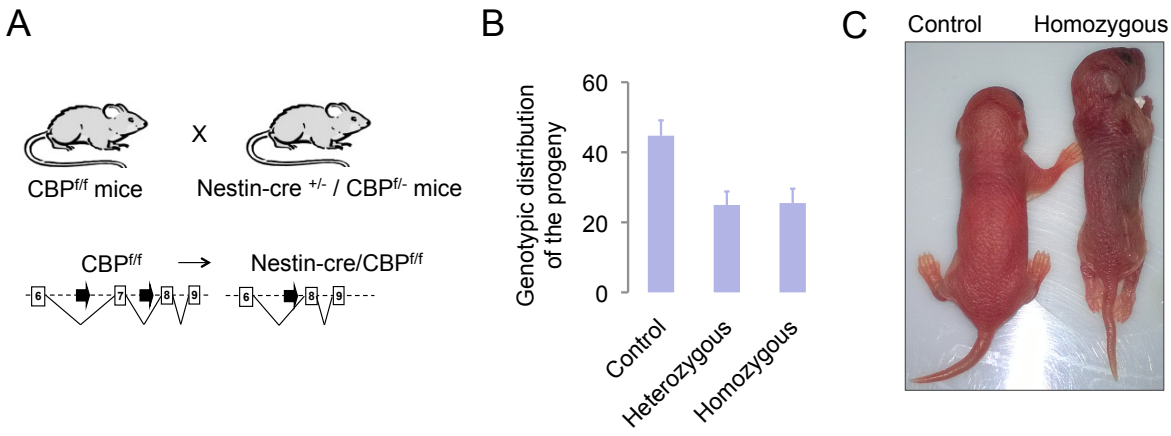

D

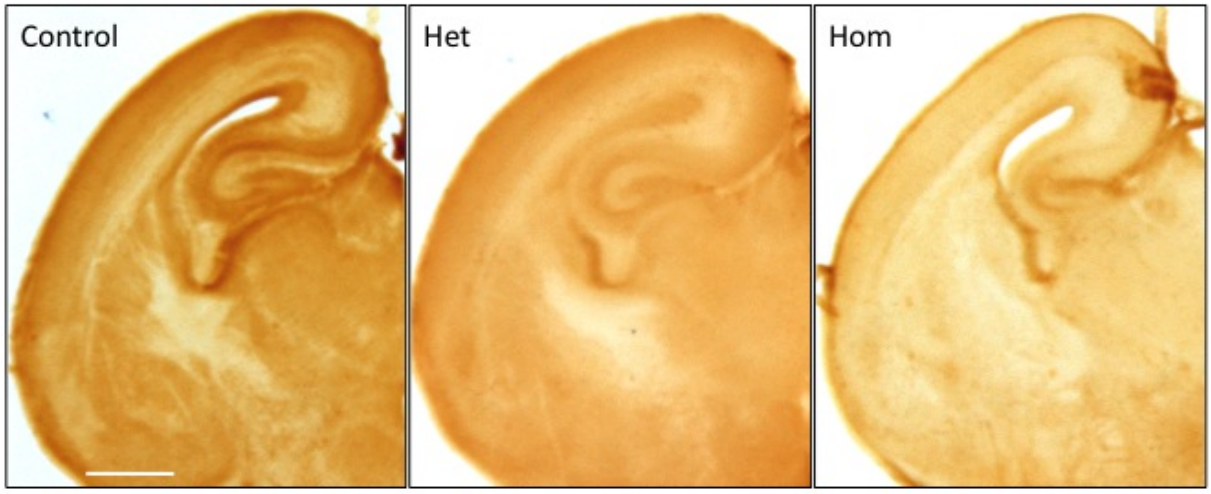

Figure 20. General characterization of Nes-cre::CBP$^{f/f}$ mouse line. A. Squeme of the crossing of CBP$^{f/f}$ mice with Nestin-cre $^{+/-}$ / CBP$^{f/-}$ mice. **B.** Genotypic distribution of the progeny. **C.** Picture showing the perinatal lethality in homozygous mice. **D.** Representative images showing the CBP expression in each condition. Scale bar, 500 µm.

Newborn animals did not show changes in the gross morphology of the brain in MR images (**Fig 21B-C**). However, the 3D reconstruction of MR images revealed that although despite the total volume of the brain was similar for all the genotypes, the hippocampus was significantly smaller in homozygous when compared with heterozygous and the control group (**Fig. 22**). The heterozygous embryos showed an intermediate volume.

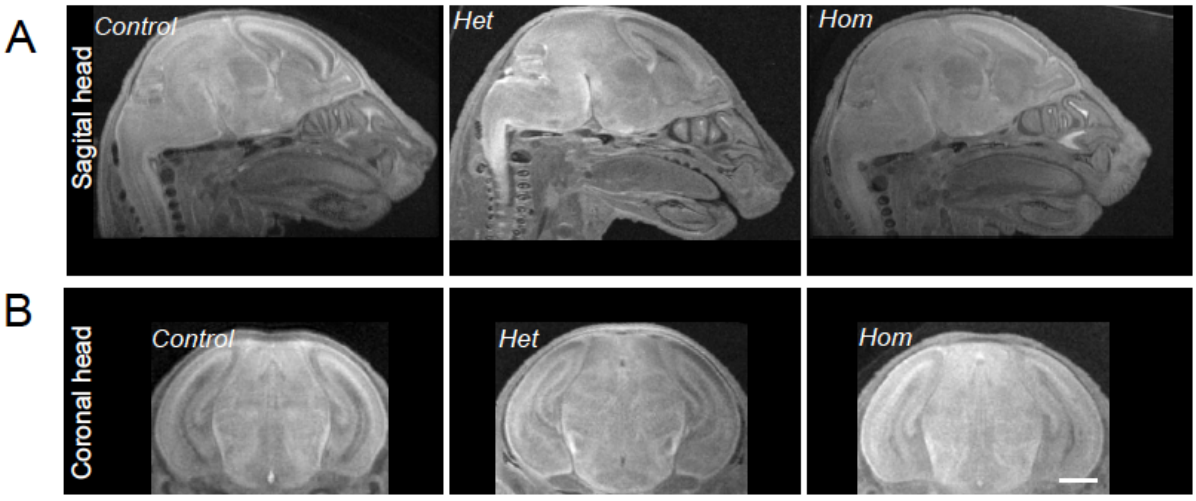

Figure 21. MRI images from sagital head and coronal head. Representative MRI images showing the sagital head (**A**) and coronal head in (**B**) of control, heterozygous (Het) and homozygous (Hom) Nes-cre::CBP$^{f/f}$ mice at P0 stage. Scale bar, 1000 µm.

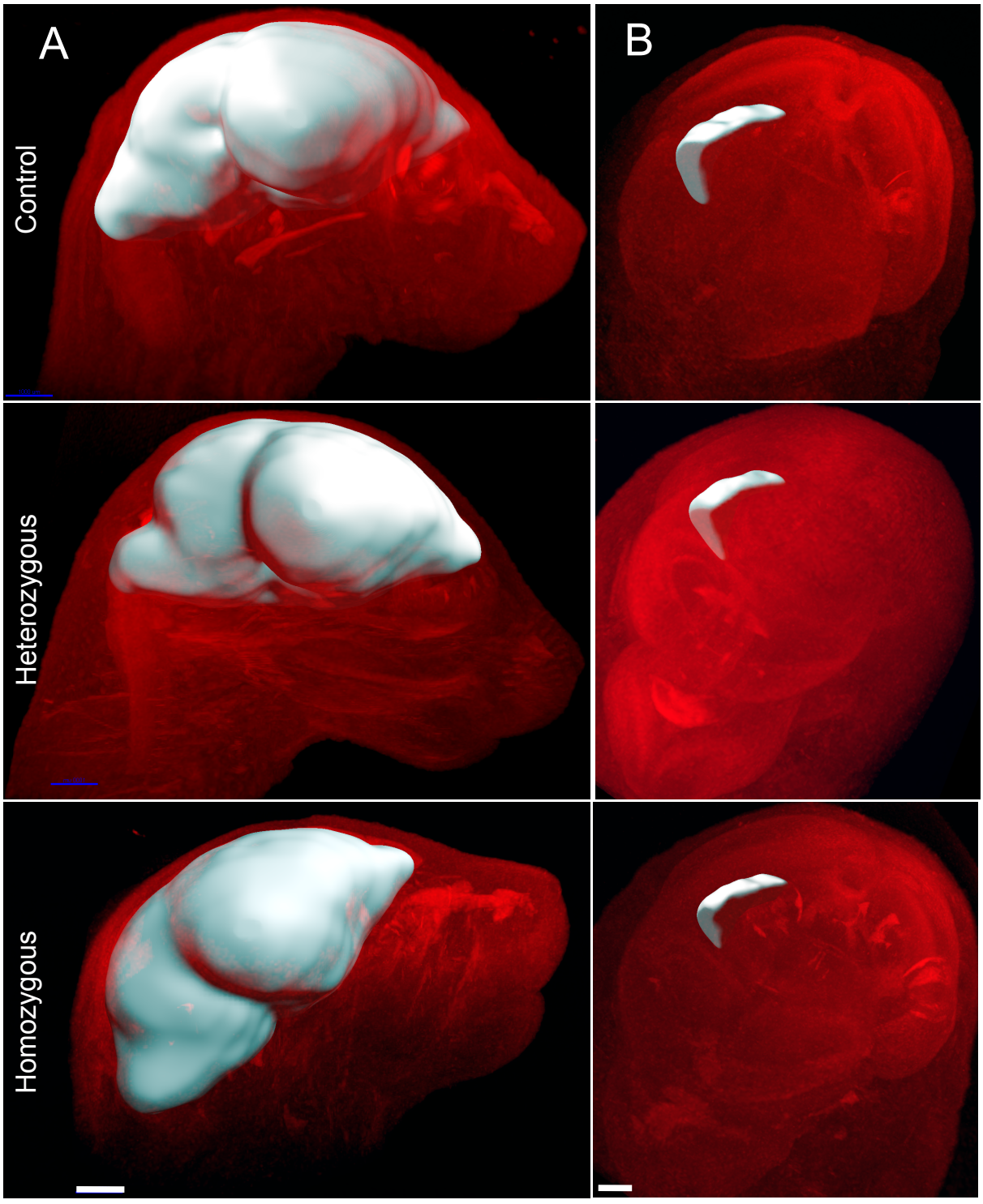
A
B
Control
Heterozygous
Homozygous

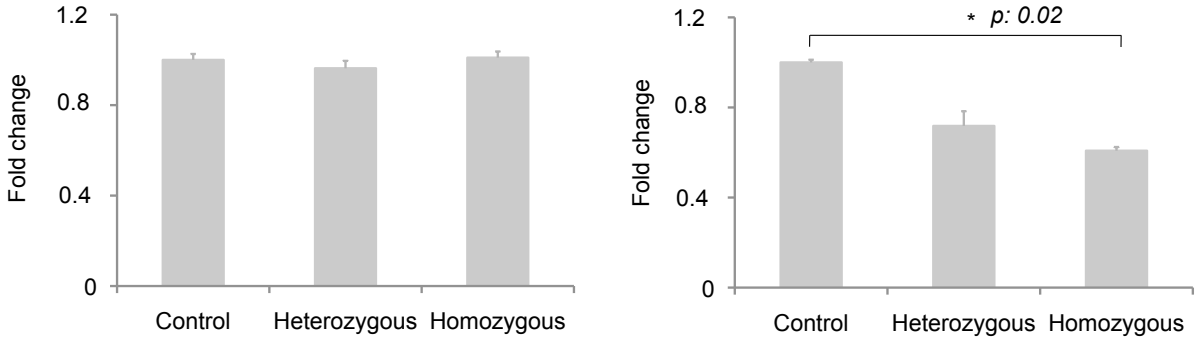

Figure 22. Three-dimensional reconstruction of MR images. Detailed views from sagital and coronal head illustrating the three-dimensional reconstruction of the brain volume (**A**) and hippocampal volume (**B**). Quantification is showed at the bottom panels. Data is represented as the mean ± SEM. Student's *t* test ($p < 0.05$). Scale bar, 1mm (**A**), 500 µm (**B**).

4.3.2 Severe neuronal growth defects of primary cultures from Nes-cre::CBP$^{f/f}$ mice

Next, we investigated whether the neurons from Nes-cre::CBP$^{f/f}$ mice can survive *in vitro*. We dissected the hippocampus from embryos with the different genotypes and we counted the number of neurons after dissociation of the tissue. This quantification did not reveal statistical differences between control and heterozygous mice, although there was a trend toward a lower number of cells in the homozygous embryos (**Fig. 23A**), in agreement with the atrophy observed in the MRI volumetry analysis. Ten days after plating equal number of cells for each condition, we performed a double staining of the cultures with the neuronal marker NeuN and the astrocyte marker GFAP (**Fig. 23B**). We observed that the number of neurons was significantly reduced in the cultures from homozygous embryos while small differences were observed between controls and heterozygous cultures. In contrast, the expression pattern of astrocytes was similar for the three conditions.

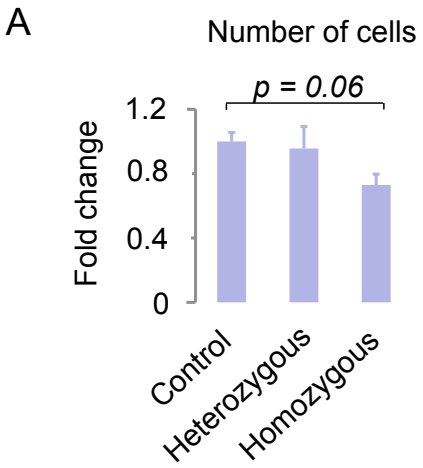

B

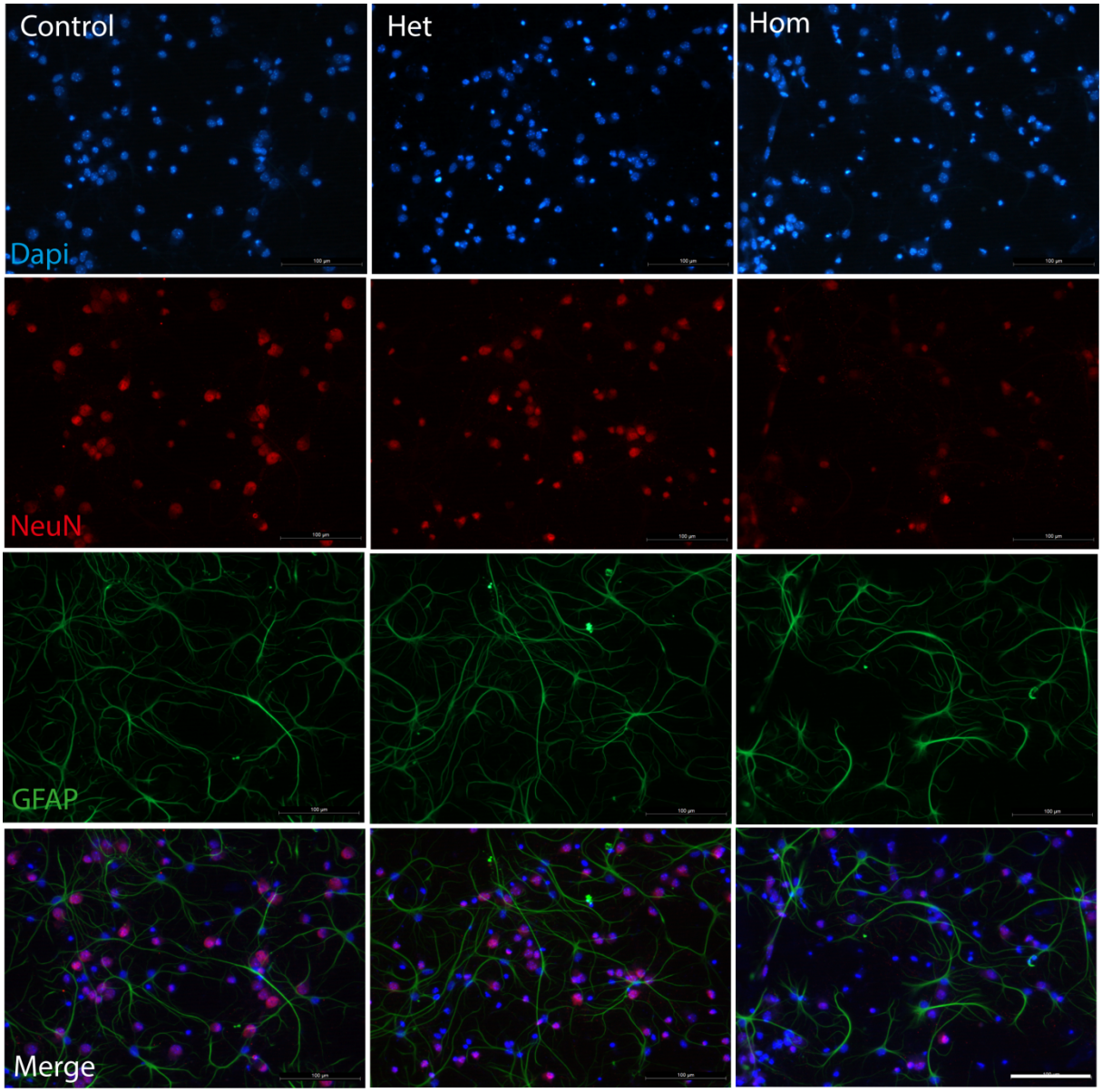

Figure 23. NeuN and GFAP staining in Nes-cre::CBP$^{f/f}$. A. Quantification of hippocampal cells from Nes-cre::CBP$^{f/f}$ embryos at E17.5 stage before the plating (1DIV). Comparison between control and homozygous conditions results statistically significant, $p = 0.06$ (Student's t-test). **B.** Hippocampal cells were stained for NeuN (red) and GFAP (green) (10DIV). Scale bar, 100 µm.

Consistent with the ablation of CBP protein in brain slices at P0 stage (**Fig. 20D**), the analysis of histone acetylation levels (H2Aac, H2Bac, H3ac and H4ac) in hippocampal cultures revealed a significant reduction for the four pan-acetylated histones (**Fig. 24**).

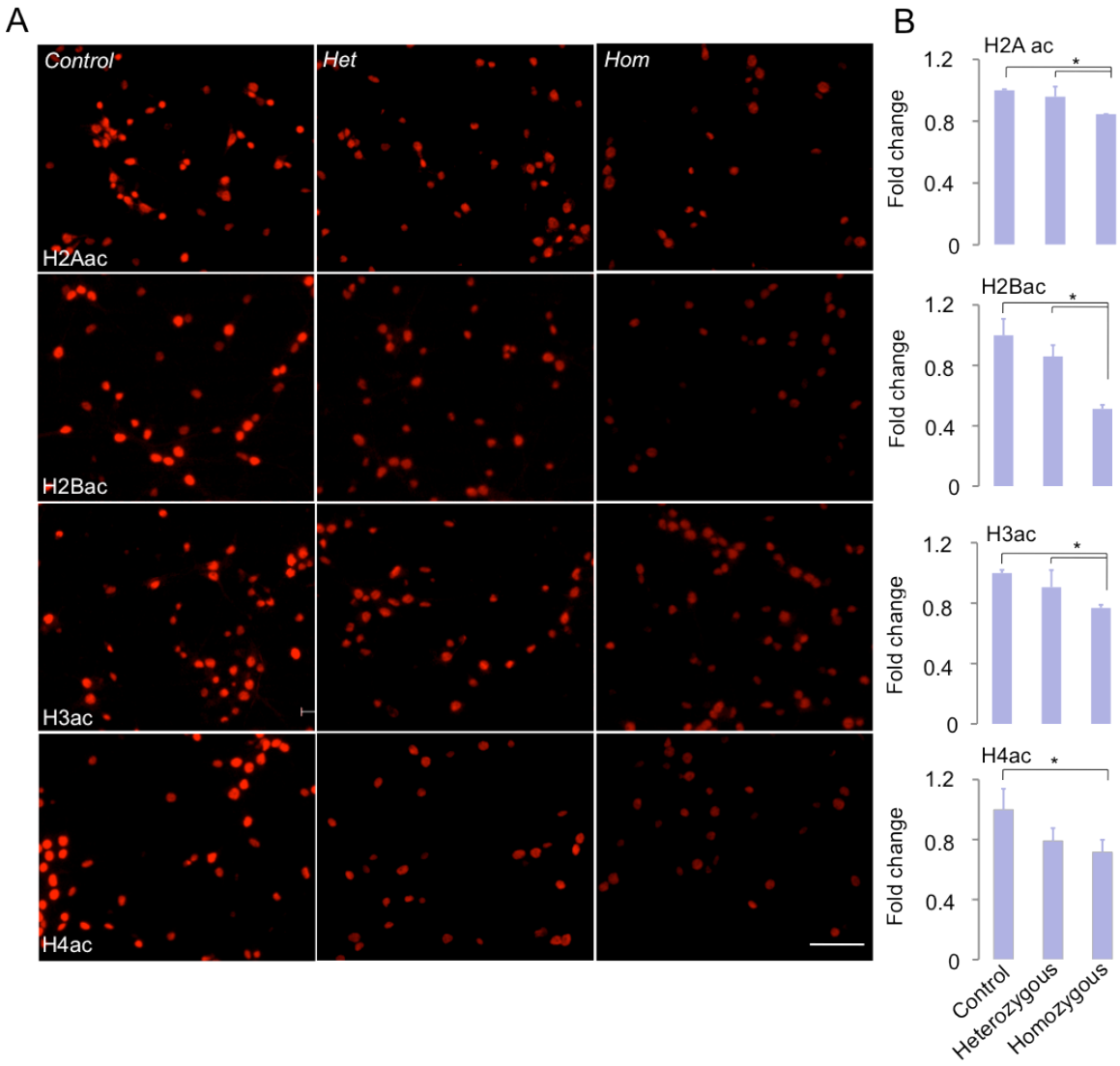

Figure 24. Nes-cre::CBP$^{f/f}$ mice show acetylation deficits in the four-nucleosome histones. A. Hippocampal neurons were stained for H2Aac, H2Bac, H2ac and H4ac (culture time: day 10). Magnification: 10x. Scale bar, 50 µm. **B.** Quantification of **A**. Data is represented as the mean ± SEM. Student's *t* test ($p < 0.05$).

In addition, when we performed the staining against MAP2, a well-known neuron-specific cytoskeletal protein, to evaluate neuronal morphology and integrity, we found an abnormal staining in hippocampal neurons from homozygous embryos compared to the control condition, indicating that the ablation of CBP affects the ability of embryonic neurons to recover after tissue disaggregation and to growth a new axon and dendritic tree (**Fig. 25**). The cultures from heterozygous embryos showed a pattern for MAP2 similar to the control cultures (data no shown).

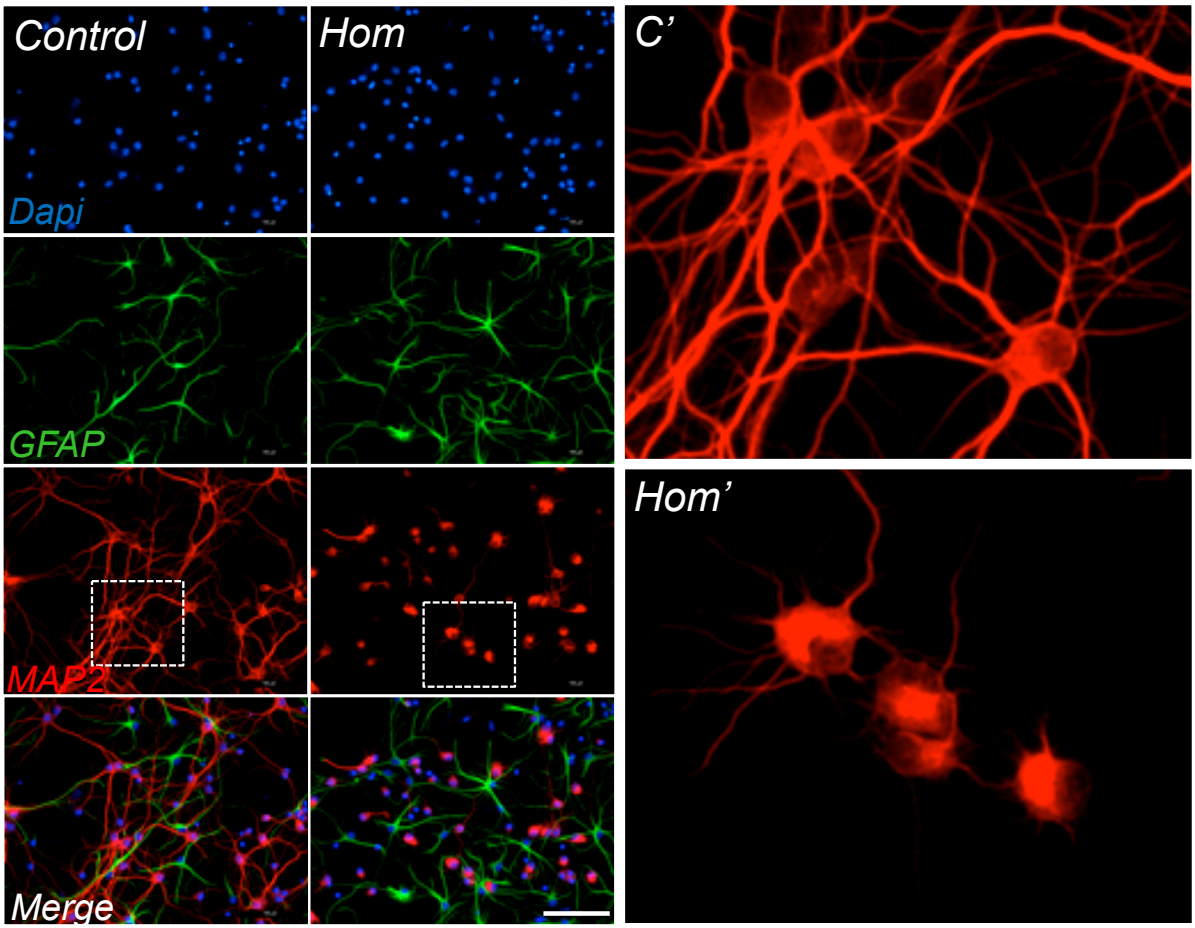

Figure 25. Nes-cre::CBP$^{f/f}$ mice show acetylation abnormal neuronal morphology. Representative images of hippocampal neurons showing altered expression of MAP2 in the homozygous condition (culture time: day 10). Magnification: 20x. Scale bar, 100 µm. C: control, Hom: homozygous.

4.4 KAT-expressing viral vector as a potential therapeutic tool to reverse neurological deficits associated with impaired lysine acetylation.

4.4.1 Generation and characterization of a KAT-expressing viral vector

The RSTS-related cellular model introduced in the previous chapter represents a good system for investigating the therapeutic potential of overexpression KAT activity. As already discussed, the uses of HDACi have been shown to ameliorate a number of neurological conditions. However, these compounds are also able to acetylate non-histone substrates, including cytoplasmic proteins (Choudhary et al., 2009; Schölz et al., 2015), they do not discriminate among cell types and excessive HDACi-induced hyperacetylation can provoke neuronal apoptosis (Boutillier et al., 2003; Fujiki et al., 2013). To minimize adverse effects of HDACi and limit the inespecificity of HDACi administration, we took advantage of genetic approaches.

To this aim, we generated a recombinant lentivirus that expresses the KAT domain of the CBP protein under the synapsin promoter to selectively overexpress KAT activity in neurons. The KAT domain was fused to GFP protein to allow the tracking of transduced cells (**Fig. 26**). This construct will be referred to as pSyn-NLS-KAT-GFP.

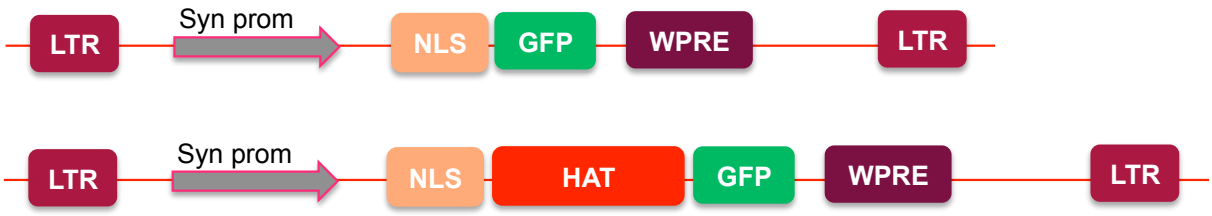

Figure 26. KAT-LV tool design. Scheme of the recombinant lentiviral constructs expressing a fusion protein of CBP's KAT domain and GFP under the synapsin promoter (Syn prom) and its control above without the KAT domain.

As a first step in the characterization of this genetic tool, we explored the specificity of the pSyn-NLS-KAT-GFP in primary dissociated hippocampal cultures. To this end, we checked the infection pattern of our pSyn-NLS-KAT-GFP vector. We found that pSyn-NLS-KAT-GFP infected only neurons since the GFP signal only colocalized with NeuN+ but not with GFAP+ cells (**Fig. 27**).

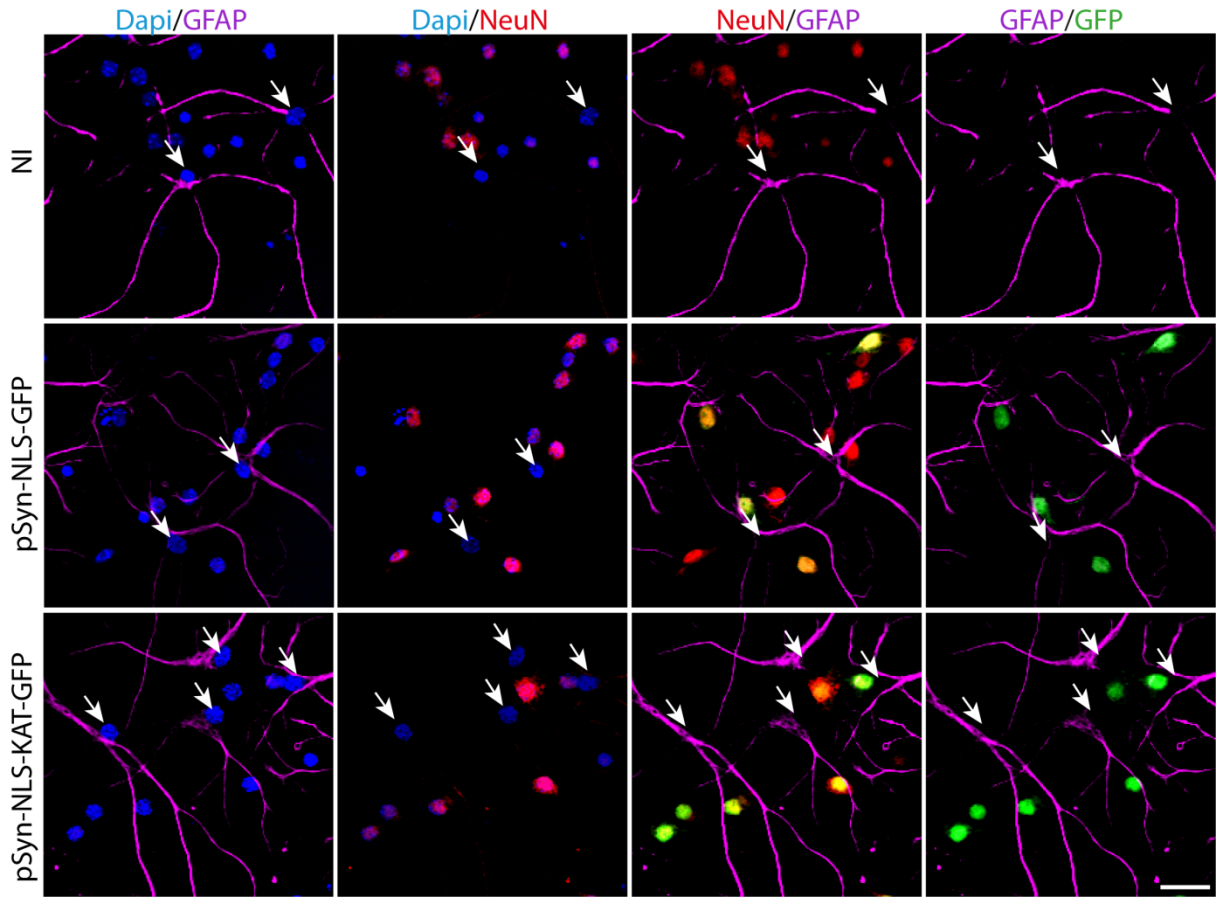

Figure 27. Selective infection of pSyn-NLS-KAT-GFP in neurons. Triple IC against NeuN (red), GFAP (magenta) and GFP (green). Magnification: 20X. Scale bar, 25 µm. NI: non-infection.

In parallel, we assayed the viability of KAT-overexpressing neurons by measuring LDH activity in the supernatant of cultured hippocampal neurons at 6DINF/10DIV, and we compared the results with the pharmacological treatment with trichostatin A (TSA), an inhibitor of class I and II HDACs (Finnin et al., 1999; Johnstone, 2002), at different time points. We included different conditions: basal (non-infection, NI), control lentiviral vector without the KAT domain (pSyn-NLS-GFP), KAT-expressing vector (pSyn-NLS-KAT-GFP), TSA-treatment (0.2 and 2 µM) and a positive excitotoxic control (NMDA 100 µM). The timeline of the experiment is outlined in **Fig. 28A**.

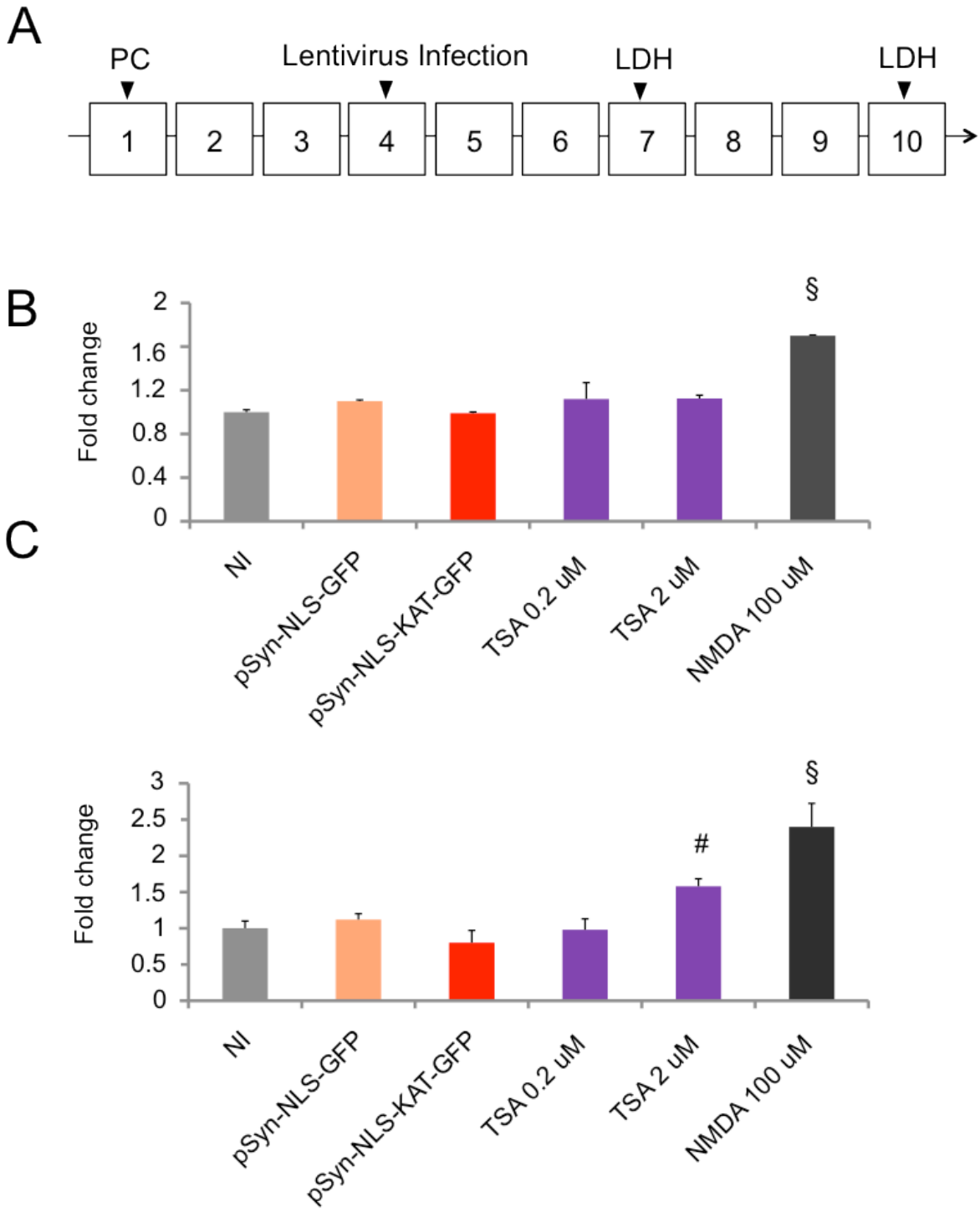

Figure 28. Experimental design and timing for KAT-overexpression experiments (**A**). Neurons were infected at 4DIV and LDH was measured at day 7 (5 h after TSA-treatment) (**B**) and day 10 (after 72 h of TSA-treatment) (**C**). NMDA was introduced 24h before the assay. PC: Plating of the culture. Data are represented as the mean ± SEM. Student's *t* test ($p < 0.05$). # and §, denote statistically significant values when compared with all others conditions. NI: non-infection.

Whereas 5 h of 2 μM TSA treatment did not show a significant difference with the non-infected/non-treated control, 72 h of treatment showed a robust increase in

LDH activity, as indicator of excitotoxic cell death. However, 6DINF with pSyn-NLS-KAT-GFP and 0.2 μM TSA treatment did not apparently produce deleterious effects in hippocampal neurons (**Fig. 29**).

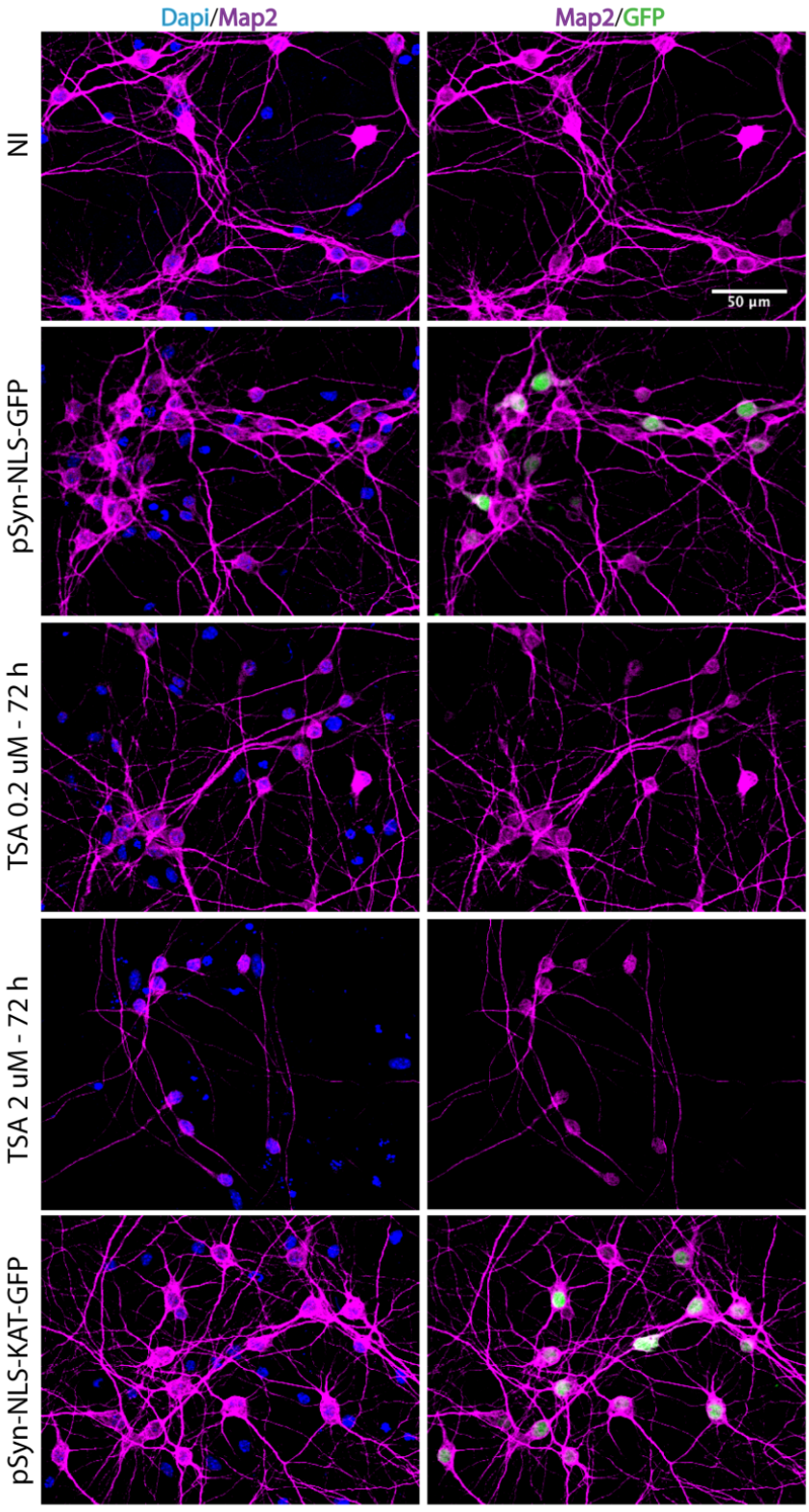

Figure 29. Representative images of hippocampal neurons under different conditions. IC against Map2 (magenta) and GFP (green). Magnification: 20X. Scale bar, 50 μm. NI: non-infection.

Next, we measured acetylation levels in all the conditions mentioned above. We observed that TSA, as expected, increased H2Bac level at both concentrations (0.2 and 2 μM) in neuronal cells. However, the impact of TSA was also very strong in glial cells when compared with basal condition (see quantifications in **Fig. 30B-C**). These results demonstrate that TSA does not exert its function in a cell type-specific manner. Remarkably, pSyn-NLS-KAT-GFP was able to increase the acetylation of H2B precisely in those infected-neurons at comparable levels with the highest TSA concentration (**Fig. 30**) in a completely innocuous manner (**Fig. 28**).

A

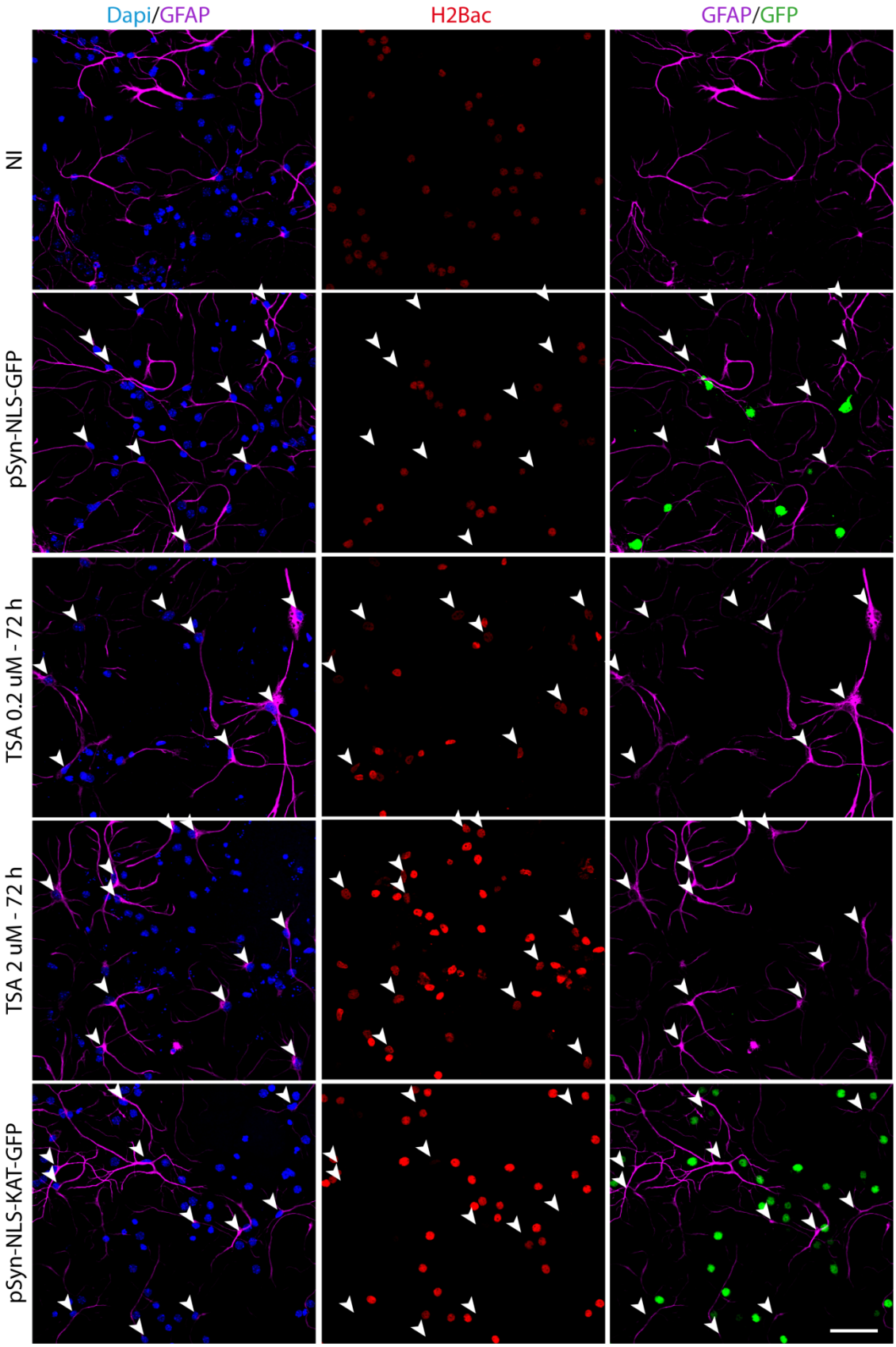
Dapi/GFAP
H2Bac
GFAP/GFP
NI
pSyn-NLS-GFP
TSA 0.2 uM - 72 h
TSA 2 uM - 72 h
pSyn-NLS-KAT-GFP

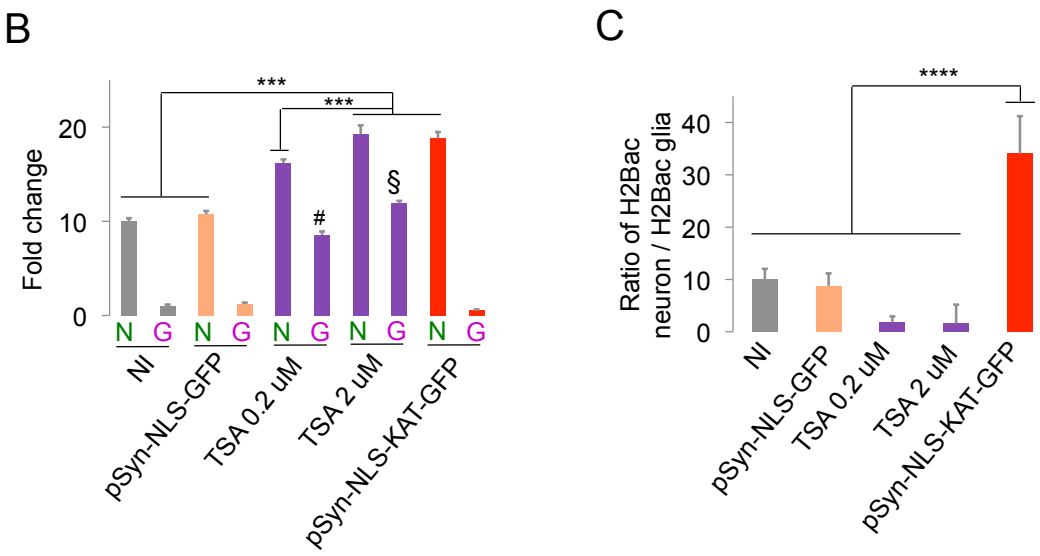

Figure 30. pSyn-NLS-KAT-GFP induce hyperacetylation selectively in neurons. A. Increased acetilated H2B level in pSyn-NLS-KAT-GFP infected neurons. Triple IC against GFAP (magenta), H2Bac (red) and GFP (green). Magnification: 20X. Scale bar, 50 µm. **B.** Quantification of H2B acetylation levels (intensity of H2Bac signal) in neurons (N) and glial cells (G) of the images showed in A. **C**. Same data as in B representing the ratio between H2Bac neuron/H2Bac glia). Data are represented as the mean ± SEM. Student's *t* test (**** $p< 0.00001$). # and § denote statistically significant values when compared with all others conditions. NI: non-infection; N: neuron; G: glia.

Notably, the expression of pSyn-NLS-KAT-GFP efficiently increases acetylation levels of the four-nucleosome histones in neurons, as demonstrated by additional IC and WB (**Fig. 31A-C**).

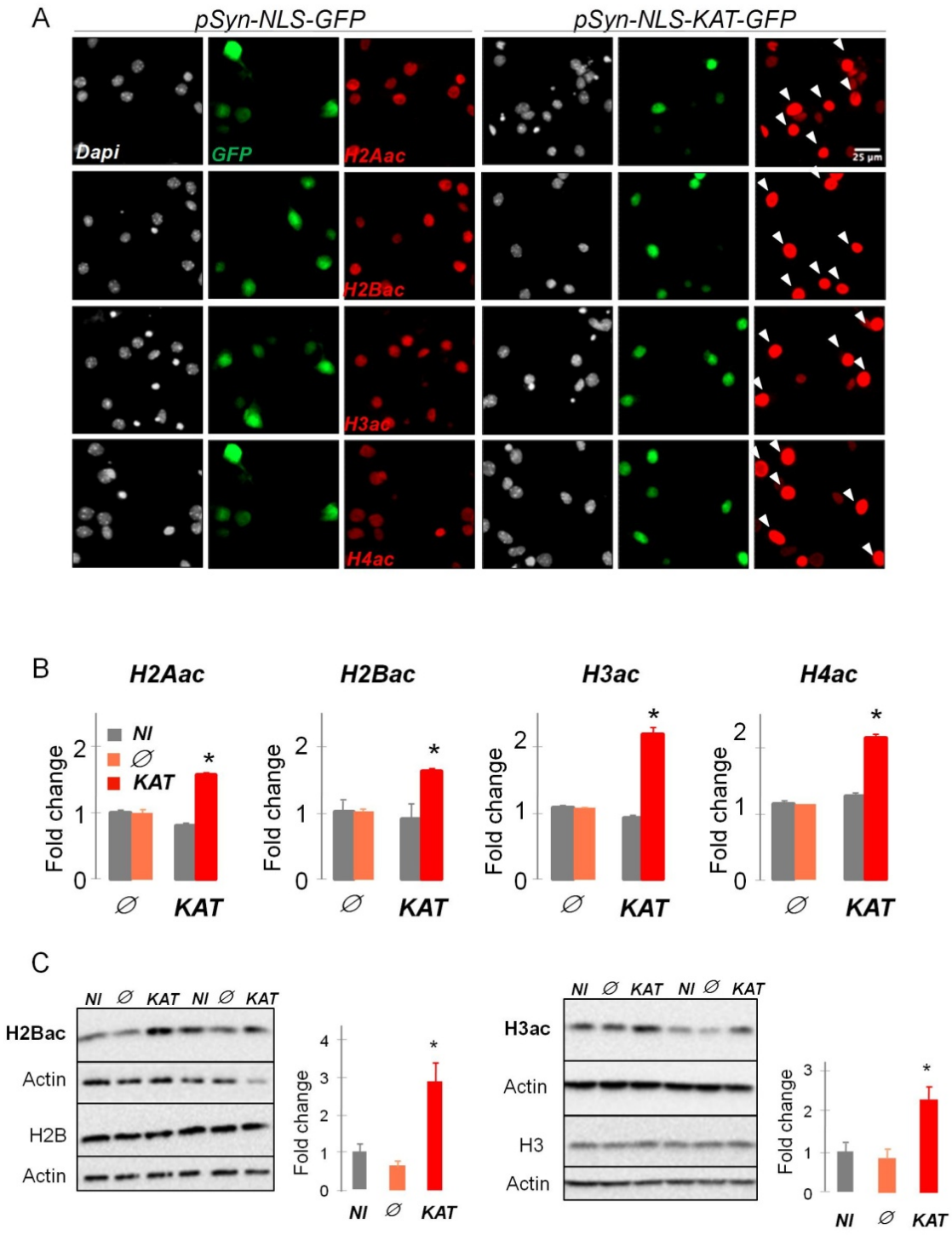

Figure 31. A. pSyn-NLS-KAT-GFP increase acetylation of the four-nucleosome histones. IC images of hippocampal neurons infected with pSyn-NLS-KAT-GFP. Magnification 20x. Scale bar, 25 µm. **B.** Quantification of A. NI: no-infection, ∅: pSyn-NLS-GFP, *KAT*: pSyn-NLS-KAT-GFP. Acetylated histones: H2Aac, H2Bac, H3ac and H4ac. **C.** Representative Western blots of protein extracts from lentiviral-infected hippocampal cultures against the pan-acetylated histones H2B (left panels) and H3 (right panels) and their corresponding total histones. Quantification was performed by normalizing acetylated fraction / total histone from two different experiments.

We also investigated whether other non-histone substrates of CBP were also affected by the overexpression of KAT activity. In agreement with previous studies that reported the acetylation of different TFs by CBP, we found that neuronal NF-κB, which plays important roles in synaptic plasticity, learning and memory, and neuroprotection (Chen et al., 2001; Zhang et al., 2010; Boersma et al., 2011; Federman et al., 2013), and the tumor suppressor protein p53 (Gu and Roeder 1997; Gaub et al., 2010) were hyperacetylated by pSyn-NLS-KAT-GFP (**Fig. 32A-B**). In contrast, we did not observe an increase in the acetylation of α-tubulin, likely because pSyn-NLS-KAT-GFP is directed to the nucleus and cannot reach this cytoplasmatic protein. Albeit TSA increased the acetylation of α-tubulin since the drug exerts its action in both the nuclear and cytoplasmic compartments (**Fig. 32C**). These results demonstrate another level of specificity in comparison with TSA, since the infection with pSyn-NLS-KAT-GFP lentivirus was restricted to the nucleus.

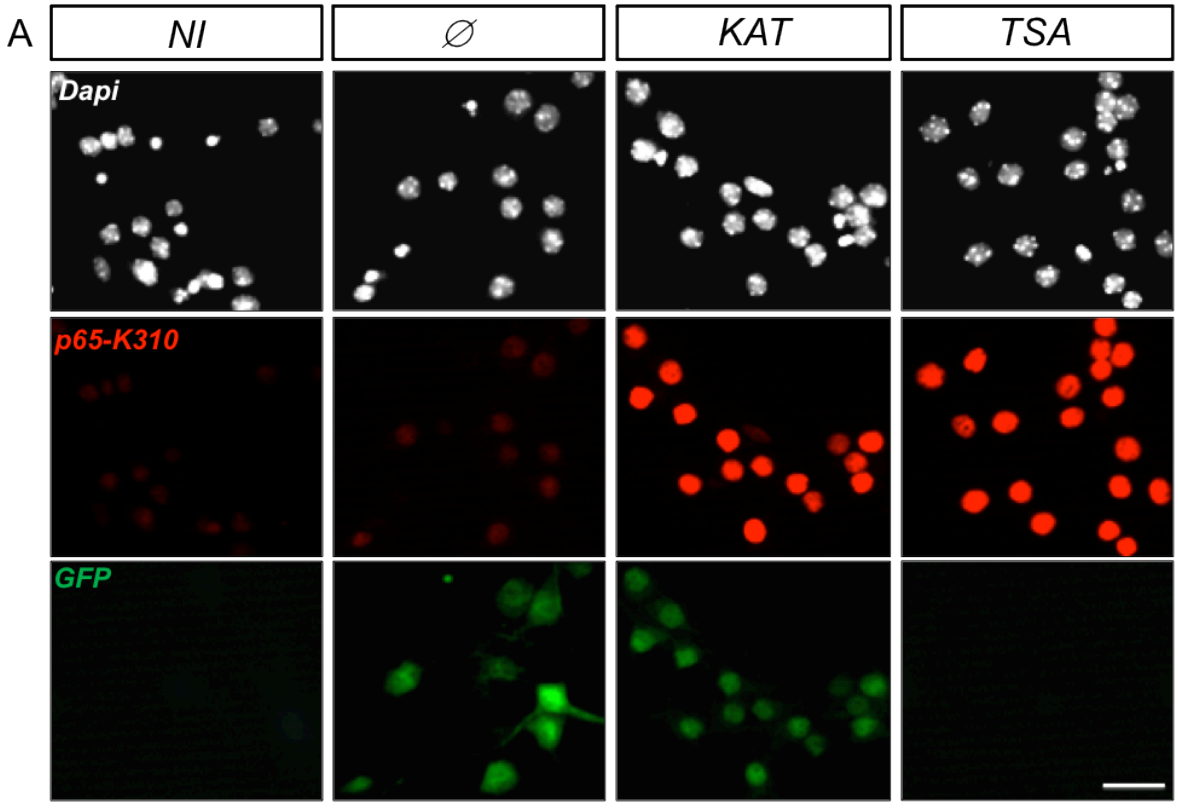

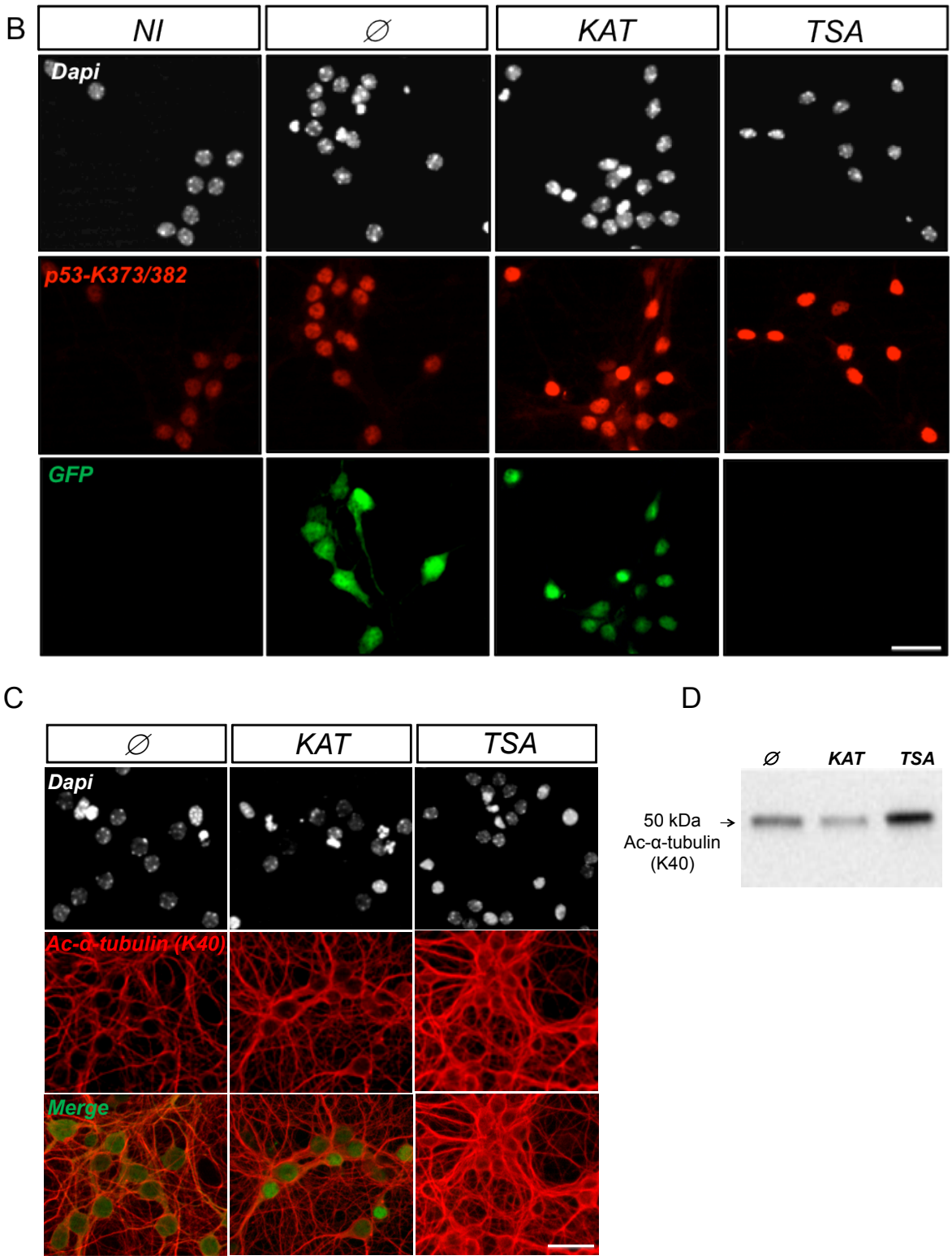

Figure 32. pSyn-NLS-KAT-GFP increase the acetylation of NF-κB and p53 TFs. Representative images of hippocampal cultures. Neurons were infected with pSyn-NLS-KAT-GFP LV, pSyn-NLS-GFP LV as a negative control and TSA as a positive control for the detection of significant acetylation changes in p65 subunit of NF-κB (K310) (**A**), in p53 (K373-382) (**B**) and in the α-tubulin (K40) (**C**). Merge images shows the overlap between GFP and the signal of the acetylated proteins. Western blot shows the difference in α-tubulin acetylation (right panel). ∅: pSyn-NLS-GFP; *KAT*: pSyn-NLS-KAT-GFP. Ac, acetylated. Magnification 20x. Scale bar, 50 μm.

Encouraged by the previous results, we planned a pilot experiment to test in vivo the acetylation induced by the KAT construct. To achieve this, we cloned the KAT domain of CBP under the control of the ubiquitous CAG promoter. Subsequently, E14 embryos were electroporated *in utero* with the CAG-NLS-KAT-GFP plasmid. Just before birth we perfused the embryos and coronal brain sections were stained against GFP and H2Bac. This staining demonstrated that transduced neurons from embryos monolaterally electroporated at the cortex show histone hyperacetylation (**Fig. 33**). These results indicate that KAT-overexpression occurs specifically only in neurons both *in vitro* and *in vivo*.

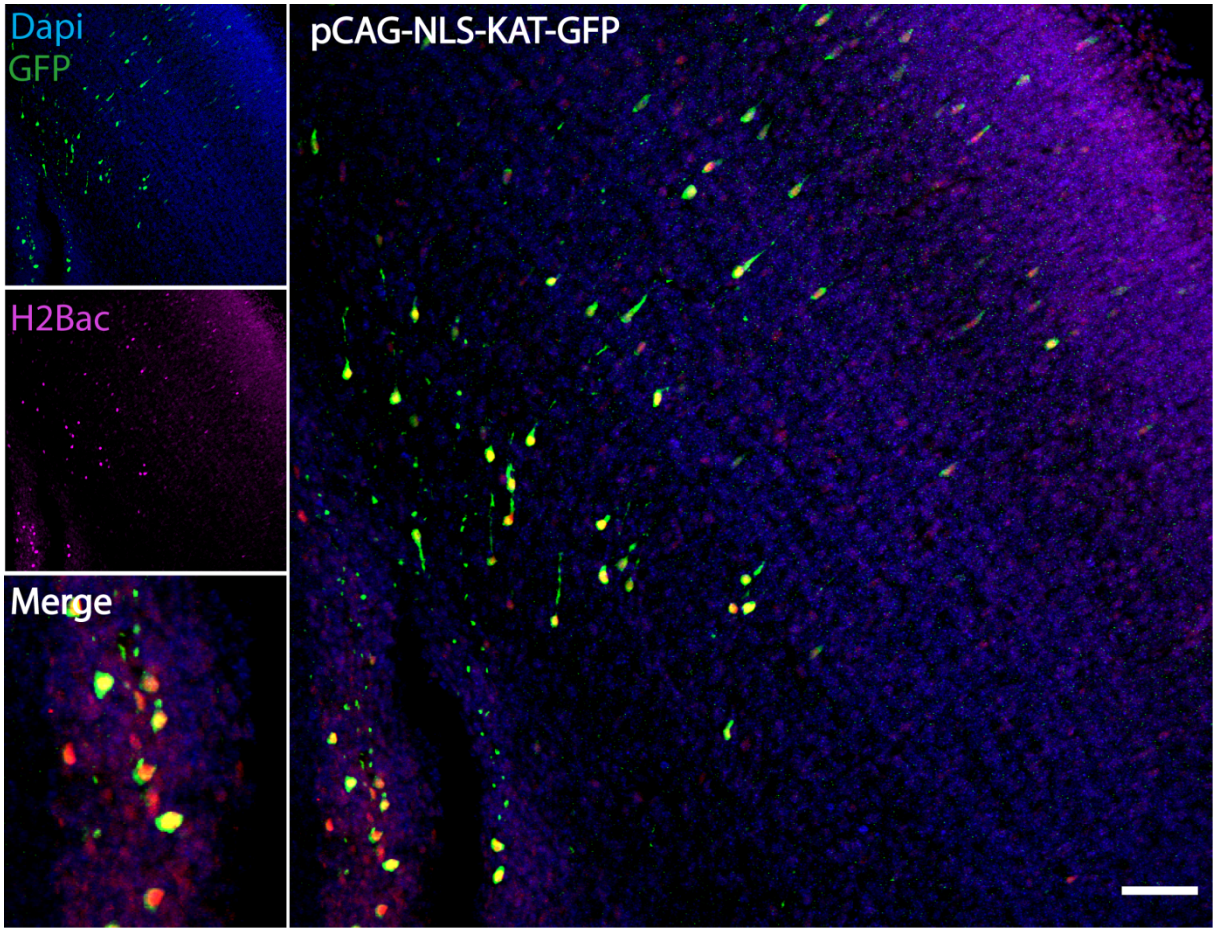

Figure 33. pCAG-NLS-KAT-GFP increase histone acetylation in an *in vivo* system. pCAG-NLS-KAT-GFP *in utero* electroporation. The image shows a coronal section, in which cortical neurons has increased acetylation of H2B (H2Bac). Magnification: 20x. Scale bar, 50 µm.

4.4.2 KAT-overexpression causes an increase in the number of synaptic protrusions in hippocampal neurons

Next, we asked whether enhancing KAT activity could affect the morphology of infected neurons. We found that the hyperacetylation of histone and non-histone substrates by pSyn-NLS-KAT-GFP correlated with an increase in the number of filopodia like-spines in comparison with control-infected neurons (**Fig. 34C**). In parallel, we also investigated the complexity of the dendritic tree (**Fig. 34B**) in pSyn-NLS-KAT-GFP and control-infected neurons and found no difference between the two groups in the Scholl analysis (**Fig. 34D**). Altogether, these data suggest that pSyn-NLS-KAT-GFP induces spine protrusions in still immature neurons without affecting global morphology.

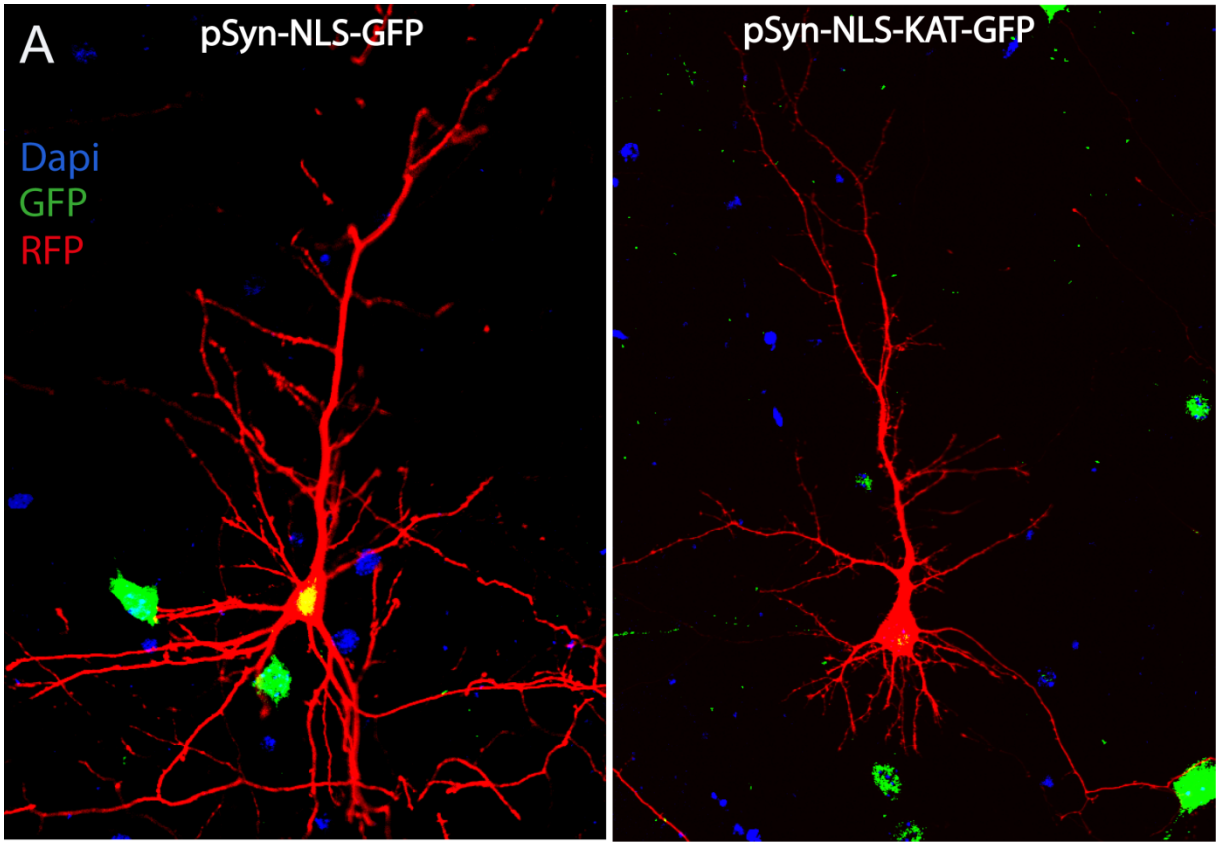

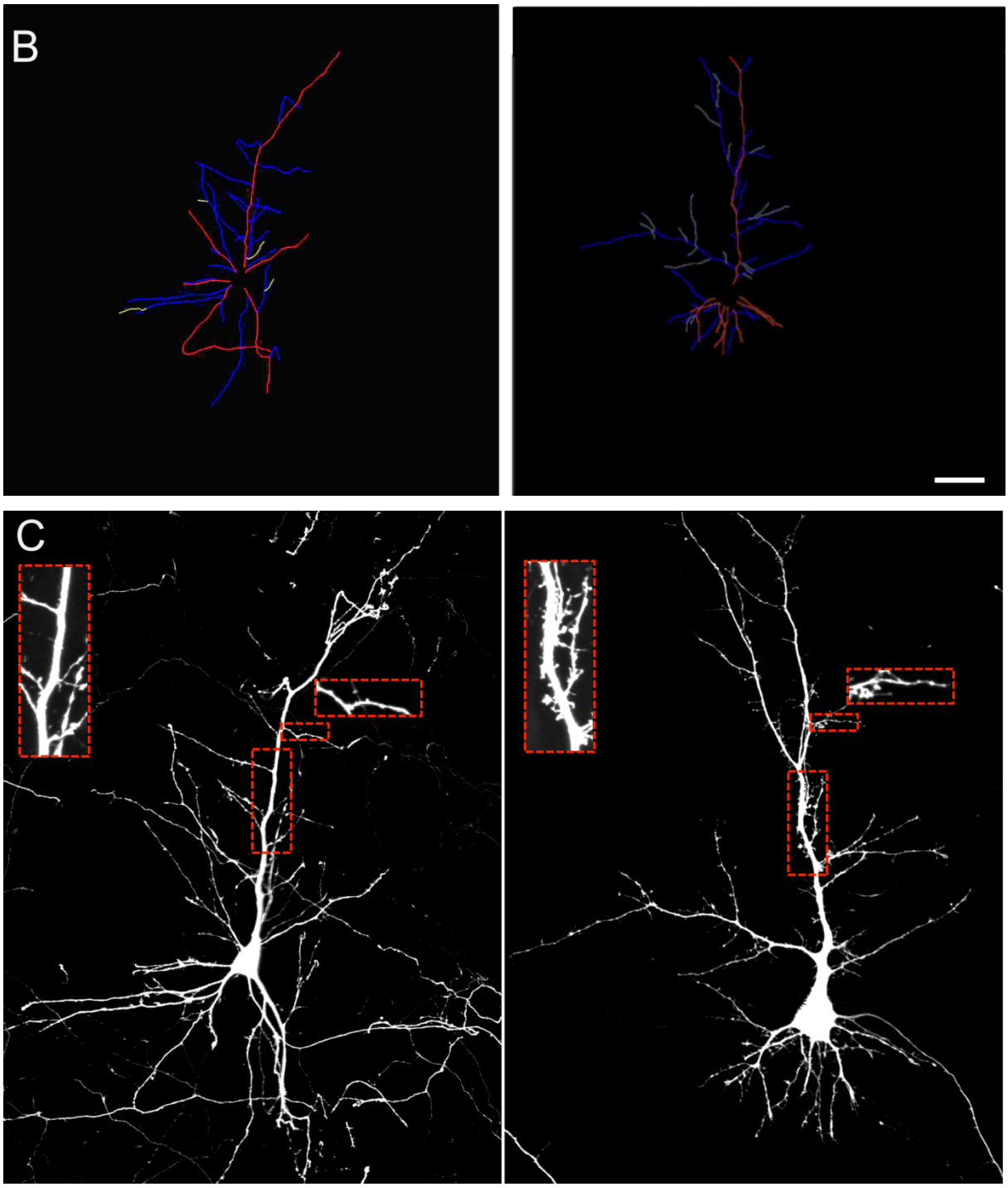
B
C

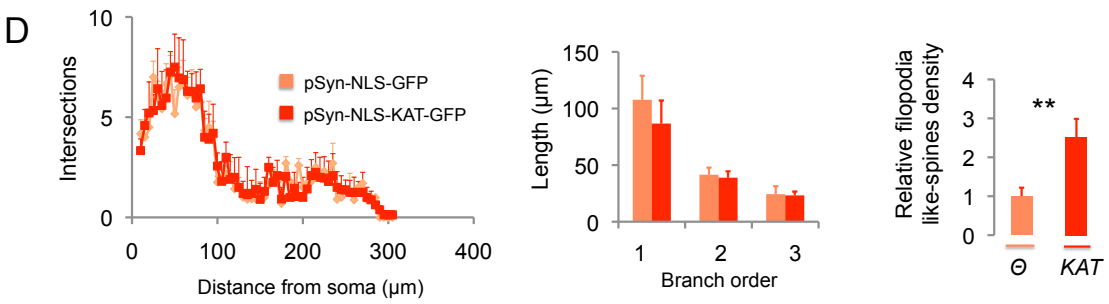
D
Intersections
10
5
0
0
100
200
300
400
Distance from soma (µm)
pSyn-NLS-GFP
pSyn-NLS-KAT-GFP
Length (µm)
150
100
50
0
1
2
3
Branch order
Relative filopodia like-spines density
4
3
2
1
0
**
Θ
KAT

Figure 34. pSyn-NLS-KAT-GFP increase the number of filopodia like-spines. **A.** Representative confocal images of pyramidal hippocampal neurons infected with pSyn-NLS-KAT-GFP and its control. Magnification 40x. **B.** Representative draws of the neurons distinguishing different dendrites. Scale bar, 20 µm. **C.** Representative images showing an increased number of filopodia like-spines in neurons infected with pSyn-NLS-KAT-GFP and its control. Magnification: 60x. Scale bar, 20 µm. **D.** Sholl analysis (left panel), quantification of the length of different order dendritic branches by ImageJ software (center panel) and quantification of the filopodia like-spines (right panel) by Imaris software. ∅: pSyn-NLS-GFP; *KAT*: pSyn-NLS-KAT-GFP.

4.4.3 The genetic reversal of lysine acetylation deficits ameliorates the neuronal growth defects

Based upon the pSyn-NLS-KAT-GFP capacity to hyperacetylate both histone and non-histone substrates in cultured neurons, we tested whether the transduction of KAT activity could restore the acetylation levels in CBP deficient neurons. To that end, we infected 4DIV cultured hippocampal neurons of all genotypes with pSyn-NLS-KAT-GFP and its control pSyn-NLS-GFP. After 6DINF/10DIV we performed a triple labeling against H3ac (to measure acetylation levels), GFP (to track the infection of the lentiviruses) and MAP2.

Remarkably, we observed a partial reversion of the abnormal MAP2 staining in neural cultures from homozygous embryos with concomitant increased histone acetylation in the neurons infected with pSyn-NLS-KAT-GFP (**Fig. 35**). This approach effectively demonstrated the capability of our genetic tool to induce hyperacetylation to restore the functional consequences of defective conditions of lysine acetylation.

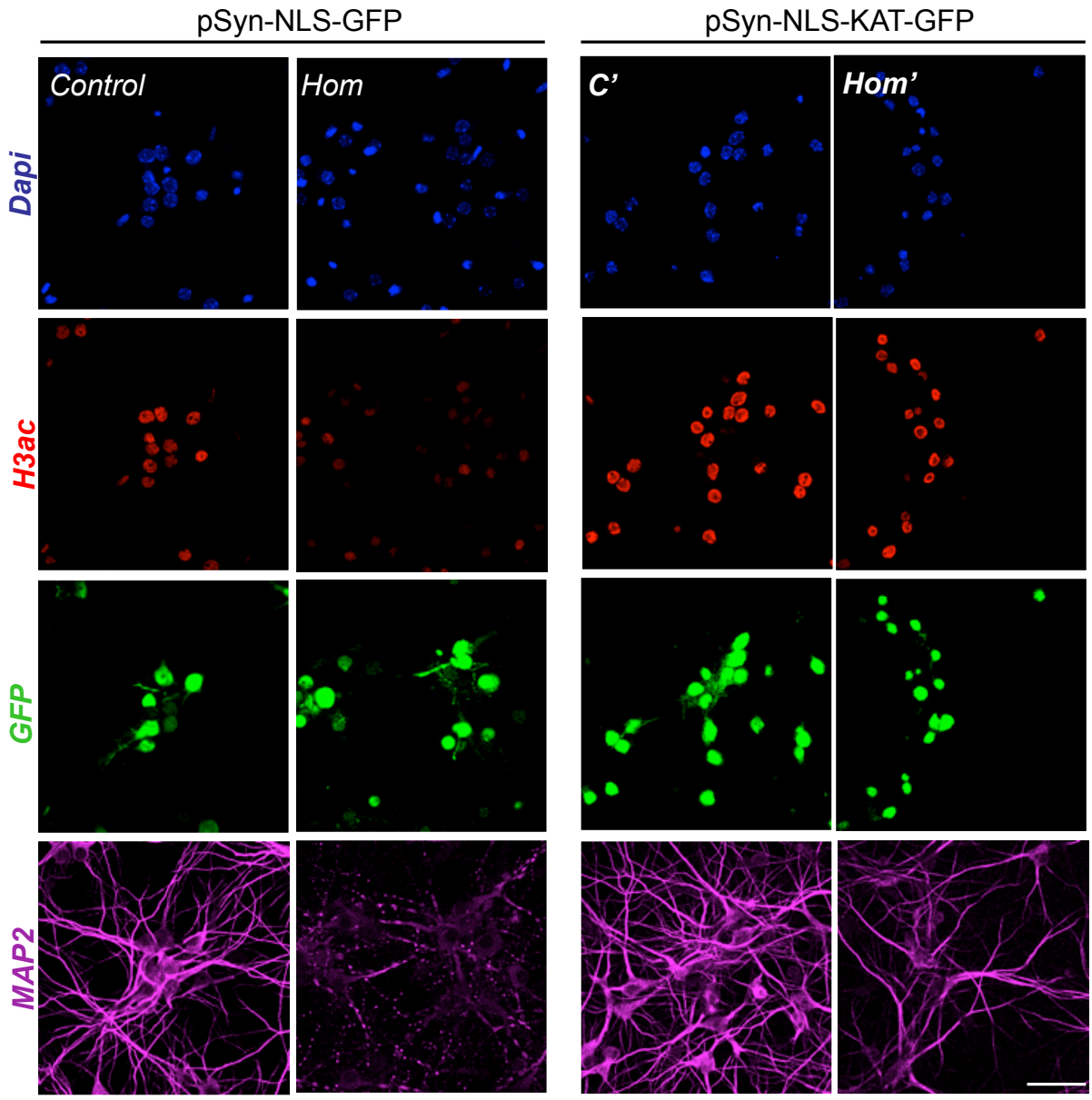

Figure 35. pSyn-NLS-KAT-GFP can restore hypoacetylation and the altered MAP2 expression pattern in Nes-cre::CBP$^{f/f}$ mice. Representative confocal images of hippocampal neurons infected with pSyn-NLS-KAT-GFP and its control pSyn-NLS-GFP (culture time: day 10). Magnification: 40x. Scale bar, 50 µm. C: control; Hom: homozygous.

4.4.4 Discussion: KAT-LV as a potential therapeutic tool in neuropathologies

It has been proposed that the cognitive and neurological deficits associated with RSTS may have two distinct components: one originated during the development of the CNS, and a second one resulting from the continued requirement of the enzymatic activity of CBP throughout life (Alarcon et al., 2004; Korzus et al., 2004). Nes-cre::CBP$^{f/f}$ mouse model represents an ideal system to investigate the role of CBP during embryonic steps considering the early lethality phenotype observed in

the CBP KO mice. We still do not know the cause of their perinatal death but, by analogy with other models, we can hypothesize that is the result of a cardiorespiration failure.

These mice showed, reduced hippocampal volume and abnormal MAP2 expression protein with concomitant hypoacetylation at the four-nucleosome histones in primary hippocampal culture. To rescue the later deficit, we designed a novel tool to increase acetylation that may offer important advantages over conventional approaches like the ones represented by pharmacological treatment with HDACis (see section 1.4).

The experiments using KAT-LV has demonstrated that selective hyperacetylation in neurons does not cause neuronal toxicity *per se*, as demonstrated by intact MAP2 pattern and LDH release. These results oppose to those observed after long-treatment with 2 μM TSA (72 h), although both of them produced the same levels of acetylation in neuronal cells. Several groups have shown that aberrant histone acetylation can also have deleterious effects as shown in several neuronal cell lines (Salminen et al., 1998; Smith et al., 2009a; Wang et al., 2009a). Intriguingly, the opposite effect, hypoacetylation, does not necessarily cause neuronal death (Chen et al., 2010; Valor et al., 2011). Comparing the neuron/glia acetylation ratio (**Fig. 30C**) together with LDH values (**Fig. 28B**) from our KAT-LV and long-treatment with 2 μM TSA (72 h), we can speculate that TSA can trigger cell death through glial-dependent hyperacetylation. Importantly, long-treatment of 0.2 μM TSA (72 h) presented a similar LDH value than KAT-LV (**Fig. 28B**), however, it showed significantly less acetylation in neurons with concomitant hyperacetylation in glial cells respect to KAT-LV (**Fig. 30B-C**). In addition, KAT-LV was able to increase the acetylation of the four- nucleosome histones as well as the acetylation of the TFs NF-kB and p53 (direct substrates of CBP's KAT activity) (Ito et al., 2001; Nadiminty et al., 2006) confirming its nuclear activity. Overall, we have designed a tool that increases lysine acetylation levels in a highly restricted pattern (nuclei of neurons) in a safe manner.

Interestingly, KAT overexpression also augmented the number of filopodia like-spines. We can speculate about two different events: KAT-LV could indirectly regulate dendritic processes through the activity of TFs that are the direct targets of KAT activity and/or KAT-LV could directly regulate the activity of proteins that shuffle between the nucleus and spines where they may have a key local role. Thus it has

been described for various proteins (e.g.: HDAC4, CtBP-1) (Darcy et al., 2010; Ivanova et al., 2015; Kravchick and Jordan, 2015) a switch in the location between the nucleus and the dendritic spines. Therefore, several mechanisms might account for the observed effect of KAT-LV regulating the formation of cytoplasmic filopodia like-spines.

We used Nes-cre::CBP$^{f/f}$ to address the effect of KAT-LV on hippocampal culture that showed hypoacetylation. Noticeably, we demonstrated the KAT-LV was able to increase histone acetylation with concomitant partial reversion of the abnormal staining of MAP2 in neurons in the homozygous condition. To reveal which nuclear function is regulated by KAT-LV is an essential question that will need to be addressed in the future in order to define the therapeutic potential of KAT-LV. In any case, the results of our rescue experiment suggest that our tool represents a promising approach for therapeutics of preclinical models of neuropathologies such as RSTS, HD and AD among others.

General discussion

5.1 The relationship between histone acetylation and transcription: an open debate

From our analysis in HD mouse models, we can conclude that histone deacetylation and transcriptional defects are early and, in general, not linked events (section 4.1.2 and 4.2.5) during the progression of the disease. Therefore, some additional mechanisms apart from histone deacetylation should to be responsible for the downstream transcriptional changes seen in HD. Different hypothesis can be considered to explain this lack of interaction: (i) the combination of histone PTMs, with well over one hundred distinct modification sites described in the literature, can differentially contribute to specific changes in gene expression (Daujat et al., 2002; Lee et al., 2010; Rando, 2012), it is possible that a particular increased acetylation mark, not explored in our study shows a better correlation with changes in transcription than the ones presented here. (ii) histone acetylation is a permissive mark that plays an allosteric role regulating chromatin complexes but it is not directly engaged in the recruitment of TFs or the RNApol complex, thereby the changes in this mark has a weak impact on transcription (Lopez-Atalaya et al., 2013; Rando et al., 2012). The later view is consistent with experiments in other models of HD (Valor, 2015) and with numerous studies in other species (Lenstra et al., 2011; Rando, 2012) that did not find a clear causal relationship between differential changes in histone acetylation and changes in gene expression. Thus, the research conducted in yeast, *Drosophila* and other organisms in which it is possible to specifically prevent the acetylation of histones at specific positions indicates that the lack of acetylation does not block or even interfere with transcription, unless that many lysines are simultaneously affected (Lopez-Atalaya and Barco, 2014). Further progress in our understanding of the role of epigenetic modifications in neuropathology will require a clear distinction between cause and effect and between epigenetics-related processes and classical transcriptional mechanisms.

Another important question refers to how HDACi treatment can ameliorate symptomatology of HD and restore the expression of a small number of genes? (Ferrante et al., 2003; Gardian et al., 2005; Stack et al., 2007). The precise mechanism by which HDACi exert their effects has not been determined. It is important to remark that acetylation regulates diverse protein classes. Lysine acetylation preferentially targets large macromolecular complexes involved in numerous functions, such as chromatin remodeling, cell cycle, splicing, nuclear transport and actin nucleation (Choudhary et al., 2009). One might therefore consider

that HDACi may exert their effects through acetylation of non-histone substrates, including TFs. In addition, HDACis comprises a heterogeneous group of compounds and it is possible that the beneficial effects of some HDACi in HD models are due to mechanisms unrelated to HDAC activity. For instance, TSA and SAHA have a hydroxamic acid group that has been involved in a neuroprotective effect independent of their HDAC inhibition properties (Sleiman et al., 2014). Similarly, valproate influences GABA transmission and NMDA-mediated excitotoxicity also by HDAC-independent mechanisms (Zadori et al., 2009). On the other hand, HDACi with higher specificity such as HDACi 4b corrected the expression of a high number of genes in the R6/2 HD strain (Thomas et al., 2008), which ameliorates the disease phenotype and transcriptional abnormalities. How this specific HDAC1/3 inhibitor can promote such profound reversion compared to more unselective HDACis remains unknown.

In this scenario, our KAT-LV, which induces hyperacetylation in a highly specific manner (see **Fig. 30** and section 4.4.4), may be a potential therapeutic tool for HD, RSTS as well as for others neurodegenerative disorders associated with reduced lysine acetylation levels. The KAT-LV represents an excellent tool to reverse this situation and assess the consequences of this reversion in transcription.

5.2 Future perspectives

In the course of this thesis, I have introduced two important technologies for the research of neurological diseases that have large potential for further development.

First, the use of next-generation sequencing (NGS) coupled with chromatin immunoprecipitation (ChIP-seq) has allowed us to obtain unprecedented view of the epigenome in poly-Q disease. In 2013, when our paper came out (Valor et al., 2013a), we presented the first parallel genome-wide analysis of transcriptional and histone acetylation deficits in a polyQ disease model. Our study, initially constrained by the high cost of these genomic methods, was pioneer exploring the relationship between acetylation and transcription applying genome-wide unbiased technology. In the last few years, NGS platforms have undergone a fast-growing period and now permit the possibility of including a large number of samples with a low cost, longer read lengths, etc. Undoubtedly, NGS-based techniques are aimed to provide fundamental biological insight into questions that were very hard to address a few years ago. They have the potential to provide comprehensive maps of how

nucleosome positioning, chromatin conformation, transcription factor binding, and the localization of histone and DNA modifications are affected through the genome in many still poorly understood brain pathologies, such as HD and RSTS (Dawson and Kouzarides, 2012).

The second development refers to epigenetic editing techniques. Recent developments based on CRISPRs/Cas9 technology now allow creating programmable tools to edit the epigenome (Hilton et al., 2015). This represent an important refinement over our seminal attend to correct epigenetic deficits using KAT-LV for increasing lysine acetylation levels specifically in neurons. In the near future, the coupling of the KAT domain with CRISPRs/dCas9 constructs will make possible to manipulate epigenetic marks in order to control cell phenotype or interrogate the connection between the epigenome and transcriptional regulation. This outstanding type of technology is the one necessary to answer complex questions related to the causal/consequential role of histone PTMs in transcription, and the impact of directed lysine acetylation in the regulation of gene networks and chromatin state dynamics.

Conclusions

1. Cerebellar and hippocampal tissues present the highest density of mHTT aggregates in the brain of HD82Q mice, which positively correlates with the severity of transcriptional dysregulation.

2. Transcriptional deficits in HD82Q mice precede the onset of chorea and weight loss, which suggests a possible role for these alterations in the etiology of these symptoms.

3. Hundreds of loci were hypoacetylated for H3K9/14 and H4K12 in the chromatin of HD82Q mice.

4. Transcriptional and histone acetylation defects in HD82Q mice show low global correlation.

5. Histone deacetylation and transcriptional dysregulation appear to be two early, but largely independent manifestations of polyglutamine disease, suggesting that additional epigenetic marks or mechanisms are required for explaining the full range of transcriptional alterations associated with this disorder.

6. Genes showing both altered gene expression and TSS-associated H3 acetylation were part of a consistent HD transcriptional signature in different HD models and in postmortem brain patients.

7. Histone H3 acetylation, is perturbed at specific loci both HD82Q and R6/1 mice, relevant for neuronal functioning.

8. The generation of Nes-cre::CBP$^{f/f}$ mice is a valuable line to improve the understanding of the role of CBP during prenatal development period in the nervous system.

9. Nes-cre::CBP$^{f/f}$ mice do not show changes in the gross morphology of the brain between genotypes, but present a significant reduction in hippocampus volume.

10. Primary hippocampal cultures derived from Nes-cre::CBP$^{f/f}$ homozygous embryos present severe neuronal growth defects, hipoacetylation for the four-nucleosome histones and abnormal staining for MAP2 protein.

11. The overexpression of the KAT activity of CBP do not shows toxic effects in neurons, increases the acetylation of both the histone tails and TFs such as NF-κB and p53, and increase the number of filopodia like-spines in primary hippocampal culture.

12. The overexpression of the KAT activity of CBP rescues the acetylation defect and abnormal growth in primary hippocampal culture from Nes-cre::CBP$^{f/f}$ homozygous embryos.

Bibliography

Abdolmaleky HM, Cheng KH, Russo A, Smith CL, Faraone SV, Wilcox M, Shafa R, Glatt SJ, Nguyen G, Ponte JF, Thiagalingam S, Tsuang MT (2005) Hypermethylation of the reelin (RELN) promoter in the brain of schizophrenic patients: a preliminary report. Am J Med Genet B Neuropsychiatr Genet 134B:60-66.

Al-Mahdawi S, Pinto RM, Ismail O, Varshney D, Lymperi S, Sandi C, Trabzuni D, Pook M (2008) The Friedreich ataxia GAA repeat expansion mutation induces comparable epigenetic changes in human and transgenic mouse brain and heart tissues. Hum Mol Genet 17:735-746.

Alarcon JM, Malleret G, Touzani K, Vronskaya S, Ishii S, Kandel ER, Barco A (2004) Chromatin acetylation, memory, and LTP are impaired in CBP+/- mice: a model for the cognitive deficit in Rubinstein-Taybi syndrome and its amelioration. Neuron 42:947-959.

Andrade MA, Bork P (1995) HEAT repeats in the Huntington's disease protein. Nat Genet 11:115-116.

Arrasate M, Finkbeiner S (2012) Protein aggregates in Huntington's disease. Exp Neurol 238:1-11.

Arrasate M, Mitra S, Schweitzer ES, Segal MR, Finkbeiner S (2004) Inclusion body formation reduces levels of mutant huntingtin and the risk of neuronal death. Nature 431:805-810.

Augood SJ, Faull RL, Emson PC (1997) Dopamine D1 and D2 receptor gene expression in the striatum in Huntington's disease. Ann Neurol 42:215-221.

Aylward EH, Codori AM, Rosenblatt A, Sherr M, Brandt J, Stine OC, Barta PE, Pearlson GD, Ross CA (2000) Rate of caudate atrophy in presymptomatic and symptomatic stages of Huntington's disease. Mov Disord 15:552-560.

Aylward EH, Li Q, Stine OC, Ranen N, Sherr M, Barta PE, Bylsma FW, Pearlson GD, Ross CA (1997) Longitudinal change in basal ganglia volume in patients with Huntington's disease. Neurology 48:394-399.

Bardai FH, Verma P, Smith C, Rawat V, Wang L, D'Mello SR (2013) Disassociation of histone deacetylase-3 from normal huntingtin underlies mutant huntingtin neurotoxicity. J Neurosci 33:11833-11838.

Barrett RM, Malvaez M, Kramar E, Matheos DP, Arrizon A, Cabrera SM, Lynch G, Greene RW, Wood MA (2011) Hippocampal focal knockout of CBP affects specific histone modifications, long-term potentiation, and long-term memory. Neuropsychopharmacology 36:1545-1556.

Bates G, Harper P, Jones L (eds.) (2004) Huntington’s disease: Oxford University Press.

Baylin SB (2005) DNA methylation and gene silencing in cancer. Nat Clin Pract Oncol 2 Suppl 1:S4-11.

Beck H, Yaari Y (2008) Plasticity of intrinsic neuronal properties in CNS disorders. Nat Rev Neurosci 9:357-369.

Bedford DC, Brindle PK (2012) Is histone acetylation the most important physiological function for CBP and p300? Aging (Albany NY) 4:247-255.

Bedford DC, Kasper LH, Fukuyama T, Brindle PK (2010) Target gene context influences the transcriptional requirement for the KAT3 family of CBP and p300 histone acetyltransferases. Epigenetics 5:9-15.

Benito E, Valor LM, Jimenez-Minchan M, Huber W, Barco A (2011) cAMP response element-binding protein is a primary hub of activity-driven neuronal gene expression. J Neurosci 31:18237-18250.

Benn CL, Butler R, Mariner L, Nixon J, Moffitt H, Mielcarek M, Woodman B, Bates GP (2009) Genetic knock-down of HDAC7 does not ameliorate disease pathogenesis in the R6/2 mouse model of Huntington's disease. PLoS One 4:e5747.

Benn CL, Landles C, Li H, Strand AD, Woodman B, Sathasivam K, Li SH, Ghazi-Noori S, Hockly E, Faruque SM, Cha JH, Sharpe PT, Olson JM, Li XJ, Bates GP (2005) Contribution of nuclear and extranuclear polyQ to neurological phenotypes in mouse models of Huntington's disease. Hum Mol Genet 14:3065-3078.

Benn CL, Sun T, Sadri-Vakili G, McFarland KN, DiRocco DP, Yohrling GJ, Clark TW, Bouzou B, Cha JH (2008) Huntingtin modulates transcription, occupies gene promoters in vivo, and binds directly to DNA in a polyglutamine-dependent manner. J Neurosci 28:10720-10733.

Berdasco M, Esteller M (2013) Genetic syndromes caused by mutations in epigenetic genes. Hum Genet 132:359-383.

Bergqvist A, Rice CM (2001) Transcriptional activation of the interleukin-2 promoter by hepatitis C virus core protein. J Virol 75:772-781.

Bhattacherjee V, Horn KH, Singh S, Webb CL, Pisano MM, Greene RM (2009) CBP/p300 and associated transcriptional co-activators exhibit distinct expression patterns during murine craniofacial and neural tube development. Int J Dev Biol 53:1097-1104.

Bliss JM, Gray EE, Dhaka A, O'Dell TJ, Colicelli J (2010) Fear learning and extinction are linked to neuronal plasticity through Rin1 signaling. J Neurosci Res 88:917-926.

Bobrowska A, Donmez G, Weiss A, Guarente L, Bates G (2012) SIRT2 ablation has no effect on tubulin acetylation in brain, cholesterol biosynthesis or the progression of Huntington's disease phenotypes in vivo. PLoS One 7:e34805.
Bobrowska A, Paganetti P, Matthias P, Bates GP (2011) Hdac6 knock-out increases tubulin acetylation but does not modify disease progression in the R6/2 mouse model of Huntington's disease. PLoS One 6:e20696.
Boersma MC, Dresselhaus EC, De Biase LM, Mihalas AB, Bergles DE, Meffert MK (2011) A requirement for nuclear factor-kappaB in developmental and plasticity-associated synaptogenesis. J Neurosci 31:5414-5425.
Bonasio R, Tu S, Reinberg D (2010) Molecular signals of epigenetic states. Science 330:612-616.
Bondarenko VA, Liu YV, Jiang YI, Studitsky VM (2003) Communication over a large distance: enhancers and insulators. Biochem Cell Biol 81:241-251.
Borovecki F, Lovrecic L, Zhou J, Jeong H, Then F, Rosas HD, Hersch SM, Hogarth P, Bouzou B, Jensen RV, Krainc D (2005) Genome-wide expression profiling of human blood reveals biomarkers for Huntington's disease. Proc Natl Acad Sci U S A 102:11023-11028.
Boutell JM, Thomas P, Neal JW, Weston VJ, Duce J, Harper PS, Jones AL (1999) Aberrant interactions of transcriptional repressor proteins with the Huntington's disease gene product, huntingtin. Hum Mol Genet 8:1647-1655.
Boutillier AL, Trinh E, Loeffler JP (2003) Selective E2F-dependent gene transcription is controlled by histone deacetylase activity during neuronal apoptosis. J Neurochem 84:814-828.
Braun S, Madhani HD (2012) Shaping the landscape: mechanistic consequences of ubiquitin modification of chromatin. EMBO Rep 13:619-630.
Burgunder JM (2014) Genetics of Huntington's disease and related disorders. Drug Discov Today.
Calabresi P, Centonze D, Bernardi G (2000) Cellular factors controlling neuronal vulnerability in the brain: a lesson from the striatum. Neurology 55:1249-1255.
Cao J, Yan Q (2012) Histone ubiquitination and deubiquitination in transcription, DNA damage response, and cancer. Front Oncol 2:26.
Carninci P, Sandelin A, Lenhard B, Katayama S, Shimokawa K, Ponjavic J, Semple CA, Taylor MS, Engstrom PG, Frith MC, Forrest AR, Alkema WB, Tan SL, Plessy C, Kodzius R, Ravasi T, Kasukawa T, Fukuda S, Kanamori-Katayama M, Kitazume Y, Kawaji H, Kai C, Nakamura M, Konno H, Nakano K, Mottagui-Tabar S, Arner P, Chesi A, Gustincich S, Persichetti F, Suzuki H, Grimmond SM, Wells CA, Orlando V, Wahlestedt C, Liu ET, Harbers M, Kawai J, Bajic VB, Hume DA, Hayashizaki Y (2006) Genome-wide analysis of mammalian promoter architecture and evolution. Nat Genet 38:626-635.
Cattaneo E, Rigamonti D, Goffredo D, Zuccato C, Squitieri F, Sipione S (2001) Loss of normal huntingtin function: new developments in Huntington's disease research. Trends Neurosci 24:182-188.
Cha JH (2007) Transcriptional signatures in Huntington's disease. Prog Neurobiol 83:228-248.
Cha JH, Kosinski CM, Kerner JA, Alsdorf SA, Mangiarini L, Davies SW, Penney JB, Bates GP, Young AB (1998) Altered brain neurotransmitter receptors in transgenic mice expressing a portion of an abnormal human huntington disease gene. Proc Natl Acad Sci U S A 95:6480-6485.
Chakrabarti S, Bhattacharyya D, Dasgupta D (2000) Structural basis of DNA recognition by anticancer antibiotics, chromomycin A(3), and mithramycin: roles of minor groove width and ligand flexibility. Biopolymers 56:85-95.
Chen G, Zou X, Watanabe H, van Deursen JM, Shen J (2010) CREB binding protein is required for both short-term and long-term memory formation. J Neurosci 30:13066-13077.
Chen L, Fischle W, Verdin E, Greene WC (2001) Duration of nuclear NF-kappaB action regulated by reversible acetylation. Science 293:1653-1657.
Chiu CT, Liu G, Leeds P, Chuang DM (2011) Combined treatment with the mood stabilizers lithium and valproate produces multiple beneficial effects in transgenic mouse models of Huntington's disease. Neuropsychopharmacology 36:2406-2421.
Choi YJ, Kim SI, Lee JW, Kwon YS, Lee HJ, Kim SS, Chun W (2012) Suppression of aggregate formation of mutant huntingtin potentiates CREB-binding protein sequestration and apoptotic cell death. Mol Cell Neurosci 49:127-137.
Choudhary C, Kumar C, Gnad F, Nielsen ML, Rehman M, Walther TC, Olsen JV, Mann M (2009) Lysine acetylation targets protein complexes and co-regulates major cellular functions. Science 325:834-840.
Choukrallah MA, Matthias P (2014) The Interplay between Chromatin and Transcription Factor Networks during B Cell Development: Who Pulls the Trigger First? Front Immunol 5:156.

Chuang DM, Leng Y, Marinova Z, Kim HJ, Chiu CT (2009) Multiple roles of HDAC inhibition in neurodegenerative conditions. Trends Neurosci 32:591-601.
Chueh AC, Tse JW, Togel L, Mariadason JM (2014) Mechanisms of Histone Deacetylase Inhibitor-Regulated Gene Expression in Cancer Cells. Antioxid Redox Signal.
Cong SY, Pepers BA, Evert BO, Rubinsztein DC, Roos RA, van Ommen GJ, Dorsman JC (2005) Mutant huntingtin represses CBP, but not p300, by binding and protein degradation. Mol Cell Neurosci 30:560-571.
Creyghton MP, Cheng AW, Welstead GG, Kooistra T, Carey BW, Steine EJ, Hanna J, Lodato MA, Frampton GM, Sharp PA, Boyer LA, Young RA, Jaenisch R (2010) Histone H3K27ac separates active from poised enhancers and predicts developmental state. Proc Natl Acad Sci U S A 107:21931-21936.
Crosio C, Heitz E, Allis CD, Borrelli E, Sassone-Corsi P (2003) Chromatin remodeling and neuronal response: multiple signaling pathways induce specific histone H3 modifications and early gene expression in hippocampal neurons. J Cell Sci 116:4905-4914.
Cui L, Jeong H, Borovecki F, Parkhurst CN, Tanese N, Krainc D (2006) Transcriptional repression of PGC-1alpha by mutant huntingtin leads to mitochondrial dysfunction and neurodegeneration. Cell 127:59-69.
Darcy MJ, Calvin K, Cavnar K, Ouimet CC (2010) Regional and subcellular distribution of HDAC4 in mouse brain. J Comp Neurol 518:722-740.
Daujat S, Bauer UM, Shah V, Turner B, Berger S, Kouzarides T (2002) Crosstalk between CARM1 methylation and CBP acetylation on histone H3. Curr Biol 12:2090-2097.
Davies SW, Turmaine M, Cozens BA, DiFiglia M, Sharp AH, Ross CA, Scherzinger E, Wanker EE, Mangiarini L, Bates GP (1997) Formation of neuronal intranuclear inclusions underlies the neurological dysfunction in mice transgenic for the HD mutation. Cell 90:537-548.
Dawson MA, Kouzarides T (2012) Cancer epigenetics: from mechanism to therapy. Cell 150:12-27.
Day JJ, Sweatt JD (2011) Epigenetic mechanisms in cognition. Neuron 70:813-829.
de Carcer G, Escobar B, Higuero AM, Garcia L, Anson A, Perez G, Mollejo M, Manning G, Melendez B, Abad-Rodriguez J, Malumbres M (2011) Plk5, a polo box domain-only protein with specific roles in neuron differentiation and glioblastoma suppression. Mol Cell Biol 31:1225-1239.
de la Monte SM, Vonsattel JP, Richardson EP, Jr. (1988) Morphometric demonstration of atrophic changes in the cerebral cortex, white matter, and neostriatum in Huntington's disease. J Neuropathol Exp Neurol 47:516-525.
Deak M, Clifton AD, Lucocq LM, Alessi DR (1998) Mitogen- and stress-activated protein kinase-1 (MSK1) is directly activated by MAPK and SAPK2/p38, and may mediate activation of CREB. EMBO J 17:4426-4441.
Deininger K, Eder M, Kramer ER, Zieglgansberger W, Dodt HU, Dornmair K, Colicelli J, Klein R (2008) The Rab5 guanylate exchange factor Rin1 regulates endocytosis of the EphA4 receptor in mature excitatory neurons. Proceedings of the National Academy of Sciences of the United States of America 105:12539-12544.
del Toro D, Canals JM, Gines S, Kojima M, Egea G, Alberch J (2006) Mutant huntingtin impairs the post-Golgi trafficking of brain-derived neurotrophic factor but not its Val66Met polymorphism. J Neurosci 26:12748-12757.
Dhaka A, Costa RM, Hu H, Irvin DK, Patel A, Kornblum HI, Silva AJ, O'Dell TJ, Colicelli J (2003) The RAS effector RIN1 modulates the formation of aversive memories. The Journal of neuroscience : the official journal of the Society for Neuroscience 23:748-757.
DiFiglia M, Sapp E, Chase K, Schwarz C, Meloni A, Young C, Martin E, Vonsattel JP, Carraway R, Reeves SA, et al. (1995) Huntingtin is a cytoplasmic protein associated with vesicles in human and rat brain neurons. Neuron 14:1075-1081.
Dokmanovic M, Perez G, Xu W, Ngo L, Clarke C, Parmigiani RB, Marks PA (2007) Histone deacetylase inhibitors selectively suppress expression of HDAC7. Mol Cancer Ther 6:2525-2534.
Dompierre JP, Godin JD, Charrin BC, Cordelieres FP, King SJ, Humbert S, Saudou F (2007) Histone deacetylase 6 inhibition compensates for the transport deficit in Huntington's disease by increasing tubulin acetylation. J Neurosci 27:3571-3583.
Ebert DH, Greenberg ME (2013) Activity-dependent neuronal signalling and autism spectrum disorder. Nature 493:327-337.
Emson PC, Arregui A, Clement-Jones V, Sandberg BE, Rossor M (1980) Regional distribution of methionine-enkephalin and substance P-like immunoreactivity in normal human brain and in Huntington's disease. Brain Res 199:147-160.
Esteller M (2011) Non-coding RNAs in human disease. Nat Rev Genet 12:861-874.

Federman N, de la Fuente V, Zalcman G, Corbi N, Onori A, Passananti C, Romano A (2013) Nuclear factor kappaB-dependent histone acetylation is specifically involved in persistent forms of memory. J Neurosci 33:7603-7614.
Feinberg AP, Ohlsson R, Henikoff S (2006) The epigenetic progenitor origin of human cancer. Nat Rev Genet 7:21-33.
Feng J, Liu T, Qin B, Zhang Y, Liu XS (2012) Identifying ChIP-seq enrichment using MACS. Nat Protoc 7:1728-1740.
Ferrante RJ, Gutekunst CA, Persichetti F, McNeil SM, Kowall NW, Gusella JF, MacDonald ME, Beal MF, Hersch SM (1997) Heterogeneous topographic and cellular distribution of huntingtin expression in the normal human neostriatum. J Neurosci 17:3052-3063.
Ferrante RJ, Kubilus JK, Lee J, Ryu H, Beesen A, Zucker B, Smith K, Kowall NW, Ratan RR, Luthi-Carter R, Hersch SM (2003) Histone deacetylase inhibition by sodium butyrate chemotherapy ameliorates the neurodegenerative phenotype in Huntington's disease mice. J Neurosci 23:9418-9427.
Fink AJ, Englund C, Daza RA, Pham D, Lau C, Nivison M, Kowalczyk T, Hevner RF (2006) Development of the deep cerebellar nuclei: transcription factors and cell migration from the rhombic lip. The Journal of neuroscience : the official journal of the Society for Neuroscience 26:3066-3076.
Finnin MS, Donigian JR, Cohen A, Richon VM, Rifkind RA, Marks PA, Breslow R, Pavletich NP (1999) Structures of a histone deacetylase homologue bound to the TSA and SAHA inhibitors. Nature 401:188-193.
Fischer A, Sananbenesi F, Mungenast A, Tsai LH (2010) Targeting the correct HDAC(s) to treat cognitive disorders. Trends Pharmacol Sci 31:605-617.
Fischle W, Dequiedt F, Hendzel MJ, Guenther MG, Lazar MA, Voelter W, Verdin E (2002) Enzymatic activity associated with class II HDACs is dependent on a multiprotein complex containing HDAC3 and SMRT/N-CoR. Mol Cell 9:45-57.
Flavell SW, Greenberg ME (2008) Signaling mechanisms linking neuronal activity to gene expression and plasticity of the nervous system. Annu Rev Neurosci 31:563-590.
Fraga MF, Ballestar E, Paz MF, Ropero S, Setien F, Ballestar ML, Heine-Suner D, Cigudosa JC, Urioste M, Benitez J, Boix-Chornet M, Sanchez-Aguilera A, Ling C, Carlsson E, Poulsen P, Vaag A, Stephan Z, Spector TD, Wu YZ, Plass C, Esteller M (2005) Epigenetic differences arise during the lifetime of monozygotic twins. Proc Natl Acad Sci U S A 102:10604-10609.
Fujiki R, Sato A, Fujitani M, Yamashita T (2013) A proapoptotic effect of valproic acid on progenitors of embryonic stem cell-derived glutamatergic neurons. Cell Death Dis 4:e677.
Fusco FR, Chen Q, Lamoreaux WJ, Figueredo-Cardenas G, Jiao Y, Coffman JA, Surmeier DJ, Honig MG, Carlock LR, Reiner A (1999) Cellular localization of huntingtin in striatal and cortical neurons in rats: lack of correlation with neuronal vulnerability in Huntington's disease. J Neurosci 19:1189-1202.
Galkina EI, Shin A, Coser KR, Shioda T, Kohane IS, Seong IS, Wheeler VC, Gusella JF, Macdonald ME, Lee JM (2014) HD CAGnome: a search tool for huntingtin CAG repeat length-correlated genes. PLoS One 9:e95556.
Garcia-Frigola C, Carreres MI, Vegar C, Herrera E (2007) Gene delivery into mouse retinal ganglion cells by in utero electroporation. BMC Dev Biol 7:103.
Gardian G, Browne SE, Choi DK, Klivenyi P, Gregorio J, Kubilus JK, Ryu H, Langley B, Ratan RR, Ferrante RJ, Beal MF (2005) Neuroprotective effects of phenylbutyrate in the N171-82Q transgenic mouse model of Huntington's disease. J Biol Chem 280:556-563.
Gascon S, Paez-Gomez JA, Diaz-Guerra M, Scheiffele P, Scholl FG (2008) Dual-promoter lentiviral vectors for constitutive and regulated gene expression in neurons. J Neurosci Methods 168:104-112.
Gasmi M, Brandon EP, Herzog CD, Wilson A, Bishop KM, Hofer EK, Cunningham JJ, Printz MA, Kordower JH, Bartus RT (2007) AAV2-mediated delivery of human neurturin to the rat nigrostriatal system: long-term efficacy and tolerability of CERE-120 for Parkinson's disease. Neurobiol Dis 27:67-76.
Gatchel JR, Watase K, Thaller C, Carson JP, Jafar-Nejad P, Shaw C, Zu T, Orr HT, Zoghbi HY (2008) The insulin-like growth factor pathway is altered in spinocerebellar ataxia type 1 and type 7. Proc Natl Acad Sci U S A 105:1291-1296.
Gaub P, Tedeschi A, Puttagunta R, Nguyen T, Schmandke A, Di Giovanni S (2010) HDAC inhibition promotes neuronal outgrowth and counteracts growth cone collapse through CBP/p300 and P/CAF-dependent p53 acetylation. Cell Death Differ 17:1392-1408.

Gerber M, Shilatifard A (2003) Transcriptional elongation by RNA polymerase II and histone methylation. J Biol Chem 278:26303-26306.
Ghosh A, Greenberg ME (1995) Calcium signaling in neurons: molecular mechanisms and cellular consequences. Science 268:239-247.
Gifford CA, Ziller MJ, Gu H, Trapnell C, Donaghey J, Tsankov A, Shalek AK, Kelley DR, Shishkin AA, Issner R, Zhang X, Coyne M, Fostel JL, Holmes L, Meldrim J, Guttman M, Epstein C, Park H, Kohlbacher O, Rinn J, Gnirke A, Lander ES, Bernstein BE, Meissner A (2013) Transcriptional and epigenetic dynamics during specification of human embryonic stem cells. Cell 153:1149-1163.
Giralt A, Puigdellivol M, Carreton O, Paoletti P, Valero J, Parra-Damas A, Saura CA, Alberch J, Gines S (2012) Long-term memory deficits in Huntington's disease are associated with reduced CBP histone acetylase activity. Hum Mol Genet 21:1203-1216.
Godin JD, Poizat G, Hickey MA, Maschat F, Humbert S (2010) Mutant huntingtin-impaired degradation of beta-catenin causes neurotoxicity in Huntington's disease. EMBO J 29:2433-2445.
Gomes AQ, Nolasco S, Soares H (2013) Non-coding RNAs: multi-tasking molecules in the cell. Int J Mol Sci 14:16010-16039.
Goodrich JA, Tjian R (1994) TBP-TAF complexes: selectivity factors for eukaryotic transcription. Curr Opin Cell Biol 6:403-409.
Govindarajan N, Agis-Balboa RC, Walter J, Sananbenesi F, Fischer A (2011) Sodium butyrate improves memory function in an Alzheimer's disease mouse model when administered at an advanced stage of disease progression. J Alzheimers Dis 26:187-197.
Graff J, Tsai LH (2013) Histone acetylation: molecular mnemonics on the chromatin. Nat Rev Neurosci 14:97-111.
Graham RK, Deng Y, Slow EJ, Haigh B, Bissada N, Lu G, Pearson J, Shehadeh J, Bertram L, Murphy Z, Warby SC, Doty CN, Roy S, Wellington CL, Leavitt BR, Raymond LA, Nicholson DW, Hayden MR (2006) Cleavage at the caspase-6 site is required for neuronal dysfunction and degeneration due to mutant huntingtin. Cell 125:1179-1191.
Gray M, Shirasaki DI, Cepeda C, Andre VM, Wilburn B, Lu XH, Tao J, Yamazaki I, Li SH, Sun YE, Li XJ, Levine MS, Yang XW (2008) Full-length human mutant huntingtin with a stable polyglutamine repeat can elicit progressive and selective neuropathogenesis in BACHD mice. J Neurosci 28:6182-6195.
Greenberg ME, Ziff EB, Greene LA (1986) Stimulation of neuronal acetylcholine receptors induces rapid gene transcription. Science 234:80-83.
Group HS (1996) Unified Huntington's Disease Rating Scale: reliability and consistency. . Mov Disord 11:136-142.
Gu W, Roeder RG (1997) Activation of p53 sequence-specific DNA binding by acetylation of the p53 C-terminal domain. Cell 90:595-606.
Guibert S, Weber M (2013) Functions of DNA methylation and hydroxymethylation in mammalian development. Curr Top Dev Biol 104:47-83.
Guzman-Karlsson MC, Meadows JP, Gavin CF, Hablitz JJ, Sweatt JD (2014) Transcriptional and epigenetic regulation of Hebbian and non-Hebbian plasticity. Neuropharmacology 80:3-17.
Haettig J, Stefanko DP, Multani ML, Figueroa DX, McQuown SC, Wood MA (2011) HDAC inhibition modulates hippocampus-dependent long-term memory for object location in a CBP-dependent manner. Learn Mem 18:71-79.
Harjes P, Wanker EE (2003) The hunt for huntingtin function: interaction partners tell many different stories. Trends Biochem Sci 28:425-433.
Harper P, Jones L (2002a) Huntington’s disease: a historical background. UK: Oxford University Press.
Harper P, Jones L (2002b) Huntington’s disease: genetic and molecular studies. UK
: Oxford University Press
Heathfield KW (1973) Huntington's chorea: a centenary review. Postgrad Med J 49:32-45.
Heintzman ND, Hon GC, Hawkins RD, Kheradpour P, Stark A, Harp LF, Ye Z, Lee LK, Stuart RK, Ching CW, Ching KA, Antosiewicz-Bourget JE, Liu H, Zhang X, Green RD, Lobanenkov VV, Stewart R, Thomson JA, Crawford GE, Kellis M, Ren B (2009) Histone modifications at human enhancers reflect global cell-type-specific gene expression. Nature 459:108-112.
Heintzman ND, Stuart RK, Hon G, Fu Y, Ching CW, Hawkins RD, Barrera LO, Van Calcar S, Qu C, Ching KA, Wang W, Weng Z, Green RD, Crawford GE, Ren B (2007) Distinct and predictive chromatin signatures of transcriptional promoters and enhancers in the human genome. Nat Genet 39:311-318.
Hennekam RC (2006) Rubinstein-Taybi syndrome. Eur J Hum Genet 14:981-985.

Herdegen T, Leah JD (1998) Inducible and constitutive transcription factors in the mammalian nervous system: control of gene expression by Jun, Fos and Krox, and CREB/ATF proteins. Brain Res Brain Res Rev 28:370-490.
Hilditch-Maguire P, Trettel F, Passani LA, Auerbach A, Persichetti F, MacDonald ME (2000) Huntingtin: an iron-regulated protein essential for normal nuclear and perinuclear organelles. Hum Mol Genet 9:2789-2797.
Hilton IB, D'Ippolito AM, Vockley CM, Thakore PI, Crawford GE, Reddy TE, Gersbach CA (2015) Epigenome editing by a CRISPR-Cas9-based acetyltransferase activates genes from promoters and enhancers. Nat Biotechnol 33:510-517.
Hodges A, Hughes G, Brooks S, Elliston L, Holmans P, Dunnett SB, Jones L (2008) Brain gene expression correlates with changes in behavior in the R6/1 mouse model of Huntington's disease. Genes Brain Behav 7:288-299.
Hodgson JG, Agopyan N, Gutekunst CA, Leavitt BR, LePiane F, Singaraja R, Smith DJ, Bissada N, McCutcheon K, Nasir J, Jamot L, Li XJ, Stevens ME, Rosemond E, Roder JC, Phillips AG, Rubin EM, Hersch SM, Hayden MR (1999) A YAC mouse model for Huntington's disease with full-length mutant huntingtin, cytoplasmic toxicity, and selective striatal neurodegeneration. Neuron 23:181-192.
Hoffner G, Kahlem P, Djian P (2002) Perinuclear localization of huntingtin as a consequence of its binding to microtubules through an interaction with beta-tubulin: relevance to Huntington's disease. J Cell Sci 115:941-948.
Holbert S, Denghien I, Kiechle T, Rosenblatt A, Wellington C, Hayden MR, Margolis RL, Ross CA, Dausset J, Ferrante RJ, Neri C (2001) The Gln-Ala repeat transcriptional activator CA150 interacts with huntingtin: neuropathologic and genetic evidence for a role in Huntington's disease pathogenesis. Proc Natl Acad Sci U S A 98:1811-1816.
Huang CC, Faber PW, Persichetti F, Mittal V, Vonsattel JP, MacDonald ME, Gusella JF (1998) Amyloid formation by mutant huntingtin: threshold, progressivity and recruitment of normal polyglutamine proteins. Somat Cell Mol Genet 24:217-233.
Huang da W, Sherman BT, Lempicki RA (2009) Systematic and integrative analysis of large gene lists using DAVID bioinformatics resources. Nat Protoc 4:44-57.
Igarashi S, Morita H, Bennett KM, Tanaka Y, Engelender S, Peters MF, Cooper JK, Wood JD, Sawa A, Ross CA (2003) Inducible PC12 cell model of Huntington's disease shows toxicity and decreased histone acetylation. Neuroreport 14:565-568.
Imhof A, Yang XJ, Ogryzko VV, Nakatani Y, Wolffe AP, Ge H (1997) Acetylation of general transcription factors by histone acetyltransferases. Curr Biol 7:689-692.
Ito A, Lai CH, Zhao X, Saito S, Hamilton MH, Appella E, Yao TP (2001) p300/CBP-mediated p53 acetylation is commonly induced by p53-activating agents and inhibited by MDM2. EMBO J 20:1331-1340.
Ivanova D, Dirks A, Montenegro-Venegas C, Schone C, Altrock WD, Marini C, Frischknecht R, Schanze D, Zenker M, Gundelfinger ED, Fejtova A (2015) Synaptic activity controls localization and function of CtBP1 via binding to Bassoon and Piccolo. EMBO J 34:1056-1077.
Jablonka E, Lamb MJ (2002) The changing concept of epigenetics. Ann N Y Acad Sci 981:82-96.
Jacobsen JC, Gregory GC, Woda JM, Thompson MN, Coser KR, Murthy V, Kohane IS, Gusella JF, Seong IS, MacDonald ME, Shioda T, Lee JM (2011) HD CAG-correlated gene expression changes support a simple dominant gain of function. Hum Mol Genet 20:2846-2860.
Janknecht R (2002) The versatile functions of the transcriptional coactivators p300 and CBP and their roles in disease. Histol Histopathol 17:657-668.
Jeong H, Then F, Melia TJ, Jr., Mazzulli JR, Cui L, Savas JN, Voisine C, Paganetti P, Tanese N, Hart AC, Yamamoto A, Krainc D (2009) Acetylation targets mutant huntingtin to autophagosomes for degradation. Cell 137:60-72.
Jia H, Pallos J, Jacques V, Lau A, Tang B, Cooper A, Syed A, Purcell J, Chen Y, Sharma S, Sangrey GR, Darnell SB, Plasterer H, Sadri-Vakili G, Gottesfeld JM, Thompson LM, Rusche JR, Marsh JL, Thomas EA (2012) Histone deacetylase (HDAC) inhibitors targeting HDAC3 and HDAC1 ameliorate polyglutamine-elicited phenotypes in model systems of Huntington's disease. Neurobiol Dis 46:351-361.
Jiang H, Poirier MA, Liang Y, Pei Z, Weiskittel CE, Smith WW, DeFranco DB, Ross CA (2006) Depletion of CBP is directly linked with cellular toxicity caused by mutant huntingtin. Neurobiol Dis 23:543-551.

Jin Q, Yu LR, Wang L, Zhang Z, Kasper LH, Lee JE, Wang C, Brindle PK, Dent SY, Ge K (2011) Distinct roles of GCN5/PCAF-mediated H3K9ac and CBP/p300-mediated H3K18/27ac in nuclear receptor transactivation. EMBO J 30:249-262.
Johnstone RW (2002) Histone-deacetylase inhibitors: novel drugs for the treatment of cancer. Nat Rev Drug Discov 1:287-299.
Kadonaga JT (2004) Regulation of RNA polymerase II transcription by sequence-specific DNA binding factors. Cell 116:247-257.
Kadonaga JT (2012) Perspectives on the RNA polymerase II core promoter. Wiley Interdiscip Rev Dev Biol 1:40-51.
Kahoud RJ, Elsen GE, Hevner RF, Hodge RD (2014) Conditional ablation of Tbr2 results in abnormal development of the olfactory bulbs and subventricular zone-rostral migratory stream. Developmental dynamics : an official publication of the American Association of Anatomists 243:440-450.
Kandel ER (2001) The molecular biology of memory storage: a dialogue between genes and synapses. Science 294:1030-1038.
Kasper LH, Brindle PK (2006) Mammalian gene expression program resiliency: the roles of multiple coactivator mechanisms in hypoxia-responsive transcription. Cell Cycle 5:142-146.
Kasper LH, Fukuyama T, Biesen MA, Boussouar F, Tong C, de Pauw A, Murray PJ, van Deursen JM, Brindle PK (2006) Conditional knockout mice reveal distinct functions for the global transcriptional coactivators CBP and p300 in T-cell development. Mol Cell Biol 26:789-809.
Kasper LH, Lerach S, Wang J, Wu S, Jeevan T, Brindle PK (2010) CBP/p300 double null cells reveal effect of coactivator level and diversity on CREB transactivation. EMBO J 29:3660-3672.
Kasten MM, Clapier CR, Cairns BR (2011) SnapShot: Chromatin remodeling: SWI/SNF. Cell 144:310 e311.
Kazantsev A, Preisinger E, Dranovsky A, Goldgaber D, Housman D (1999) Insoluble detergent-resistant aggregates form between pathological and nonpathological lengths of polyglutamine in mammalian cells. Proc Natl Acad Sci U S A 96:11404-11409.
Kazantsev AG, Thompson LM (2008) Therapeutic application of histone deacetylase inhibitors for central nervous system disorders. Nat Rev Drug Discov 7:854-868.
Kegel KB, Meloni AR, Yi Y, Kim YJ, Doyle E, Cuiffo BG, Sapp E, Wang Y, Qin ZH, Chen JD, Nevins JR, Aronin N, DiFiglia M (2002) Huntingtin is present in the nucleus, interacts with the transcriptional corepressor C-terminal binding protein, and represses transcription. J Biol Chem 277:7466-7476.
Kent WJ, Sugnet CW, Furey TS, Roskin KM, Pringle TH, Zahler AM, Haussler D (2002) The human genome browser at UCSC. Genome Res 12:996-1006.
Kim K, Doi A, Wen B, Ng K, Zhao R, Cahan P, Kim J, Aryee MJ, Ji H, Ehrlich LI, Yabuuchi A, Takeuchi A, Cunniff KC, Hongguang H, McKinney-Freeman S, Naveiras O, Yoon TJ, Irizarry RA, Jung N, Seita J, Hanna J, Murakami P, Jaenisch R, Weissleder R, Orkin SH, Weissman IL, Feinberg AP, Daley GQ (2010) Epigenetic memory in induced pluripotent stem cells. Nature 467:285-290.
Kim M, Lee HS, LaForet G, McIntyre C, Martin EJ, Chang P, Kim TW, Williams M, Reddy PH, Tagle D, Boyce FM, Won L, Heller A, Aronin N, DiFiglia M (1999) Mutant huntingtin expression in clonal striatal cells: dissociation of inclusion formation and neuronal survival by caspase inhibition. J Neurosci 19:964-973.
Kipps CM, Duggins AJ, Mahant N, Gomes L, Ashburner J, McCusker EA (2005) Progression of structural neuropathology in preclinical Huntington's disease: a tensor based morphometry study. J Neurol Neurosurg Psychiatry 76:650-655.
Kleine-Kohlbrecher D, Christensen J, Vandamme J, Abarrategui I, Bak M, Tommerup N, Shi X, Gozani O, Rappsilber J, Salcini AE, Helin K (2010) A functional link between the histone demethylase PHF8 and the transcription factor ZNF711 in X-linked mental retardation. Mol Cell 38:165-178.
Klevytska AM, Tebbenkamp AT, Savonenko AV, Borchelt DR (2010) Partial depletion of CREB-binding protein reduces life expectancy in a mouse model of Huntington disease. J Neuropathol Exp Neurol 69:396-404.
Kornberg A, and Baker, T.A. (1992) (1992) DNA Replication. Book Second Ed.
Kornberg RD (1977) Structure of chromatin. Annu Rev Biochem 46:931-954.
Korzus E, Rosenfeld MG, Mayford M (2004) CBP histone acetyltransferase activity is a critical component of memory consolidation. Neuron 42:961-972.
Kouzarides T (2007) Chromatin modifications and their function. Cell 128:693-705.
Kravchick DO, Jordan BA (2015) Presynapses go nuclear! EMBO J 34:984-986.

Kuhn A, Goldstein DR, Hodges A, Strand AD, Sengstag T, Kooperberg C, Becanovic K, Pouladi MA, Sathasivam K, Cha JH, Hannan AJ, Hayden MR, Leavitt BR, Dunnett SB, Ferrante RJ, Albin R, Shelbourne P, Delorenzi M, Augood SJ, Faull RL, Olson JM, Bates GP, Jones L, Luthi-Carter R (2007) Mutant huntingtin's effects on striatal gene expression in mice recapitulate changes observed in human Huntington's disease brain and do not differ with mutant huntingtin length or wild-type huntingtin dosage. Hum Mol Genet 16:1845-1861.

Kung AL, Rebel VI, Bronson RT, Ch'ng LE, Sieff CA, Livingston DM, Yao TP (2000) Gene dose-dependent control of hematopoiesis and hematologic tumor suppression by CBP. Genes Dev 14:272-277.

Lagrange T, Kapanidis AN, Tang H, Reinberg D, Ebright RH (1998) New core promoter element in RNA polymerase II-dependent transcription: sequence-specific DNA binding by transcription factor IIB. Genes Dev 12:34-44.

Lahm A, Paolini C, Pallaoro M, Nardi MC, Jones P, Neddermann P, Sambucini S, Bottomley MJ, Lo Surdo P, Carfi A, Koch U, De Francesco R, Steinkuhler C, Gallinari P (2007) Unraveling the hidden catalytic activity of vertebrate class IIa histone deacetylases. Proc Natl Acad Sci U S A 104:17335-17340.

Landles C, Bates GP (2004) Huntingtin and the molecular pathogenesis of Huntington's disease. Fourth in molecular medicine review series. EMBO Rep 5:958-963.

Langbehn DR, Brinkman RR, Falush D, Paulsen JS, Hayden MR (2004) A new model for prediction of the age of onset and penetrance for Huntington's disease based on CAG length. Clin Genet 65:267-277.

Lanska DJ (2000) George Huntington (1850-1916) and hereditary chorea. J Hist Neurosci 9:76-89.

Lanska DJ (2010) Chapter 33: the history of movement disorders. Handb Clin Neurol 95:501-546.

Lee CY, Cantle JP, Yang XW (2013a) Genetic manipulations of mutant huntingtin in mice: new insights into Huntington's disease pathogenesis. FEBS J 280:4382-4394.

Lee JM, Galkina EI, Levantovsky RM, Fossale E, Anne Anderson M, Gillis T, Srinidhi Mysore J, Coser KR, Shioda T, Zhang B, Furia MD, Derry J, Kohane IS, Seong IS, Wheeler VC, Gusella JF, MacDonald ME (2013b) Dominant effects of the Huntington's disease HTT CAG repeat length are captured in gene-expression data sets by a continuous analysis mathematical modeling strategy. Hum Mol Genet 22:3227-3238.

Lee JS, Smith E, Shilatifard A (2010) The language of histone crosstalk. Cell 142:682-685.

Leegwater-Kim J, Cha JH (2004) The paradigm of Huntington's disease: therapeutic opportunities in neurodegeneration. NeuroRx 1:128-138.

Lenstra TL, Benschop JJ, Kim T, Schulze JM, Brabers NA, Margaritis T, van de Pasch LA, van Heesch SA, Brok MO, Groot Koerkamp MJ, Ko CW, van Leenen D, Sameith K, van Hooff SR, Lijnzaad P, Kemmeren P, Hentrich T, Kobor MS, Buratowski S, Holstege FC (2011) The specificity and topology of chromatin interaction pathways in yeast. Mol Cell 42:536-549.

Li H, Durbin R (2010) Fast and accurate long-read alignment with Burrows-Wheeler transform. Bioinformatics 26:589-595.

Li JY, Plomann M, Brundin P (2003) Huntington's disease: a synaptopathy? Trends Mol Med 9:414-420.

Li SH, Li XJ (2004) Huntingtin-protein interactions and the pathogenesis of Huntington's disease. Trends Genet 20:146-154.

Liang K, Keles S (2012) Detecting differential binding of transcription factors with ChIP-seq. Bioinformatics 28:121-122.

Lifton RP, Goldberg ML, Karp RW, Hogness DS (1978) The organization of the histone genes in Drosophila melanogaster: functional and evolutionary implications. Cold Spring Harb Symp Quant Biol 42 Pt 2:1047-1051.

Lim S, Chesser AS, Grima JC, Rappold PM, Blum D, Przedborski S, Tieu K (2011) D-beta-hydroxybutyrate is protective in mouse models of Huntington's disease. PLoS One 6:e24620.

Liot G, Zala D, Pla P, Mottet G, Piel M, Saudou F (2013) Mutant Huntingtin alters retrograde transport of TrkB receptors in striatal dendrites. J Neurosci 33:6298-6309.

Liu R, Lei JX, Luo C, Lan X, Chi L, Deng P, Lei S, Ghribi O, Liu QY (2012) Increased EID1 nuclear translocation impairs synaptic plasticity and memory function associated with pathogenesis of Alzheimer's disease. Neurobiol Dis 45:902-912.

Lo Sardo V, Zuccato C, Gaudenzi G, Vitali B, Ramos C, Tartari M, Myre MA, Walker JA, Pistocchi A, Conti L, Valenza M, Drung B, Schmidt B, Gusella J, Zeitlin S, Cotelli F, Cattaneo E (2012) An evolutionary recent neuroepithelial cell adhesion function of huntingtin implicates ADAM10-Ncadherin. Nat Neurosci 15:713-721.

Loebrich S, Nedivi E (2009) The function of activity-regulated genes in the nervous system. Physiol Rev 89:1079-1103.
Lopez-Atalaya JP, Barco A (2014) Can changes in histone acetylation contribute to memory formation? Trends Genet 30:529-539.
Lopez-Atalaya JP, Ciccarelli A, Viosca J, Valor LM, Jimenez-Minchan M, Canals S, Giustetto M, Barco A (2011) CBP is required for environmental enrichment-induced neurogenesis and cognitive enhancement. EMBO J 30:4287-4298.
Lopez-Atalaya JP, Gervasini C, Mottadelli F, Spena S, Piccione M, Scarano G, Selicorni A, Barco A, Larizza L (2012) Histone acetylation deficits in lymphoblastoid cell lines from patients with Rubinstein-Taybi syndrome. J Med Genet 49:66-74.
Lopez-Atalaya JP, Ito S, Valor LM, Benito E, Barco A (2013) Genomic targets, and histone acetylation and gene expression profiling of neural HDAC inhibition. Nucleic acids research 41:8072-8084.
Lopez-Atalaya JP, Valor LM, Barco A (2014) Epigenetic factors in intellectual disability: the Rubinstein-Taybi syndrome as a paradigm of neurodevelopmental disorder with epigenetic origin. Prog Mol Biol Transl Sci 128:139-176.
Ma C, D'Mello SR (2011) Neuroprotection by histone deacetylase-7 (HDAC7) occurs by inhibition of c-jun expression through a deacetylase-independent mechanism. J Biol Chem 286:4819-4828.
Mahadevan LC, Willis AC, Barratt MJ (1991) Rapid histone H3 phosphorylation in response to growth factors, phorbol esters, okadaic acid, and protein synthesis inhibitors. Cell 65:775-783.
Mangiarini L, Sathasivam K, Seller M, Cozens B, Harper A, Hetherington C, Lawton M, Trottier Y, Lehrach H, Davies SW, Bates GP (1996) Exon 1 of the HD gene with an expanded CAG repeat is sufficient to cause a progressive neurological phenotype in transgenic mice. Cell 87:493-506.
Mayr B, Montminy M (2001) Transcriptional regulation by the phosphorylation-dependent factor CREB. Nat Rev Mol Cell Biol 2:599-609.
McBride JL, Kordower JH (2002) Neuroprotection for Parkinson's disease using viral vector-mediated delivery of GDNF. Prog Brain Res 138:421-432.
McCampbell A, Taye AA, Whitty L, Penney E, Steffan JS, Fischbeck KH (2001) Histone deacetylase inhibitors reduce polyglutamine toxicity. Proc Natl Acad Sci U S A 98:15179-15184.
McFarland KN, Das S, Sun TT, Leyfer D, Xia E, Sangrey GR, Kuhn A, Luthi-Carter R, Clark TW, Sadri-Vakili G, Cha JH (2012) Genome-wide histone acetylation is altered in a transgenic mouse model of Huntington's disease. PLoS One 7:e41423.
McGeer EG, McGeer PL (1976) Duplication of biochemical changes of Huntington's chorea by intrastriatal injections of glutamic and kainic acids. Nature 263:517-519.
McGhee JD, Felsenfeld G (1980) Nucleosome structure. Annu Rev Biochem 49:1115-1156.
Metzler M, Legendre-Guillemin V, Gan L, Chopra V, Kwok A, McPherson PS, Hayden MR (2001) HIP1 functions in clathrin-mediated endocytosis through binding to clathrin and adaptor protein 2. J Biol Chem 276:39271-39276.
Michail J, Matsoukas J, Theodorou S (1957) [Arched, clubbed thumb in strong abduction-extension & other concomitant symptoms]. Rev Chir Orthop Reparatrice Appar Mot 43:142-146.
Miller CA, Sweatt JD (2007) Covalent modification of DNA regulates memory formation. Neuron 53:857-869.
Miller J, Arrasate M, Shaby BA, Mitra S, Masliah E, Finkbeiner S (2010) Quantitative relationships between huntingtin levels, polyglutamine length, inclusion body formation, and neuronal death provide novel insight into huntington's disease molecular pathogenesis. J Neurosci 30:10541-10550.
Mione M, Baldessari D, Deflorian G, Nappo G, Santoriello C (2008) How neuronal migration contributes to the morphogenesis of the CNS: insights from the zebrafish. Developmental neuroscience 30:65-81.
Moumne L, Betuing S, Caboche J (2013) Multiple Aspects of Gene Dysregulation in Huntington's Disease. Front Neurol 4:127.
Moumne L, Campbell K, Howland D, Ouyang Y, Bates GP (2012) Genetic knock-down of HDAC3 does not modify disease-related phenotypes in a mouse model of Huntington's disease. PLoS One 7:e31080.
Mullighan CG, Zhang J, Kasper LH, Lerach S, Payne-Turner D, Phillips LA, Heatley SL, Holmfeldt L, Collins-Underwood JR, Ma J, Buetow KH, Pui CH, Baker SD, Brindle PK, Downing JR (2011) CREBBP mutations in relapsed acute lymphoblastic leukaemia. Nature 471:235-239.
Myers RH (2004) Huntington's disease genetics. NeuroRx 1:255-262.

Nadiminty N, Lou W, Lee SO, Lin X, Trump DL, Gao AC (2006) Stat3 activation of NF-{kappa}B p100 processing involves CBP/p300-mediated acetylation. Proc Natl Acad Sci U S A 103:7264-7269.

Nagasaka Y, Dillner K, Ebise H, Teramoto R, Nakagawa H, Lilius L, Axelman K, Forsell C, Ito A, Winblad B, Kimura T, Graff C (2005) A unique gene expression signature discriminates familial Alzheimer's disease mutation carriers from their wild-type siblings. Proc Natl Acad Sci U S A 102:14854-14859.

Nance MA, Myers RH (2001) Juvenile onset Huntington's disease--clinical and research perspectives. Ment Retard Dev Disabil Res Rev 7:153-157.

Narayan PJ, Lill C, Faull R, Curtis MA, Dragunow M (2015) Increased acetyl and total histone levels in post-mortem Alzheimer's disease brain. Neurobiology of disease 74:281-294.

Nasir J, Floresco SB, O'Kusky JR, Diewert VM, Richman JM, Zeisler J, Borowski A, Marth JD, Phillips AG, Hayden MR (1995) Targeted disruption of the Huntington's disease gene results in embryonic lethality and behavioral and morphological changes in heterozygotes. Cell 81:811-823.

Nicolas G, Devys D, Goldenberg A, Maltete D, Herve C, Hannequin D, Guyant-Marechal L (2011) Juvenile Huntington disease in an 18-month-old boy revealed by global developmental delay and reduced cerebellar volume. Am J Med Genet A 155A:815-818.

Norman C, Runswick M, Pollock R, Treisman R (1988) Isolation and properties of cDNA clones encoding SRF, a transcription factor that binds to the c-fos serum response element. Cell 55:989-1003.

Novak MJ, Warren JD, Henley SM, Draganski B, Frackowiak RS, Tabrizi SJ (2012) Altered brain mechanisms of emotion processing in pre-manifest Huntington's disease. Brain 135:1165-1179.

Nowak SJ, Corces VG (2000) Phosphorylation of histone H3 correlates with transcriptionally active loci. Genes Dev 14:3003-3013.

Nucifora FC, Jr., Sasaki M, Peters MF, Huang H, Cooper JK, Yamada M, Takahashi H, Tsuji S, Troncoso J, Dawson VL, Dawson TM, Ross CA (2001) Interference by huntingtin and atrophin-1 with cbp-mediated transcription leading to cellular toxicity. Science 291:2423-2428.

Oike Y, Hata A, Mamiya T, Kaname T, Noda Y, Suzuki M, Yasue H, Nabeshima T, Araki K, Yamamura K (1999) Truncated CBP protein leads to classical Rubinstein-Taybi syndrome phenotypes in mice: implications for a dominant-negative mechanism. Hum Mol Genet 8:387-396.

Orphanides G, Reinberg D (2002) A unified theory of gene expression. Cell 108:439-451.

Orr HT, Zoghbi HY (2007) Trinucleotide repeat disorders. Annu Rev Neurosci 30:575-621.

Padfield CJ, Partington MW, Simpson NE (1968) The Rubinstein-Taybi syndrome. Arch Dis Child 43:94-101.

Paradiso S, Turner BM, Paulsen JS, Jorge R, Ponto LL, Robinson RG (2008) Neural bases of dysphoria in early Huntington's disease. Psychiatry Res 162:73-87.

Pardo R, Molina-Calavita M, Poizat G, Keryer G, Humbert S, Saudou F (2010) pARIS-htt: an optimised expression platform to study huntingtin reveals functional domains required for vesicular trafficking. Mol Brain 3:17.

Parkel S, Lopez-Atalaya JP, Barco A (2013) Histone H3 lysine methylation in cognition and intellectual disability disorders. Learn Mem 20:570-579.

Parker D, Ferreri K, Nakajima T, LaMorte VJ, Evans R, Koerber SC, Hoeger C, Montminy MR (1996) Phosphorylation of CREB at Ser-133 induces complex formation with CREB-binding protein via a direct mechanism. Mol Cell Biol 16:694-703.

Partanen A, Motoyama J, Hui CC (1999) Developmentally regulated expression of the transcriptional cofactors/histone acetyltransferases CBP and p300 during mouse embryogenesis. Int J Dev Biol 43:487-494.

Pasqualucci L, Dominguez-Sola D, Chiarenza A, Fabbri G, Grunn A, Trifonov V, Kasper LH, Lerach S, Tang H, Ma J, Rossi D, Chadburn A, Murty VV, Mullighan CG, Gaidano G, Rabadan R, Brindle PK, Dalla-Favera R (2011) Inactivating mutations of acetyltransferase genes in B-cell lymphoma. Nature 471:189-195.

Peixoto L, Abel T (2013) The role of histone acetylation in memory formation and cognitive impairments. Neuropsychopharmacology 38:62-76.

Petrij F, Giles RH, Dauwerse HG, Saris JJ, Hennekam RC, Masuno M, Tommerup N, van Ommen GJ, Goodman RH, Peters DJ, et al. (1995) Rubinstein-Taybi syndrome caused by mutations in the transcriptional co-activator CBP. Nature 376:348-351.

Piekarski M, Jelinska A (2013) Anthracyclines still prove effective in anticancer therapy. Mini Rev Med Chem 13:627-634.
Pillai JA, Hansen LA, Masliah E, Goldstein JL, Edland SD, Corey-Bloom J (2012) Clinical severity of Huntington's disease does not always correlate with neuropathologic stage. Mov Disord 27:1099-1103.
Poirier R, Cheval H, Mailhes C, Charnay P, Davis S, Laroche S (2007) Paradoxical role of an Egr transcription factor family member, Egr2/Krox20, in learning and memory. Front Behav Neurosci 1:6.
Polesskaya A, Harel-Bellan A (2001) Acetylation of MyoD by p300 requires more than its histone acetyltransferase domain. J Biol Chem 276:44502-44503.
Porrua O, Libri D (2015) Transcription termination and the control of the transcriptome: why, where and how to stop. Nat Rev Mol Cell Biol 16:190-202.
Qiao D, Xu J, Le C, Huang E, Liu C, Qiu P, Lin Z, Xie WB, Wang H (2014) Insulin-like growth factor binding protein 5 (IGFBP5) mediates methamphetamine-induced dopaminergic neuron apoptosis. Toxicology letters 230:444-453.
Qin ZH, Wang Y, Sapp E, Cuiffo B, Wanker E, Hayden MR, Kegel KB, Aronin N, DiFiglia M (2004) Huntingtin bodies sequester vesicle-associated proteins by a polyproline-dependent interaction. J Neurosci 24:269-281.
Quarrell O, O'Donovan KL, Bandmann O, Strong M (2012) The Prevalence of Juvenile Huntington's Disease: A Review of the Literature and Meta-Analysis. PLoS Curr 4:e4f8606b8742ef8603.
Ramaswamy S, McBride JL, Herzog CD, Brandon E, Gasmi M, Bartus RT, Kordower JH (2007) Neurturin gene therapy improves motor function and prevents death of striatal neurons in a 3-nitropropionic acid rat model of Huntington's disease. Neurobiol Dis 26:375-384.
Rando OJ (2012) Combinatorial complexity in chromatin structure and function: revisiting the histone code. Curr Opin Genet Dev 22:148-155.
Ransome MI, Hannan AJ (2013) Impaired basal and running-induced hippocampal neurogenesis coincides with reduced Akt signaling in adult R6/1 HD mice. Mol Cell Neurosci 54:93-107.
Ransome MI, Renoir T, Hannan AJ (2012) Hippocampal neurogenesis, cognitive deficits and affective disorder in Huntington's disease. Neural Plast 2012:874387.
Reiner A, Albin RL, Anderson KD, D'Amato CJ, Penney JB, Young AB (1988) Differential loss of striatal projection neurons in Huntington disease. Proc Natl Acad Sci U S A 85:5733-5737.
Reiner A, Dragatsis I, Zeitlin S, Goldowitz D (2003) Wild-type huntingtin plays a role in brain development and neuronal survival. Mol Neurobiol 28:259-276.
Rigamonti D, Bauer JH, De-Fraja C, Conti L, Sipione S, Sciorati C, Clementi E, Hackam A, Hayden MR, Li Y, Cooper JK, Ross CA, Govoni S, Vincenz C, Cattaneo E (2000) Wild-type huntingtin protects from apoptosis upstream of caspase-3. J Neurosci 20:3705-3713.
Roelfsema JH, White SJ, Ariyurek Y, Bartholdi D, Niedrist D, Papadia F, Bacino CA, den Dunnen JT, van Ommen GJ, Breuning MH, Hennekam RC, Peters DJ (2005) Genetic heterogeneity in Rubinstein-Taybi syndrome: mutations in both the CBP and EP300 genes cause disease. Am J Hum Genet 76:572-580.
Roh TY, Cuddapah S, Zhao K (2005) Active chromatin domains are defined by acetylation islands revealed by genome-wide mapping. Genes Dev 19:542-552.
Rosas HD, Hevelone ND, Zaleta AK, Greve DN, Salat DH, Fischl B (2005) Regional cortical thinning in preclinical Huntington disease and its relationship to cognition. Neurology 65:745-747.
Rouaux C, Jokic N, Mbebi C, Boutillier S, Loeffler JP, Boutillier AL (2003) Critical loss of CBP/p300 histone acetylase activity by caspase-6 during neurodegeneration. EMBO J 22:6537-6549.
Rountree MR, Bachman KE, Herman JG, Baylin SB (2001) DNA methylation, chromatin inheritance, and cancer. Oncogene 20:3156-3165.
Rubinstein JH, Taybi H (1963) Broad thumbs and toes and facial abnormalities. A possible mental retardation syndrome. Am J Dis Child 105:588-608.
Rudenko A, Tsai LH (2014) Epigenetic modifications in the nervous system and their impact upon cognitive impairments. Neuropharmacology 80:70-82.
Sadri-Vakili G, Bouzou B, Benn CL, Kim MO, Chawla P, Overland RP, Glajch KE, Xia E, Qiu Z, Hersch SM, Clark TW, Yohrling GJ, Cha JH (2007) Histones associated with downregulated genes are hypo-acetylated in Huntington's disease models. Hum Mol Genet 16:1293-1306.
Saha RN, Pahan K (2006) HATs and HDACs in neurodegeneration: a tale of disconcerted acetylation homeostasis. Cell Death Differ 13:539-550.
Salminen A, Tapiola T, Korhonen P, Suuronen T (1998) Neuronal apoptosis induced by histone deacetylase inhibitors. Brain Res Mol Brain Res 61:203-206.

Sapp E, Schwarz C, Chase K, Bhide PG, Young AB, Penney J, Vonsattel JP, Aronin N, DiFiglia M (1997) Huntingtin localization in brains of normal and Huntington's disease patients. Ann Neurol 42:604-612.
Sastry L, Johnson T, Hobson MJ, Smucker B, Cornetta K (2002) Titering lentiviral vectors: comparison of DNA, RNA and marker expression methods. Gene Ther 9:1155-1162.
Saudou F, Finkbeiner S, Devys D, Greenberg ME (1998) Huntingtin acts in the nucleus to induce apoptosis but death does not correlate with the formation of intranuclear inclusions. Cell 95:55-66.
Sax DS, O'Donnell B, Butters N, Menzer L, Montgomery K, Kayne HL (1983) Computed tomographic, neurologic, and neuropsychological correlates of Huntington's disease. Int J Neurosci 18:21-36.
Schilling G, Becher MW, Sharp AH, Jinnah HA, Duan K, Kotzuk JA, Slunt HH, Ratovitski T, Cooper JK, Jenkins NA, Copeland NG, Price DL, Ross CA, Borchelt DR (1999) Intranuclear inclusions and neuritic aggregates in transgenic mice expressing a mutant N-terminal fragment of huntingtin. Hum Mol Genet 8:397-407.
Schilling G, Savonenko AV, Klevytska A, Morton JL, Tucker SM, Poirier M, Gale A, Chan N, Gonzales V, Slunt HH, Coonfield ML, Jenkins NA, Copeland NG, Ross CA, Borchelt DR (2004) Nuclear-targeting of mutant huntingtin fragments produces Huntington's disease-like phenotypes in transgenic mice. Hum Mol Genet 13:1599-1610.
Schorry EK, Keddache M, Lanphear N, Rubinstein JH, Srodulski S, Fletcher D, Blough-Pfau RI, Grabowski GA (2008) Genotype-phenotype correlations in Rubinstein-Taybi syndrome. Am J Med Genet A 146A:2512-2519.
Sehgal M, Song C, Ehlers VL, Moyer JR, Jr. (2013) Learning to learn - intrinsic plasticity as a metaplasticity mechanism for memory formation. Neurobiol Learn Mem 105:186-199.
Seneca S, Fagnart D, Keymolen K, Lissens W, Hasaerts D, Debulpaep S, Desprechins B, Liebaers I, De Meirleir L (2004) Early onset Huntington disease: a neuronal degeneration syndrome. Eur J Pediatr 163:717-721.
Seong IS, Woda JM, Song JJ, Lloret A, Abeyrathne PD, Woo CJ, Gregory G, Lee JM, Wheeler VC, Walz T, Kingston RE, Gusella JF, Conlon RA, MacDonald ME (2010) Huntingtin facilitates polycomb repressive complex 2. Hum Mol Genet 19:573-583.
Shang H, Danek A, Landwehrmeyer B, Burgunder JM (2012) Huntington's disease: new aspects on phenotype and genotype. Parkinsonism Relat Disord 18 Suppl 1:S107-109.
Sheng M, Greenberg ME (1990) The regulation and function of c-fos and other immediate early genes in the nervous system. Neuron 4:477-485.
Sleiman SF, Olson DE, Bourassa MW, Karuppagounder SS, Zhang YL, Gale J, Wagner FF, Basso M, Coppola G, Pinto JT, Holson EB, Ratan RR (2014) Hydroxamic acid-based histone deacetylase (HDAC) inhibitors can mediate neuroprotection independent of HDAC inhibition. J Neurosci 34:14328-14337.
Slow EJ, van Raamsdonk J, Rogers D, Coleman SH, Graham RK, Deng Y, Oh R, Bissada N, Hossain SM, Yang YZ, Li XJ, Simpson EM, Gutekunst CA, Leavitt BR, Hayden MR (2003) Selective striatal neuronal loss in a YAC128 mouse model of Huntington disease. Hum Mol Genet 12:1555-1567.
Smale ST, Baltimore D (1989) The "initiator" as a transcription control element. Cell 57:103-113.
Smith DL, Pozueta J, Gong B, Arancio O, Shelanski M (2009a) Reversal of long-term dendritic spine alterations in Alzheimer disease models. Proc Natl Acad Sci U S A 106:16877-16882.
Smith R, Bacos K, Fedele V, Soulet D, Walz HA, Obermuller S, Lindqvist A, Bjorkqvist M, Klein P, Onnerfjord P, Brundin P, Mulder H, Li JY (2009b) Mutant huntingtin interacts with {beta}-tubulin and disrupts vesicular transport and insulin secretion. Hum Mol Genet 18:3942-3954.
Soria G, Polo SE, Almouzni G (2012) Prime, repair, restore: the active role of chromatin in the DNA damage response. Mol Cell 46:722-734.
Stack EC, Del Signore SJ, Luthi-Carter R, Soh BY, Goldstein DR, Matson S, Goodrich S, Markey AL, Cormier K, Hagerty SW, Smith K, Ryu H, Ferrante RJ (2007) Modulation of nucleosome dynamics in Huntington's disease. Hum Mol Genet 16:1164-1175.
Stefanko DP, Barrett RM, Ly AR, Reolon GK, Wood MA (2009) Modulation of long-term memory for object recognition via HDAC inhibition. Proc Natl Acad Sci U S A 106:9447-9452.
Steffan JS, Bodai L, Pallos J, Poelman M, McCampbell A, Apostol BL, Kazantsev A, Schmidt E, Zhu YZ, Greenwald M, Kurokawa R, Housman DE, Jackson GR, Marsh JL, Thompson LM (2001) Histone deacetylase inhibitors arrest polyglutamine-dependent neurodegeneration in Drosophila. Nature 413:739-743.

Steffan JS, Kazantsev A, Spasic-Boskovic O, Greenwald M, Zhu YZ, Gohler H, Wanker EE, Bates GP, Housman DE, Thompson LM (2000) The Huntington's disease protein interacts with p53 and CREB-binding protein and represses transcription. Proc Natl Acad Sci U S A 97:6763-6768.

Sterner DE, Wang X, Bloom MH, Simon GM, Berger SL (2002) The SANT domain of Ada2 is required for normal acetylation of histones by the yeast SAGA complex. J Biol Chem 277:8178-8186.

Sun Z, Feng D, Fang B, Mullican SE, You SH, Lim HW, Everett LJ, Nabel CS, Li Y, Selvakumaran V, Won KJ, Lazar MA (2013) Deacetylase-independent function of HDAC3 in transcription and metabolism requires nuclear receptor corepressor. Mol Cell 52:769-782.

Tallaksen-Greene SJ, Crouse AB, Hunter JM, Detloff PJ, Albin RL (2005) Neuronal intranuclear inclusions and neuropil aggregates in HdhCAG(150) knockin mice. Neuroscience 131:843-852.

Tanaka Y, Naruse I, Hongo T, Xu M, Nakahata T, Maekawa T, Ishii S (2000) Extensive brain hemorrhage and embryonic lethality in a mouse null mutant of CREB-binding protein. Mech Dev 95:133-145.

Tanaka Y, Naruse I, Maekawa T, Masuya H, Shiroishi T, Ishii S (1997) Abnormal skeletal patterning in embryos lacking a single Cbp allele: a partial similarity with Rubinstein-Taybi syndrome. Proc Natl Acad Sci U S A 94:10215-10220.

Thomas EA (2014) Involvement of HDAC1 and HDAC3 in the Pathology of Polyglutamine Disorders: Therapeutic Implications for Selective HDAC1/HDAC3 Inhibitors. Pharmaceuticals (Basel) 7:634-661.

Thomas EA, Coppola G, Desplats PA, Tang B, Soragni E, Burnett R, Gao F, Fitzgerald KM, Borok JF, Herman D, Geschwind DH, Gottesfeld JM (2008) The HDAC inhibitor 4b ameliorates the disease phenotype and transcriptional abnormalities in Huntington's disease transgenic mice. Proc Natl Acad Sci U S A 105:15564-15569.

Trembath MK, Horton ZA, Tippett L, Hogg V, Collins VR, Churchyard A, Velakoulis D, Roxburgh R, Delatycki MB (2010) A retrospective study of the impact of lifestyle on age at onset of Huntington disease. Mov Disord 25:1444-1450.

Trottier Y, Lutz Y, Stevanin G, Imbert G, Devys D, Cancel G, Saudou F, Weber C, David G, Tora L, et al. (1995) Polyglutamine expansion as a pathological epitope in Huntington's disease and four dominant cerebellar ataxias. Nature 378:403-406.

Tsui D, Voronova A, Gallagher D, Kaplan DR, Miller FD, Wang J (2014) CBP regulates the differentiation of interneurons from ventral forebrain neural precursors during murine development. Dev Biol 385:230-241.

Uchida H, Sasaki K, Ma L, Ueda H (2010) Neuron-restrictive silencer factor causes epigenetic silencing of Kv4.3 gene after peripheral nerve injury. Neuroscience 166:1-4.

Urdinguio RG, Sanchez-Mut JV, Esteller M (2009) Epigenetic mechanisms in neurological diseases: genes, syndromes, and therapies. Lancet Neurol 8:1056-1072.

Valor LM (2014) Transcription, Epigenetics and Ameliorative Strategies in Huntington's Disease: a Genome-Wide Perspective. Mol Neurobiol.

Valor LM (2015) Transcription, epigenetics and ameliorative strategies in Huntington's Disease: a genome-wide perspective. Molecular neurobiology 51:406-423.

Valor LM, Guiretti D (2014) What's wrong with epigenetics in Huntington's disease? Neuropharmacology 80:103-114.

Valor LM, Guiretti D, Lopez-Atalaya JP, Barco A (2013a) Genomic landscape of transcriptional and epigenetic dysregulation in early onset polyglutamine disease. J Neurosci 33:10471-10482.

Valor LM, Pulopulos MM, Jimenez-Minchan M, Olivares R, Lutz B, Barco A (2011) Ablation of CBP in forebrain principal neurons causes modest memory and transcriptional defects and a dramatic reduction of histone acetylation but does not affect cell viability. J Neurosci 31:1652-1663.

Valor LM, Viosca J, Lopez-Atalaya JP, Barco A (2013b) Lysine acetyltransferases CBP and p300 as therapeutic targets in cognitive and neurodegenerative disorders. Curr Pharm Des.

Van Raamsdonk JM, Murphy Z, Slow EJ, Leavitt BR, Hayden MR (2005) Selective degeneration and nuclear localization of mutant huntingtin in the YAC128 mouse model of Huntington disease. Hum Mol Genet 14:3823-3835.

Van Raamsdonk JM, Warby SC, Hayden MR (2007) Selective degeneration in YAC mouse models of Huntington disease. Brain Res Bull 72:124-131.

Vashishtha M, Ng CW, Yildirim F, Gipson TA, Kratter IH, Bodai L, Song W, Lau A, Labadorf A, Vogel-Ciernia A, Troncosco J, Ross CA, Bates GP, Krainc D, Sadri-Vakili G, Finkbeiner S, Marsh JL, Housman DE, Fraenkel E, Thompson LM (2013) Targeting H3K4 trimethylation in Huntington

disease. Proceedings of the National Academy of Sciences of the United States of America 110:E3027-3036.
Vecsey CG, Hawk JD, Lattal KM, Stein JM, Fabian SA, Attner MA, Cabrera SM, McDonough CB, Brindle PK, Abel T, Wood MA (2007) Histone deacetylase inhibitors enhance memory and synaptic plasticity via CREB:CBP-dependent transcriptional activation. J Neurosci 27:6128-6140.
Velier J, Kim M, Schwarz C, Kim TW, Sapp E, Chase K, Aronin N, DiFiglia M (1998) Wild-type and mutant huntingtins function in vesicle trafficking in the secretory and endocytic pathways. Exp Neurol 152:34-40.
Vessie PR (1932) On the transmission of Huntington's chorea for 300 years-the Bures family group. Journal of Nervous and Mental Diseases 76.
Viosca J, Lopez-Atalaya JP, Olivares R, Eckner R, Barco A (2010) Syndromic features and mild cognitive impairment in mice with genetic reduction on p300 activity: Differential contribution of p300 and CBP to Rubinstein-Taybi syndrome etiology. Neurobiol Dis 37:186-194.
Viosca J, Malleret G, Bourtchouladze R, Benito E, Vronskava S, Kandel ER, Barco A (2009) Chronic enhancement of CREB activity in the hippocampus interferes with the retrieval of spatial information. Learn Mem 16:198-209.
Vonsattel JP, Myers RH, Stevens TJ, Ferrante RJ, Bird ED, Richardson EP, Jr. (1985) Neuropathological classification of Huntington's disease. J Neuropathol Exp Neurol 44:559-577.
Waddington CH (2012) The epigenotype. 1942. Int J Epidemiol 41:10-13.
Walling HW, Baldassare JJ, Westfall TC (1998) Molecular aspects of Huntington's disease. J Neurosci Res 54:301-308.
Wang J, Weaver IC, Gauthier-Fisher A, Wang H, He L, Yeomans J, Wondisford F, Kaplan DR, Miller FD (2010) CBP histone acetyltransferase activity regulates embryonic neural differentiation in the normal and Rubinstein-Taybi syndrome brain. Dev Cell 18:114-125.
Wang Y, Wang X, Liu L, Wang X (2009a) HDAC inhibitor trichostatin A-inhibited survival of dopaminergic neuronal cells. Neurosci Lett 467:212-216.
Wang Z, Zang C, Cui K, Schones DE, Barski A, Peng W, Zhao K (2009b) Genome-wide mapping of HATs and HDACs reveals distinct functions in active and inactive genes. Cell 138:1019-1031.
West AE, Greenberg ME (2011) Neuronal activity-regulated gene transcription in synapse development and cognitive function. Cold Spring Harb Perspect Biol 3.
Wexler NS (2012) Huntington's disease: advocacy driving science. Annu Rev Med 63:1-22.
White JK, Auerbach W, Duyao MP, Vonsattel JP, Gusella JF, Joyner AL, MacDonald ME (1997) Huntingtin is required for neurogenesis and is not impaired by the Huntington's disease CAG expansion. Nat Genet 17:404-410.
Wiley S, Swayne S, Rubinstein JH, Lanphear NE, Stevens CA (2003) Rubinstein-Taybi syndrome medical guidelines. Am J Med Genet A 119A:101-110.
Wood MA, Hawk JD, Abel T (2006) Combinatorial chromatin modifications and memory storage: a code for memory? Learn Mem 13:241-244.
Wyttenbach A, Swartz J, Kita H, Thykjaer T, Carmichael J, Bradley J, Brown R, Maxwell M, Schapira A, Orntoft TF, Kato K, Rubinsztein DC (2001) Polyglutamine expansions cause decreased CRE-mediated transcription and early gene expression changes prior to cell death in an inducible cell model of Huntington's disease. Hum Mol Genet 10:1829-1845.
Xie W, Schultz MD, Lister R, Hou Z, Rajagopal N, Ray P, Whitaker JW, Tian S, Hawkins RD, Leung D, Yang H, Wang T, Lee AY, Swanson SA, Zhang J, Zhu Y, Kim A, Nery JR, Urich MA, Kuan S, Yen CA, Klugman S, Yu P, Suknuntha K, Propson NE, Chen H, Edsall LE, Wagner U, Li Y, Ye Z, Kulkarni A, Xuan Z, Chung WY, Chi NC, Antosiewicz-Bourget JE, Slukvin I, Stewart R, Zhang MQ, Wang W, Thomson JA, Ecker JR, Ren B (2013) Epigenomic analysis of multilineage differentiation of human embryonic stem cells. Cell 153:1134-1148.
Xu W, Fukuyama T, Ney PA, Wang D, Rehg J, Boyd K, van Deursen JM, Brindle PK (2006) Global transcriptional coactivators CREB-binding protein and p300 are highly essential collectively but not individually in peripheral B cells. Blood 107:4407-4416.
Xu W, Kasper LH, Lerach S, Jeevan T, Brindle PK (2007) Individual CREB-target genes dictate usage of distinct cAMP-responsive coactivation mechanisms. EMBO J 26:2890-2903.
Yamanaka T, Miyazaki H, Oyama F, Kurosawa M, Washizu C, Doi H, Nukina N (2008) Mutant Huntingtin reduces HSP70 expression through the sequestration of NF-Y transcription factor. EMBO J 27:827-839.

Yang SH, Cheng PH, Banta H, Piotrowska-Nitsche K, Yang JJ, Cheng EC, Snyder B, Larkin K, Liu J, Orkin J, Fang ZH, Smith Y, Bachevalier J, Zola SM, Li SH, Li XJ, Chan AW (2008) Towards a transgenic model of Huntington's disease in a non-human primate. Nature 453:921-924.

Yao TP, Oh SP, Fuchs M, Zhou ND, Ch'ng LE, Newsome D, Bronson RT, Li E, Livingston DM, Eckner R (1998) Gene dosage-dependent embryonic development and proliferation defects in mice lacking the transcriptional integrator p300. Cell 93:361-372.

Ye T, Krebs AR, Choukrallah MA, Keime C, Plewniak F, Davidson I, Tora L (2011) seqMINER: an integrated ChIP-seq data interpretation platform. Nucleic Acids Res 39:e35.

Yeh HH, Young D, Gelovani JG, Robinson A, Davidson Y, Herholz K, Mann DM (2013) Histone deacetylase class II and acetylated core histone immunohistochemistry in human brains with Huntington's disease. Brain Res 1504:16-24.

Young AB, Greenamyre JT, Hollingsworth Z, Albin R, D'Amato C, Shoulson I, Penney JB (1988) NMDA receptor losses in putamen from patients with Huntington's disease. Science 241:981-983.

Zadori D, Geisz A, Vamos E, Vecsei L, Klivenyi P (2009) Valproate ameliorates the survival and the motor performance in a transgenic mouse model of Huntington's disease. Pharmacol Biochem Behav 94:148-153.

Zaidi SK, Young DW, Choi JY, Pratap J, Javed A, Montecino M, Stein JL, van Wijnen AJ, Lian JB, Stein GS (2005) The dynamic organization of gene-regulatory machinery in nuclear microenvironments. EMBO Rep 6:128-133.

Zajac MS, Pang TY, Wong N, Weinrich B, Leang LS, Craig JM, Saffery R, Hannan AJ (2010) Wheel running and environmental enrichment differentially modify exon-specific BDNF expression in the hippocampus of wild-type and pre-motor symptomatic male and female Huntington's disease mice. Hippocampus 20:621-636.

Zambelli F, Pesole G, Pavesi G (2009) Pscan: finding over-represented transcription factor binding site motifs in sequences from co-regulated or co-expressed genes. Nucleic Acids Res 37:W247-252.

Zeitlin S, Liu JP, Chapman DL, Papaioannou VE, Efstratiadis A (1995) Increased apoptosis and early embryonic lethality in mice nullizygous for the Huntington's disease gene homologue. Nat Genet 11:155-163.

Zhang LX, Zhao Y, Cheng G, Guo TL, Chin YE, Liu PY, Zhao TC (2010) Targeted deletion of NF-kappaB p50 diminishes the cardioprotection of histone deacetylase inhibition. Am J Physiol Heart Circ Physiol 298:H2154-2163.

Zhang SJ, Steijaert MN, Lau D, Schutz G, Delucinge-Vivier C, Descombes P, Bading H (2007) Decoding NMDA receptor signaling: identification of genomic programs specifying neuronal survival and death. Neuron 53:549-562.

Zhang Y, Friedlander RM (2011) Using non-coding small RNAs to develop therapies for Huntington's disease. Gene Ther 18:1139-1149.

Zhang Y, Liu T, Meyer CA, Eeckhoute J, Johnson DS, Bernstein BE, Nusbaum C, Myers RM, Brown M, Li W, Liu XS (2008) Model-based analysis of ChIP-Seq (MACS). Genome Biol 9:R137.

Zhong J, Deng J, Phan J, Dlouhy S, Wu H, Yao W, Ye P, D'Ercole AJ, Lee WH (2005) Insulin-like growth factor-I protects granule neurons from apoptosis and improves ataxia in weaver mice. Journal of neuroscience research 80:481-490.

Zhu J, Adli M, Zou JY, Verstappen G, Coyne M, Zhang X, Durham T, Miri M, Deshpande V, De Jager PL, Bennett DA, Houmard JA, Muoio DM, Onder TT, Camahort R, Cowan CA, Meissner A, Epstein CB, Shoresh N, Bernstein BE (2013) Genome-wide chromatin state transitions associated with developmental and environmental cues. Cell 152:642-654.

Zhu LJ, Gazin C, Lawson ND, Pages H, Lin SM, Lapointe DS, Green MR (2010) ChIPpeakAnno: a Bioconductor package to annotate ChIP-seq and ChIP-chip data. BMC Bioinformatics 11:237.

Zuccato C, Tartari M, Crotti A, Goffredo D, Valenza M, Conti L, Cataudella T, Leavitt BR, Hayden MR, Timmusk T, Rigamonti D, Cattaneo E (2003) Huntingtin interacts with REST/NRSF to modulate the transcription of NRSE-controlled neuronal genes. Nat Genet 35:76-83.

Zuccato C, Valenza M, Cattaneo E (2010) Molecular mechanisms and potential therapeutical targets in Huntington's disease. Physiol Rev 90:905-981.

Annex: Published review during the thesis period

Neuropharmacology xxx (2013) 1–12

Contents lists available at ScienceDirect

Neuropharmacology

journal homepage: www.elsevier.com/locate/neuropharm

Invited review

What's wrong with epigenetics in Huntington's disease?

Luis M. Valor*, Deisy Guiretti

Instituto de Neurociencias de Alicante (Universidad Miguel Hernández, Consejo Superior de Investigaciones Científicas), Av. Santiago Ramón y Cajal s/n, Sant Joan d'Alacant, 03550 Alicante, Spain

ARTICLE INFO

Article history:
Received 29 August 2013
Received in revised form
16 October 2013
Accepted 21 October 2013

Keywords:
Polyglutamine
Histone
Post-translational modification
KAT
HDAC
DNA methylation
Amelioration

ABSTRACT

Huntington's disease (HD) can be considered the paradigm of epigenetic dysregulation in neurodegenerative disorders. In this review, we attempted to compile the evidence that indicates, on the one hand, that several epigenetic marks (histone acetylation, methylation, ubiquitylation, phosphorylation and DNA modifications) are altered in multiple models and in postmortem patient samples, and on the other hand, that pharmacological treatments aimed to reverse such alterations have beneficial effects on HD phenotypic and biochemical traits. However, the working hypotheses regarding the biological significance of epigenetic dysregulation in this disease and the mechanisms of action of the tested ameliorative strategies need to be refined. Understanding the complexity of the epigenetics in HD will provide useful insights to examine the role of epigenetic dysregulation in other neuropathologies, such as Alzheimer's or Parkinson's diseases.

1. Introduction

The relevance of epigenetics in human disease has been extended from the field of cancer research to several diverse conditions, including a vast variety of neuropathologies, as reviewed in articles of this Special Issue and elsewhere (Day and Sweatt, 2012; Jakovcevski and Akbarian, 2012). Huntington's disease (HD) is the most common polyglutamine (polyQ) disorder and has emerged as a prototypical paradigm of epigenetic dysregulation in a neurodegenerative condition. Pioneering work in HD and other polyQ disorders at the beginning of the last decade suggested a relevant role of epigenetics in neuronal malfunction and cell loss, and proposed for the first time a corrective strategy based on epigenetics in neurodegeneration. These seminal results were soon translated to more common neurodegenerative disorders like Alzheimer's disease, leading to the general hypothesis of epigenetic imbalance as an important feature in neurodegeneration. Nonetheless, our knowledge of the primary cause of HD makes the proposal of general principles more feasible compared to other pathologies of uncertain origin.

HD is inherited in a fully penetrant, autosomal-dominant manner, with a prevalence of 5–10 cases per 100,000 worldwide (Bates et al., 2004). Onset commonly occurs around the 30s and 40s, although juvenile cases have been documented. Classical HD is characterized by personality changes, weight loss, cognitive disorders and motor impairment, including the hallmark feature of chorea (involuntary jerky movements of the face and limbs), and gait abnormalities. The disease lasts 15 years on average, until the death of the patient. Currently, HD has no effective therapy. A prominent morphological feature is a marked degeneration in medium spiny GABAergic neurons of the striatum, although several neuronal types and brain areas become more affected as its pathology progresses (Bates et al., 2004). In all cases, HD is caused by an aberrant expansion of the trinucleotide sequence CAG (>36) in a polymorphic region encoding a polyQ stretch located in the N-terminus of the huntingtin (Htt) protein (see Fig. 1 for a scheme of the primary sequence). This mutation causes two types of effects (Zuccato et al., 2010): 1) depletion of the normal Htt, which plays roles in endocytosis and vesicle trafficking, among others, and this can compromise its prosurvival and synaptic functions; and 2) the formation of a misfolded mutant Htt (mHtt) that can affect the activities of several components of multiple cellular processes. mHtt is cleaved and forms intracellular aggregates in the cell nucleus, cytoplasm, neurites and terminals, which constitutes a universal hallmark of HD despite the controversial role of these aggregates in the pathogenesis of the disease. Whether soluble or aggregated, aberrant interaction of mHtt with transcription factors and chromatin-remodeling proteins is the primary basis of the

* Corresponding author. Tel.: +34 965 919531; fax: +34 965 919492.
E-mail address: lmv@umh.es (L.M. Valor).

0028-3908/$ – see front matter © 2013 Elsevier Ltd. All rights reserved.
http://dx.doi.org/10.1016/j.neuropharm.2013.10.025

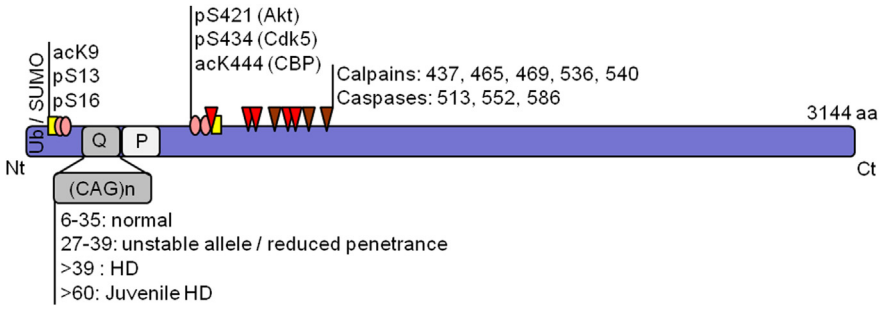

Fig. 1. Scheme of the human huntingtin. Polyglutamine (Q) and polyproline (P) tracts are indicated, in addition to the polymorphic range of CAG repeats found in human population. Cleavage sites and post-translational modifications are also shown, together with the residue number: Ub/SUMO, ubiquitylation/SUMOylation; yellow square, acetylation; pink oval, phosphorylation; red and brown triangles, calpain and caspase cleavage sites, respectively. Nt and Ct, amino- and carboxy-termini, respectively.

prominent transcriptional dysregulation observed in several HD models and in patients, which can occur in presymptomatic stages and in peripheral samples (Cha, 2007; Seredenina and Luthi-Carter, 2012).

Epigenetic mechanisms can be classified into DNA modifications (methylation and hydroxymethylation), post-translational histone modifications (acetylation, methylation, phosphorylation, ubiquitylation, SUMOylation, ADP ribosylation, etc.) and exchange of histone variants (e.g., H1, H3.3, H2A.Z, H2A.X). More recently, certain non-coding RNA species have been considered as part of epigenetics as they can influence the chromatin (Kanduri, 2011). In the following sections, we will review the epigenetic alterations that have been documented for more than 10 years in both cellular and animal HD models (see Zuccato et al., 2010 for a description of HD models), together with tantalizing findings in postmortem human samples, and the examined upstream mechanisms that may lead to such alterations (Fig. 2). Next, we will summarize the ameliorative strategies that reverse epigenetic dysregulation and their accompanying beneficial effects at the behavioral and molecular levels. Finally, we will discuss the biological significance of these outcomes, as recent evidence challenges the classical view of the roles of epigenetics in regulating gene expression and in HD amelioration.

2. Altered epigenetics in Huntington's disease

2.1. Histone acetylation

Histone acetylation is the most studied epigenetic mark in cognition and neuropathology. It is associated with a relaxed chromatin conformation that facilitates the recruitment of transcription factors and the basal machinery to regulatory sequences in the DNA, and it is regulated by two opposing enzymatic activities: histone (or lysine) acetyltransferase (KAT) and histone deacetylase (HDAC) (Valor et al., 2013b). The first evidence of histone acetylation dysregulation in HD came from the observation that CREB-binding protein (CBP), which has KAT activity, was found in intracellular inclusions in *in vitro* preparations, animal model brains and postmortem tissue from patients (Kazantsev et al., 1999; Steffan et al., 2000; Nucifora et al., 2001), suggesting that depletion of soluble CBP may affect the transcriptional regulation of neuronal genes relevant to cell survival. In agreement with this view, overexpression experiments rescued the deficits in exogenous CBP/CREB-dependent transcription and the toxicity induced by mHtt in cell culture (Nucifora et al., 2001). In a parallel report, Steffan et al., 2001 discovered global hypoacetylation of histones H3 and H4 in stably transfected PC12 cells expressing mHtt.

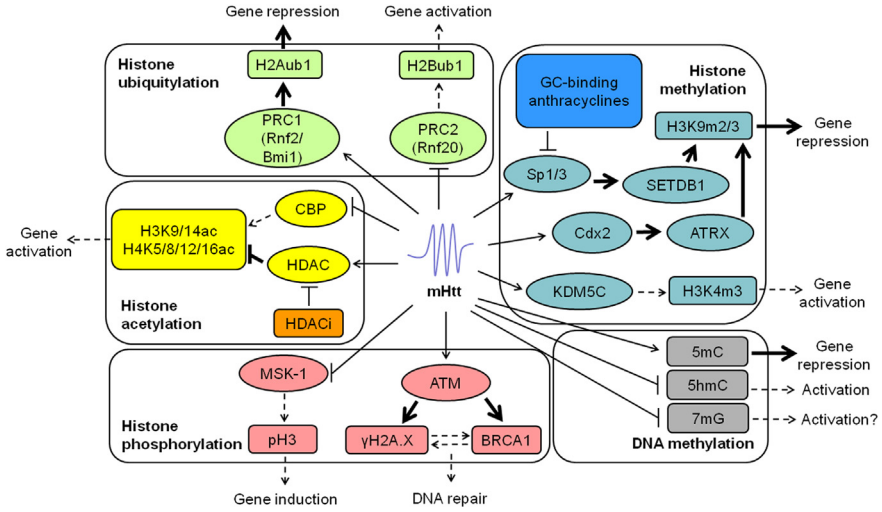

Fig. 2. Summary of the disrupted epigenetic mechanisms in HD and the tested ameliorative strategies. A gain-of-function effect is inferred because most of the HD models are based on transgenic or exogenous mHtt expression. Nonetheless, altered interactions between wt-Htt and chromatin-remodeling proteins are possible in HD (e.g., Htt-HDAC3). Actions by mHtt: regular arrow, activation; blunt end, inhibition. Resulting effects in the relationship between transcription factors and chromatin-remodeling proteins and their downstream targets and related processes are represented by dashed (reduced activity/effect) and thick arrows (enhanced activity/effect). No intermediate enzyme has been examined in altered DNA methylation. Ameliorative pharmacological compounds are also depicted. See main text for full acronyms description.

From these seminal findings, altered histone acetylation has been demonstrated in a vast array of HD models by independent research groups and, recently, in neuronal populations from patients (Yeh et al., 2013). However, while some reports validated the reduction in the levels of bulk-acetylated histones (Ferrante et al., 2003; Igarashi et al., 2003; Gardian et al., 2005; Jiang et al., 2006; Stack et al., 2007; Chiu et al., 2011; Lim et al., 2011; Giralt et al., 2012), others did not find such profound molecular changes, even using the same murine models (Hockly et al., 2003; Oliveira et al., 2006; Sadri-Vakili et al., 2007; Klevytska et al., 2010; Valor et al., 2013a). In the latter cases, histone dysregulation was confined to specific loci (Sadri-Vakili et al., 2007; Thomas et al., 2008; McFarland et al., 2012; Valor et al., 2013a), containing examples of promoter hypoacetylation correlated with gene downregulation and a small number of hyperacetylation events. In parallel, both KATs and HDACs were examined to explain these acetylation deficits.

2.1.1. CBP

This protein is the better characterized KAT enzyme in cognitive functions, and it is associated with the Rubinstein–Taybi mental retardation syndrome (OMIM #180849) and several neurodegenerative diseases (Valor et al., 2013b). CBP activity can be altered in HD, and manipulation of CBP level can therefore modulate the pathology. Thus, the cell toxicity, histone hypoacetylation and reduced CBP-dependent transcription of polyQ-expressing systems are reversed by CBP overexpression (McCampbell et al., 2000; Steffan et al., 2001; Taylor et al., 2003; Jiang et al., 2006), whereas a 50% reduction of CBP expression exacerbates neurodegeneration in a *Caenorhabditis elegans* HD model (Bates et al., 2006) and diminishes the median life expectancy in the murine N171-82Q strain (Klevytska et al., 2010).

Three main mechanisms have been described for endogenous CBP activity disruption: i) sequestration into mHtt aggregates; ii) inhibition by soluble mHtt; and iii) degradation of the CBP protein. In addition to the aforementioned study (Nucifora et al., 2001), sequestration has been observed in different transfected preparations (Jiang et al., 2003, 2006; Kim et al., 2005; Klevytska et al., 2010). Interaction of the aberrantly expanded Htt fragment with the polyQ tract at the C-terminus of CBP was the proposed mechanism for sequestration (Kazantsev et al., 1999; Nucifora et al., 2001). However, a direct and inhibitory interaction with the acetyltransferase domain of KAT enzymes was also reported independently of the presence of a polyQ tract in the primary sequence of these proteins (Steffan et al., 2001). Moreover, inclusions of mHtt were unable to significantly alter the nuclear distribution of CBP and other transcription factors, as the examined proteins did not show a significant colocalization with aggregates in *Hdh*CAG150, R6/2 and N171-82Q mice (Yu et al., 2002; Obrietan and Hoyt, 2004; Tallaksen-Greene et al., 2005). In agreement with these results, in a stably inducible PC12 cell line, soluble mHtt interacted with CBP and inhibited KAT activity before the formation of visible inclusions, and in a later stage of polyQ expression, CBP was marginally located within the aggregates (Cong et al., 2005). More recently, an expanded polyQ fragment engineered to be mostly soluble interacted better with CBP and potentiated cytotoxicity more than an aggregative version (Choi et al., 2012). As an alternative mechanism, CBP level can be decreased by the ubiquitin–proteasome system (UPS) (Jiang et al., 2003; Giampa et al., 2009; Giralt et al., 2012), indicating abnormal degradation. Overall, these results are in concordance with the observation that altered gene expression is not necessarily associated with the formation of nuclear Htt aggregates in HD mice (Dunah et al., 2002; Sadri-Vakili et al., 2006) and can occur in their absence (Kita et al., 2002; Sipione et al., 2002). Thus, soluble mHtt might interact with transcription factors and chromatin-remodeling proteins to mediate early pathological changes before the formation of nuclear inclusions. These discrepancies can be due to different and non-exclusive explanations: first, *in vitro* overexpression of mHtt and CBP may force co-aggregation; second, the cellular response to mHtt expression is not uniform, even in apparently homogeneous cell cultures (Jiang et al., 2003, 2006; Klevytska et al., 2010), and in the absence of quantification, some reports might be describing marginal events; and third, unforeseen factors dependent on the experimental conditions might favor one mechanism over another.

Although altered CBP activity has been associated with mHtt-induced cell death (Jiang et al., 2003, 2006; Choi et al., 2012), the precise role of both CBP and histone acetylation in neurodegeneration is still unclear, as reviewed in Valor et al. (2013b). Conditional knockout of CBP in postmitotic forebrain neurons reduced the bulk levels of histone acetylation without apparently compromising cell viability (Chen et al., 2010; Valor et al., 2011), suggesting additional factors may converge to induce effective cell loss. Nonetheless, CBP may play a prominent role in the cognitive impairments observed in HD patients because *Hdh*Q7/Q111-knockin mice exhibit deficits in spatial and recognition memories concomitant to diminished levels of CBP and acetylated histone H3 (Giralt et al., 2012).

2.1.2. Other KATs

Although mHtt can potentially interfere with any KAT activity (Steffan et al., 2001), the involvement of other KAT enzymes in HD remains largely unexplored, as only two additional members have been examined so far. Despite the high similarity to CBP, p300 is absent in the intracellular inclusions, is not capable of rescuing cell toxicity in overexpression experiments (Nucifora et al., 2001) and is not degraded in the presence of mHtt (Cong et al., 2005). However, p300 may have a more relevant role in peripheral tissues (Andreassen et al., 2002). In the case of p300/CBP-associated factor (P/CAF), its loss of function in a *Drosophila* HD model further reduced survival, most likely due to an indirect effect, as P/CAF level was unaltered and overexpression did not rescue the neurodegenerative phenotype (Bodai et al., 2012).

2.1.3. HDACs

Due to the beneficial effects of HDAC inhibitors (HDACis), as we will see later, and the observations on the interacting partner of HDAC1/2, the corepressor mSin3a, in HD models (Boutell et al., 1999; Steffan et al., 2000, 2001), it is reasonable to consider that HDAC activity can also be affected in HD in an opposite manner to KATs. These enzymes are classified into classes I (HDACs 1–3 and 8), II (HDACs 4–7, 9 and 10), III (NAD^+-dependent family of sirtuins) and IV (HDAC11). Whereas RNA levels were not affected, protein levels and nuclear distribution of class I and II HDACs showed some perturbations. However, they were not entirely consistent in successive studies and HD models (Table 1), suggesting more refined approaches are needed to properly explore the amounts of HDACs. The functional involvement of HDACs in HD is being systematically examined by Bates et al. So far, reduction of single HDACs (namely HDAC3, 6, 7 and Sirt2) from the R6/2 strain in crossing experiments did not ameliorate the pathological phenotype and did not rescue transcriptional deficits (Benn et al., 2009; Bobrowska et al., 2011, 2012; Moumne et al., 2012). A similar approach in invertebrate models has been more successful, although with some limitations. Knocking down the HDAC3 ortholog in worms suppressed the mHtt-induced degeneration of ASH sensory neurons; however, reducing any of the other orthologs of classes I–III enhanced neurodegeneration, contrary to expectations (Bates et al., 2006). In HD flies, decreasing specifically the expression of Rpd3 (ortholog to HDAC1/2/8) or Sir2 (Sirt1) was neuroprotective, but without rescuing their shortened life span (Pallos et al., 2008).

Table 1
Altered histone deacetylases (HDACs) in HD.

HDAC	HD model and brain area	Altered levels and distribution
HDAC1	Infected HeLa cells and cortical neurons (htt-111Q) [1]	No total protein change/no increase in agg+ cells
	R6/2 Ctx and Str (4, 9 and 12w) [2]	Increased total protein levels
	R6/2 Ctx and BrSt (9w) [3]	No total RNA change
	*Hdh*CAG140 Ctx (8 and 24m) [2]	No total protein change
	N171-82Q Ctx [4]	Reduced cytosolic and increased nuclear protein
	Postmortem brain from HD patients [1, 2]	No staining change in Str and Ctx [1]
		No total protein change [2]
HDAC2	Infected HeLa cells and cortical neurons (htt-111Q) [1]	No total protein change
	R6/2 Ctx and BrSt (9w) [3]	No total RNA change
	*Hdh*CAG140 Ctx (8 and 24m) [2]	No total protein change
	N171-82Q Ctx [4]	No change in cytosolic and nuclear protein levels
HDAC3	Infected HeLa cells and cortical neurons (htt-111Q) [1]	No total protein change
	R6/2 Ctx and Str (4, 9 and 12w) [2]	
	R6/2 Ctx and BrSt (9w) [3]	No total RNA change
	R6/2 Ctx, Str and Cb (15w) [5]	
	*Hdh*CAG140 Ctx (8 and 24m) [2]	No total protein change
	N171-82Q Ctx [4]	Reduced cytosolic and increased nuclear protein
HDAC4	Infected HeLa cells and cortical neurons (htt-111Q) [1]	No total protein change
	R6/2 Str (9w) [2]	
	R6/2 Ctx (4 and 12w) [2]	Increased total protein levels (12w)
	R6/2 Ctx and BrSt (9w) [3]	No total RNA change
	*Hdh*CAG140 Ctx (8 and 24m) [2]	No total protein change
	N171-82Q Ctx [4]	No change in cytosolic protein levels
	Postmortem brain from HD patients [6]	Increased protein levels in cingulate Ctx
		No protein change in CN and PNJ cells
HDAC5	Infected HeLa cells (htt-111Q) [1]	No protein change/slight increase in agg+ cells
	Infected cortical neurons (htt-111Q) [1]	No protein change/no increase in agg+ cells
	Postmortem brain from HD patients [1]	Increase in nuclear staining (Str > Ctx)
	R6/2 Str (9w) [2]	No total protein change
	R6/2 Ctx (4 and 12w) [2]	Increased total protein levels (12w)
	R6/2 Ctx and BrSt (9w) [3]	No total RNA change
	*Hdh*CAG140 Ctx (8 and 24m) [2]	No total protein change
	Postmortem brain from HD patients [6]	Increased protein levels in cingulate Ctx
		No protein change in CN and PNJ cells
HDAC6	R6/2 Str and Ctx (9 and 12w) [2]	Increased total protein levels
	R6/2 Ctx and BrSt (9w) [3]	No total RNA change
	R6/2 Str, Ctx and Cb (4, 9, 15w) [7]	
	*Hdh*CAG140 Ctx (8 and 24m) [2]	No total protein change
HDAC7	R6/2 Ctx and BrSt (9w) [3]	No total RNA change
	R6/2 Str and Cb (14w) [8]	
	R6/2 Ctx (14w) [7]	No total protein change
	R6/2 Str (6w) [9]	Decreased total RNA and protein levels
	N171-82Q Ctx [4]	No change in cytosolic protein levels
HDAC8	Infected HeLa cells and cortical neurons (htt-111Q) [1]	No total protein change
	R6/2 Ctx and BrSt (9w) [3]	No total RNA change
	Postmortem brain from HD patients [1]	No protein staining change in Ctx and Str
HDAC9	R6/2 Ctx and BrSt (9w) [3]	No total RNA change
HDAC10		
HDAC11		
Sirt2	R6/2 Ctx, Str and Cb (4 and 15w) [10]	No total RNA change

Ctx, cortex; Str, striatum; BrSt, brain stem; Cb, cerebellum; CN, caudate nucleus; PNJ, Purkinje; agg+, positive to mHtt aggregates. References: [1] (Hoshino et al., 2003), [2] (Quinti et al., 2010), [3] (Mielcarek et al., 2011), [4] (Jia et al., 2012b), [5] (Moumne et al., 2012), [6] (Yeh et al., 2013), [7] (Bobrowska et al., 2011), [8] (Benn et al., 2009), [9] (Ma and D'Mello, 2011), [10] (Bobrowska et al., 2012).

Of note, in cell lines challenged with cytotoxic insults, neuroprotection has been achieved by overexpressing HDAC7, independently of its HDAC activity (Ma and D'Mello, 2011), and by overexpressing wild-type Htt, which physically interacts with HDAC3 to damper its activity (Bardai et al., 2013). In R6/2 mice the Htt-HDAC3 interaction is actually disturbed. In summary, these results add more complexity for understanding the precise roles of HDACs in HD.

2.2. Histone methylation

Similarly to acetylation, histone methylation is also involved in cognition and linked to intellectual disabilities, especially in the case of histone H3 (reviewed in Parkel et al., 2013). The repressive marks di-methylation (m2) and tri-methylation (m3) of H3K9 are elevated in brain tissues of R6/2 and N171-82Q mice and in HD patients (Ferrante et al., 2004; Gardian et al., 2005; Ryu et al., 2006; Stack et al., 2007). H3K9 methylation and acetylation are mutually exclusive (Wang et al., 2008), so it is not surprising that their levels become imbalanced in opposite directions in murine models (Stack et al., 2007) to negatively affect the expression of genes with neuronal functions.

Histone H3K9 hypermethylation has been explained as a result of altered upregulation of upstream chromatin factors. Ferrante et al. (Ryu et al., 2006) showed concurrently increased levels of H3K9me3 and its specific histone–lysine *N*-methyltransferase SET (SU(VAR)3-9, enhancer of Zeste, Trithorax) domain bifurcated 1 (SETDB1), also known as ERG-associated protein with SET domain (ESET). GC-box-binding transcription factors Sp1 and Sp3 were proposed to be responsible for the SETDB1 transcriptional upregulation. This view is in agreement with the reported enhancement of Sp1 activity in HD (Qiu et al., 2006; Benn et al., 2008) but in apparent contradiction

with other works (Dunah et al., 2002; Li et al., 2002; Chen-Plotkin et al., 2006). Therefore, the effect of Sp factors dysregulation should be explained on the basis of specific loci. Another example is alpha-thalassemia/mental retardation X-linked (ATRX), a DNA-dependent ATPase/helicase that specifically recognizes H3K9me2/3 in pericentromeric heterochromatin (Eustermann et al., 2011; Iwase et al., 2011) and is associated with the mental retardation syndrome that carries the same name (OMIM #301040). Increased ATRX has been observed in different HD animal and cellular models, and it colocalizes with H3K9me3 and heterochromatin-binding protein 1 alpha (HP1α) (Lee et al., 2012). Moreover, neurotoxicity induced by mHtt is influenced by genetic manipulation of ATRX level in *Drosophila*. In accordance with ATRX's role in heterochromatin condensation, an increase in the volume of pericentromeric heterochromatin clusters was subsequently confirmed in HD (Lee et al., 2013). To explain this upregulation, the expression level of the transcription factor caudal type homeobox 2 (Cdx2) and its binding occupancy at the ATRX promoter were augmented in R6/2 striatum (Lee et al., 2012). It is documented that Cdx2 expression is restricted to metastatic adenocarcinomas and intestinal epithelium and related tissues in non-neoplastic conditions (Strickland-Marmol et al., 2007), so the presence of Cdx2 in adult brain remains intriguing.

In contrast, the methylation mark associated with active genes, H3K4me3 (Parkel et al., 2013), exhibited reduced binding at the promoters of representative downregulated genes in cortical and striatal areas of R6/2 mice and patients (Vashishtha et al., 2013). This correlation was extended to other genes in a genome-wide occupancy survey in the murine strain. The proposed cause of H3K4me3 hypomethylation was the upregulation of the specific histone demethylase lysine (K)-specific demethylase 5C (KDM5C), also known as Smcy homolog, X-linked (SMCX) or Jumonji/ARID domain-containing protein 1C (Jarid1c), associated with the X-linked Claus-Jensen type mental retardation syndrome (OMIM #300534). As a validation of this effect, knockdown of KDM5C increased the transcript levels of selected HD-deregulated genes and ameliorated the toxicity in mHtt-expressing flies (Vashishtha et al., 2013).

2.3. Histone ubiquitylation

Next we summarize the most relevant aspects of histone monoubiquitylation for the purposes of this review. For further details, see the reviews by Cao and Yan (2012), Braun and Madhani, 2012, and references therein. Histone monoubiquitylation is the result of the covalent attachment of ubiquitin protein to lysine residues by the enzymatic action of E3 ubiquitin ligases. On the one hand, H2A is monoubiquitylated at K119 by the Polycomb repressor complex PRC1 and has been linked to the silencing of developmental genes, pericentromeric regions and the inactive X-chromosome. A general requirement for H2A monoubiquitylation (H2Aub1) is the previous methylation of H3K27 by the Polycomb complex PRC2. On the other hand, H2B is monoubiquitylated at K120 and is frequently associated with active genes. H2B monoubiquitylation (H2Bub1) is required for the establishment of two downstream active marks: methylated H3K4 and H3K79. In addition, H2Bub1 determines the general structure of the chromatin by ensuring the integrity of histone positioning throughout the genome.

In R6/2 mouse brain, the bulk H2Aub1 level was increased independently of the ubiquitin–proteasome system in two studies (Kim et al., 2008; Bett et al., 2009), whereas H2Bub1 was reduced (Kim et al., 2008). These changes were correlated at the level of promoter binding and transcriptional expression of selected genes: negatively in the case of H2Aub1 and positively in the case of H2Bub1, in concordance with a repressive and active mark, respectively. Similar deficits were observed in the HD ST*Hdh*Q111/Q111 cell line, which allows the manipulation of E3 ubiquitin ligases (Kim et al., 2008). Thus, ring finger protein 2 (Rnf2 or Ring2) can regulate H2Aub1 and the downstream methylation of H3K9, whereas Rnf20 (homolog to yeast Bre1) can regulate H2Bub1 and the downstream methylation of H3K4, suggesting the potential involvement of the Polycomb repressive complexes in the etiology and/or progression of HD.

2.4. Histone phosphorylation

An early report suggested an aberrant phosphorylation of histone H3 in polyQ diseases (Yazawa et al., 2003), but only years later was it demonstrated that the induction of pH3 and its downstream target gene c-Fos was impaired in striatal neurons transfected with an expanded version of a Htt fragment (Roze et al., 2008). The phosphorylation level of histone H3 at serine 10 is extremely low under basal conditions, but it is highly induced after neuronal activation in a rapid and transient manner (Crosio et al., 2003; Tsankova et al., 2004; Sng et al., 2006). Impaired pH3 induction has been explained by downregulation of the upstream kinase mitogen- and stress-activated protein kinase-1 (MSK-1). Overexpression of MSK-1 restored full induction of the pH3 and c-Fos expression and abrogated striatal death *in vitro* and *in vivo* (Roze et al., 2008; Martin et al., 2011) by acting cooperatively with transcription factors such as CREB to activate prosurvival factors.

Another completely different aspect of histone phosphorylation implicates histone H2A.X. This universal variant differs from the canonical H2A in the C-terminus and in a few amino acids. H2A.X became phosphorylated at S139 by ataxia telangiectasia mutated kinase (ATM) to create γH2A.X in both cellular and R6/2 models in response to DNA damage (Giuliano et al., 2003; Illuzzi et al., 2009). Activation of γH2A.X fosters a structural environment that facilitates DNA repair (reviewed in Bonisch and Hake, 2012). However, in mHtt-expressing conditions, this activation did not lead to an efficient repair, due to the uncoupling between γH2A.X and breast cancer-associated 1 (BRCA1), another ATM substrate, making neurons more susceptible to DNA breaks under stress conditions (Jeon et al., 2012).

2.5. DNA methylation

In the nervous system, altered DNA methylation has been implicated in a variety of neurodevelopmental and psychiatric disorders (Jakovcevski and Akbarian, 2012; Grayson and Guidotti, 2013). This modification is most familiar from its prominent role during development in processes such as gene imprinting and tissue-specific gene silencing (Guibert and Weber, 2013) and has been regarded as a highly stable mark that makes possible the maintenance of cell identity in adulthood. Nonetheless, a more dynamic view for this epigenetic mark has recently arisen in neuronal activation and cognition (Day and Sweatt, 2011; Guo et al., 2011a).

Methylation of carbon 5 in cytosine is the most abundant DNA modification and is highly represented in vertebrates. In mammals it is found almost exclusively in CpG dinucleotides. CpG islands (CGIs) are genomic sequences enriched in CpG dinucleotides, usually located in gene promoters and generally involved in gene regulation (Deaton and Bird, 2011). The modification is catalyzed by DNA methyltransferases (DNMTs), which create 5-methylcytosines (5mCs). This can be followed by an additional step of 5 mC oxidization to create hydroxymethylcytosines (5 hmCs), which are catalyzed by ten-eleven translocation (TET) proteins and are thought to be an intermediate state prior to DNA demethylation (Guo et al., 2011b). To oversimplify, 5 mC in a promoter is associated with gene repression, while 5 hmC is associated with relief of transcriptional silencing (Guibert and Weber, 2013), as demonstrated during the brain development (Lister et al., 2013).

Altered patterns of CpG methylation in HD have been examined in two downregulated gene products in multiple HD models and in patients (Seredenina and Luthi-Carter, 2012): brain-derived neurotrophic factor (BDNF), important for the function and survival of mature neurons, and adenosine A_{2A} receptor (Adora2a), which stimulates the activity of adenylyl cyclase. No overall methylation changes have been observed in the CGIs distributed along the alternative promoters and 5′-UTRs of these genes. In the case of BDNF, examination of single CpG dinucleotides revealed very little influence of mHtt expression in the R6/1 hippocampus (Zajac et al., 2010). In the case of Adora2a, an immunoprecipitation approach was used to discriminate 5 mC and 5 hmC changes at specific CpGs (Villar-Menendez et al., 2013), which is not possible using methods such as bisulfite sequencing (Huang et al., 2010; Jin et al., 2010; Nestor et al., 2010). Whereas 5 mC changes were inconsistent, 5 hmC levels were decreased in a similar location in the 5′-end of the Adora2a gene in murine and human striata.

Genome-wide surveys have been more informative than gene-single studies. In the first study, a modified bisulfite sequencing protocol was used to measure DNA methylation at the base pair resolution comparing ST*Hdh*Q111/Q111 and the control Q7/Q7 cell lines (Ng et al., 2013). There was a bias toward hypomethylation, which was more concentrated at CpG-poor regions, which are more likely to be associated with distal and intergenic regions. However, methylation changes at CpG-rich regions, which are largely associated with transcription start sites (TSS), were inversely correlated with gene expression changes. To determine whether specific DNA sequences may regulate methylation changes at the CpG-poor distal regions in ST*Hdh* cell line, a ChIP-seq analysis demonstrated differential binding of the transcription factors Sox2 and the AP-1 members Fra2 and JunD that were positively correlated with differential DNA methylation. In another study, the global level of 5 hmC was reduced in striatum and cortex of YAC128 mice in presymptomatic stages (Wang et al., 2013). The genomic distribution of this mark confirmed this differential hypomethylation at several loci, although hypermethylation was also detected to a lesser extent. Despite a positive correlation between the presence of differential 5 hmC regions and gene expression, the subset of examined genes was too small to infer the precise contribution of 5 hmC deficits in HD transcriptional dysregulation.

In any case, the analysis of DNA methylation in neurodegenerative disorders is still immature. Most of the methylation properties are inferred from proliferative cells and may not apply to post-mitotic cells. For instance, CpG dinucleotides have been the focus of DNA methylation, but brain tissue exhibits a significant fraction of non-CpG methylation (Xie et al., 2012; Varley et al., 2013), as it is prominent in the neuronal genome (Lister et al., 2013). In addition, the brain shows possibly the highest levels of 5 hmC in the body (Globisch et al., 2010; Li and Liu, 2011; Song et al., 2011), although the parallel reduction of 5 hmC and gene expression in HD may be not in the line with the proposed function of this modification without a concomitant persistence of 5 mC at the same positions. Finally, there exist more DNA modifications that may also be relevant to HD pathology. For example, the global level of 7-methylguanine (7 mG) was reduced in nuclear fractions of HD models (both knockin and transgenic mice) and in the motor cortex of HD patients, whereas 7 mG was increased in cytoplasmic (RNA) fractions (Thomas et al., 2013).

3. Epigenetic-based ameliorative strategies

3.1. HDAC inhibitors

These drugs generally exert a broad action on HDACs (excluding class III), although HDACi 4b and related compounds may have more specificity against HDAC1 and 3 (Jia et al., 2012b). Their involvement in HD was discovered in parallel to the observation of CBP deficits in HD. In two seminal works, HDACis belonging to different families (sodium butyrate (NaB), suberoylanilide hydroxamic acid (SAHA) and trichostatin A (TSA)) were able to rescue degeneration and cell death in models of polyQ disorders (McCampbell et al., 2001; Steffan et al., 2001). Since then, beneficial effects of HDACis have been described in cellular, invertebrate and murine models of HD, although overdose has deleterious effects (see Table 2 for further details). The main proposed ameliorative mechanism is that HDACi administration dramatically induces histone acetylation, potentially reversing any deficit that affects gene expression. Thus, chronic treatment may permanently increase the association of acetylated histones with downregulated genes that eventually correct mRNA abnormalities. Interestingly, due to the cross-talk between different histone modifications, some HDACis additionally influenced other marks, for instance by reducing the repressive H3K9me2 and H2Aub1 marks (Gardian et al., 2005; Sadri-Vakili et al., 2007). These effects may help HDACis restore native gene expression. Interestingly, chronic treatment with HDACi SAHA can modulate the expression of HDAC2 and 4 at the protein level, and HDAC7 and 11 at the RNA levels, as a hypothetical mechanism for amelioration (Benn et al., 2009; Mielcarek et al., 2011).

3.2. Anthracyclines

To date, no methyltransferase inhibitor has been tested in a HD model. However, it is possible to manipulate histone methylation indirectly, by using GC-binding anthracyclines, such as mithramycin A and chromomycin, a group of bacterial compounds with anticancer and antibiotic properties (Piekarski and Jelinska, 2013). It has been proposed that interaction with the minor groove of DNA can inhibit the binding of GC-rich-binding transcription factors such as Sp1 family members, thereby correcting the expression level of the methyltransferase SETDB1 and reversing the hypermethylation of H3K9 in HD animal models (Ryu et al., 2006). However, the action of GC-binding anthracyclines seems to be wider, as they can also reverse the hypoacetylation of histones H3 and H4 (Stack et al., 2007). In any case, amelioration has been achieved in the tested animal models (Ferrante et al., 2004; Ryu et al., 2006; Stack et al., 2007), in the latter case concomitant to a partial reversal of the HD transcriptional dysregulation (Table 3).

4. Revisiting the role of epigenetics in Huntington's disease

4.1. The complex interplay between epigenetics and gene expression

For years, researchers have worked under the hypothesis that altered epigenetics is one of the main causes of the transcriptional dysregulation observed in HD models and postmortem brain patients, and therefore that the reversal of such epigenetic dysregulation can restore, at least partially, the original transcriptional program and ameliorate particular pathophenotypic traits. In principle this hypothesis has been supported by single-gene experiments, as commented in the previous section. The introduction of global techniques to map the genomic distribution of epigenetic marks widened our perspective about epigenetic-based transcriptional dysregulation and demonstrated that the relationship between altered epigenetic and transcription is more complex than previously envisaged. Thus, overlap between transcriptional changes and various altered epigenetic modifications has proven far from fully satisfactory, although seemingly better correlations were obtained using next-generation sequencing approaches (ChIP-seq, RNA-seq), which allow nucleosome resolution and an

Table 2
Summary of the effects of HDACi treatment in HD.

Compound	HD model and optimal dose[a]	Effects
Hydroxamic acids		
SAHA (suberoylanilide hydroxamic acid)	*Drosophila* UAS-Q93Httex1p and UAS-Q48 + myc/flag: 10 μM in food, 6 d [1]	*Amelioration:* Rhabdomeres degeneration, adult death *No change:* mHtt transgene expression
	R6/2 (4–5w) mice: 0.67 g/L (with HOP-β-CD) in drinking water, 4–5w	*Amelioration:* Cortical Bdnf defective expression [2], expression of toxic metabolites of the kynurenine pathway [3] Cellular atrophy [4], mHtt aggregation in cortex and brain stem [2] Rotarod performance impairment [4] *No change:* Body weight loss, grip strength deficits [4] mHtt expression, hippocampal mHtt aggregation [2,4]
	R6/2 (4–5w) mice: 1.33 g/L (with HOP-β-CD) in drinking water	*Side effects:* Weight loss, death [4]
	R6/2 (P7) hippocampal slices: 2.5 μM, 4w [4] R6/2 microglia cultures: 10 μM, 6 h [3]	*No change:* mHtt aggregation *Amelioration:* Expression of toxic metabolites of the kynurenine pathway
TSA (trichostatin A)	*C. elegans* Htn-Q150: 150 μg/ml in medium, 8 d [5]	*Amelioration:* Neuronal degeneration
	ST*Hdh*Q111 and Q7 cells: 10 nM, 24 h YAC128 striatal culture: 50 nM 7DIV	*Amelioration:* Inefficient mitochondrial Ca^{2+} handling in Ca^{2+} induced toxicity [6]
	*Hdh*Q7/Q111 mice: 2 mg/kg i.p. 2 h before training [7]	*Amelioration*: H3 hypoacetylation, c-Fos downregulation Long-term memory impairment (novel object recognition task)
Aliphatic acids		
Sodium butyrate	PC12/Httex1Q103-EGFP cells: 5 mM, 24 h [1]	*Amelioration*: H3 and H4 hypoacetylation
	Drosophila UAS-Q93Httex1p and UAS-Q48 + myc/flag: 100 mM in diet, 6 d [1]	*Amelioration*: Rhabdomeres degeneration, adult death *No change:* mHtt transgene expression
	R6/2 (21 d) mice: 1.2 g/kg/d i.p. 21 or 69 d [8]	*Amelioration:* H3 and H4 hypoacetylation. Subset of differential expressed genes in striatum, including α- and β-globins and MKP-1 Premature death, weight loss. Rotarod performance impairment Gross brain and striatal atrophy. Neuronal soma reduction. 3-NP-induced lesion. *No change*: mHtt transgene expression and aggregation. Differentially expressed genes, including Penk1
	R6/2 (21 d) mice: 5 g/kg/d i.p. [8]	*Side effects*: Morbidity and death
	ST*Hdh*Q111 and Q7 cells: 1 mM, 24 h YAC128 striatal culture: 500 μM 7DIV	*Amelioration*: Inefficient mitochondrial Ca^{2+} handling in Ca^{2+} induced toxicity [6]
	ST*Hdh*Q111 and Q7 cells: 10 mM, 24 h [9]	*Amelioration:* H3 hypoacetylation and transcript downregulation of selected genes (Vdr, Inhbb, Dhrs4, Tcf7), H2AK119 hyperubiquitylation
Sodium phenylbutyrate	N171-82Q (75d) mice: 100 mg/kg, 6 d per week i.p. 15–45 d [10]	*Amelioration:* H3 and H4 hypoacetylation and H3K9 hyperdimethylation. Subset of deregulated striatal genes, including Gfer, Gstm3, Psma3, Casp9, Cflar and Prkce Premature death. Brain and neuronal atrophy *No change*: Body weight loss, mHtt aggregation. Rotarod performance impairment
	R6/2 (8w): 400 mg/kg/d 7 d [9]	*Amelioration*: H3 hypoacetylation and transcript downregulation of selected genes (Drd2, Penk)
	HD patients: 18 g/d [19]	*Side effects*: Nausea, fatigue, gait instability, lightheadedness, etc.
D-β-HB (D-β-hydrobutyrate)	3-NP (21w) treated mice: 1.6 mmol/kg/d subcutaneous minipumps, 6 d [12]	*Amelioration*: Death. Striatal lesion Spontaneous locomotor activity
	R6/2 (6w) treated mice: 1.6 mmol/kg/d subcutaneous minipumps, 10w [12]	*Amelioration:* H4 hypoacetylation Premature death *No change:* Spontaneous locomotor activity,[b] striatal atrophy, mHtt aggregation
Sodium valproate	N171-82Q (7w) mice: 100 mg/kg 5 d per week i.p. 9w [13]	*Amelioration:* Premature death, ambulatory and spontaneous locomotor activity deficits
	N171-82Q (7w) mice: 25 g/kg in diet, 15w [14]	*Amelioration:* H3 hypoacetylation Premature death, depressive-like behavior[c] *No change:* Body weight loss (exacerbated), spontaneous locomotor activity deficits, rotarod performance impairment, GSK-3β hyperactivation
	YAC128 (3m) mice: 25 g/kg in diet, 9m [14]	*Amelioration:* H3 hypoacetylation, GSK-3β hyperactivation Body weight gain, anxiety-like behavior[c] *No change:* Spontaneous locomotor activity deficits, depressive-like behavior
Sodium valproate + lithium (mood stabilizer)	N171-82Q (7w) mice: 25 g/kg + 3 g/kg in diet, 15w [14]	*Amelioration:* H3 hypoacetylation, GSK-3β hyperactivation Premature death, spontaneous locomotor activity, rotarod performance impairment, depressive-like behavior *No change:* Body weight loss (exacerbated)
	YAC128 (3m) mice: 25 g/kg + 3 g/kg in diet, 9m [14]	*Amelioration:* H3 hypoacetylation, GSK-3β hyperactivation Body weight gain, spontaneous locomotor activity deficits, anxiety-like and depressive-like behavior

(*continued on next page*)

Table 2 (*continued*)

Compound	HD model and optimal dose[a]	Effects
Pimelic diphenylamides		
4b	R6/2 (4m) mice: 150 mg/kg/day (with HOP-β-CD) in drinking water, 67 d [15]	*Amelioration*: Subset of differentially deregulated genes in striatum, cortex, and cerebellum. H3 hypoacetylation at promoters of selected downregulated genes: Cldn1, Calml4, Aqp1, Folr1, Clic6, Enpp2 Gross brain striatal atrophy Body weight loss. Feet clasping phenotype, kyphosis, spontaneous locomotor activity, gait instability. Rotarod performance deficits *No change:* Endogenous Htt and mHtt expression mHtt aggregation
	R6/2 mice: 150 mg/kg/d s.c., 3 d[d] [16]	*Amelioration:* Subset of downregulated genes: Hrh3, Cnih2, Ccr6
	Drosophila UAS-Q93Httex1p: 100 μM in diet, 6 d[d] [16]	*Amelioration:* Rhabdomeres degeneration
	ST*Hdh*Q111 cells: 10 μM 1–2 d[d] [16]	*Amelioration:* Mitochondrial metabolic dysfunction
	N171-82Q (8w) mice: 50–100 mg/kg 2.5 s.c. per week, 10w [17]	*Amelioration:* Differentially deregulated genes related with ubiquitin–proteasome pathway (e.g., Ubqln2, Pml, Ube2e3, Ube2k, Sumo2, etc.) mHtt aggregation Body weight loss (female). Rotarod performance impairment, T-maze cognitive, ambulatory and spontaneous locomotion deficits
	R6/2 (17w) mice: 0.85 mg/ml (with HOP-β-CD) in drinking water, 10w [18]	*Amelioration:* Brain weight loss, striatal atrophy, feet clasping phenotype *No change:* Premature death, body weight loss, spontaneous locomotor activity, rotarod performance deficits, kyphosis
	N171-82Q (9w) mice: 0.85 mg/ml (with HOP-β-CD) in drinking water, 10w [18]	*No change:* Premature death, body weight loss, spontaneous locomotor activity, rotarod performance deficits, feet clasping phenotype, late kyphosis
136	R6/2 mice: 150 mg/kg/d s.c., 3 d[d] [16]	*Amelioration:* Subset of downregulated genes: Ppp1r1b, Ngef, Hrh3, Cnih2, Ccr6
	Drosophila UAS-Q93Httex1p: 10 μM in diet, 6 d[d] [16]	*Amelioration:* Rhabdomeres degeneration
	ST*Hdh*Q111 cells: 1 mM 1–2 d[d] [16]	*Amelioration:* Mitochondrial metabolic dysfunction
233 971 974	*Drosophila* UAS-Q93Httex1p: 1 μM in diet, 6 d[d] [16]	*Amelioration:* Rhabdomeres degeneration
874	N171-82Q (8w) mice: 50–100 mg/kg 2.5 s.c. per week, 6w [17]	*Amelioration:* mHtt aggregation

[a] In brackets, the starting age of treatment followed by the dose, way and duration of administration (where indicated). Note that representative age and duration are indicated as they can vary in the same report, dependent on the experiment.
[b] Claimed to improve locomotor deficits.
[c] The amelioration was not observed in all the tasks that measured the referred behavior.
[d] Partial results of a study assessing several related compounds; only the most effective were shown. HOP-β-CD, 2-hydroxypropyl-β-cyclodextrin; i.p., intraperitoneal injection; s.c., subcutaneous injection; MKP-1, MAP kinase phosphatase 1 (Dusp1); 3-NP, 3-nitropropionic acid; Penk1, proenkephalin; Vdr, vitamin D receptor; Inhbb, inhibin β B; Dhrs4, dehydrogenase/reductase (SDR family) member 4; Tcf7, transcription factor 7 (T-cell specific, HMG-box); Gfer, growth factor, augmenter of liver regeneration; Gstm3, Glutathione S-transferase M3 (brain); Psma3, proteasome (prosome, macropain) subunit, alpha type, 3; Casp9, caspase 9, apoptosis-related cysteine peptidase; Cflar, CASP8 and FADD-like apoptosis regulator; Prkce, protein kinase C, epsilon; Drd2; dopamine receptor D2; GSK-3β Glycogen synthase kinase 3β; Cldn1, claudin 1; Calml4, calmodulin-like 4; Aqp1, aquaporin 1 (Colton blood group); Folr1, folate receptor 1 (adult); Clic6, chloride intracellular channel 6; Enpp2, ectonucleotide pyrophosphatase/phosphodiesterase 2; Ppp1r1b, protein phosphatase 1, regulatory (inhibitor) subunit 1B (DARPP-2); Ngef, neuronal guanine nucleotide exchange factor; Hrh3, histamine receptor H3; Cnih2, cornichon homolog 2 (Drosophila); Ccr6, chemokine (C–C motif) receptor 6; Ubqln2, ubiquilin 2; Pml, promyelocytic leukemia; Ube2e3, ubiquitin-conjugating enzyme E2E 3; Ube2k, ubiquitin-conjugating enzyme E2K; Sumo2, SMT3 suppressor of mif two 3 homolog 2 (*Saccharomyces cerevisiae*). References: [1] (Steffan et al., 2001), [2] (Mielcarek et al., 2011), [3] (Giorgini et al., 2008), [4] (Hockly et al., 2003), [5] (Bates et al., 2006), [6] (Oliveira et al., 2006), [7] (Giralt et al., 2012), [8] (Ferrante et al., 2003), [9] (Sadri-Vakili et al., 2007), [10] (Gardian et al., 2005), [11] (Hogarth et al., 2007), [12] (Lim et al., 2011), [13] (Zadori et al., 2009), [14], (Chiu et al., 2011), [15] (Thomas et al., 2008), [16] (Jia et al., 2012b), [17] (Jia et al., 2012a), [18] (Chen et al., 2013), [19] (Hogarth et al., 2007).

unbiased interrogation of the genome, in comparison with array-based techniques (ChIP-on-chip, gene expression microarrays) (Valor and Barco, 2012). Furthermore, changes in the opposite direction (hyperacetylation, hypomethylation in repressive marks and hypermethylation in active marks) do not fit with the proposed perturbed activities of KATs, methyltransferases and demethylases, unless we consider homeostatic responses or activation of secondary responses. So far, the following epigenetic marks have been explored with a genomic perspective: H3K9/14ac, limited to promoters and adjacent regions in R6/2 striatum (McFarland et al., 2012); H3K9/14ac and H4K12ac in N171-82Q hippocampus (Valor et al., 2013a); H3K9me3 (Lee et al., 2013) and DNA methylation (Ng et al., 2013) in ST*Hdh*Q111/Q111 striatal cells; and H3K4me3 in R6/2 cortex and striatum (Vashishtha et al., 2013).

These puzzling results prove our poor understanding of the role of epigenetics under normal conditions. Our current view regarding how epigenetic mechanisms regulate gene expression is being challenged (Anamika et al., 2010; Henikoff and Shilatifard, 2011; Bedford and Brindle, 2012; Rando, 2012): 1) mutations in the post-translational modification sites of histone genes produce surprisingly moderate phenotypes and gene expression changes in yeast and invertebrates; 2) multiple epigenetic marks and chromatin-remodeling factors tend to concur at the same loci, an argument against the extreme combinatorial possibilities predicted by the 'histone code' hypothesis; 3) the co-occurrence of changes in gene expression and epigenetic modifications does not imply a causal relationship; and 4) chromatin-remodeling factors may have additional activities more relevant for transcriptional regulation than their epigenetic actions, as exemplified by CBP/p300, which can be substituted by cofactors lacking KAT activity to regulate the CREB-dependent transcriptional response to cAMP (Bedford and Brindle, 2012).

Table 3
Summary of the effects of anthracyclines treatment in HD.

Compound	HD model and optimal dose[a]	Effects
Mithramycin A	R6/2 (21–28 d): 150 μg/kg/d, i.p. 52 d	*Amelioration:* H3K9 hyperdimethylation [1]. Subset of differentially expressed genes in cortex [2]. Gross brain and striatal atrophy, neuroprotection (3-NP insult) [1]. Premature death, rotarod performance [1]. *No change:* mHtt transgene expression and aggregation, body weight loss [1]
	R6/2 (21–28 d): 300 μg/kg/d, i.p. N171-82Q (28 d): 100 μg/kg/d, i.p. [2]	*Side effect:* Morbidity and death [1] *Amelioration:* Oxidative DNA damage (8-OH_2dG levels). Premature death. Brain and striatal atrophy. *No change:* Weight loss
	N171-82Q (28 d): 200 μg/kg/d, i.p. [2]	*Side effect:* Enhanced weight loss and premature death
Mithramycin A + cystamine (transglutaminase inhibitor) [3]	R6/2 (28 d): 150 μg/kg/d, i.p. + 112 mg/kg/d in drinking water, 62 d	*Amelioration:* SETDB1 upregulation, H3K9me3 hypermethylation. Enhanced survival compared to mithramycin alone, rotarod performance. Gross brain and striatal atrophy, brain weight, neuronal size, mHtt aggregates. *No change:* Weight loss[b]
Chromomycin [2]	R6/2 (28 d): 100 μg/kg/d, i.p. N171-82Q (28 d): 100 μg/kg/d, i.p.	*Amelioration:* H3K9 hypertrimethylation, H3K9 and H4 hypoacetylation. Oxidative DNA damage (8-OH_2dG levels). Premature death, ambulatory deficits. Gross brain and striatal atrophy. *No change:* Weight loss
Dystamicin (AT-binding anthracycline) [1]	R6/2: 50–300 μg/kg/d	*No change:* Survival, rotarod performance

[a] In brackets, the starting age of treatment followed by the dose, way and duration of administration (where indicated). Note that representative age and duration are indicated as they can vary in the same report, dependent on the experiment.
[b] Amelioration of weight loss was apparently due to enhanced survival and not due to a direct effect (authors' claim). i.p., intraperitoneal injection; 3-NP, 3-nitropropionic acid; 8-OH_2dG, 8-hydroxy-2′-deoxyguanosine. References: [1] (Ferrante et al., 2004), [2] (Stack et al., 2007), [3] (Ryu et al., 2006).

These concerns are also applicable to the genomic effects of HDACi treatments. Acute treatment with TSA preferentially hyperacetylated active loci already premarked with H3K4me3 and H3K9/14ac at the TSS without substantially affecting the number of genes containing these active marks (Lopez-Atalaya et al., 2013), suggesting that HDAC inhibition seems to favor transcriptionally permissive states rather than modulate transcriptional rates. This situation may change during chronic treatments and at defective loci. Nonetheless, a closer inspection of the microarray studies revealed a relatively small number of corrected genes in HD models (Ferrante et al., 2003; Gardian et al., 2005; Stack et al., 2007), with the notable exception of HDACi 4b (Thomas et al., 2008). Of course, although low in number, these reversions can be sufficient to justify phenotypic amelioration because they affect genes involved in highly relevant functions such as neuronal signaling and protein degradation.

In any case, the newly generated genome-wide data on HD could help in determining the exact contribution of epigenetic changes to transcriptional dysregulation. For example, only specific deficits at specific loci are more prone to be correlated with the gene expression deficits promoted by mHtt (Ng et al., 2013; Valor et al., 2013a; Vashishtha et al., 2013). This is the case of TSS regions, indicating distinct roles of epigenetic modifications depending on their genomic location.

4.2. The role of epigenetics in CAG instability

As a general theme in polyQ and other trinucleotide-repeat disorders, repeat instability increases the risk of triplet expansions over time. This phenomenon underlines anticipation (as further expansions in the germline worsen the disease in successive generations) and also accelerates the progression of the disease in sensitive somatic cells (Telenius et al., 1994). Surprisingly, repeat instability can be controlled by epigenetic mechanisms. Thus, the relevance of histone acetylation to CAG instability over generations is demonstrated by an increase in CBP-deficient mutants and a reduction after TSA treatment in *Drosophila* (Jung and Bonini, 2007). In cell cultures, trinucleotide expansions are at least dependent on the activity of HDAC3 and CBP/p300 in a bidirectional manner, through the transcriptional regulation of factors involved in DNA repair (Debacker et al., 2012). More direct mechanisms imply DNA demethylation in the germline (Gorbunova et al., 2004) and transcription elongation in somatic tissues (Goula et al., 2012) in the Htt locus. In R6/1 and R6/2 mice, CAG instability was strongly correlated with transcription elongation marks (e.g., H3K36me3), but not with transcription initiation marks (H3K9ac and H3K4me3), and only in striatum, suggesting a tissue-specific transcriptional regulation of the Htt gene that may play an important role in the development and progression of HD pathology.

4.3. The non-histone targets of HDAC inhibitors

Hundreds of proteins are susceptible to acetylation (Lundby et al., 2012) and, most importantly, can be influenced by HDAC inhibition (Choudhary et al., 2009). Thus, ameliorative strategies based on the use of HDACis can be a consequence of the combinatorial effects over histone and non-histone substrates that include transcription factors, cytoskeletal and mitochondrial proteins and many others. For example, post-translational modification of Htt can promote its clearance by the autophagic-lysosomal system, which is different from the UPS. This is the case for AcK444, which is regulated by the opposing activities of CBP and HDAC1 (Jeong et al., 2009). Therefore, CBP dysfunction contributes to accumulation, whereas HDACi treatment potentiates mHtt degradation in HD. In agreement with this notion, the triad AcK9/pS13/pS16 (also linked to autophagic degradation (Thompson et al., 2009)) can be regulated by HDACi 4b (Jia et al., 2012a, see Fig. 1 for a schematic representation of these residues). Another example is α-tubulin, whose acetylated form is reduced in postmortem striatal tissue from patients (Dompierre et al., 2007). Specific HDACis can increase tubulin acetylation at lysine 40 and rescue *in vitro* microtubule-dependent transport, including trafficking of BDNF-containing vesicles. This trafficking is disrupted in HD (Cattaneo et al., 2005), so HDACi treatment may also ameliorate HD symptomatology by restoring the cortical supply of BDNF to the striatum.

5. Concluding remarks

Both transcriptional and epigenetic dysregulation in HD models are important and early molecular events in the pathology. However, it is not clear to what extent altered epigenetics has a

causative role in the altered transcriptional program observed in HD. Although several epigenetic marks remain to be examined, it is plausible that the association of epigenetically dysregulated genomic regions with particular DNA sequences, as predicted *in silico* in the aforementioned genome-wide studies, may indicate the convergence of disrupted activities of both transcription factors and chromatin-remodeling proteins at the same loci, effectively altering gene expression. Moreover, non-histone nuclear proteins can be covalently modified using similar pathways as histones. This fact, together with alleviation of multiple pathological processes in pharmacological approaches (not only transcriptional dysregulation but also triplet instability, impairment in vesicle trafficking and protein degradation, among others), should be taken into consideration for the development of selective inhibitors in HD therapy.

Acknowledgments

LMV's research is supported by a Ramón Cajal contract and grant SAF2011-22506 from the Spanish Ministry of Economy and Competitiveness. DG is supported by a predoctoral fellowship (JAE-pre) from the Program "Junta para la Ampliación de Estudios" co-funded by the Fondo Social Europeo (FSE) and grants from the Fundació Gent per Gent and the Spanish Ministry of Economy and Competitiveness (SAF2011-22855).

References

Anamika, K., Krebs, A.R., Thompson, J., Poch, O., Devys, D., Tora, L., 2010. Lessons from genome-wide studies: an integrated definition of the coactivator function of histone acetyl transferases. Epigenetics Chromatin 3, 18.

Andreassen, O.A., Dedeoglu, A., Stanojevic, V., Hughes, D.B., Browne, S.E., Leech, C.A., Ferrante, R.J., Habener, J.F., Beal, M.F., Thomas, M.K., 2002. Huntington's disease of the endocrine pancreas: insulin deficiency and diabetes mellitus due to impaired insulin gene expression. Neurobiol. Dis. 11, 410–424.

Bardai, F.H., Verma, P., Smith, C., Rawat, V., Wang, L., D'Mello, S.R., 2013. Disassociation of histone deacetylase-3 from normal huntingtin underlies mutant huntingtin neurotoxicity. J. Neurosci. 33, 11833–11838.

Bates, G., Harper, P., Jones, L. (Eds.), 2004. Huntington's Disease. Oxford University Press.

Bates, E.A., Victor, M., Jones, A.K., Shi, Y., Hart, A.C., 2006. Differential contributions of *Caenorhabditis elegans* histone deacetylases to huntingtin polyglutamine toxicity. J. Neurosci. 26, 2830–2838.

Bedford, D.C., Brindle, P.K., 2012. Is histone acetylation the most important physiological function for CBP and p300? Aging (Albany NY) 4, 247–255.

Benn, C.L., Sun, T., Sadri-Vakili, G., McFarland, K.N., DiRocco, D.P., Yohrling, G.J., Clark, T.W., Bouzou, B., Cha, J.H., 2008. Huntingtin modulates transcription, occupies gene promoters in vivo, and binds directly to DNA in a polyglutamine-dependent manner. J. Neurosci. 28, 10720–10733.

Benn, C.L., Butler, R., Mariner, L., Nixon, J., Moffitt, H., Mielcarek, M., Woodman, B., Bates, G.P., 2009. Genetic knock-down of HDAC7 does not ameliorate disease pathogenesis in the R6/2 mouse model of Huntington's disease. PLoS One 4, e5747.

Bett, J.S., Benn, C.L., Ryu, K.Y., Kopito, R.R., Bates, G.P., 2009. The polyubiquitin Ubc gene modulates histone H2A monoubiquitylation in the R6/2 mouse model of Huntington's disease. J. Cell. Mol. Med. 13, 2645–2657.

Bobrowska, A., Paganetti, P., Matthias, P., Bates, G.P., 2011. Hdac6 knock-out increases tubulin acetylation but does not modify disease progression in the R6/2 mouse model of Huntington's disease. PLoS One 6, e20696.

Bobrowska, A., Donmez, G., Weiss, A., Guarente, L., Bates, G., 2012. SIRT2 ablation has no effect on tubulin acetylation in brain, cholesterol biosynthesis or the progression of Huntington's disease phenotypes in vivo. PLoS One 7, e34805.

Bodai, L., Pallos, J., Thompson, L.M., Marsh, J.L., 2012. Pcaf modulates polyglutamine pathology in a Drosophila model of Huntington's disease. Neurodegener Dis. 9, 104–106.

Bonisch, C., Hake, S.B., 2012. Histone H2A variants in nucleosomes and chromatin: more or less stable? Nucleic Acids Res. 40, 10719–10741.

Boutell, J.M., Thomas, P., Neal, J.W., Weston, V.J., Duce, J., Harper, P.S., Jones, A.L., 1999. Aberrant interactions of transcriptional repressor proteins with the Huntington's disease gene product, huntingtin. Hum. Mol. Genet. 8, 1647–1655.

Braun, S., Madhani, H.D., 2012. Shaping the landscape: mechanistic consequences of ubiquitin modification of chromatin. EMBO Rep. 13, 619–630.

Cao, J., Yan, Q., 2012. Histone ubiquitination and deubiquitination in transcription, DNA damage response, and cancer. Front. Oncol. 2, 26.

Cattaneo, E., Zuccato, C., Tartari, M., 2005. Normal huntingtin function: an alternative approach to Huntington's disease. Nat. Rev. Neurosci. 6, 919–930.

Cong, S.Y., Pepers, B.A., Evert, B.O., Rubinsztein, D.C., Roos, R.A., van Ommen, G.J., Dorsman, J.C., 2005. Mutant huntingtin represses CBP, but not p300, by binding and protein degradation. Mol. Cell. Neurosci. 30, 560–571.

Crosio, C., Heitz, E., Allis, C.D., Borrelli, E., Sassone-Corsi, P., 2003. Chromatin remodeling and neuronal response: multiple signaling pathways induce specific histone H3 modifications and early gene expression in hippocampal neurons. J. Cell Sci. 116, 4905–4914.

Cha, J.H., 2007. Transcriptional signatures in Huntington's disease. Prog. Neurobiol. 83, 228–248.

Chen-Plotkin, A.S., Sadri-Vakili, G., Yohrling, G.J., Braveman, M.W., Benn, C.L., Glajch, K.E., DiRocco, D.P., Farrell, L.A., Krainc, D., Gines, S., MacDonald, M.E., Cha, J.H., 2006. Decreased association of the transcription factor Sp1 with genes downregulated in Huntington's disease. Neurobiol. Dis. 22, 233–241.

Chen, G., Zou, X., Watanabe, H., van Deursen, J.M., Shen, J., 2010. CREB binding protein is required for both short-term and long-term memory formation. J. Neurosci. 30, 13066–13077.

Chen, J.Y., Wang, E., Galvan, L., Huynh, M., Joshi, P., Cepeda, C., Levine, M.S., 2013. Effects of the pimelic diphenylamide histone deacetylase inhibitor HDACi 4b on the R6/2 and N171-82Q mouse models of Huntington's disease. PLoS Curr. 5.

Chiu, C.T., Liu, G., Leeds, P., Chuang, D.M., 2011. Combined treatment with the mood stabilizers lithium and valproate produces multiple beneficial effects in transgenic mouse models of Huntington's disease. Neuropsychopharmacology 36, 2406–2421.

Choi, Y.J., Kim, S.I., Lee, J.W., Kwon, Y.S., Lee, H.J., Kim, S.S., Chun, W., 2012. Suppression of aggregate formation of mutant huntingtin potentiates CREB-binding protein sequestration and apoptotic cell death. Mol. Cell. Neurosci. 49, 127–137.

Choudhary, C., Kumar, C., Gnad, F., Nielsen, M.L., Rehman, M., Walther, T.C., Olsen, J.V., Mann, M., 2009. Lysine acetylation targets protein complexes and co-regulates major cellular functions. Science 325, 834–840.

Day, J.J., Sweatt, J.D., 2011. Epigenetic mechanisms in cognition. Neuron 70, 813–829.

Day, J.J., Sweatt, J.D., 2012. Epigenetic treatments for cognitive impairments. Neuropsychopharmacology 37, 247–260.

Deaton, A.M., Bird, A., 2011. CpG islands and the regulation of transcription. Genes Dev. 25, 1010–1022.

Debacker, K., Frizzell, A., Gleeson, O., Kirkham-McCarthy, L., Mertz, T., Lahue, R.S., 2012. Histone deacetylase complexes promote trinucleotide repeat expansions. PLoS Biol. 10, e1001257.

Dompierre, J.P., Godin, J.D., Charrin, B.C., Cordelieres, F.P., King, S.J., Humbert, S., Saudou, F., 2007. Histone deacetylase 6 inhibition compensates for the transport deficit in Huntington's disease by increasing tubulin acetylation. J. Neurosci. 27, 3571–3583.

Dunah, A.W., Jeong, H., Griffin, A., Kim, Y.M., Standaert, D.G., Hersch, S.M., Mouradian, M.M., Young, A.B., Tanese, N., Krainc, D., 2002. Sp1 and TAFII130 transcriptional activity disrupted in early Huntington's disease. Science 296, 2238–2243.

Eustermann, S., Yang, J.C., Law, M.J., Amos, R., Chapman, L.M., Jelinska, C., Garrick, D., Clynes, D., Gibbons, R.J., Rhodes, D., Higgs, D.R., Neuhaus, D., 2011. Combinatorial readout of histone H3 modifications specifies localization of ATRX to heterochromatin. Nat. Struct. Mol. Biol. 18, 777–782.

Ferrante, R.J., Kubilus, J.K., Lee, J., Ryu, H., Beesen, A., Zucker, B., Smith, K., Kowall, N.W., Ratan, R.R., Luthi-Carter, R., Hersch, S.M., 2003. Histone deacetylase inhibition by sodium butyrate chemotherapy ameliorates the neurodegenerative phenotype in Huntington's disease mice. J. Neurosci. 23, 9418–9427.

Ferrante, R.J., Ryu, H., Kubilus, J.K., D'Mello, S., Sugars, K.L., Lee, J., Lu, P., Smith, K., Browne, S., Beal, M.F., Kristal, B.S., Stavrovskaya, I.G., Hewett, S., Rubinsztein, D.C., Langley, B., Ratan, R.R., 2004. Chemotherapy for the brain: the antitumor antibiotic mithramycin prolongs survival in a mouse model of Huntington's disease. J. Neurosci. 24, 10335–10342.

Gardian, G., Browne, S.E., Choi, D.K., Klivenyi, P., Gregorio, J., Kubilus, J.K., Ryu, H., Langley, B., Ratan, R.R., Ferrante, R.J., Beal, M.F., 2005. Neuroprotective effects of phenylbutyrate in the N171-82Q transgenic mouse model of Huntington's disease. J. Biol. Chem. 280, 556–563.

Giampa, C., Middei, S., Patassini, S., Borreca, A., Marullo, F., Laurenti, D., Bernardi, G., Ammassari-Teule, M., Fusco, F.R., 2009. Phosphodiesterase type IV inhibition prevents sequestration of CREB binding protein, protects striatal parvalbumin interneurons and rescues motor deficits in the R6/2 mouse model of Huntington's disease. Eur. J. Neurosci. 29, 902–910.

Giorgini, F., Moller, T., Kwan, W., Zwilling, D., Wacker, J.L., Hong, S., Tsai, L.C., Cheah, C.S., Schwarcz, R., Guidetti, P., Muchowski, P.J., 2008. Histone deacetylase inhibition modulates kynurenine pathway activation in yeast, microglia, and mice expressing a mutant huntingtin fragment. J. Biol. Chem. 283, 7390–7400.

Giralt, A., Puigdellivol, M., Carreton, O., Paoletti, P., Valero, J., Parra-Damas, A., Saura, C.A., Alberch, J., Gines, S., 2012. Long-term memory deficits in Huntington's disease are associated with reduced CBP histone acetylase activity. Hum. Mol. Genet. 21, 1203–1216.

Giuliano, P., De Cristofaro, T., Affaitati, A., Pizzulo, G.M., Feliciello, A., Criscuolo, C., De Michele, G., Filla, A., Avvedimento, E.V., Varrone, S., 2003. DNA damage induced by polyglutamine-expanded proteins. Hum. Mol. Genet. 12, 2301–2309.

Globisch, D., Munzel, M., Muller, M., Michalakis, S., Wagner, M., Koch, S., Bruckl, T., Biel, M., Carell, T., 2010. Tissue distribution of 5-hydroxymethylcytosine and search for active demethylation intermediates. PLoS One 5, e15367.

Gorbunova, V., Seluanov, A., Mittelman, D., Wilson, J.H., 2004. Genome-wide demethylation destabilizes CTG.CAG trinucleotide repeats in mammalian cells. Hum. Mol. Genet. 13, 2979–2989.

Goula, A.V., Stys, A., Chan, J.P., Trottier, Y., Festenstein, R., Merienne, K., 2012. Transcription elongation and tissue-specific somatic CAG instability. PLoS Genet. 8, e1003051.

Grayson, D.R., Guidotti, A., 2013. The dynamics of DNA methylation in schizophrenia and related psychiatric disorders. Neuropsychopharmacology 38, 138–166.
Guibert, S., Weber, M., 2013. Functions of DNA methylation and hydroxymethylation in mammalian development. Curr. Top. Dev. Biol. 104, 47–83.
Guo, J.U., Ma, D.K., Mo, H., Ball, M.P., Jang, M.H., Bonaguidi, M.A., Balazer, J.A., Eaves, H.L., Xie, B., Ford, E., Zhang, K., Ming, G.L., Gao, Y., Song, H., 2011a. Neuronal activity modifies the DNA methylation landscape in the adult brain. Nat. Neurosci. 14, 1345–1351.
Guo, J.U., Su, Y., Zhong, C., Ming, G.L., Song, H., 2011b. Hydroxylation of 5-methylcytosine by TET1 promotes active DNA demethylation in the adult brain. Cell 145, 423–434.
Henikoff, S., Shilatifard, A., 2011. Histone modification: cause or cog? Trends Genet. 27, 389–396.
Hockly, E., Richon, V.M., Woodman, B., Smith, D.L., Zhou, X., Rosa, E., Sathasivam, K., Ghazi-Noori, S., Mahal, A., Lowden, P.A., Steffan, J.S., Marsh, J.L., Thompson, L.M., Lewis, C.M., Marks, P.A., Bates, G.P., 2003. Suberoylanilide hydroxamic acid, a histone deacetylase inhibitor, ameliorates motor deficits in a mouse model of Huntington's disease. Proc. Natl. Acad. Sci. U.S.A. 100, 2041–2046.
Hogarth, P., Lovrecic, L., Krainc, D., 2007. Sodium phenylbutyrate in Huntington's disease: a dose-finding study. Mov. Disord. 22, 1962–1964.
Hoshino, M., Tagawa, K., Okuda, T., Murata, M., Oyanagi, K., Arai, N., Mizutani, T., Kanazawa, I., Wanker, E.E., Okazawa, H., 2003. Histone deacetylase activity is retained in primary neurons expressing mutant huntingtin protein. J. Neurochem. 87, 257–267.
Huang, Y., Pastor, W.A., Shen, Y., Tahiliani, M., Liu, D.R., Rao, A., 2010. The behaviour of 5-hydroxymethylcytosine in bisulfite sequencing. PLoS One 5, e8888.
Igarashi, S., Morita, H., Bennett, K.M., Tanaka, Y., Engelender, S., Peters, M.F., Cooper, J.K., Wood, J.D., Sawa, A., Ross, C.A., 2003. Inducible PC12 cell model of Huntington's disease shows toxicity and decreased histone acetylation. Neuroreport 14, 565–568.
Illuzzi, J., Yerkes, S., Parekh-Olmedo, H., Kmiec, E.B., 2009. DNA breakage and induction of DNA damage response proteins precede the appearance of visible mutant huntingtin aggregates. J. Neurosci. Res. 87, 733–747.
Iwase, S., Xiang, B., Ghosh, S., Ren, T., Lewis, P.W., Cochrane, J.C., Allis, C.D., Picketts, D.J., Patel, D.J., Li, H., Shi, Y., 2011. ATRX ADD domain links an atypical histone methylation recognition mechanism to human mental-retardation syndrome. Nat. Struct. Mol. Biol. 18, 769–776.
Jakovcevski, M., Akbarian, S., 2012. Epigenetic mechanisms in neurological disease. Nat. Med. 18, 1194–1204.
Jeon, G.S., Kim, K.Y., Hwang, Y.J., Jung, M.K., An, S., Ouchi, M., Ouchi, T., Kowall, N., Lee, J., Ryu, H., 2012. Deregulation of BRCA1 leads to impaired spatiotemporal dynamics of gamma-H2AX and DNA damage responses in Huntington's disease. Mol. Neurobiol. 45, 550–563.
Jeong, H., Then, F., Melia Jr., T.J., Mazzulli, J.R., Cui, L., Savas, J.N., Voisine, C., Paganetti, P., Tanese, N., Hart, A.C., Yamamoto, A., Krainc, D., 2009. Acetylation targets mutant huntingtin to autophagosomes for degradation. Cell 137, 60–72.
Jia, H., Kast, R.J., Steffan, J.S., Thomas, E.A., 2012a. Selective histone deacetylase (HDAC) inhibition imparts beneficial effects in Huntington's disease mice: implications for the ubiquitin-proteasomal and autophagy systems. Hum. Mol. Genet. 21, 5280–5293.
Jia, H., Pallos, J., Jacques, V., Lau, A., Tang, B., Cooper, A., Syed, A., Purcell, J., Chen, Y., Sharma, S., Sangrey, G.R., Darnell, S.B., Plasterer, H., Sadri-Vakili, G., Gottesfeld, J.M., Thompson, L.M., Rusche, J.R., Marsh, J.L., Thomas, E.A., 2012b. Histone deacetylase (HDAC) inhibitors targeting HDAC3 and HDAC1 ameliorate polyglutamine-elicited phenotypes in model systems of Huntington's disease. Neurobiol. Dis. 46, 351–361.
Jiang, H., Nucifora Jr., F.C., Ross, C.A., DeFranco, D.B., 2003. Cell death triggered by polyglutamine-expanded huntingtin in a neuronal cell line is associated with degradation of CREB-binding protein. Hum. Mol. Genet. 12, 1–12.
Jiang, H., Poirier, M.A., Liang, Y., Pei, Z., Weiskittel, C.E., Smith, W.W., DeFranco, D.B., Ross, C.A., 2006. Depletion of CBP is directly linked with cellular toxicity caused by mutant huntingtin. Neurobiol. Dis. 23, 543–551.
Jin, S.G., Kadam, S., Pfeifer, G.P., 2010. Examination of the specificity of DNA methylation profiling techniques towards 5-methylcytosine and 5-hydroxymethylcytosine. Nucleic Acids Res. 38, e125.
Jung, J., Bonini, N., 2007. CREB-binding protein modulates repeat instability in a Drosophila model for polyQ disease. Science 315, 1857–1859.
Kanduri, C., 2011. Long noncoding RNA and epigenomics. Adv. Exp. Med. Biol. 722, 174–195.
Kazantsev, A., Preisinger, E., Dranovsky, A., Goldgaber, D., Housman, D., 1999. Insoluble detergent-resistant aggregates form between pathological and non-pathological lengths of polyglutamine in mammalian cells. Proc. Natl. Acad. Sci. U.S.A. 96, 11404–11409.
Kim, W.Y., Fayazi, Z., Bao, X., Higgins, D., Kazemi-Esfarjani, P., 2005. Evidence for sequestration of polyglutamine inclusions by Drosophila myeloid leukemia factor. Mol. Cell. Neurosci. 29, 536–544.
Kim, M.O., Chawla, P., Overland, R.P., Xia, E., Sadri-Vakili, G., Cha, J.H., 2008. Altered histone monoubiquitylation mediated by mutant huntingtin induces transcriptional dysregulation. J. Neurosci. 28, 3947–3957.
Kita, H., Carmichael, J., Swartz, J., Muro, S., Wyttenbach, A., Matsubara, K., Rubinsztein, D.C., Kato, K., 2002. Modulation of polyglutamine-induced cell death by genes identified by expression profiling. Hum. Mol. Genet. 11, 2279–2287.
Klevytska, A.M., Tebbenkamp, A.T., Savonenko, A.V., Borchelt, D.R., 2010. Partial depletion of CREB-binding protein reduces life expectancy in a mouse model of Huntington disease. J. Neuropathol. Exp. Neurol. 69, 396–404.
Lee, J., Hong, Y.K., Jeon, G.S., Hwang, Y.J., Kim, K.Y., Seong, K.H., Jung, M.K., Picketts, D.J., Kowall, N.W., Cho, K.S., Ryu, H., 2012. ATRX induction by mutant huntingtin via Cdx2 modulates heterochromatin condensation and pathology in Huntington's disease. Cell Death Differ. 19, 1109–1116.
Lee, J., Hwang, Y.J., Shin, J.Y., Lee, W.C., Wie, J., Kim, K.Y., Lee, M.Y., Hwang, D., Ratan, R.R., Pae, A.N., Kowall, N.W., So, I., Kim, J.I., Ryu, H., 2013. Epigenetic regulation of cholinergic receptor M1 (CHRM1) by histone H3K9me3 impairs Ca(2+) signaling in Huntington's disease. Acta Neuropathol. 125, 727–739.
Li, W., Liu, M., 2011. Distribution of 5-hydroxymethylcytosine in different human tissues. J. Nucleic Acids 2011, 870726.
Li, S.H., Cheng, A.L., Zhou, H., Lam, S., Rao, M., Li, H., Li, X.J., 2002. Interaction of Huntington disease protein with transcriptional activator Sp1. Mol. Cell. Biol. 22, 1277–1287.
Lim, S., Chesser, A.S., Grima, J.C., Rappold, P.M., Blum, D., Przedborski, S., Tieu, K., 2011. D-beta-hydroxybutyrate is protective in mouse models of Huntington's disease. PLoS One 6, e24620.
Lister, R., Mukamel, E.A., Nery, J.R., Urich, M., Puddifoot, C.A., Johnson, N.D., Lucero, J., Huang, Y., Dwork, A.J., Schultz, M.D., Yu, M., Tonti-Filippini, J., Heyn, H., Hu, S., Wu, J.C., Rao, A., Esteller, M., He, C., Haghighi, F.G., Sejnowski, T.J., Behrens, M.M., Ecker, J.R., 2013. Global epigenomic reconfiguration during mammalian brain development. Science 341, 1237905.
Lopez-Atalaya, J.P., Ito, S., Valor, L.M., Benito, E., Barco, A., 2013. Genomic targets, and histone acetylation and gene expression profiling of neural HDAC inhibition. Nucleic Acids Res. 41, 8072–8084.
Lundby, A., Lage, K., Weinert, B.T., Bekker-Jensen, D.B., Secher, A., Skovgaard, T., Kelstrup, C.D., Dmytriyev, A., Choudhary, C., Lundby, C., Olsen, J.V., 2012. Proteomic analysis of lysine acetylation sites in rat tissues reveals organ specificity and subcellular patterns. Cell Rep. 2, 419–431.
Ma, C., D'Mello, S.R., 2011. Neuroprotection by histone deacetylase-7 (HDAC7) occurs by inhibition of c-jun expression through a deacetylase-independent mechanism. J. Biol. Chem. 286, 4819–4828.
Martin, E., Betuing, S., Pages, C., Cambon, K., Auregan, G., Deglon, N., Roze, E., Caboche, J., 2011. Mitogen- and stress-activated protein kinase 1-induced neuroprotection in Huntington's disease: role on chromatin remodeling at the PGC-1-alpha promoter. Hum. Mol. Genet. 20, 2422–2434.
McCampbell, A., Taylor, J.P., Taye, A.A., Robitschek, J., Li, M., Walcott, J., Merry, D., Chai, Y., Paulson, H., Sobue, G., Fischbeck, K.H., 2000. CREB-binding protein sequestration by expanded polyglutamine. Hum. Mol. Genet. 9, 2197–2202.
McCampbell, A., Taye, A.A., Whitty, L., Penney, E., Steffan, J.S., Fischbeck, K.H., 2001. Histone deacetylase inhibitors reduce polyglutamine toxicity. Proc. Natl. Acad. Sci. U.S.A. 98, 15179–15184.
McFarland, K.N., Das, S., Sun, T.T., Leyfer, D., Xia, E., Sangrey, G.R., Kuhn, A., Luthi-Carter, R., Clark, T.W., Sadri-Vakili, G., Cha, J.H., 2012. Genome-wide histone acetylation is altered in a transgenic mouse model of Huntington's disease. PLoS One 7, e41423.
Mielcarek, M., Benn, C.L., Franklin, S.A., Smith, D.L., Woodman, B., Marks, P.A., Bates, G.P., 2011. SAHA decreases HDAC 2 and 4 levels in vivo and improves molecular phenotypes in the R6/2 mouse model of Huntington's disease. PLoS One 6, e27746.
Moumne, L., Campbell, K., Howland, D., Ouyang, Y., Bates, G.P., 2012. Genetic knockdown of HDAC3 does not modify disease-related phenotypes in a mouse model of Huntington's disease. PLoS One 7, e31080.
Nestor, C., Ruzov, A., Meehan, R., Dunican, D., 2010. Enzymatic approaches and bisulfite sequencing cannot distinguish between 5-methylcytosine and 5-hydroxymethylcytosine in DNA. Biotechniques 48, 317–319.
Ng, C.W., Yildirim, F., Yap, Y.S., Dalin, S., Matthews, B.J., Velez, P.J., Labadorf, A., Housman, D.E., Fraenkel, E., 2013. Extensive changes in DNA methylation are associated with expression of mutant huntingtin. Proc. Natl. Acad. Sci. U.S.A. 110, 2354–2359.
Nucifora Jr., F.C., Sasaki, M., Peters, M.F., Huang, H., Cooper, J.K., Yamada, M., Takahashi, H., Tsuji, S., Troncoso, J., Dawson, V.L., Dawson, T.M., Ross, C.A., 2001. Interference by huntingtin and atrophin-1 with cbp-mediated transcription leading to cellular toxicity. Science 291, 2423–2428.
Obrietan, K., Hoyt, K.R., 2004. CRE-mediated transcription is increased in Huntington's disease transgenic mice. J. Neurosci. 24, 791–796.
Oliveira, J.M., Chen, S., Almeida, S., Riley, R., Goncalves, J., Oliveira, C.R., Hayden, M.R., Nicholls, D.G., Ellerby, L.M., Rego, A.C., 2006. Mitochondrial-dependent Ca^{2+} handling in Huntington's disease striatal cells: effect of histone deacetylase inhibitors. J. Neurosci. 26, 11174–11186.
Pallos, J., Bodai, L., Lukacsovich, T., Purcell, J.M., Steffan, J.S., Thompson, L.M., Marsh, J.L., 2008. Inhibition of specific HDACs and sirtuins suppresses pathogenesis in a Drosophila model of Huntington's disease. Hum. Mol. Genet. 17, 3767–3775.
Parkel, S., Lopez-Atalaya, J., Barco, A., 2013. Histone H3 lysine methylation in cognition and intellectual disability disorders. Learn Mem. 20, 570–579.
Piekarski, M., Jelinska, A., 2013. Anthracyclines still prove effective in anticancer therapy. Mini Rev. Med. Chem. 13, 627–634.
Qiu, Z., Norflus, F., Singh, B., Swindell, M.K., Buzescu, R., Bejarano, M., Chopra, R., Zucker, B., Benn, C.L., DiRocco, D.P., Cha, J.H., Ferrante, R.J., Hersch, S.M., 2006. Sp1 is up-regulated in cellular and transgenic models of Huntington disease, and its reduction is neuroprotective. J. Biol. Chem. 281, 16672–16680.
Quinti, L., Chopra, V., Rotili, D., Valente, S., Amore, A., Franci, G., Meade, S., Valenza, M., Altucci, L., Maxwell, M.M., Cattaneo, E., Hersch, S., Mai, A., Kazantsev, A., 2010. Evaluation of histone deacetylases as drug targets in Huntington's disease models. Study of HDACs in brain tissues from R6/2 and

CAG140 knock-in HD mouse models and human patients and in a neuronal HD cell model. PLoS Curr. 2.
Rando, O.J., 2012. Combinatorial complexity in chromatin structure and function: revisiting the histone code. Curr. Opin. Genet. Dev. 22, 148–155.
Roze, E., Betuing, S., Deyts, C., Marcon, E., Brami-Cherrier, K., Pages, C., Humbert, S., Merienne, K., Caboche, J., 2008. Mitogen- and stress-activated protein kinase-1 deficiency is involved in expanded-huntingtin-induced transcriptional dysregulation and striatal death. FASEB J. 22, 1083–1093.
Ryu, H., Lee, J., Hagerty, S.W., Soh, B.Y., McAlpin, S.E., Cormier, K.A., Smith, K.M., Ferrante, R.J., 2006. ESET/SETDB1 gene expression and histone H3 (K9) trimethylation in Huntington's disease. Proc. Natl. Acad. Sci. U.S.A. 103, 19176–19181.
Sadri-Vakili, G., Menon, A.S., Farrell, L.A., Keller-McGandy, C.E., Cantuti-Castelvetri, I., Standaert, D.G., Augood, S.J., Yohrling, G.J., Cha, J.H., 2006. Huntingtin inclusions do not down-regulate specific genes in the R6/2 Huntington's disease mouse. Eur. J. Neurosci. 23, 3171–3175.
Sadri-Vakili, G., Bouzou, B., Benn, C.L., Kim, M.O., Chawla, P., Overland, R.P., Glajch, K.E., Xia, E., Qiu, Z., Hersch, S.M., Clark, T.W., Yohrling, G.J., Cha, J.H., 2007. Histones associated with downregulated genes are hypo-acetylated in Huntington's disease models. Hum. Mol. Genet. 16, 1293–1306.
Seredenina, T., Luthi-Carter, R., 2012. What have we learned from gene expression profiles in Huntington's disease? Neurobiol. Dis. 45, 83–98.
Sipione, S., Rigamonti, D., Valenza, M., Zuccato, C., Conti, L., Pritchard, J., Kooperberg, C., Olson, J.M., Cattaneo, E., 2002. Early transcriptional profiles in huntingtin-inducible striatal cells by microarray analyses. Hum. Mol. Genet. 11, 1953–1965.
Sng, J.C., Taniura, H., Yoneda, Y., 2006. Histone modifications in kainate-induced status epilepticus. Eur. J. Neurosci. 23, 1269–1282.
Song, C.X., Szulwach, K.E., Fu, Y., Dai, Q., Yi, C., Li, X., Li, Y., Chen, C.H., Zhang, W., Jian, X., Wang, J., Zhang, L., Looney, T.J., Zhang, B., Godley, L.A., Hicks, L.M., Lahn, B.T., Jin, P., He, C., 2011. Selective chemical labeling reveals the genome-wide distribution of 5-hydroxymethylcytosine. Nat. Biotechnol. 29, 68–72.
Stack, E.C., Del Signore, S.J., Luthi-Carter, R., Soh, B.Y., Goldstein, D.R., Matson, S., Goodrich, S., Markey, A.L., Cormier, K., Hagerty, S.W., Smith, K., Ryu, H., Ferrante, R.J., 2007. Modulation of nucleosome dynamics in Huntington's disease. Hum. Mol. Genet. 16, 1164–1175.
Steffan, J.S., Kazantsev, A., Spasic-Boskovic, O., Greenwald, M., Zhu, Y.Z., Gohler, H., Wanker, E.E., Bates, G.P., Housman, D.E., Thompson, L.M., 2000. The Huntington's disease protein interacts with p53 and CREB-binding protein and represses transcription. Proc. Natl. Acad. Sci. U.S.A. 97, 6763–6768.
Steffan, J.S., Bodai, L., Pallos, J., Poelman, M., McCampbell, A., Apostol, B.L., Kazantsev, A., Schmidt, E., Zhu, Y.Z., Greenwald, M., Kurokawa, R., Housman, D.E., Jackson, G.R., Marsh, J.L., Thompson, L.M., 2001. Histone deacetylase inhibitors arrest polyglutamine-dependent neurodegeneration in Drosophila. Nature 413, 739–743.
Strickland-Marmol, L.B., Khoor, A., Livingston, S.K., Rojiani, A., 2007. Utility of tissue-specific transcription factors thyroid transcription factor 1 and Cdx2 in determining the primary site of metastatic adenocarcinomas to the brain. Arch. Pathol. Lab. Med. 131, 1686–1690.
Tallaksen-Greene, S.J., Crouse, A.B., Hunter, J.M., Detloff, P.J., Albin, R.L., 2005. Neuronal intranuclear inclusions and neuropil aggregates in HdhCAG(150) knockin mice. Neuroscience 131, 843–852.
Taylor, J.P., Taye, A.A., Campbell, C., Kazemi-Esfarjani, P., Fischbeck, K.H., Min, K.T., 2003. Aberrant histone acetylation, altered transcription, and retinal degeneration in a Drosophila model of polyglutamine disease are rescued by CREB-binding protein. Genes Dev. 17, 1463–1468.
Telenius, H., Kremer, B., Goldberg, Y.P., Theilmann, J., Andrew, S.E., Zeisler, J., Adam, S., Greenberg, C., Ives, E.J., Clarke, L.A., et al., 1994. Somatic and gonadal mosaicism of the Huntington disease gene CAG repeat in brain and sperm. Nat. Genet. 6, 409–414.
Thomas, E.A., Coppola, G., Desplats, P.A., Tang, B., Soragni, E., Burnett, R., Gao, F., Fitzgerald, K.M., Borok, J.F., Herman, D., Geschwind, D.H., Gottesfeld, J.M., 2008. The HDAC inhibitor 4b ameliorates the disease phenotype and transcriptional abnormalities in Huntington's disease transgenic mice. Proc. Natl. Acad. Sci. U.S.A. 105, 15564–15569.
Thomas, B., Matson, S., Chopra, V., Sun, L., Sharma, S., Hersch, S., Rosas, H.D., Scherzer, C., Ferrante, R., Matson, W., 2013. A novel method for detecting 7-methyl guanine reveals aberrant methylation levels in Huntington disease. Anal. Biochem. 436, 112–120.
Thompson, L.M., Aiken, C.T., Kaltenbach, L.S., Agrawal, N., Illes, K., Khoshnan, A., Martinez-Vincente, M., Arrasate, M., O'Rourke, J.G., Khashwji, H., Lukacsovich, T., Zhu, Y.Z., Lau, A.L., Massey, A., Hayden, M.R., Zeitlin, S.O., Finkbeiner, S., Green, K.N., LaFerla, F.M., Bates, G., Huang, L., Patterson, P.H., Lo, D.C., Cuervo, A.M., Marsh, J.L., Steffan, J.S., 2009. IKK phosphorylates Huntingtin and targets it for degradation by the proteasome and lysosome. J. Cell Biol. 187, 1083–1099.
Tsankova, N.M., Kumar, A., Nestler, E.J., 2004. Histone modifications at gene promoter regions in rat hippocampus after acute and chronic electroconvulsive seizures. J. Neurosci. 24, 5603–5610.
Valor, L.M., Barco, A., 2012. Hippocampal gene profiling: towards a systems biology of the hippocampus. Hippocampus 22, 929–941.
Valor, L.M., Pulopulos, M.M., Jimenez-Minchan, M., Olivares, R., Lutz, B., Barco, A., 2011. Ablation of CBP in forebrain principal neurons causes modest memory and transcriptional defects and a dramatic reduction of histone acetylation but does not affect cell viability. J. Neurosci. 31, 1652–1663.
Valor, L.M., Guiretti, D., Lopez-Atalaya, J.P., Barco, A., 2013a. Genomic landscape of transcriptional and epigenetic dysregulation in early onset polyglutamine disease. J. Neurosci. 33, 10471–10482.
Valor, L.M., Viosca, J., Lopez-Atalaya, J.P., Barco, A., 2013b. Lysine acetyltransferases CBP and p300 as therapeutic targets in cognitive and neurodegenerative disorders. Curr. Pharm. Des. 19, 5051–5064.
Varley, K.E., Gertz, J., Bowling, K.M., Parker, S.L., Reddy, T.E., Pauli-Behn, F., Cross, M.K., Williams, B.A., Stamatoyannopoulos, J.A., Crawford, G.E., Absher, D.M., Wold, B.J., Myers, R.M., 2013. Dynamic DNA methylation across diverse human cell lines and tissues. Genome Res. 23, 555–567.
Vashishtha, M., Ng, C.W., Yildirim, F., Gipson, T.A., Kratter, I.H., Bodai, L., Song, W., Lau, A., Labadorf, A., Vogel-Ciernia, A., Troncosco, J., Ross, C.A., Bates, G.P., Krainc, D., Sadri-Vakili, G., Finkbeiner, S., Marsh, J.L., Housman, D.E., Fraenkel, E., Thompson, L.M., 2013. Targeting H3K4 trimethylation in Huntington disease. Proc. Natl. Acad. Sci. U.S.A. 110, E3027–3036.
Villar-Menendez, I., Blanch, M., Tyebji, S., Pereira-Veiga, T., Albasanz, J.L., Martin, M., Ferrer, I., Perez-Navarro, E., Barrachina, M., 2013. Increased 5-methylcytosine and decreased 5-hydroxymethylcytosine levels are associated with reduced striatal A2AR levels in Huntington's disease. Neuromolecular Med. 15, 295–309.
Wang, Z., Zang, C., Rosenfeld, J.A., Schones, D.E., Barski, A., Cuddapah, S., Cui, K., Roh, T.Y., Peng, W., Zhang, M.Q., Zhao, K., 2008. Combinatorial patterns of histone acetylations and methylations in the human genome. Nat. Genet. 40, 897–903.
Wang, F., Yang, Y., Lin, X., Wang, J.Q., Wu, Y.S., Xie, W., Wang, D., Zhu, S., Liao, Y.Q., Sun, Q., Yang, Y.G., Luo, H.R., Guo, C., Han, C., Tang, T.S., 2013. Genome-wide loss of 5-hmC is a novel epigenetic feature of Huntington's disease. Hum. Mol. Genet. 22, 3641–3653.
Xie, W., Barr, C.L., Kim, A., Yue, F., Lee, A.Y., Eubanks, J., Dempster, E.L., Ren, B., 2012. Base-resolution analyses of sequence and parent-of-origin dependent DNA methylation in the mouse genome. Cell 148, 816–831.
Yazawa, I., Hazeki, N., Nakase, H., Kanazawa, I., Tanaka, M., 2003. Histone H3 is aberrantly phosphorylated in glutamine-repeat diseases. Biochem. Biophys. Res. Commun. 302, 144–149.
Yeh, H.H., Young, D., Gelovani, J.G., Robinson, A., Davidson, Y., Herholz, K., Mann, D.M., 2013. Histone deacetylase class II and acetylated core histone immunohistochemistry in human brains with Huntington's disease. Brain Res. 1504, 16–24.
Yu, Z.X., Li, S.H., Nguyen, H.P., Li, X.J., 2002. Huntingtin inclusions do not deplete polyglutamine-containing transcription factors in HD mice. Hum. Mol. Genet. 11, 905–914.
Zadori, D., Geisz, A., Vamos, E., Vecsei, L., Klivenyi, P., 2009. Valproate ameliorates the survival and the motor performance in a transgenic mouse model of Huntington's disease. Pharmacol. Biochem. Behav. 94, 148–153.
Zajac, M.S., Pang, T.Y., Wong, N., Weinrich, B., Leang, L.S., Craig, J.M., Saffery, R., Hannan, A.J., 2010. Wheel running and environmental enrichment differentially modify exon-specific BDNF expression in the hippocampus of wild-type and pre-motor symptomatic male and female Huntington's disease mice. Hippocampus 20, 621–636.
Zuccato, C., Valenza, M., Cattaneo, E., 2010. Molecular mechanisms and potential therapeutical targets in Huntington's disease. Physiol. Rev. 90, 905–981.